

**HYDROGEOCHEMICAL INVESTIGATION
OF REACTIVE TAILINGS AT THE WAITE-
AMULET TAILINGS SITE, NORANDA,
QUÉBEC, "GENERATION AND EVOLUTION
OF ACIDIC PORE WATERS AT THE WAITE
AMULET TAILINGS - FINAL REPORT"**

MEND Project 1.17.1d

April 1990

**GENERATION AND EVOLUTION OF
ACIDIC PORE WATERS
AT THE WAITE AMULET TAILINGS**

**Final Report
by**

**Authors: E.K. Yanful, L. St-Arnaud, and R. Prairie
Project Manager: R. Siwik
Project No: EN2-8523H: RR 89-1
Centre de Technologie Noranda
240 Boulevard Hymus
Pointe Claire, Quebec
H9R 1G5**

**DSS Contract Number:
CANMET Scientific Authority:**

**09SQ.23440-8-9162
Dr. N.K. Dave**

April 1990

DISTRIBUTION

Dr. N. Dave (CANMET Scientific Authority)	10 copies
Mr. M. Fillion (Secretary, MEND Program)	40 copies
Noranda Internal Distribution	30 copies

ACKNOWLEDGEMENTS

The authors would wish to thank Dr R. Nicholson of the University of Waterloo and Dr N. Dave of CANMET for reviewing the report. R. Blackport of Terraqua Investigations Ltd provided essential comments on the hydrological and hydrogeological sections. Discussions were held with D. Blowes of the University of Waterloo. Input from R. Siwik and K. Wheeland of Noranda Technology Centre is also gratefully acknowledged. This work would not have been realized without the cooperation of Noranda Minerals, Horne Division, and the participation of several technicians, students, and temporary personnel, in particular S. Payant of the Noranda Technology Centre.

This project was jointly funded by Noranda Inc. and CANMET.

KEY WORDS

Acid Mine Drainage
Acid Generation
Hydrogeochemistry
Tailings
MEND Program
Sulphides
Waite Amulet

TABLE OF CONTENTS

	<u>Page</u>
EXECUTIVE SUMMARY	x
SOMMAIRE EXECUTIF	xii
TECHNICAL SUMMARY	1
1. INTRODUCTION	17
1.1 Background and Objectives	17
1.2 Scope	19
1.3 Site Location	19
2. SITE HISTORY	20
2.1 Mining Activity	20
2.2 Mineral Processing	20
2.3 Tailings Disposal	21
2.4 Tailings Reclamation	21
3. THEORY OF ACID GENERATION	24
3.1 Oxidation Processes	24
3.2 Factors Controlling Oxidation	26
3.2.1 Oxygen Transport	26
3.2.2 Temperature	27
3.2.3 Sulphide Content, Morphology, and Surface Area	28
3.2.4 Bacterial Activity	29
3.2.5 pH	30
3.2.6 Carbon Dioxide Transport	31
3.2.7 Nutrients	32
4. ACID GENERATION AT WAITE AMULET	33
4.1 Sampling Locations	33
4.2 Oxygen Distribution	33
4.3 Temperature Profiles	34
4.4 Sulphide Content	36
4.5 Bacteria Populations	38
4.6 pH Profiles	39
4.7 Carbon Dioxide Concentrations	40
4.8 Nutrient Availability	41

TABLE OF CONTENTS (Cont'd)

	<u>Page</u>
5. PORE WATER GEOCHEMISTRY	42
5.1 Unsaturated Zone	42
5.2 Saturated Zone	44
6. HYDROGEOLOGY	56
6.1 Site Conditions	56
6.2 Unsaturated Zone Pore Water Flow	57
6.3 Saturated Zone Pore Water Flow and Storage	58
7. HYDROLOGY	60
7.1 Water Balance Equation	60
7.2 Evaporation and Precipitation	61
7.3 Infiltration and Run-off	62
7.4 Seepage	64
7.5 Water Balance Evaluation	68
8. FLOW MODELLING	72
8.1 Method	72
8.2 Results	74
8.3 Discussion	74
9. PORE WATER EVOLUTION	78
10. GEOTECHNIQUE AND HYDROGEOCHEMISTRY OF CLAYEY SUBSOIL	80
10.1 Introduction	80
10.2 Sampling	80
10.2.1 Field Sampling of Clay	80
10.2.2 Laboratory Sampling	80
10.3 Analyses	81
10.3.1 Pore Water Analysis	81
10.3.2 Soil Analysis	82
10.3.3 Mineralogy	82
10.4 Geotechnical Testing	82
10.4.1 Index Properties	82
10.4.2 Shear Strength	83
10.4.3 Hydraulic Conductivity	83
10.5 Quality Assurance and Quality Control	85
10.6 Results	86
10.6.1 Geotechnique	86
10.6.2 Hydrogeochemistry	88
10.7 Discussions	90

TABLE OF CONTENTS (Cont'd)

iv

	<u>Page</u>
11. CONCLUSIONS	93
12. RECOMMENDATIONS	94
REFERENCES	96
APPENDICES	
APPENDIX A	WATER TREATMENT
APPENDIX B	METHODS OF INVESTIGATION AND QA/QC
APPENDIX C	MODELLING
APPENDIX D	METEOROLOGICAL DATA

LIST OF TABLES

		<u>Page</u>
Table 1.1	Waite Amulet and West MacDonald Metallurgy and Reagents (1956).	22
Table 5.1	Heavy Metal Concentrations at WA-15, October 1986.	47
Table 5.2	Heavy Metal Concentrations at WA-17, October 1986.	49
Table 5.3	Heavy Metal Concentrations at WA-11, October 1986.	51
Table 5.4	Physico-Chemical, Metal, and Major Ion Concentration Values, October 1986 (a) and November 1988 (b).	52
Table 7.1	Monthly Precipitation and Evaporation Data for Waite Amulet Tailings Site.	61
Table 7.2	Concentrations and Loading Values from Samples Collected at Station 1.	65
Table 7.3	Rainfall Duration and Peak Flows for Conditions of High Seepage at Station 2 During May and November 1988.	66
Table 7.4	Input Parameters for Help Model.	69
Table 7.5	Annual Water Balance at the Waite Amulet Site.	70
Table 8.1	Description of Flow Simulation Parameters.	73
Table 8.2	Calibrated and Measured Potentials of Piezometers Along Section A-A'.	75
Table 8.3	Calibrated and Measured Potentials of Piezometers Along Section B-B'.	76
Table 10.1	Chemical Composition of Simulated Pore Water Used in the Hydraulic Conductivity Tests.	85
Table 10.2	Summary of Index Properties of Clay Underneath the Tailings Impoundment.	87
Table 10.3	Adsorbed Cation Composition of Clay Beneath Tailings Dam WA-20.	92

LIST OF FIGURES

- Figure 1.1 Location of Waite Amulet Tailings Area
- Figure 1.2 Waite Amulet Concentrator Flowsheet
- Figure 4.1 Location of Waite Amulet Monitoring Stations
- Figure 4.2 Gaseous Oxygen Concentration versus Depth at (a) Locations WA-11, WA-17 in 1986 and (b) Location WA-8 in 1987
- Figure 4.3 Diurnal Temperature Variations of Air and Tailings at 15 and 45 cm Depth in August 1988
- Figure 4.4 Diurnal Temperature Variation of Air and Tailings at 15 and 45 cm Depth in November 1988
- Figure 4.5 Temperature versus Depth at Location WA-2
- Figure 4.6 Temperature versus Depth at Location WA-20
- Figure 4.7 Temperature versus Depth at Location WA-21
- Figure 4.8 Temperature versus Depth at Location WA-22
- Figure 4.9 Variation in Sulphides and Alteration Products versus Depth for <37 micron Particles at WA-20
- Figure 4.10 Variation in Sulphide and Alteration Products versus Depth for >37 micron Particles at WA-20
- Figure 4.11 Variation in pH, Sulphide Alteration Intensity, Sulphate, Elemental Sulphur and Pore Gas with Depth at WA-2
- Figure 4.12 Variation in pH, Sulphide Alteration Intensity, Sulphate, Elemental Sulphur and Pore Gas with Depth at WA-11
- Figure 4.13 T. Ferroxidans, Sulphate Reducers, Pore Gas, pH and Sulphide Alteration Intensity versus Depth for WA-20
- Figure 4.14 T. Ferroxidans, Sulphate Reducers, Pore Gas, pH and Sulphide Alteration Intensity versus Depth for WA-22
- Figure 4.15 Variation in Oxygen and Carbon Dioxide versus Depth at WA-24

LIST OF FIGURES (Cont'd)

- Figure 5.1 Ion Concentration Profiles at WA-2, WA-11, WA-20, and WA-21, October 1986. Fe, Ca and Na are represented by circles; SO₄, Mg and K are represented by squares.
- Figure 5.2 Pore Water Chemistry Profiles at WA-15, October 1986
- Figure 5.3 Pore Water Chemistry Profiles at WA-15, October 1986
- Figure 5.4 Pore Water Chemistry Profiles at WA-15, November 1988
- Figure 5.5 Pore Water Chemistry Profiles at WA-17
- Figure 5.6 Pore Water Chemistry Profiles at WA-17
- Figure 5.7 Pore Water Chemistry Profiles at WA-11
- Figure 5.8 Pore Water Chemistry Profiles at WA-11
- Figure 5.9 Pore Water Chemistry Profiles at WA-11
- Figure 5.10 Pore Water Chemistry Profiles at WA-11
- Figure 6.1 Grain Size Distribution Curves for Waite Amulet Tailings at WA-2 and WA-20
- Figure 6.2 Water Table at Waite Amulet, October 1986
- Figure 7.1 Hydrogeologic Cycle for Waite Amulet Tailings Site
- Figure 7.2 Location of Meteorological and Surface Water Monitoring Stations
- Figure 7.3 Cumulative Rainfall and Storm Hydrograph at Station 1 for September 1988
- Figure 7.4 Cumulative Rainfall and Storm Hydrographs at Station 1 for 26 August, 24 and 27 September, and 5 November 1988
- Figure 7.5 Flow and Fe_T Concentrations Versus Time at Station 2, November 1988
- Figure 8.1 Plan of Tailings Showing Locations of Piezometer Nests and Sections A-A' and B-B'.
- Figure 8.2 Boundary Conditions for Two-Dimensional Flow Modelling of Waite Amulet Tailings

LIST OF FIGURES (Cont'd)

- Figure 8.3** Calibrated Flow Net Section A-A, Waite Amulet Tailings
- Figure 8.4** Calibrated Flow Net Section B-B, Waite Amulet Tailings
- Figure 10.1** Triaxial Panel and Cell Used in the Hydraulic Conductivity Tests.
- Figure 10.2** Applied Squeeze Pressures vs Pore Water Cation Concentrations in Background Waite Amulet Clay.
- Figure 10.3** Geotechnical Profiles at WA-11.
- Figure 10.4** Geotechnical Profiles at WA-20.
- Figure 10.5** A Typical Grain Size Distribution of Waite Amulet Clay.
- Figure 10.6** Hydraulic Conductivity of Clay Soil Near the Tailings/Clay Interface at WA-20 Permeated with Distilled Water.
- Figure 10.7** Hydraulic Conductivity of Clay Soil Near the Tailings/Clay Interface at WA-20 Permeated with Simulated Pore Water.
- Figure 10.8** Iron Concentrations in Bulk Clay Soil and Pore Water at WA-11.
- Figure 10.9** Zinc Concentrations in Bulk Clay Soil and Pore Water at WA-11.
- Figure 10.10** Lead Concentrations in Bulk Clay Soil and Pore Water at WA-11.
- Figure 10.11** Copper Concentrations in Bulk Clay Soil and Pore Water at WA-11.
- Figure 10.12** Aluminum Concentrations in Bulk Clay Soil and Pore Water at WA-11.
- Figure 10.13** Sulphate Concentrations in Bulk Clay Soil and Pore Water at WA-11.
- Figure 10.14** Soil Solution and Clay Pore Water pH Profiles at WA-11.
- Figure 10.15** Iron Concentrations in Bulk Clay Soil and Pore Water at WA-20.
- Figure 10.16** Zinc Concentrations in Bulk Clay Soil and Pore Water at WA-20.
- Figure 10.17** Lead Concentrations in Bulk Clay Soil and Pore Water at WA-20.
- Figure 10.18** Copper Concentrations in Bulk Clay Soil and Pore Water at WA-20.

LIST OF FIGURES (Cont'd)

Figure 10.19 Aluminum Concentrations in Bulk Clay Soil and Pore Water at WA-20.

Figure 10.20 Sulphate Concentrations in Bulk Clay Soil and Pore Water at WA-20.

Figure 10.21 Soil Solution and Clay Pore Water pH Profiles at WA-11.

Figure 10.22 Major Cation Profiles at WA-11.

Figure 10.23 Major Cation Profiles at WA-20.

EXECUTIVE SUMMARY

This final report presents the results of studies conducted at the Waite Amulet tailings site during the four-year period from 1985 to 1988. These studies were performed under the national MEND (Mine Environment Neutral Drainage) program, a combined industry-government consortium committed to the development of practical techniques to reduce the environmental impact of acid mine drainage.

The influence of various factors (gaseous oxygen and carbon dioxide concentrations, temperature, bacteria, sulphide content and pH) on acid generation at Waite Amulet are presented and discussed along with unsaturated and saturated zone pore water geochemistry, tailings hydrogeology, and surface hydrology. Results of simulations of pore water flow by a two-dimensional steady state finite element model are also given. The evolution of acidic pore waters at the tailings site is discussed.

The study verified that the most important control on the pyrite oxidation process is the availability of oxygen. In addition to contributing directly to oxidation, oxygen influences the production of ferric iron and the density of bacterial populations. Oxygen concentration distribution with depth in the tailings defines the depth of active oxidation, and show that oxygen movement within the tailings is controlled by diffusion.

The oxidation of sulphides in the deep unsaturated zone occurs at a rate dependent on pH, and will be very low. Acidic porewater is partly neutralized by mineral dissolution and precipitation reactions in the deeper unsaturated zone. As sulphides in the shallow zone are depleted, the oxidation front will move downwards. The remaining acidity and dissolved metals will flow downwards with the pore water in the unsaturated zone until it reaches the water table. Acid conditions in the shallow saturated zone become more neutral with depth due to more buffering.

Pore water in the saturated zone flows in a direction which varies across the area of the tailings. Flow in the central part of the tailings is vertical and downwards while flow along the perimeter of the tailings is horizontal. Anisotropy in the hydraulic properties of the tailings is a major control on the flow of porewater in the tailings. The anisotropy is produced by the presence of fine-grained, horizontal ("slime") layers. It has the effect of promoting horizontal flow over vertical downward flow.

Along the west side of the tailings, a surface drainage ditch collects most of the water infiltrating the tailings. Analysis of porewater quality and calculation of groundwater velocity suggested that tailings porewater does not penetrate deep into the clayey horizon underlying the south section of the tailings. In the northwest section, a small portion of the porewater (approximately 10%) flows through the bottom of the tailings into the underlying geological units. Sulphate levels above background values, observed in the deeper layer of the clay, may be attributed to migration by diffusion.

By monitoring run-off and seepage water quality over a period of five months, it was found that acid water collected in surface ditches around the tailings impoundment is produced by seepage rather than run-off.

Acid generation will last longer along the tailings dam and in the south section of the impoundment. In these areas, the coarse-grained nature of the tailings results in lower water table levels and hence larger volumes of unsaturated tailings available for oxidation. Recommendations are made for future tailings impoundments, such as the promotion of high water tables by selective placement of fine-grained tailings across the site. Coarse-grained material, such as rock fill, should be avoided in tailings dam construction, unless design features are incorporated to prevent water tables from dropping excessively. Horizontal flow should be promoted by selective placement of horizontal fine-grained layers across the area of the tailings deposits. This could reduce downward vertical flow considerably, and facilitate the collection of acid mine drainage around the perimeter of the impoundments.

SOMMAIRE EXECUTIF

Ce rapport final présente les résultats d'études menées au parc à résidus miniers de Waite-Amulet de 1985 à 1988. Ces études furent faites sous le parrainage du programme national NEDEM (Neutralisation des Eaux de Drainage dans l'Environnement Minier), qui fut créé par un comité composé de représentants de l'industrie et des gouvernements pour le développement de techniques pour réduire l'impact environnemental du drainage minier acide.

L'influence de divers facteurs (concentrations d'oxygène gazeux et de dioxyde de carbone, température, présence de bactéries, contenu en minéraux sulfureux, et pH) sur la génération d'acide à Waite-Amulet est présentée, en même temps que la géochimie des eaux interstitielles dans les zones saturée et non-saturée, l'hydrogéologie, et l'hydrologie du site. Les résultats de simulations de l'écoulement des eaux interstitielles au moyen d'un modèle numérique en deux dimensions sont présentés, de même qu'une discussion sur l'évolution des eaux interstitielles à l'intérieur du parc.

L'étude a permis de vérifier que l'oxydation de la pyrite dans les résidus miniers est contrôlée principalement par la disponibilité d'oxygène. En plus de contribuer directement à l'oxydation, l'oxygène influence la production de fer ferreux et la densité des populations bactériennes catalysatrices. Les profils de distribution des concentrations d'oxygène en profondeur permettent de définir la profondeur d'oxydation active, et de déterminer que le mouvement de l'oxygène à l'intérieur du parc à résidus s'effectue par diffusion.

L'oxydation des sulfures aux niveaux inférieurs de la zone non-saturée s'effectue à un taux qui dépend du pH, et sera très faible. A ce niveau, un effet tampon est produit par des réactions de dissolution et de précipitation qui neutralisent partiellement les eaux interstitielles acides. A mesure que les minéraux sulfureux des niveaux supérieurs sont consommés par l'oxydation, le front d'oxydation se déplace vers les niveaux plus profonds. L'excédent d'acidité et les métaux dissous qui lui sont reliés s'écoulent vers le bas pour atteindre la surface phréatique. Les conditions acides toujours existantes aux niveaux supérieurs de la zone saturée s'estompent avec la profondeur sous l'effet des réactions tampon.

Les directions d'écoulement de l'eau interstitielle dans la zone saturée sont variables. Dans la partie centrale du parc, l'écoulement sera vertical et vers le bas, tandis qu'en périphérie, il sera horizontal. Une anisotropie au niveau des propriétés hydrauliques des résidus a un effet important sur l'écoulement des eaux interstitielles. Cette anisotropie est produite par la présence de résidus à granulométrie très fine formant des couches horizontales minces, et a pour effet de promouvoir l'écoulement horizontal au détriment de l'écoulement vertical.

Sur le côté ouest du parc à résidus, un fossé latéral de drainage intercepte la quasi-totalité de l'eau interstitielle du parc à résidus. L'analyse de la qualité de l'eau interstitielle et le calcul des vitesses d'écoulement à l'intérieur de la couche argileuse située sous le parc à résidus suggèrent que l'eau du parc à résidus ne pénètre pas profondément dans cette couche dans la partie sud-ouest du parc. Dans la partie nord-ouest, une certaine portion de l'eau interstitielle (environ 10%) s'écoule à travers la base du parc. Les concentrations de sulfates observées en profondeur dans la couche argileuse sont légèrement au-dessus des valeurs régionales, et peuvent être attribuées à l'effet de migration par diffusion.

En monitorant la qualité du ruissellement de surface et du suintement autour du périmètre du parc au cours d'une période de cinq mois, il a été déterminé que le drainage acide produit par le site est relié au suintement plutôt qu'au ruissellement.

La production d'acide devrait durer plus longtemps à l'intérieur de la digue et dans la section sud du parc. A ces endroits, la granulométrie plus grossière des résidus induit un niveau de nappe phréatique plus profond, ce qui accroît le volume de résidus non-saturé à oxyder. Des recommandations ont été incluses à cet effet, tel que le placement sélectif de résidus fins afin de d'élever le niveau de saturation. L'utilisation de matériel grossier, tel que les blocs de roche stérile, est à éviter dans la construction des digues, à moins que leur désign incorpore des mesures pour prévenir un abaissement excessif du niveau de saturation. L'écoulement horizontal devrait être accru à l'aide d'un placement sélectif de résidus fins en couches horizontales à travers l'étendue des nouveaux parcs à résidus. Ceci pourrait réduire considérablement l'écoulement vertical, et faciliter grandement la collection de drainage acide en périphérie des sites.

TECHNICAL SUMMARY

INTRODUCTION

The Waite Amulet tailings area, which is situated approximately 20 km north of Noranda, ceased operation in 1962, leaving 5.9 million tonnes of reactive sulphide tailings in an elevated 41 hectare dam and tailings spills in a lower area. Acid seepage and tailings surface run-off are collected in an acid water reservoir. A computer-controlled water treatment plant uses lime to neutralize the acid water to remove metals, producing a high density sludge and providing an acceptable effluent.

In an effort to minimize perpetual maintenance of acid generating mine sites, the national MEND program was created by industry and government in a collaborative effort to develop walk-away solutions to mine closure problems. The Waite Amulet hydrogeochemical study was undertaken as part of the MEND program to understand the geochemical processes controlling sulphide oxidation and subsequent pore water evolution.

Project reports which included results of each year's study were submitted to CANMET, along with recommendations, proposals and work plans for the subsequent year. The specific study objectives and work conducted during each year were as follows:

Phase 1 (1985) The first-year objective was to define the tailings hydrogeology, geochemistry and biochemistry.

Work conducted in 1985 included site investigation involving drilling and the use of geophysical methods for the analysis and sampling of the tailings and underlying deposits. A hydrogeochemical investigation was also conducted to define the pore water chemistry in the tailings and underlying formation. The 1985 field program indicated that elevated pore water metal levels reached the water table, and that the unsaturated (vadose) zone should be investigated.

Phase 2 (1986)

The study objectives in the second year were to finalize the definition of tailings hydrogeology, evaluate the geochemistry of the unsaturated zone, and propose oxidation control measures.

In accordance with the stated objectives, more piezometers were installed to further define the site hydrogeochemistry. A study of the unsaturated zone pore water and mineralogy was also undertaken to determine the extent of oxidation and pore water evolution. The 1986 field program indicated the need to further examine the role of gaseous oxygen in controlling sulphide oxidation, and to develop a mass balance to define pore water evolution.

Phase 3 (1987)

The work plan in the third year of the project was to assess water and metal balance in the tailings, evaluate gaseous O₂ profiles in different areas of the tailings, and, in conjunction with CANMET and the University of Waterloo, relate the mineralogy of the tailings to the unsaturated pore water geochemistry.

The 1987 field program evaluated the O₂ profiles with depth in the tailings. Tailings moisture contents and grain size distributions were also obtained. Results of work conducted in Phases 1 to 3 showed that infiltration, acidification, flow and release of acidic pore waters occur along sections of the tailings dam face. It was therefore decided that an adequate understanding of acid generation, pore water evolution and metal transport would require a detailed study of the west tailings dam.

Phase 4 (1988)

The intent of the Phase 4 program was to develop a realistic metal and water balance and evaluate pore water evolution and transport mechanisms along the west seepage face using a numerical flow model.

In accordance with these objectives, the 1988 field program included flow monitoring to provide information on metal loadings from overland and baseflow conditions. Piezometers were installed to obtain complete data along two sections on the western face. Steady state flow modelling was then conducted to determine pore water transport in the tailings.

ACID GENERATION AT WAITE AMULET

Oxygen Transport

The importance of oxygen in the reactive sulphide oxidation process lies in the fact that its presence is critical to the formation of Fe^{2+} and Fe^{3+} . Sulphide oxidation in reactive tailings is effectively limited to the vadose zone because oxygen transport in the saturated zone is restricted. The rate at which oxygen enters the tailings surface controls the maximum rate of oxidation and hence the rate of acid generation. The depth of penetration of oxygen defines the zone of active oxidation in tailings.

Gaseous oxygen profiles for the main tailings area of the Waite Amulet site suggest penetration of oxygen to a depth of 0.5 to 0.7 m in the unsaturated zone. Effective oxygen diffusion coefficients calculated from theoretical best-fits of observed oxygen concentrations were in the range of 3.0 to $4.2 \times 10^{-7} \text{ m}^2/\text{s}$. From these diffusion coefficients, sulphide oxidation in the vadose zone is estimated to continue for the next 600 years.

Temperature

The influence of temperature on biological ferrous iron oxidation by Thiobacillus ferrooxidans is similar to the influence of temperature on chemical oxidation. Temperature profiles in tailings deposits can therefore give an indication of the zone of active oxidation. Temperature

fluctuations measured in the Waite Amulet tailings at 15 and 45 cm depths indicated that changes in the ambient air temperature induce small fluctuations in temperatures at the 15 cm depth, while the temperature at 45 cm depth is nearly constant.

Oxygen and bacteria profiles indicate that at the Waite Amulet tailings site, the zone of active oxidation is located in the shallow tailings (0.5 to 0.7 m from surface). The temperature data suggest that very high summer surface or air temperatures could have a major influence on oxidation reactions in the shallow tailings zone through an increase in the level of bacteria activity. It appears that the surface temperature has completely masked any possible increases in temperature that could result from pyritic oxidation.

Sulphide Content

Profiles of tailings sulphide content and alteration products on the bench along the western side of the dam indicate that the main sulphide minerals are pyrite and pyrrhotite. Minor sulphides were reported to be sphalerite and chalcopyrite.

A study of the mineralogical character of the sulphide alteration products is also presented. In general, three zones of alteration are identified, as follows :

- i) a strongly oxidized near-surface zone depleted in sulphides;
- ii) an intermediate zone in which pyrrhotite (the sulphide most susceptible to oxidation) has extensively altered but not obliterated; and
- iii) a bottom zone of weak alteration in which pyrrhotite is largely preserved but has variable alteration rims from narrow, to incomplete, to absent.

Bacterial Activity

Pyrite oxidation via inorganic pathways occurs slowly under normal conditions. However, certain iron oxidizing bacteria, especially the genus T. ferrooxidans, have been known to catalyze the oxidation reactions involved in acid generation. For example, the oxidation rate in

the presence of T. ferrooxidans has been observed to increase by five to six orders of magnitude especially at shallow depths where oxygen is readily available. The major role of these bacteria in the oxidation process is to catalyze the oxidation of Fe^{2+} to Fe^{3+} .

Results of bacterial counts for T. ferrooxidans presented as the most probable number (MPN) of bacteria per gram of dry mass of tailings sample indicate a high population of T. ferrooxidans at 100,000 MPN/g at the 0.5 m depth in the south-end main tailings and decreases sharply to almost zero at 1.1 m. On the tailings dam, the T. ferrooxidans population ranges from near-zero at 0.4 m to a maximum of 63,000 MPN/g at 1.0 m, and then decreases to about 10,000 MPN/g at the 1.5 m depth. T. ferrooxidans are absent below the water table at both stations. These results indicate a strong presence of iron oxidizing bacteria T. ferrooxidans in the shallow unsaturated zone which correlates closely with the gaseous oxygen profile. The observed low populations of sulphate-reducing bacteria in the saturated zone may be due to the insufficiency of organic compounds required as energy source(s) for metabolism.

pH

The pH of the groundwater can influence the rate of both chemical and biological oxidation. The role of pH in the chemical oxidation process can be seen by considering the rate of oxidation of Fe^{2+} to Fe^{3+} . This reaction has been shown to be the rate-determining step in the pyrite oxidation process.

In general, the shallow oxidized zone of the Waite Amulet tailings is characterized by acidic pore waters with pH of less than 4. The pH increases to about 5.5 near the water table and to about 6.0 to 6.5 for the unaltered tailings at depth.

In the saturated zone, the pH increases to 6.0, suggesting buffering of acidic pore waters migrating from the unsaturated zone. The pH data suggest that further oxidization of the remaining sulphides in the deeper unsaturated zone will occur at a rate dependent on pH, as well as on oxygen concentration.

Carbon Dioxide Transport

The rate-determining step in the sulphide mineral oxidation is the oxidation of Fe^{2+} to form Fe^{3+} . This reaction is catalyzed by bacteria in the pH range of 3.5 and below. Thus, the oxidation rate depends on factors such as the availability of carbon dioxide, which controls the kinetics of bacterial growth. Carbon dioxide, CO_2 , is the main source of carbon used by I. ferrooxidans for growth.

Carbon dioxide concentrations in the unsaturated zone tailings at Waite Amulet are also presented. The observed levels ranged from 0.2 to 6.5 percent. In general, the CO_2 levels increased slightly to maximum levels at greater depths in the unsaturated zone, where the O_2 profiles terminate. This increase is presumably due to carbonate-consuming buffering reactions.

PORE WATER GEOCHEMISTRY

Unsaturated Zone

The entire unsaturated zone shows high Fe^{2+} concentrations (up to 10 g/L) generated by sulphide oxidation. Low pH conditions (pH 2.5 to 3.0) are, however, restricted to only shallow depths in the unsaturated zone, as a result of H^+ -consuming reactions occurring in the vadose zone. Redox potentials, E_h , generally show oxidizing conditions in the entire vadose zone, with values ranging from 200 to 700 mV. Sulphate levels are also high and like Fe^{2+} , are up to 10 g/L. The alkaline (Na, K) and alkaline earth (Ca, Mg) metal concentrations are low (less than 100 mg/L).

Saturation indices calculated for $\text{Fe}(\text{OH})_3$, goethite and lepidocrocite showed undersaturation of the pore water with respect to these ferric oxyhydroxide phases at shallow depths (0 to 50 cm from the tailings surface).

The undersaturation suggests re-dissolution of these oxyhydroxides previously deposited in the shallow unsaturated zone from sulphide oxidation. In the north-central portion of the tailings impoundment, saturation with respect to goethite and lepidocrocite occurs. In the shallow

unsaturated zone where sulphide is obliterated, goethite and lepidocrocite have been shown to co-exist as intimate mixtures that have replaced individual grains of pyrrhotite. Gypsum is the most abundant sulphate mineral in the tailings.

Heavy metal (Co, Mn, Cu, Ni, Pb, and Zn) profiles obtained for the unsaturated zone pore water show a concentration and mobility order similar to what has been observed at the Nordic Main pyritic uranium tailings near Elliot Lake, Ontario: $Fe = Mn \geq Zn > Ni > Co > Pb > Cu$.

These metals are released into the tailings pore water as a result of sulphide oxidation. Their subsequent mobility is apparently controlled by complex reactions such as precipitation-dissolution, solid-solution substitution, coprecipitation and adsorption-desorption.

Saturated Zone

Chemical data obtained on pore waters from the shallow saturated zone indicate pH values ranging from 4.5 to 6.0. Electrical conductivity is 2000 to 3000 $\mu\text{s}/\text{cm}$ in this zone but decreases to about 1000 $\mu\text{s}/\text{cm}$ at greater depths.

In the shallow saturated zone acidity ranges from 500 to 1800 mg/L CaCO_3 and then decreases rapidly to 70 mg/L at greater depths. Observed redox potentials, E_H , reach a maximum of 700 mV in the near-surface tailings in the unsaturated zone, and decrease to about 100 mV at greater depths.

In general, dissolved ferrous iron, Fe^{2+} , at shallow depths is high and reaches a maximum of 6000 mg/L and then decreases rapidly with depth. Sulphate concentrations decrease from about 13000 mg/L in the shallow saturated zone to about 2000 mg/L at greater depths. Concentrations of all other heavy metals (Cu, Pb, Zn, Cr, Ni, and Al), with the exception of manganese (Mn), are generally low (less than 0.05 mg/L) in the saturated zone. At one station, the manganese concentration in the shallow saturated zone pore water is about 70 mg/L and decreases to about 3 mg/L at greater depths. In the shallow saturated zone, observed sodium and potassium concentrations in the tailings pore water are much lower than those of calcium and magnesium. The higher calcium and magnesium levels are probably derived from dissolved carbonates from limestone added during the revegetation program. Sodium concentrations increase at greater depths which may reflect competitive ion exchange with calcium and magnesium (Barone and others, 1989).

Geochemical calculations carried out using the equilibrium metal speciation model MINTEQA2 indicated that the tailings pore water in the shallow unsaturated zone is saturated with gypsum ($\text{CaSO}_4 \cdot 2\text{H}_2\text{O}$) and supersaturated with respect to Na and K-jarosite ($\text{Na-KFe}_3(\text{SO}_4)_2(\text{OH})_6$), goethite and lepidocrocite ($\text{FeO} \cdot \text{OH}$). Also in this zone, saturation with respect to anglesite (PbSO_4) occurs.

HYDROGEOLOGY

Site Features

Bedrock topography, as defined by seismic geophysical work, indicates extremely variable bedrock topography, especially in the northern section of the tailings. The bedrock and clay which gently dips south and west with thicknesses ranging from 2 m to about 20 m thickness ranging from 2 m in the north to about 15 m in the south is a moderately fractured acidic volcanic rock (probably a granodiorite).

In the northern section, the water table is just below the tailings surface and decreases in elevation towards the south end, where it is about 5.5 m below the tailings surface. The highest water levels occur in the central portion of the site.

The tailings are much more fine-grained in the northern region than in the south. The data also indicate that the fine-grained tailings in the north consist of 17 to 22 percent clay and 10 percent silt size fractions. The coarse-grained south tailings show only 5 percent clay size and 1 to 3 percent silt size materials. Fine-grained tailings were also encountered across the site as distinct, thin, horizontal "slime" layers. These layers were probably produced by changes in the rate of spilling of the tailings, and on environmental conditions, such as wave action, at the time of deposition.

Unsaturated Zone Pore Water Flow

Pore water flow in the unsaturated (vadose) zone is mainly vertical, and its magnitude depends on the physical parameters of the tailings.

Measured values of field-saturated hydraulic conductivity in the vadose zone, K_s , were between 10^{-5} and 10^{-4} cm/s. An estimate of the downward pore water velocity in the unsaturated zone was calculated to be between 0.03 and 0.3 m/day.

Saturated Zone Pore Water Flow

Saturated zone pore water flow occurs from the middle of the tailings deposit towards the sides. Pore water velocities along two sections across the tailings dam were estimated using field measured hydraulic conductivities and water table profiles.

The horizontal gradient across the dam was observed to be about 0.05 (November 1988). Measured hydraulic conductivities were between 5×10^{-6} to 2×10^{-4} cm/s along the section. Using these values, pore water velocity was calculated to be in the range of 0.2 to 9.0 m/a. These velocities could likely increase to 35 m/a in the higher permeability, steeper sections of the dam.

Vertical gradients at most of the monitoring stations were downwards and ranged from 0.002 to 0.06. Because of the presence of the horizontal fine-grained slime lenses, it is believed that the tailings hydraulic conductivity is anisotropic, with horizontal hydraulic conductivity being greater than the vertical hydraulic conductivity. With the type of layering observed in the tailings core, an anisotropy factor of 10 to 100 may be expected. Vertical pore water velocities could range from 0.07 to 10 m/a. The degree of downward movement of the pore water will depend on several factors such as inflow quantities, thickness of the underlying clay layer, slope of the clay layer and proximity of the discharge ditch.

It was found that a high variability in clay hydraulic conductivity could influence the flow system in the tailings.

HYDROLOGY

Two monitoring stations were installed in July 1987. Station 1 was located on the top of the northern tailings section to monitor precipitation, evaporation and surface run-off quantity and quality. Station 2, located along the western seepage face, monitored seepage quantity and quality of the western half of the main tailings dam.

Monthly rainfall quantities ranged between 50 and 240 mm; daily values were between 1.5 and 7.6 mm. The evaporation rates varied between 1.8 and 3.8 mm per day.

Infiltration

The measured saturated hydraulic conductivity in the shallow unsaturated zone of 0.03 m/day would represent a minimal infiltration rate for water recharging into the unsaturated zone. This rate would exist, for example, during a long, intense recharge event. Theoretically, the infiltration rate could be higher than 0.03 m/day at the beginning of a recharge event.

Run-off

The dry conditions encountered in late spring and early summer caused the tailings water table level to fall, limiting the surface run-off on the top of the tailings to mean flows usually below 0.5 m³/h.

This suggests that the preceding rainfall events gradually raised the water table in the tailings until the tailings were saturated, a pond was formed on top of the tailings, and the overland ditch could immediately respond to a rainfall event. Therefore, the flow rate of this overland ditch is directly related to the assimilative storage capacity of the tailings.

The metal concentrations were usually less than 10 mg/L Fe, 3.5 mg/L Fe⁺², 1 mg/L Cu, 0.2 mg/L Pb, 5 mg/L Zn, 400 mg/L Ca, 150 mg/L Mg and 200 mg/L SO₄. The metal concentrations did not vary significantly between high and low flow conditions. This suggests that the flow at this location represents a very small fraction of the total metal loading to be treated at the lime neutralizing plant.

Samples collected in the ditch below the Station 1 flume at various occasions indicate an increase in metal concentrations. This is probably due to intermittent seepage coming out of the tailings.

Seepage

Seepage along the west dam of the Waite Amulet tailings resulted in base flows between 1.5 and 4.1 m³/h, for a mean of approximately 2.5 m³/h. These fluctuations are related to the water table levels in the tailings. The volume of water in addition to baseflow during rainfall events and the recorded rainfall accumulation suggest that drainage area of the seepage ditch is approximately 10,000 m².

The ion concentrations rarely exceeded 2.5 g/L Fe (1.3 g/L Fe⁺²) 2.5 mg/L for Cu, 0.6 mg/L for Pb, 8.0 mg/L for Zn, 500 mg/L for Ca, 800 mg/L for Mg and 7.5 g/L SO₄. The Fe total at low flow (<10 m³/h) ranged between 1.1 and 1.6 g/L. Also, about 60% of the Fe total was generally present as Fe²⁺ in the water samples collected in the seepage ditch.

Linear regression parameter values indicated a high correlation ($r^2 = 0.92$) between the overall Fe_T loading values and the corresponding flow, since the loading is a factor of the flow and the variations in metal concentrations are rather small (C.V. 20%).

Water balance evaluation

The water balance components on the Waite-Amulet tailings site were evaluated based on short-term field observations, data from the Quebec Ministry of the Environment, and empirical relations included in the HELP model. Estimations are the following: 100 cm of water falls annually as precipitation, 19 cm flows overland as run-off, 56 cm evapotranspires, and 24 cm infiltrates the tailings.

Flow modelling

It can be seen that, because of the tailings geometry and the effect of anisotropy in the hydraulic properties, flow in the tailings would be dominantly horizontal and shallow.

Average horizontal velocities calculated from the simulations were 7.5 m/a for Section A-A (north side) and 9.3 m/a for Section B-B (south side). Average downward velocities in the tailings were 0.45 m/a (Section A-A) and 0.49 m/a (Section B-B). The values obtained with the numerical model confirmed and refined previous estimates of pore water horizontal velocities which ranged from 0.2 to 9.0 m/a, with higher velocities of 35 m/a in the tailings dam.

Along the west side of the tailings, the surface ditch collects most of the water infiltrating the tailings; in the northwest section of the impoundment, the model showed that a portion of the pore water (approximately 10 %) could flow through the bottom of the tailings into the underlying geological units.

Pore Water evolution

The simulated flowlines suggest that flow occurring in the vicinity of the seepage ditch is horizontal. Acid water produced at the east and west boundaries of the impoundment will therefore move horizontally towards the seepage ditches. Acid waters generated in the central portion of the impoundment will most likely flow downwards and reach the tailings-clay interface, along which it will flow. A small amount of seepage will slowly infiltrate into the clay.

Reaction of ferrous iron with carbonates to form FeCO_3 will most likely occur in the deep central portion of the tailings deposit. The reaction will not take place within pore waters at the limits of the impoundment, along the tailings dam and benches mainly because (1) shorter travel paths to the drainage ditches allowed high-pH process waters to escape from the tailings and (2) shorter residence time in the tailings does not allow the precipitation reaction to occur.

Ferrous iron, still in solution when the seepage is released to the surface drainage system, is the main contributor to acidification; Fe^{2+} oxidizes to Fe^{3+} rapidly once oxygen becomes readily available, iron hydroxide forms and coats the bottom of the ditch with red sludge and releases acidity.

Iron precipitation does not take place within pore water originating from the edges of the impoundment. Hence, this area is currently the major contributor to acid loading. It is expected that, as time goes on, the pH at the bottom of the tailings will become more acidic and iron precipitation will cease. More acid loading to the collection ditches will then be produced at the centre of the impoundment. Ultimately, reduction of acid loading will occur once all the pyrite in the tailings unsaturated zone becomes oxidized and all acid pore water has drained out of the impoundment. Acid generation should first terminate in the northern section of the tailings, where the water table is high. In the southern section and along the tailings dam, acid generation should still continue for several hundred years due to the larger volume of unsaturated sulphide material.

CONCLUSIONS

The study of acid pore water generation and movement in the Waite Amulet tailings has demonstrated that:

- 1) The most important control on the pyrite oxidation process is the availability of oxygen. In addition to contributing directly to oxidation, oxygen influences the production of ferric iron and the density of bacterial populations.
- 2) Oxygen concentration distribution with depth in the tailings defines the depth of active oxidation. Oxygen movement within the tailings is controlled by diffusion.

- 3) Oxidation of sulphides in the deep unsaturated zone occurs at a rate dependent on pH, and will be very low. As sulphide in the shallow zone is depleted, the oxidation front will move downwards.
- 4) Acidic pore water is partly neutralized by buffering reactions occurring in the deeper unsaturated zone. The remaining acidity and dissolved metals will flow downwards with the pore water in the unsaturated zone until the water table is reached.
- 5) Acid conditions in the shallow saturated zone become more neutral with depth due to buffering reactions, such as mineral dissolution and precipitation of minerals.
- 6) Pore water in the saturated zone will flow in a direction which varies across the area of the tailings. Flow in the central part of the tailings will be vertical and downwards; flow along the perimeter of the tailings will be horizontal.
- 7) Anisotropy in the hydraulic properties of the tailings is a major control on the flow of pore water in the tailings. The anisotropy is produced by the presence of fine-grained, horizontal ("slime") layers. It has the effect of promoting horizontal flow over vertical downward flow.
- 8) Along the west side of the tailings, the surface ditch collects most of the water infiltrating the tailings; in the northwest section of the impoundment, a small portion of the pore water flows through the bottom of the tailings into the underlying geological units.
- 9) Acid water collected in surface ditches around the tailings impoundment is produced by seepage rather than run-off.
- 10) Analysis of pore water quality and calculation of groundwater velocity in the clay suggest that tailings pore water does not penetrate deep into the clay layer on the south side of the tailings. Sulphate levels above background values, observed in the deeper layer of the clay, may be attributed to migration by diffusion.

- 11) Acid generation will last longer along the tailings dam and in the south section of the impoundment. In these areas, coarser tailings grain sizes induce lower water table levels, and larger volumes of unsaturated tailings available for oxidation.

RECOMMENDATIONS

General recommendations should apply to present and future tailings impoundments:

- 1) Mineralogy and hydrogeochemical parameters, such as dissolved metal and major ion concentrations, should be determined at reactive tailings impoundments to provide information on AMD generation and loading.
- 2) Measurement of infiltration and hydraulic conductivity of tailings should be performed at reactive tailings impoundments to enable the characterization of tailings pore water flow systems.
- 3) Characterization of soil layers underneath reactive tailings impoundments should be performed routinely to evaluate the potential for downward migration of oxidation products.
- 4) High water tables should be promoted by selective placement of fine-grained tailings across the site. Coarse-grained material, such as rock fill, should be avoided in tailings dam construction, unless design features are incorporated to prevent water tables from dropping excessively.
- 5) Horizontal flow should be promoted by selective placement of horizontal fine-grained layers across the area of the tailings deposits. This could reduce downward vertical flow considerably, and facilitate the collection of AMD around the perimeter of the impoundments.

- 6) **A standardized method for computation of water balances in inactive tailings impoundments should be developed. This could be based on methods used in the present study, such as the Guelph permeameter, the SCS method, and/or the HELP model.**

Specific recommendations are made for the Waite-Amulet site, which might have later implications for other tailings sites:

- 1) **Small-scale monitoring of rainfall and pore water pressures in the Waite-Amulet tailings should be done during rainfall events to confirm the effect of the rapid rise of the water table in the tension-saturated zone and its effect on seepage water quality.**
- 2) **The long-term compatibility of Waite-Amulet clay with acid water solutions should be determined through laboratory-scale testing.**
- 3) **Data collected at the Waite-Amulet site should be used to model the long-term acid generation rates of the tailings.**
- 4) **Data from the Waite-Amulet site should be used as background to study the effect of remediation options such as natural soil barriers.**

1. INTRODUCTION

1.1 Background and Objectives

Canada's current inventory of sulphide tailings covers approximately 25,000 hectares. Current tailings management practices for decommissioning are revegetation and long-term treatment of the acidic seepage from the tailings area. In an effort to minimize perpetual maintenance of these sites, the Mine Environment Neutral Drainage (MEND)¹ program was initiated. The MEND program is jointly funded by the federal government, the provinces, and the mining industry. The objective is to develop an inventory of practical techniques to achieve sufficient reduction in the impact of acid-generating tailings and wasterock to permit ultimate abandonment without on-going treatment or maintenance.

The Waite Amulet project was initiated by Noranda with the overall objective of developing a better understanding of the hydrogeochemical processes controlling sulphide oxidation and subsequent pore water evolution in an acid-generating tailings area. This would lead to the development of closure technologies for improved long-term tailings management practices. The Waite Amulet project was approved by the MEND program and initiated in 1985 through a five-year \$500,000 joint funding by Noranda Inc. and CANMET.

Project reports which included results of each year's study were submitted to CANMET, along with recommendations, proposals and work plans for the subsequent year. The specific study objectives and work conducted during each year were as follows:

Phase 1 (1985) The first-year objective was to define the tailings hydrogeology, geochemistry and biochemistry.

Accordingly, a preliminary site reconnaissance and drilling program was completed. A geophysical investigation and drilling program were conducted to sample the tailings and underlying deposits for mineralogical and bacterial analyses. Piezometers were installed at

1. Formerly called RATS, Reactive Acid Tailings Stabilization Program.

depth to define the pore water chemistry in the tailings and underlying formation. The 1985 field program indicated that elevated pore water metal levels reached the water table, and that the unsaturated (vadose) zone should be investigated.

Phase 2 (1986)

The study objectives in the second year were to finalize the definition of tailings hydrogeology, evaluate the geochemistry of the unsaturated zone, and propose oxidation control measures.

Work conducted in this phase included installation of more piezometers to further define the site hydrogeochemistry. A study of the unsaturated zone pore water and mineralogy was also undertaken to determine the extent of oxidation and pore water evolution. The 1986 field program indicated the need to further examine the role of gaseous oxygen in controlling sulphide oxidation, and to develop a mass balance to define pore water evolution.

Phase 3 (1987)

The work plan in the third year of the project was to assess water and metal balance in the tailings, evaluate gaseous O₂ profiles in different areas of the tailings, and, in conjunction with CANMET and the University of Waterloo, relate the mineralogy of the tailings to the unsaturated pore water geochemistry.

The 1987 field program evaluated the O₂ profiles with depth in the tailings. Piezometers were sampled to determine the pore water chemistry. Tailings moisture contents and grain size distributions were also obtained. Results of work conducted in Phases 1 to 3 showed that infiltration, acidification, flow and release of acidic pore waters occur along sections of the tailings dam face. It was therefore decided that an adequate understanding of acid generation, pore water evolution and metal transport would require a detailed study of the west tailings dam.

Phase 4 (1988)

The intent of the Phase 4 program was to develop a realistic metal and water balance and evaluate pore water evolution, and transport mechanisms along the west seepage face using a numerical flow model.

In accordance with these objectives, the 1988 field program included flow monitoring to provide information on metal loadings from overland and baseflow conditions. Piezometers were installed to obtain complete data along two sections on the western face. Steady state flow modelling was then conducted to determine pore water transport in the tailings.

1.2 Scope

The current document presents the overall hydrogeochemistry of the Waite Amulet tailings site through discussions of the processes governing the generation and evolution of acidic pore waters. The theory of acid generation is briefly reviewed. Data on the extent of oxidation are presented along with the geochemistry of the unsaturated and saturated zones pore waters. The site hydrology and hydrogeology are presented to show the direction and rates of movement of pore water in the tailings and seepage into surface ditches.

The document integrates studies conducted by the Noranda Technology Centre, the University of Waterloo and CANMET. Noranda Inc. funded a study of the unsaturated zone geochemistry by Mr. Dave Blowes, Ph.D. student at the University of Waterloo. Dr. John Jambor of CANMET conducted mineralogical studies on the unsaturated zone tailings. All saturated zone and surface hydrology work was conducted by the Noranda Technology Centre. A summary of recent work on Waite Amulet is given in St-Arnaud et al (1989).

1.3 Site Location

The Waite Amulet tailings area is situated approximately 20 km north of Noranda, Quebec, as shown in Figure 1.1. The tailings area lies in low marshland surrounded by a few steep hills. The hills are typical of the regional topography controlled by the bedrock of volcanic origin. The main nearby water body is Lake Dufault to the east of the site. Drainage from the site is treated and discharged into Duprat Creek, which flows eastward and reports to Lake Dufault.

2. SITE HISTORY

2.1 Mining Activity

The mining of the Amulet ore began in August 1928, with the ore averaging 8.1% Cu, 4.9% Zn, and 2 oz/ton Ag. The ore was shipped to the Noranda Horne smelter operations (Siwik, 1986) until 1929 when the 272 tonnes/day Amulet mill was constructed. In 1933, the Waite-Ackerman-Montgomery and Amulet shares were incorporated into Waite Amulet Mines Ltd. With the war demand for zinc, a new 1088 tonnes/day mill went into production to treat 816 tonnes/day of Cu-Zn ore from the Amulet Dufault and 272 tonnes/day from the Waite ore bodies. A 300 tonnes/day mill extension went into operation in 1943. The mill then treated 907 tonnes/day of Lower "A" ore, 408 tonnes/day of Waite ore, and 317 tonnes/day from the Amulet "C" ore body. The original Waite mine closed in 1948. The Amulet "C" ore body was exhausted in 1951.

The mill capacity was increased in 1955 to treat 907 tonnes/day of West MacDonald ore. Waite Amulet production was reduced to 907 tonnes/day. A pyrite flotation circuit was installed to produce a pyrite concentrate. An aerial tramway was used to transport the West MacDonald ore situated on the east side of Lake Dufault, to the Waite Amulet mill. The West MacDonald operation ceased in 1958. The only remaining ore body, the Amulet Dufault Lower "A", was exhausted in October 1962.

In total, ten ore bodies were milled and the tailings disposed of in the Waite Amulet mill tailings area. Approximately 8.74 million tonnes were milled from the nine Waite Amulet and Amulet Dufault ore bodies, of which 2.65 million came from the Waite-Ackerman-Montgomery property, 1.17 million from the Amulet, and 4.63 million from the Lower "A" Amulet ore bodies. The West MacDonald ore body contributed approximately 0.81 million tonnes.

2.2 Mineral Processing

The 1814 tonnes/day mill treated 91 tonnes/day of West MacDonald ore and 907 tonnes/day of Waite Amulet and Amulet Dufault ores. The Waite ores were approximately 60% sulphides (chalcopyrite, marmatite, pyrite and pyrrhotite), and the West MacDonald ore consisted of 95%

sulphides (mainly pyrite and marmatite with minor amounts of chalcopyrite, pyrrhotite and galena). The Waite gangue consisted of diabase and feldspar porphyry. Gangue from the West MacDonald ore consisted of lamprophyre and rhyolite.

The Waite Amulet mill flowsheet is illustrated in Figure 1.2. The Waite Amulet and West MacDonald grades and reagent consumption are detailed in Table 1.1

2.3 Tailings Disposal

There are no records regarding the placement and operation of the 41 hectare main tailings dam. The tailings were gravity fed from the mill via a wood stave pipeline and trestle. The method of tailings dam construction may have been with original waste rock starter dams with subsequent lift construction using coarser spigotted tailings. The tailings were end-spilled during winter operation in the central north and south sections.

The area between the concentrator and main tailings dam contains varying depths of tailings (1 to 2 m). Placement details are not known, but in the early 1920-1930's, tailings were probably disposed of in this lower region. Later, spills from the wood stave pipeline probably contributed.

Tailings disposal ceased in 1962. Approximately 5.9 million tonnes of reactive sulphide tailings now occupy the elevated 41 hectare dam. Some tailings were spilled in adjacent lower areas.

2.4 Tailings Reclamation

The majority of the main sulphide tailings dam was revegetated in 1978 and 1979. The tailings surface was neutralized with 44 tonnes/hectare of agricultural limestone. Up to 5.5 tonnes per ha of fertilizer was used because these tailings were devoid of any nutrients. Birdsfoot trefoil and a companion crop of creeping red fescue were planted.

TABLE 1.1

WAITE AMULET AND WEST MACDONALD METALLURGY AND REAGENTS (1956)

<u>METALLURGY</u>					
	Cu %	Zn %	S %	Au oz/ton	Ag oz/ton
Waite Amulet ore	3.89	3.95	18.91	0.041	8.93
Recoveries (%)	94.49			65.41	65.33
West Macdonald ore	0.13	2.41	46.47	0.027	0.82
Recoveries (%)	7.62			7.53	6.47
Combined zinc recovery (%)		85.6			
Pyrite recovery (%)			83.2		
Pyrite tailings	0.16	0.26	12.82		
<u>REAGENTS</u>					
	Waite Amulet Cu Flotation	West Macdonald Cu-Ag-Au Flotation	Zinc Flotation	Pyrite Flotation	
Sodium sulphide (lb/ton)	1.086	0.302			
NaCN	0.028	0.007	1.870		
Soda Ash	2.336	1.650			
Aerofloat 242	0.066	0.013			
Z-5	0.074				
Frother 73	0.073	0.012	0.065	0.017	
Aerofloat 208		0.005	0.093		
Ca(OH) ₂			0.329		
CuSO ₄			1.437		
(NH ₄) ₂ SO ₄			0.185		
Aerofloat 343					0.162

Monitoring of drainage water from the tailings after revegetation showed no improvement in water quality (Veldhuizen et al, 1987). Since 1984, the seepage and surface run-off from the site has been collected in surface ditches along the periphery of the site. The acid water is collected in a reservoir and treated in an automated computer-controlled water treatment plant. Details of water treatment methods are given in Appendix A.

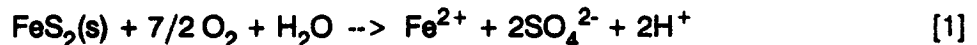
3. THEORY OF ACID GENERATION

3.1 Oxidation Processes

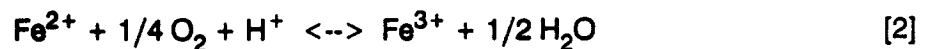
Sulphide oxidation in reactive tailings affects other geochemical processes, such as acidification, and the subsequent dissolution of other tailings constituents, including metals (Stumm and Morgan, 1981). The oxidation process, in the absence of appreciable buffer materials, releases acidity and metals into waters draining from tailings impoundments. An understanding of the sulphide oxidation process and the controlling mechanisms is therefore a key requirement for developing measures to prevent the formation of acid waters or to minimize their adverse environmental impact.

The two sulphides of primary concern in reactive tailings are pyrite (FeS_2) and pyrrhotite (Fe_{1-x}S , where x values are between 0 and 0.2, Hurlbut and Klein, 1977). Since the chemical compositions of these minerals are similar, oxidation and the resulting acidification processes are also similar for both minerals. Pyrite is the dominant mineral and is used as the example in the chemical reactions presented in this section.

The oxidation of pyrite in the presence of oxygen and water can be represented by the following equation:

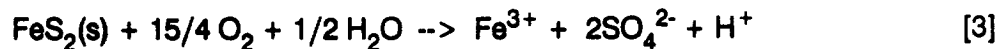


The dissolved Fe^{2+} , SO_4^{2-} , and H^+ represent an increase in total dissolved solids and acidity of the water. For a low-pH system (i.e. pH 1.5 to 3.5) in which oxygen is readily available, subsequent oxidation of ferrous iron, Fe^{2+} , will occur, producing ferric iron, Fe^{3+} , as follows:

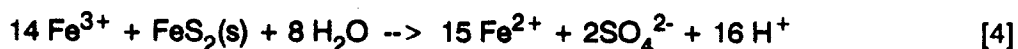


Ferrous oxidation to ferric iron in the pH range 1.5 to 3.5, Equation [2], is sometimes catalyzed by the iron bacteria, Thiobacillus ferrooxidans.

The reactions in Equations (1) and (2) can be combined to yield:

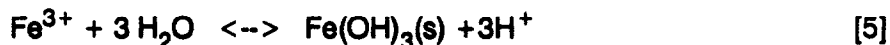


The reaction in Equation (3) indicates that, during pyrite oxidation, both the Fe^{2+} and S_2^{2-} of $\text{FeS}_2(\text{s})$ can oxidize, resulting in the formation of two moles of SO_4^{2-} and one mole of H^+ for each mole of FeS_2 oxidized. Ferric iron, Fe^{3+} , released as in either Equation (2) or Equation (3), will further oxidize pyrite, thereby generating additional dissolved ferrous iron and acidity, as shown by the following equation:



In comparison with Equation [1], Equation [4] shows that 16 moles of H^+ are generated for every mole of pyrite oxidized. Thus Equation [4] underscores the important role played by the presence of dissolved ferric iron in the whole oxidation process and subsequent generation of acidity.

At slightly higher pH values (say 4 or greater), hydrolysis of Fe^{3+} will occur, resulting in the precipitation of ferric hydroxide and further generation of acidity as indicated by



The hydrolysis reaction, Equation [5], is reversible and indicates that $\text{Fe}(\text{OH})_3(\text{s})$ is more stable at higher pH values or decreasing concentrations of H^+ . When the pH decreases, $\text{Fe}(\text{OH})_3(\text{s})$ becomes more soluble and Fe^{3+} more stable. Under these conditions, reaction (5) does not contribute significantly to acidification. Any Fe^{3+} from reaction [2] that does not precipitate from solution through reaction [5] may be used to oxidize additional pyrite, as in reaction [4].

The overall process of pyrite oxidation can be represented by combining Equations [3] and [5] to give the following:



3.2 Factors Controlling Oxidation

The most important controls on the pyrite oxidation process appear to be oxygen, water and ferric iron (Stumm and Morgan, 1981). However, Equations [1] and [2] indicate that if oxygen is not available, Fe^{3+} will not be generated and the oxidation process will not occur. Thus, the role of Fe^{3+} is intermediate. Oxygen availability and transport is therefore the most important consideration in any reactive tailings management strategy. In addition to oxygen and water, other factors found to influence the oxidation of pyrite include sulphide content and morphology, ferric iron concentration and bacterial population density (Siwik et al, 1987). Bacteria play a major role, in some cases, in accelerating the rate of acid generation.

3.2.1 Oxygen Transport

The importance of oxygen in the reactive sulphide oxidation process lies in the fact that its presence, as illustrated in Equations [1] and [3], is critical to the formation of Fe^{2+} and Fe^{3+} . The primary role of oxygen is in the control of the inorganic chemical oxidation process. The limiting concentration in the bacterial oxidation process has been reported to be 5% of the water saturation levels (Myerson, 1981). Below this level, the rate of oxidation has been shown by Stumm and Lee (1961) and Nicholson (1984) to be related to oxygen concentration by the relation:

$$-dN/dt = \theta KC \exp(-E_a/RT)/(1 + KC) \quad [7]$$

where C is the oxygen concentration, K the oxygen-adsorption constant for pyrite, T the absolute temperature, E_a the activation energy, R the gas constant, and θ a constant dependent on the surface area of pyrite and the ratio of stoichiometric coefficients relating FeS_2 and O_2 in equation [6], Section 3.1.

Sulphide oxidation in reactive tailings is eventually limited to the vadose zone because oxygen transport in the saturated zone is restricted. The rate at which oxygen enters the tailings surface controls the maximum rate of oxidation and hence the rate of acid generation.

3.2.2 Temperature

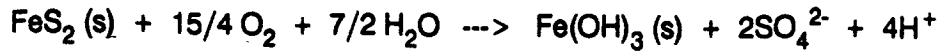
The rates of both chemical and biological oxidation of pyrite are affected by temperature. Kinetic studies by Nicholson (1984) suggest that the temperature dependence on the oxidation rate follows the Arrhenius equation:

$$K_c = A \exp (-E_a/RT) \quad [8]$$

where K_c is the rate constant, A the pre-exponential factor, E_a the activation energy, R the universal gas constant and T the absolute temperature. From least square fit of experimental data, Nicholson (1984) calculated an activation energy, E_a , of 88 kJ mol^{-1} which implies that the rate of oxidation approximately triples for a 10°C rise in temperature. Activation energies reported for a variety of experimental conditions by Lawson (1982) range from 39 to 88 kJ mol^{-1} . In the lower range, the temperature dependence on the rate of oxidation may be slower than predicted by Nicholson (1984). For example, Nordstrom (1982) has indicated that the rate will double for every 10°C rise in temperature.

The influence of temperature on biological ferrous iron oxidation by Thiobacillus ferrooxidans is similar to that of chemical oxidation. In the temperature range of 3 to 24°C , the biological rate is approximately doubled for every 10°C rise in temperature (Knapp, 1987). A few investigators (Razzell and Trussell, 1963; Torma et al, 1970) have reported the optimum temperature for biological oxidation to be in the range of 30 to 35°C . Below 30°C and above approximately 35°C , the rate of biological oxidation decreases.

Temperature profiles in tailings deposits can give an indication of the zone of active oxidation. Daniel et al (1980) and Harries and Ritchie (1981, 1985) used temperature profiles to identify oxidation sites in waste rock dumps at the Rum Jungle mine in the Northern Territory of Australia. Unlike acidity and drainage metal concentration, temperature provides a very good indication of the location of oxidation sites in tailings and/or rate of oxidation. Pyrite oxidation is an exothermic reaction, that is, it releases heat (Harries and Ritchie, 1981). To illustrate this, the standard enthalpy change of the overall oxidation (Equation [6], Section 3.1) can be calculated as follows:



$$\text{Enthalpy change of reaction, } H_R^\circ = H_f^\circ \text{ products} - H_f^\circ \text{ reactants} \quad [9]$$

Using thermodynamic data (at 25°C and one atmosphere) from IUPAC (1985),

$$\begin{aligned} H_R^\circ &= -823.0 + 2(-909.27) + 2(0) - (-178.2) - 15/4 (0) - 7/2 (-285.83) \\ &= -823.0 - 1818.54 + 178.2 + 1000.41 \\ &= -1462.93 \text{ kJ mol}^{-1} \end{aligned}$$

Thus, when pyrite is oxidized, as in the above reaction, approximately 390 kJ of heat is evolved for each mole of oxygen used.

3.2.3 Sulphide Content, Morphology, and Surface Area

Pyrite can vary significantly in grain size and morphology. The most reactive form appears to be framboidal pyrite which is fine-grained and consists of crystals less than 1 μm in size. This reactivity is due to the large surface area provided by the fine granularity. Framboidal pyrite has been found to be more reactive than the euhedral form (Geidel and Caruccio, 1977; Caruccio et al, 1977). In another study (Pugh, 1979), the following order of increasing reactivity was reported: massive pyrite < framboidal pyrite < museum pyrite < marcasite, for bacterially assisted oxidation of material crushed or sieved to a common grain size. The high reaction rate for the museum grade pyrite was attributed to the production of fresh surfaces during crushing.

The influence of the surface area of pyrite on the rate of oxidation has received very little attention. A few studies reported in the literature (Stenhouse and Armstrong, 1952; Warren, 1956; Cornelius and Woodcock, 1958) appears to suggest that the rate is linearly related to the surface area.

Reported oxidation rate-surface area relationships generally take the following forms (Lowson, 1982):

- i) rate $\propto 1/d^2$, d = average particle diameter [10]
- ii) rate $\propto A$
- iii) rate $\propto A^n$, A = surface area, n = a roughness factor for coarser particle sizes

Thus, the characteristics of the pyrite present in the tailings, as well as the quantity, are factors influencing the prediction of potential acidity problems. Pyrrhotite activity is likely to vary in a similar manner.

3.2.4 Bacterial Activity

Pyrite oxidation via inorganic pathways occurs slowly under normal conditions. However, certain iron oxidizing bacteria, especially the genus T. ferrooxidans, have been known to catalyze the oxidation reactions involved in acid generation (Kleinmann et al, 1981; Caruccio and Geidel, 1987; Walsh and Mitchell, 1972; and Nordstrom, 1982). For example, the oxidation rate in the presence of T. ferrooxidans has been observed to increase by five to six orders of magnitude (Lacey and Lawson, 1970; Singer and Stumm, 1970), especially at shallow depths where oxygen is readily available. The major role of these bacteria in the oxidation process is to catalyze the oxidation of Fe^{2+} to Fe^{3+} (Equation [2]). They also appear to catalyze the oxidation directly on the pyrite surface.

Thiobacillus ferrooxidans is an obligate, chemoautotrophic, acidophilic bacterium which exhibits optimum activity at pH values in the range of 1.5 to 3.5 (Torma et al, 1970; Nicholson et al, 1989). It can tolerate high metal concentrations and thrives on inorganic compounds such as ferrous iron, reduced sulphur compounds, carbon dioxide, oxygen, and ammonium sulphate (Torma et al, 1970). The optimum temperature range reported for T. ferrooxidans activity is 28 to 40°C (Silverman and Lundgren, 1959; Torma et al, 1970).

Another genus of bacteria which has been implicated in the oxidation of pyrite and, hence, acid generation processes is Metallogenium. It has been suggested that this bacterium, which is acid-tolerant and iron-oxidizing, optimally oxidizes iron between pH values of 3.5 and 5. Once Metallogenium brings the pH to 3.5 then T. ferrooxidans takes over and reduces the pH to below 3.5 (Walsh and Mitchell, 1972). Other heterotrophs and autotrophs which normally occur in soil horizons may also play a role in the oxidation process (Nordstrom, 1982).

Regardless of the genus of bacteria and the mechanism, catalysis appears to be the key role played by bacteria in pyrite oxidation and acid generation.

3.2.5 pH

The pH of the groundwater can influence the rate of both chemical and biological oxidation. The pH plays a role in biological oxidation in that it determines the activity of the various catalyzing bacteria. In the absence of calcareous (buffering) materials, the pH of the ground water could be less than 5.5 and enhance the survival and growth of T. ferrooxidans (Geidel and Carruccio, 1977). This will lead to increased oxidation and hence acid production. The role of pH in the chemical oxidation process can be seen by considering the rate of oxidation of Fe^{2+} to Fe^{3+} . This reaction has been shown to be the rate-determining step in the pyrite oxidation process (Stumm and Lee, 1961). At pH values greater than 4.5, the rate law is given by:

$$-d[\text{Fe}^{2+}]/dt = K [\text{Fe}^{2+}][\text{OH}^-]^2 \text{PO}_2 \quad [11]$$

where K is a reaction constant, values of which are given by Stumm and Lee (1961), and PO_2 is the partial pressure of oxygen. As more H^+ ions are produced, the hydroxide ion concentration, $[\text{OH}^-]$, is decreased by reaction with $[\text{H}^+]$ to form H_2O . Thus, the chemical oxidation rate decreases with decreasing pH. At pH values below 3.5, oxidation proceeds at a rate independent of pH and the resulting rate law (Stumm and Lee, 1961) is:

$$-d[\text{Fe}^{2+}]/dt = K' [\text{Fe}^{2+}] \text{PO}_2 \quad [12]$$

where, again, K' is a reaction constant.

At pH values below 5.5, the solubility of iron is increased and in accordance with Equation [4], production of acidity increases which, in turn, puts more iron in solution and releases another 16 moles of H^+ . Thus, the mechanism becomes self-propagating (Geidel and Caruccio, 1977).

Laboratory studies (Smith and Shumate, 1970) suggest that the rate of chemical oxidation of pyrite in water at 25°C and an oxygen partial pressure of 0.1 MPa increases non-linearly as the pH is raised from 1 to 10. Studies on the effect of pH on the rate of bacterial oxidation by T. ferrooxidans indicated a maximum rate of oxidation over a pH range of 3.0 to 3.5, while other work suggests that the maximum activity falls in the range between 2.5 and 4.0 (Silverman and Lundgren, 1959; Landesman et al, 1966; Torma, 1970).

3.2.6 Carbon Dioxide Transport

As noted earlier, the rate-determining step in the sulphide mineral oxidation is the oxidation of Fe^{2+} to form Fe^{3+} . This reaction is catalyzed by bacteria in the pH range of 3.5 and below. Thus, the oxidation rate depends on factors such as the availability of carbon dioxide, which controls the kinetics of bacterial growth (Nordstrom, 1982; Knapp, 1987). Carbon dioxide, CO_2 , is the main source of carbon used by T. ferrooxidans for growth. The presence of a calcareous component in the tailings (or waste rock) should provide an ample supply of CO_2 for bacterial growth (Harries and Ritchie, 1983). Bacterial activity can be increased by raising the carbon dioxide content in the gas phase. Research has shown that a CO_2 level of 0.22 percent is optimal (Torma et al, 1972). High concentrations of CO_2 have been observed by Blowes et al (1987) in the Elliot Lake tailings, as a result of degassing of CO_2 formed during neutralization of acid water by tailings carbonate materials.

The carbon dioxide requirements in the unsaturated zone may also be met by periodic infiltration of rain water into the tailings (Tuovinen and Kelly, 1972). This will slow down the neutralization process and increase the rate of acidification.

3.2.7 Nutrients

Nutrient availability appears to be an important factor in the rate of oxidation of pyrite since it can influence the growth kinetics of T. ferrooxidans. However, nutrient requirements (such as nitrogen, phosphorous and potassium) are not limiting to the growth of T. ferrooxidans because very small concentrations are quite sufficient for growth (Nordstrom, 1982). T. ferrooxidans can grow in the absence of any added nitrogen compound which suggests that it may fix atmospheric nitrogen (Tuovinen and Kelly, 1972; MacKintosh, 1978). Experimental study (Torma et al, 1970) has shown that phosphorous increases the activity of T. ferrooxidans and hence leaching of zinc sulphide. The growth of T. ferrooxidans depends also on ferrous iron concentration in the environment. For example, laboratory study showed that 9,000 mg/L of ferrous iron was optimal in yielding the highest number of cells. Growth of the organism, however, ceased when all the ferrous iron was oxidized (Silverman and Lundgren, 1959).

4. ACID GENERATION AT WAITE AMULET

4.1 Sampling Locations

To characterize acid generation at the Waite Amulet tailings, pore water, solid and gas samples were taken at different locations on the impoundment. Samples were taken at different depths at each station using methods described in Appendix B. Figure 4.1 shows locations of stations used in the following discussions.

4.2 Oxygen Distribution

Gaseous oxygen profiles at Stations WA-11 and WA-17 (Figure 4.2a), obtained by Blowes and Jambor (1989) for the main tailings area suggest oxygen consumption in the top 0.5 to 0.7 m in the unsaturated zone. Results of field investigations on pyritic uranium tailings indicate that oxygen concentrations in partially gas-filled pore spaces in the tailings decrease rapidly below the tailings surface (Feenstra et al, 1981; Dubrovsky et al, 1985).

The depth of penetration of oxygen defines the zone of active oxidation in tailings. Thus at Stations WA-11 and WA-17, where the thickness of tailings has been observed to be about 10 to 12 m, the oxygen profiles suggest that the zone of active oxidation is confined to the shallow depths (less than 0.7 m) below the tailings surface.

Oxygen movement through porous media has been shown to be dominated by diffusion through partially gas-filled pores (Kimball and Lemon, 1971). Harries and Ritchie (1981) concluded from oxidation rate measurements in waste rock that diffusion is the main mechanism of oxygen transport through the pore spaces of the dumps. A series of mathematical models has been developed to characterize the pyrite oxidation process (Davis and Ritchie, 1986, 1987). The approximate analytical solution developed by Davis and Ritchie (1986) assumes that the supply of oxygen to the oxidizing particles occurs by diffusion through the pore space and into the tailings particles to a moving reaction front. Using this solution, Blowes and Jambor (1989) calculated oxygen concentration profiles at Stations WA-17 and WA-18 of the Waite Amulet tailings which agree reasonably with their measured profiles. From the measured and calculated best-fit profiles, they estimated effective oxygen diffusion

coefficients in the range of 3.0 to $4.2 \times 10^{-7} \text{ m}^2/\text{s}$. From these diffusion coefficients, Blowes and Jambor (1989) also estimated that sulphide oxidation in the vadose zone will continue for the next 600 years.

Figure 4.2b shows oxygen profiles obtained in 1987 (Siwik et al, 1988). The profiles are similar to those obtained by Blowes and Jambor, and confirm that gaseous oxygen is present at only shallow depths in the tailings.

4.3 Temperature Profiles

It has been noted that since tailings have a low thermal conductivity, the heat released in the oxidation process should result in a temperature rise in the region of the oxidation site (Harris and Ritchie, 1981). This suggests that temperature profiles in tailings undergoing pyritic oxidation may be useful in delineating the zone of active oxidation and probably provide an indication of the rate of oxidation in the zone.

Figures 4.3 and 4.4 show temperature fluctuations in the Waite Amulet tailings at 15 and 45 cm depths (at approximately 100 m north of WA-21) and in the air (at Station 2) during selected periods in August and November, 1988. The temperatures were obtained from thermocouples installed at the site using the method of installation and measurement detailed in Appendix B. As illustrated, daily fluctuations in the air temperature induce similar but smaller fluctuations in temperatures at the shallower depth with a certain time delay; the temperature at 45 cm depth is nearly constant.

The August graphs show that, for maximum day and minimum night temperatures of 34 and 3°C respectively, the tailings temperature at the two depths varies only slightly from 16 to 19°C . These hot day temperatures followed by those of cool nights are probably responsible for the almost homogenous temperature of the tailings profile. A typical summer temperature profile would show a colder temperature in the deepest section of the tailings than near the surface.

The graph for November (Figure 4.4) show a temperature difference of 1.5°C between the shallower depth and the 45 cm depth. The temperature at 45 cm is higher than at 15 cm from the surface. This is typical of fall conditions when tailings progressively freeze at depth. During the 5th and 6th, the air temperature increased from 1°C to 8°C , resulting in corresponding

increases in the tailings temperature at the 15 cm depth. The temperature at the 45 cm depth, however, decreased slightly. This unusual observation may be explained by snow which melted as a result of the temperature increase, bringing to the unsaturated zone an input of cold water. From 4th to 10th November, temperature variations were observed at the 15 cm depth, the air temperature being above 0°C for most of the period. After the 14th, when the air temperature was below 0°C; only a slight increase in tailings temperature occurred.

Temperature profiles in the tailings at four different locations, WA-2, WA-20, WA-21 and WA-22, are presented in Figures 4.5 to 4.8 along with corresponding air temperatures. These data were obtained during 9 to 26 August 1988. For each station, two sets of data are presented: a) mean temperatures during the period of 9 to 16 August 1988 and the corresponding 95% confidence limits, and b) mean temperatures during 17 to 18 August and 26 August 1988 when the surface or air temperatures were lower than those observed during 9 to 16 August 1988.

As shown from the 95% confidence limits for all the stations, greater deviations from the mean occur in the near-surface (top 0.35 m depth), indicating the influence of the surface temperature on the tailings temperature. This influence is better illustrated by the profiles which compare the temperature data observed during the 9 to 16, 17 to 18, and 26 August 1988 (Figures 4.5, 4.6, 4.7 and 4.8). As shown, during 17 to 18 August 1988, when surface temperatures decreased the tailings temperature also decreased with the near-surface tailings showing the greater response. The drop in the air temperature observed on 17 to 18 August reflects the diurnal variations.

The oxygen and bacteria profiles discussed in the preceding sections suggest that at the Waite Amulet tailings site, the zone of active oxidation is located in the shallow tailings (0.5 to 0.7 m from surface). Therefore, surface or air temperature has a much greater influence on the near-surface tailings temperature than the oxidation reaction. This is confirmed by the temperature profile presented in Figures 4.5 to 4.8. The results, however, do suggest that very high summer surface or air temperatures could have a major influence on oxidation reactions in the shallow tailings zone through an increase in the level of bacteria activity. It appears that the surface temperature has completely masked any possible increases in temperature that could result from pyritic oxidation. For the same reason, the observed temperatures may not give any indication of the bacteria activity. Therefore, the data cannot be used to calculate heat production in the tailings, as was done for the waste rock dump at Rum Jungle by Harries and Ritchie (1981).

4.4 Sulphide Content

Figures 4.9 and 4.10 show profiles of tailings sulphide content and alteration products at Station WA-20, located on the bench along the western side of the dam (Petruk and Pinard 1986). Separate profiles are presented for the coarse ($>37\ \mu\text{m}$) and fine ($<37\ \mu\text{m}$) fractions. The data are based on quantitative energy dispersive X-ray analysis and image analysis of screened polished sections of tailings samples. The profiles indicate that the main sulphide minerals are pyrite and pyrrhotite. Minor sulphides were reported to be sphalerite and chalcopyrite. Sulphides are consumed in the shallow unsaturated zone by oxidation. As shown in Figures 4.9 and 4.10, the pyrite content ranges from 0.5% at 0.25 m depth to about 30% at the water table.

In the saturated zone, pyrite reaches 60% of the $>37\ \mu\text{m}$ fraction (Figure 4.10). Pyrrhotite, on the other hand, is absent in the top 0 to 0.75 m and does not exceed 18% of the $>37\ \mu\text{m}$ fraction in both the unsaturated and saturated zones. The alteration products (silicates and magnetite) are abundant in the zone of oxidation. The amount of goethite remains essentially constant in the entire profile, except for the slight increase at the 0.3 m depth. The near-surface sample from the 0.3 m depth has a high goethite content in both the $>37\ \mu\text{m}$ and $<37\ \mu\text{m}$ fractions but essentially very little pyrite and pyrrhotite.

The observed silicate minerals included quartz, orthoclase, amphibole and/or pyroxene, chlorite and a minor amount of mica (Petruk and Pinard, 1986). In addition to the main oxides magnetite (Fe_3O_4) and goethite ($\text{FeO}\cdot\text{OH}$), minor amounts of cassiterite were also observed in the sulphide alteration products. The dominant sulphates were found to be of the form FeSO_4 ; only small amounts of jarosite were reported in samples at the 0.3 and 1.8 m depths. The $<37\ \mu\text{m}$ fraction of the tailings (Figure 4.9) show the same trends as noted above for the coarse fraction ($>37\ \mu\text{m}$).

As noted earlier, an indicator of sulphide oxidation reactions in the Waite Amulet tailings is the abrupt decline in the gaseous O_2 concentration in the near surface zone. Another indicator is the depletion of sulphide minerals (for example, pyrrhotite) in the top 0.6 to 0.7 m of the tailings

at Station WA-20, as shown in Figures 4.9 and 4.10. A detailed investigation of the mineralogical character of the sulphide alteration products using the coarser ($>37\ \mu\text{m}$) fractions of the tailings was also conducted. Three general zones of alteration were identified:

- i) a strongly oxidized near-surface zone depleted in sulphides;
- ii) an intermediate zone in which pyrrhotite (the sulphide most susceptible to oxidation) has been extensively altered but not obliterated;
- iii) a bottom zone of weak alteration in which pyrrhotite is largely preserved but has variable alteration rims (from narrow to incomplete to absent).

A classification scheme using a relative scale of 0 to 10 was assigned to characterize the degree of alteration of the Waite Amulet tailings. A sulphide alteration index (S.A.I.) of 10 denotes complete obliteration of pyrrhotite and pyrite with only traces of minor sulphides, such as chalcopyrite, present. An S.A.I. value in the range of 0 to 1 indicates a limited alteration of pyrrhotite grains along rims and fractures with at least 95% of the grains possessing sharp, fresh margins. A detailed definition of the sulphide alteration index is presented elsewhere (Jambor, 1987).

Figure 4.11 presents S.A.I. values for tailings cores obtained at Stations WA-2 in the northern section of the tailings. The intensity of sulphide oxidation shows a decrease with increasing depth at both locations and corresponds closely to the abrupt decline in the gaseous oxygen concentration. Similar trends have been observed at other locations in the tailings pile (Jambor, 1987). The principal alteration products identified in the unsaturated zone were iron oxyhydroxides (goethite, lepidocrocite and ferrihydrite) and sulphates (jarosite and gypsum). Figures 4.11 and 4.12 also show the sulphate (soluble and insoluble), soluble iron, and elemental sulphur contents of the tailings at Stations WA-2 and WA-11. The jarosite content was obtained as the difference between the total sulphate and water-soluble sulphate. At Station WA-2, calculated CaSO_4 shows a value of 2.4 wt. % near the top of the tailings and decreases to about 1 wt. % at the water table. A further decrease occurs below the water table, although the slight increase from 0.15 to 0.5 wt. % at the 0.8 m depth suggests movement from the oxidized zone. The Ca in the near-surface tailings is derived from lime added during revegetation.

The water-soluble Fe content of the tailings occurs at about 0.05 to 0.14 wt. % above the water table, at 0.1 wt. % in the saturated zone, and then decreases to about 0.02 wt. % at the 1 m depth. This trend suggests a depletion in the strongly oxidized saturated zone and accumulation in the saturated zone. The jarosite content decreases steadily from 2.4 wt. % at near-surface to about 1.7 wt. % at the 0.75 m depth in the saturated zone. The shape of the jarosite profile at WA-2 suggests that fluctuations in the water table elevation might have occurred. A lowering of the water table to the 0.8 m depth would better explain the CaSO_4 and water-soluble Fe profiles. It would appear that CaSO_4 and soluble Fe produced in the upper strongly oxidized zone have moved downwards and accumulated in the intermediate moderately oxidized zone.

Sulphide alteration indices (S.A.I.) obtained for the fine-grained tailings profile at Station WA-11 are presented in Figure 4.12, along with profiles for sulphate (soluble and insoluble), water-soluble Fe and elemental sulphur. The S.A.I. values decrease from 9.5 at near-surface to 2.0 at the 0.1 m depth, increase to about 8.0 at 0.8 m, and then decrease to zero at the 1.4 m depth. This trend indicates a decrease in the intensity of oxidation with increasing depth and, again, corresponds to the sharp decrease in the gaseous O_2 concentration. The O_2 profile, however, suggests that oxygen is consumed at the 0.4 m depth.

4.5 Bacteria Populations

Figures 4.13 and 4.14 show the results of bacterial counts for T. ferrooxidans presented as the most probable number (MPN) of bacteria per gram of dry mass of tailings sample at Stations WA-20 and WA-22. The data indicate a high population of T. ferrooxidans at 100,000 MPN/g at the 0.5 m depth in the south-end main tailings (Station WA-22), which decreased sharply to almost zero at 1.1 m. At WA-20 on the tailings dam, the T. ferrooxidans population ranges from near-zero at 0.4 m to a maximum of 63,000 MPN/g at 1.0 m, and then decreases to about 10,000 MPN/g at the 1.5 m depth. T. ferrooxidans are absent below the water table at both stations. These results indicate a strong presence of iron oxidizing bacteria T. ferrooxidans in the shallow unsaturated zone which correlates closely with the abrupt change in the gaseous oxygen profile. The bacteria profile is also related to the pH profile indicating the preference of T. ferrooxidans for an aerobic, acidic environment. Figures 4.13 and 4.14 also show the presence of very low populations of sulphate-reducing bacteria (<270 MPN/g at WA-22 and <550 MPN/g at WA-20) in the saturated zone. Sulphate-reducing bacteria are obligate

anaerobes and are very sensitive to oxygen. They are unable to grow in the presence of oxygen. This explains their absence in the shallow unsaturated zone. The observed low populations in the saturated zone may be due to the absence of sufficient organic compounds required as energy source(s) for metabolism.

4.6 pH Profiles

Figures 4.11, 4.12, 4.13 and 4.14 show pH profiles for the tailings pore water at Stations WA-2, WA-11, WA-20 and WA-22. The pH of the water soluble fraction of tailings is also presented for all the stations, except WA-20.

In general, the shallow oxidized zone of the tailings is characterized by acidic pore waters with pH of less than 4. The pH increases to about 5.5 near the water table and to about 6.0 to 6.5 for the unaltered tailings at depth. The pH of the water soluble tailings shows the same trends, although the values tend to be slightly lower than those of the pore water and may be an artifact of the extraction technique (Jambor, 1987).

The low pH condition that occurs in the unsaturated zone is clearly a result of pyrite oxidation, as demonstrated by the strong correlation of pH with the gaseous O₂ concentration, sulphide alteration intensity (S.A.I.) and bacteria population. There is only limited information available on the carbonate-mineral content of the Waite Amulet tailings(see Section 5.1), however, the presence of the low pH zones suggests that in these zones, carbonate buffering materials have been consumed by acidic pore waters. The presence of approximately 10 to 40 percent total sulphides in the >37 μm fraction of the tailings in the unsaturated zone (Figure 4.10), along with the low pH, indicate that the acid-neutralizing capacity of the tailings in this zone has been exhausted.

In the saturated zone, the pH increases to 6.0, suggesting buffering of acidic pore waters migrating from the unsaturated zone. The pH profile for the tailings pore water at Station WA-22 show values close to 6.5 in the deeper unsaturated zone. This location is in the coarse-grained south section of the tailings deposit where the water table is deeper (close to 6 m). These relatively high pH values in the unsaturated zone confirm the fact that the zone of active oxidation is restricted to very shallow depths (0 to 0.50 m).

The pH data for Waite Amulet presented here suggest that further oxidation of the remaining sulphides in the deeper unsaturated zone will occur at a rate dependent on pH, as well as the oxygen concentration. In view of the shallow oxygen penetration, this rate may, however, be expected to be very low.

4.7 Carbon Dioxide Concentrations

Carbon dioxide concentrations measured in the unsaturated zone tailings at Waite Amulet are presented in Figure 4.15. The observed levels were low and ranged from 0.2 to 6.5 percent. The highest concentration of 6.5 percent was reported at depth 1.40 m for Station WA-24 where the water table occurs at 3 m. In general, the CO₂ levels increased slightly to maximum levels at greater depths in the unsaturated zone, where the O₂ profiles terminate. This increase is presumably due to carbonate-consuming buffering reactions of the form (Blowes et al, 1987):



Subsequently, degassing in the unsaturated zone leads to an increase in the CO₂ level in the gas phase. As already mentioned, the optimal CO₂ level for autotrophic Thiobacilli is only 0.22 percent. At Stations WA-20 and WA-22, maximum Thiobacilli populations (Figures 4.13 and 4.14) were observed at depths where the CO₂ concentrations were about 0.2 to 0.3 percent. This correlation suggests that Thiobacilli may in fact be using CO₂ as a carbon source for metabolism.

At Station WA-24 in the south section, the tailings are more coarse-grained; accordingly, the oxygen profile penetrates deeper (Smyth, 1981; Dubrovsky et al, 1985). The CO₂ concentrations reach maximum at depths where the oxygen is consumed, indicating that CO₂ is derived from buffering of acidic pore water.

4.8 Nutrient Availability

Little information exists on nutrient availability in the Waite Amulet tailings. Available data show that ferrous iron in the tailings pore water range from 500 to about 7000 mg/L in the shallow unsaturated zone across the tailings. Potassium levels are up to about 170 mg/L. Elemental sulphur is also present in the tailings at 0.01 to 0.33 wt. %. Phosphorus and nitrogen levels are not known. It is, however, conceivable that sufficient nutrients are available in the unsaturated zone, in view of the observed high Thiobacilli population presented earlier.

5. PORE WATER GEOCHEMISTRY

5.1 Unsaturated Zone

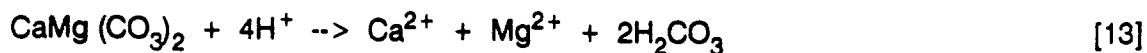
The vadose zone pore water chemistry of the Waite Amulet tailings has been assessed through extensive field and laboratory investigations (Blowes and Cherry, 1986; Blowes and Jambor, 1989). The investigation included the determination of bulk and particle densities and porosities on tailings sub-samples cored with soil augers. The pore water was extracted from cores using the miscible displacement technique (Patterson et al, 1978; Smyth, 1981). The methods of investigation are described by Blowes and Jambor (1989).

Iron and Sulphate

The entire unsaturated zone shows high Fe^{2+} concentrations (up to 10 g/L) generated by sulphide oxidation. Low pH conditions (pH 2.5 to 3.0) are, however, restricted to only shallow depths in the unsaturated zone, as a result of H^+ -consuming reactions occurring in the vadose zone. The H^+ -consuming reactions, which tend to result in tailings pore water neutralization, include dissolution of carbonate, alumino silicate and iron and aluminium hydroxide minerals (Dubrovsky et al, 1984). Redox potentials, E_h , show values ranging from 200 to 700 mV in the vadose zone. Sulphate levels are also high and, like Fe^{2+} , are up to 10 g/L. Figure 5.1 presents the Fe^{2+} and SO_4^{2-} profiles for two stations (WA-2 and WA-11) in the main tailings and two other stations (WA-21 and WA-20) on the dam. The data were obtained during the 1986 program. At Stations WA-11 and WA-21, the shapes of Fe^{2+} and SO_4^{2-} profiles are similar; high Fe^{2+} levels correspond to high SO_4^{2-} concentrations.

Alkaline and Alkaline Earth Metals

The alkaline (Na, K) and alkaline earth (Ca, Mg) metal profiles are presented in Figure 5.3. The Na and K profiles show nearly uniform concentrations with depth. At Station WA-11 however, K^+ concentrations increase slightly with depth. Pore water Mg^{2+} concentrations of the unsaturated zone tailings generally increase with depth from values of 2 to 5 mg/L near the tailings surface to 500 to 850 mg/L at about 2 m depth. The Ca^{2+} profiles are relatively more uniform and are typically about 400 to 600 mg/L at all the stations shown. The high Ca^{2+} and Mg^{2+} concentrations presumably results from dissolution of dolomite and calcite in reactions typified by the following:



An examination of the Ca^{2+} profiles shows further that the concentrations are similar at the four locations. The variations in the Mg^{2+} concentrations from station to station, on the other hand, may reflect differences in the Mg content of the carbonate minerals originally present in the tailings and added during the revegetation program. The carbonate mineral content of the tailings solids obtained at depths 1 and 2 m (the zone not affected by carbonate addition during revegetation) showed levels of more than 0.5 wt% CaCO_3 at all the four stations.

Heavy Metals

Heavy metal (Co, Mn, Cu, Ni, Pb, and Zn) profiles obtained for the unsaturated zone pore water show a concentration and mobility order similar to that observed by Dubrovsky (1986) at the Nordic Main pyritic uranium tailings near Elliot Lake, Ontario: $\text{Fe} = \text{Mn} \geq \text{Zn} > \text{Ni} > \text{Co} > \text{Pb} > \text{Cu}$. These metals are released into the tailings pore water as a result of sulphide oxidation. Their subsequent mobility is apparently controlled by complex reactions such as precipitation-dissolution, solid-solution substitution, coprecipitation and adsorption-desorption.

Aqueous Equilibrium Calculations

The unsaturated zone pore water geochemistry was assessed by aqueous equilibrium method using the computer code MINTeq (Felmy et al, 1984). The results indicated undersaturation of the pore water with respect to calcite, dolomite and siderite.

The pore water near the tailings surface also contains high concentrations of dissolved aluminum. The high Al levels have been attributed to the dissolution of alumino-silicates (Blowes and Jambor, 1989). In general, alumino-silicate dissolution tends to increase the pH, however, a large source of potential acidity still remains because Al further reprecipitates as hydroxide minerals in reactions which tend to consume OH^- and release H^+ . The alumino-silicate dissolution also releases major cations (for example, K, Na, Mg and Ca) into solution which, in turn, contributes to the formation of secondary minerals such as gypsum and Na and K jarosites.

Saturation indices calculated for $\text{Fe}(\text{OH})_3$, goethite and lepidocrocite showed undersaturation of the pore water with respect to these ferric oxyhydroxide phases at shallow depths (0 to 50 cm from the tailings surface). The undersaturation suggests re-dissolution of these oxyhydroxides previously deposited in the shallow unsaturated zone from sulphide oxidation. In the north-central portion of the tailings impoundment, saturation with respect to goethite and lepidocrocite occurs. The presence of these secondary ferric oxyhydroxides in the tailings solids was confirmed by mineralogical and X-ray diffraction analyses. In the shallow unsaturated zone where sulphide is obliterated, goethite and lepidocrocite have been shown to co-exist as intimate mixtures that have replaced individual grains of pyrrhotite.

Gypsum is the most abundant sulphate mineral in the tailings. Gypsum saturation indices (SI) derived from MINTEQ runs on the water quality data ranged from -0.20 to +0.20 which suggest that the tailings pore water is at or close to saturation with respect to gypsum.

5.2 Saturated Zone

In the saturated zone, the tailings pore water was sampled from installed PVC piezometers. A detailed description of the methods of piezometer installation and sampling and analyses of the pore water is presented in Appendix B. The chemistry of the pore water is discussed below for Stations WA-15, WA-17, WA-11, WA-20 and WA-21.

Station WA-15

pH, Acidity and Redox

The results of tailings pore water chemistry in the saturated zone are presented as profiles for piezometer WA-15 on the west dam face in Figures 5.2 and 5.3. During the two sampling dates in October 1986 and November 1988, the pH was observed to be close to 7.0. In the shallow saturated zone, a pH depression to 4.5 was observed in November 1988. Electrical conductivity, E_c , was 2000 to 3000 $\mu\text{S}/\text{cm}$ in the shallow zone (that is, down to 2 m below the water table) and decreased to about 1000 $\mu\text{S}/\text{cm}$ in the deeper zone. Observed acidities in the shallow zone were much higher in 1988 than in 1986. The 1988 values were in the range of 350 to 500 mg/L CaCO_3 in the top 3 m below the water table (Figure 5.2).

Alkaline and Alkaline Earth Metals

The saturated zone pore water concentrations of alkaline (Na, K) and alkaline earth (Ca and Mg) metals are presented as profiles in Figure 5.3. With the exception of Na^+ , these metals show high concentrations (up to 800 mg/L) at the 6.5 m depth and then decrease to less than 200 mg/L deeper in the profiles. The profiles are similar in shape to the sulphate (SO_4^{2-}) and electrical conductivity (E_c) profiles and may reflect alumino-silicate dissolution resulting from infiltration of acidic pore water generated in the unsaturated zone.

Iron and Sulphate

The sulphate levels in the saturated zone pore water did not show much change between October 1986 and November 1988, with values in the range of 2000 to 4500 mg/L (Figures 5.2 and 5.3). Dissolved ferrous iron, Fe^{2+} , concentrations in the deeper saturated zone were observed to be about 8 to 10 mg/L in October 1986 (Figure 5.3) and less than 2 mg/L in November 1988. In the shallow saturated zone, however, the Fe^{2+} concentrations reached 150 mg/L in November 1988 (Figure 5.4). Total dissolved iron, Fe_T , was also higher (close to 200 mg/L) in the shallow zone in 1988.

Heavy Metals

Heavy metal levels (Pb, Cu, and Zn) observed in 1988 were less than 6 mg/L at all depths in the saturated zone. As shown in Figure 5.4, only Zn showed concentrations of up to 6 mg/L near the water table. The saturated zone pore water Zn concentrations observed in piezometer WA-15 in October 1986 were below detection (<0.01 mg/L) at all sampling depths (Table 5.1).

Station WA-17

pH, Acidity and Redox

Station WA-17 is located in the south-end tailings along an east-west section (Figure 4.1). Chemical profiles for WA-17 obtained in October 1986 are presented in Figures 5.5 and 5.6. The pH was slightly less than 6.0 in the shallow saturated zone (about 1.5 m below the water table) but reached 7.0 in the rest of the profile. Redox potentials, E_h , were almost constant at about 350 mV in the entire profile. The electrical conductivity, E_c , showed values of 4000 to 5000 $\mu\text{S}/\text{cm}$ near the water table, which decreased uniformly to 600 $\mu\text{S}/\text{cm}$ at depth.

Acidity showed the same trends and decreased from 880 mg/L CaCO_3 at the 18 m depth. The alkalinity profile (Figure 5.6) shows low values of about 30 mg/L CaCO_3 near the water table and increases to about 300 mg/L CaCO_3 at depth.

Alkaline and Alkaline Earth Metals

In the shallow saturated zone, magnesium and calcium (Figure 5.6) concentrations are much higher (1000 and 350 mg/L, respectively) than in the deeper zone. The magnesium and calcium profiles appear to correlate very well with those of alkalinity and acidity. High magnesium and slightly high calcium levels in the shallow zone may be due to dissolution of carbonate buffering minerals resulting from the ingress of acidic pore water from the active oxidation zone. Potassium concentrations shown in Figure 5.6 increase slightly (up to 150 mg/L) in the 4 to 6 m depth and may reflect release from aluminosilicates dissolution.

TABLE 5.1
HEAVY METAL CONCENTRATIONS AT WA-15, OCTOBER 1986

Piezometer No.	Depth m	Al mg/L	Mn mg/L	Cu mg/L	Cd mg/L	Cr mg/L	Ni mg/L	Pb mg/L	Zn mg/L	Fe ²⁺ mg/L
15-1	6.5	<2.5	1.62	<0.02	<0.005	<0.05	<0.05	<0.05	<0.01	12.00
15-2	3.5	<2.5	-	<0.02	<0.005	<0.05	<0.05	<0.05	<0.01	-
15-3	11.0	<1.0	0.52	<0.02	<0.005	<0.05	<0.05	<0.05	<0.01	<1.10
15-4	7.9	<1.0	0.30	<0.02	<0.005	<0.05	<0.05	<0.05	<0.01	16.00

Iron and Sulphate

Dissolved iron (either as Fe^{2+} or Fe^{3+}) was more abundant in the shallow saturated zone (at about 0.9 m below the water table) than at depth (Figure 5.5). The ferrous iron (Fe^{2+}) concentration is close to 2200 mg/L in the shallow zone and decreases rapidly to less than 50 mg/L at the 5.2 m depth and then to less than 10 mg/L at greater depths. Ferric (Fe^{3+}) iron shows essentially the same trends, although the levels are much lower (about 420 mg/L maximum) than those of ferrous iron. As expected from pore water derived from sulphide oxidation, the dissolved sulphate (SO_4^{2-}) concentrations were high and reached 12,000 mg/L in the shallow saturated zone (Figure 5.6) which decreased to about 2800 mg/L at the 6.5 m depth.

Heavy Metals

Levels of heavy metals observed in the saturated zone tailings pore water at Station WA-17 are illustrated in Table 5.2 for October 1986. Manganese occurred at about 30 mg/L close to the water table (Figure 5.6) and decreased to less than 1 mg/L at depth. Other metals such as Pb, Zn and Cu were all below 0.3 mg/L in concentration.

Station WA-11

Figures 5.7 to 5.10 present chemical profiles of the saturated zone tailings pore water at WA-11, further west of WA-17. The profiles represent data obtained in December 1985, October 1986, and November 1988. Since the data do not show any major differences in the various chemical parameters from one sampling date to the other, only the October 1986 profiles are discussed in detail.

pH, Acidity and Redox

The 1986 profiles also include limited unsaturated zone data adapted from Blowes and Jambor (1989), which were used to demonstrate the continuity of chemical profiles along the tailings section. The results indicate that in the shallow saturated zone (that is, down to 2 m below the water table), acidity is about 1750 mg/L; it decreases rapidly to 12 mg/L at greater depths. Although alkalinity is reported only for the 5.3 and 8.6 m depths, values in the shallow saturated

TABLE 5.2
HEAVY METAL CONCENTRATIONS AT WA-17, OCTOBER 1986

Piezometer No.	Depth m	Al mg/L	Mn mg/L	Cu mg/L	Cd mg/L	Cr mg/L	Ni mg/L	Pb mg/L	Zn mg/L	Fe ²⁺ mg/L
17-1	6.8	<2.5	0.93	<0.02	<0.005	<0.05	<0.05	<0.05	<0.01	<1.10
17-2	5.7	<2.5	2.20	<0.02	<0.005	<0.05	<0.05	<0.05	<0.01	<1.10
17-3	4.2	<2.5	29.90	<0.02	<0.005	0.08	<0.05	<0.05	0.12	2820.00
17-4	3.3	<2.5	13.40	<0.02	<0.005	<0.05	<0.05	<0.05	0.25	-
17-5	5.4	<2.5	2.10	<0.02	<0.005	<0.05	<0.05	<0.05	<0.01	18.00
17-6	18.5	<2.5	0.52	<0.02	<0.005	<0.05	<0.05	<0.05	<0.01	<1.10

zone will be much lower because of increased acidity. In the unsaturated zone, the pH is about 3.8 near the tailings surface and increases to 5.9 in the region just above the water table. With the exception of the data point in the shallow saturated zone (3.3 m depth), it appears that a continuous pH profile ranging from 3.8 at near-surface to 8.0 at 8.6 m depth exists at this station. The pH of 4.3 recorded at 3.3 m is relatively low and may reflect fluctuating water table conditions. The observed redox potentials, E_H , are as high as 700 mV in the near-surface tailings in the unsaturated zone, and are around 100 mV at greater depths. The electrical conductivity, E_c , profile in the saturated zone is near-vertical with a value of 2600 $\mu\text{S}/\text{cm}$ in the shallow zone, which decreases only slightly to 2100 $\mu\text{S}/\text{cm}$ at greater depths. The unsaturated zone electrical conductivity is rather high with an average of about 20,000 $\mu\text{S}/\text{cm}$.

Iron and Sulphate

Iron and sulphate profiles shown in Figure 5.7 correlate with pH and acidity profiles. Dissolved ferrous iron, Fe^{2+} , at depth 1 m below the water table, is as high as 6000 mg/L and decreases rapidly to about 15 mg/L at a depth of 6 m below the water table. Water samples close to the water table in the unsaturated zone show iron values that are lower than those in the shallow saturated zone. The trends in the iron profile are similar to those noted above for pH. Sulphate concentrations decrease from about 13000 mg/L at 2 m below the water table to 2000 mg/L at 8.6 m depth.

Heavy Metals

As shown in Table 5.3, concentrations of all other heavy metals (Cu, Pb, Zn, Cr, Ni, and Al), with the exception of manganese (Mn), are generally low (less than 0.05 mg/L) in the saturated zone. Manganese shows values of 79 mg/L in the shallow saturated zone and decreases to about 3 mg/L at 5.3 m below surface.

TABLE 5.3
HEAVY METAL CONCENTRATIONS AT WA-11, OCTOBER 1986

WELL NO.	Al DEPTH	Cu mg/L	Mn mg/L	Cr mg/L	Ni mg/L	Pb mg/L	Zn mg/L	Fe ²⁺ mg/L	mg/L
11-3	2.96	<2.5	<0.02	79.30	<0.05	0.11	0.36	0.19	6048.00
11-2	5.15	<2.5	<0.02	3.47	<0.05	<0.05	<0.05	<0.01	144.00
11-1	8.16	<2.5	<0.02	0.12	<0.05	<0.05	<0.05	<0.01	12.00

Alkaline and Alkaline Earth Metals

In the shallow saturated zone, observed sodium and potassium concentrations in the tailings pore water are much lower than those of calcium and magnesium. The higher calcium and magnesium levels are probably derived from dissolved carbonates from limestone added during the revegetation program. As shown in Figure 5.8, sodium concentrations increase at greater depths which may reflect competitive ion exchange with calcium and magnesium (Barone et al, 1989).

Station WA-20

Station WA-20 is located at the toe of the tailings dam on the south side of the impoundment, approximately 30 m from the west collection ditch. Chemical results for Station WA-20 obtained in October 1986 and November 1988 are presented in Tables 5.4 (a) and (b). The two monitoring points at WA-20 are located at depths of 2.9 and 5.2 m below surface.

TABLE 5.4

PHYSICO-CHEMICAL, METAL, AND MAJOR ION CONCENTRATION

VALUES, OCTOBER 1986 (a) AND NOVEMBER 1988 (b).

		20-1	20-2	21-1	21-2
Tip elev	(m)	308.30	310.49	307.41	308.80
Depth of tip	(m)	5.12	2.94	4.55	3.13
pH		7.62	6.38	7.51	5.92
Eh	(mV)	272	259	287	305
Ec Field	uS	1000	4350	2350	4000
Temp.Fld	deg.C	11	11	9	9
Acidity	mg/L CaCO ₃	17.60	1012.00	26.40	
Alkalinity	mg/L CaCO ₃	678.60	97.50	207.68	15.60
Fe+2	mg/L	12.00	696.00	12.00	2496.00
Zn	mg/L				0.04
Ca	mg/L	29	400	125	335
K	mg/L	25.00	100.00	58.00	90.00
Mg	mg/L	9.60	1135.00	185.00	410.00
Mn	mg/L	0.34	5.64	0.06	21.40
Na	mg/L	405.00	22.00	475.00	16.00
SULPHATE	mg/L	195	7200	2400	7500

(a)

		20-1	20-2	21-1	21-2
Tip elev	(m)	308.30	310.49	307.41	308.80
Depth of tip	(m)	5.12	2.94	4.55	3.13
pH		7.3	6.65	7.5	6.85
Eh	(mV)	270	220	167	325
Ec Field	uS	1636	3320	3230	4510
Acidity	mg/L CaCO ₃	50	1550	50	5100
Fe+2	mg/L	2	700	3.4	2600
Zn	mg/L	0.4	0.46	0.39	0.51
Ca	mg/L	30.4	396	144	369
Mg	mg/L	11.2	789	219	449
SULPHATE	mg/L	350	4700	2300	9500

(b)

pH, Acidity and Redox

As for the other stations, acidity at WA-20 was found to decrease with depth. However, the difference in acidity with depth was much greater than at the stations located on top of the impoundment, passing from 1012 to 17 mg/L CaCO₃ within a vertical distance of slightly more than 2 m. Although not as drastic, changes in pH reflected the differences in acidity; redox was slightly higher at depth.

Iron and Sulphate

Iron and sulphate levels were high at the shallowest level, and decreased very rapidly with depth, following the same trend as the acidity values. As with the other stations, almost all dissolved iron was in the reduced (Fe²⁺) form.

Heavy Metals

Table 5.4 reports values of Mn which decreased with depth, from 5.6 mg/L to 0.3 mg/L/. All other heavy metals (Cu, Pb, Zn, Cr, Ni and Al) were below detection limits and are not reported in the table.

Alkaline and Alkaline Earth Metals

Calcium and magnesium vertical concentration gradients were very high; concentration changes were lower in the case of potassium. Sodium concentrations increased with depth, as at Station WA-11.

Station WA-21

Station WA-21 is located at the toe of the tailings dam on the north side of the impoundment. Chemical results are included in Tables 5.4 (a) and (b). The two monitoring points (21-1 and 21-2) are located at depths of 4.5 m and 3.1 m below surface.

pH, Acidity and Redox

As for Station WA-20, important decreases of acidity with depth were measured at the two monitoring points at WA-21 (Table 5.4 (b)). Redox potential decreased with depth, and pH increased by approximately 1 unit.

Metals and Sulphate

Metal levels were slightly higher at WA-21 than at WA-20. Ferrous iron was in excess of 2500 mg/L at 21-2, and decreased to less than 15 mg/L at 21-1. A zinc concentration of 0.04 mg/L was recorded at the shallowest depth. Again, manganese decreased with depth. Sulphate levels decreased with depth, but remained quite high (around 2400 mg/L), even at the deeper monitoring level. However it is likely that sulphate levels would be decreasing to less than 200 mg/L at the bottom of the tailings, which is approximately 2 m below the deepest monitoring point (21-1).

Alkaline and Alkaline Earth Metals

Again, typical high levels of calcium, magnesium and potassium, due to dissolution reactions, were encountered at the shallowest level. An increase in sodium concentration with depth was also observed, with values changing from 16 to 475 mg/L.

Aqueous Equilibrium Calculations

All the profiles presented suggest that oxidized products in the unsaturated zone have been transported by infiltrating water into the saturated zone, as was observed by Boorman and Watson (1976) at the Heath Steele tailings site in New Brunswick and confirmed by Blowes and others (1988) at various other tailings sites, including Waite Amulet.

In order to assess which mineral phases have the potential to form in the saturated zone, geochemical calculations were carried out using the equilibrium metal speciation model MINTeq (Felmy et al, 1984). The results for Stations WA-11, WA-15 and WA-17 indicated that the tailings pore water in the shallow saturated zone is saturated with gypsum ($\text{CaSO}_4 \cdot 2\text{H}_2\text{O}$) and supersaturated with respect to Na and K-jarosite ($\text{Na-KFe}_3(\text{SO}_4)_2(\text{OH})_6$), goethite and lepidocrocite ($\text{FeO} \cdot \text{OH}$). Calculated saturation indices for gypsum are between 0.00 and 0.25. The saturated indices for the jarosites were from 10.00 to 13.00. Also in this zone, saturation with respect to anglesite (PbSO_4) occurs. Blowes and Jambor (1989) have confirmed the presence of these mineral phases in the unsaturated zone. In the deeper zone, slightly higher alkalinity values were observed resulting in supersaturation with respect to siderite (FeCO_3). Siderite has been previously found by mineralogical observation in tailings cores at the deeper locations of station WA-20. Siderite formation is limited to the deeper parts of the tailings because it can occur only at relatively high pH (generally greater than 6). Morin and Cherry (1986) have reviewed the mechanisms of siderite formation in mine tailings, and have observed that siderite precipitation can produce significant retardation of migrating ions in pore water solutions. The pore water in this zone is also supersaturated with respect to jarosite, gypsum and goethite. Calculated saturation index for rhodochrosite (MnCO_3) in this zone was -0.96, which is close to saturation.

The precipitation of mineral phases in the saturated zone is a function of pH buffering by carbonate dissolution reactions. As carbonates become depleted, it can be expected that less mineral precipitation will occur. Carbonate minerals are likely to be depleted in the shallow, saturated zone; hence, pore water in the shallow saturated zone may not undergo any buffering. This explains the acidic pH and high metal and sulphate levels observed in the shallow saturated zone at Stations WA-15, WA-17 and WA-11.

6. HYDROGEOLOGY

6.1 Site Conditions

Extensive geological and hydrogeological investigations of the Waite Amulet tailings site were conducted in 1985. The results of the investigations have provided the pertinent data to define the extent and variation of the tailings deposit and the type of geologic materials underlying the tailings.

A geophysical survey using the seismic refraction method, reported by Dave et al (1986), indicated extremely variable bedrock topography, especially in the northern section of the tailings. The survey showed the presence of a clay layer underlying the tailings. The clay gently dips south and west with thicknesses ranging from 2 m to about 20 m. The tailings also vary in thickness ranging from 2 m in the north to about 15 m in the south.

Sampling confirmed the presence of the clay unit; the unit was found to be of variable composition across the site. In the south section, dense, varved clay was encountered in the deeper clay horizons and mottled, silty clay was intersected along the shallower horizons. In the north section, the clay unit was generally thin, and was composed of a clayey to sandy silt. Varved clay was also encountered in the north section, but the total thickness of the varved zones were generally only about 0.6 m.

Rock coring conducted during the 1986 drilling campaign indicated that the bedrock at Station WA-2 is a moderately fractured acidic volcanic rock (probably a granodiorite). The bedrock at Station WA-9 in the central portion of the site is less fractured than at Station WA-2.

The tailings are more fine-grained in the northern region than in the south. This is illustrated in Figure 6.1 by the grain size distribution curves for Stations WA-2 and WA-22. At WA-2 in the north, the d_{50} (that is, the grain size at which 50 percent of the tailings is finer) is about 0.007 mm, compared to 0.14 to 0.16 mm for WA-22 in the south. The corresponding d_{10} values (the grain size at which 10 percent of tailings in finer) are about 0.001 mm for WA-2 and 0.02 for WA-22. The data also indicate that the

fine-grained tailings in the north consist of 17 to 22 percent clay and 10 percent silt size fractions. The coarse-grained tailings in the south end show only 5 percent clay and 1 to 3 percent silt size materials. The gradations shown in Figure 6.1 are similar to those reported in the literature for copper and zinc tailings (Vick, 1983). Fine-grained tailings were also encountered across the site as distinct, thin, horizontal "slime" layers. These layers were probably produced by changes in the rate of spilling of the tailings, and/or environmental conditions, such as wave action, at the time of deposition.

Tailings water content and porosity were measured at Stations WA-2 and WA-22. Average water contents, based on dry mass, were 12 and 25 percent for the unsaturated and saturated tailings, respectively.

The water table configuration for October 1986, shown in Figure 6.2, indicates that the highest water levels occur in the central portion of the site. In the northern section, the water table is just below the tailings surface and decreases in elevation towards the south end, where it is about 5.5 m below the tailings surface. The highest water levels occur in the north-central portion of the site.

6.2 Unsaturated Zone Pore Water Flow

Pore water flow in the unsaturated zone is mainly vertical, and its magnitude depends on the physical parameters of the tailings. Hydraulic conductivity in unsaturated porous media such as tailings is a complex function of the volumetric water content, which varies with depth and is controlled by the hydraulic pressure head. This value is difficult to measure, and approximations are often used for practical applications.

For the Waite Amulet site, the saturated hydraulic conductivity (K_s) in the top of the unsaturated zone of the tailings was measured at selected locations using the Guelph Permeameter method of Reynolds et al (1985) described in Appendix B. Values of K_s were between 10^{-5} and 10^{-4} cm/s. An estimate of the maximum downward pore water velocity in the unsaturated zone can be obtained by assuming a unit gradient ($i = 1$) between the tailings surface and the saturated zone and with the relation:

$$V = K_s i/n \quad [14]$$

where n is the porosity and is equal to 0.30. The calculated velocity V is between 0.03 and 0.3 m/day.

The actual downward vertical velocity in the unsaturated zone could be lower than calculated above due to the effect of the fine-grained slime tailings layers which would decrease the effective vertical hydraulic conductivity and promote some horizontal flow in the unsaturated zone. Because all methods to evaluate hydraulic conductivity in the unsaturated zone mostly measure the horizontal component of hydraulic conductivity, it is difficult to evaluate the vertical velocities in the unsaturated zone and the extent of the horizontal flow component.

6.3 Saturated Zone Pore Water Flow and Storage

As indicated by Figure 6.2, pore water flow occurs in the saturated zone from the middle of the tailings deposit towards the sides. Pore water velocities along Sections A-A and B-B were estimated using field measured hydraulic conductivities, and water table profiles, and by applying Darcy's law:

$$V = Ki/n \quad [15]$$

where V is the average linear groundwater velocity, K is the hydraulic conductivity, i is the hydraulic gradient, and n is the porosity.

In November 1988, the horizontal gradient across the dam was observed to be about 0.05. Measured hydraulic conductivities were between 5×10^{-6} and 2×10^{-4} cm/s along the section. Using these values, pore water velocity was calculated to be in the range of 0.2 to 9.0 m/a. These velocities could likely increase to 35 m/a in the higher permeability, steeper sections of the dam.

Vertical gradients at most of the monitoring stations were downwards and ranged from 0.002 to 0.06. Because of the presence of the horizontal fine-grained slime lenses, it is believed that the tailings hydraulic conductivity is anisotropic, with horizontal hydraulic conductivity (K_H) being greater than the vertical hydraulic conductivity (K_V). Although piezometers and drive-point piezometers such as the ones installed at Waite Amulet have been considered to be biased towards K_H , it will be assumed that the measured hydraulic conductivity (K_M) is close to the geometric mean, that is:

$$K_M = \sqrt{K_H \cdot K_V} \quad [16]$$

With the type of layering observed in the tailings core, an anisotropy factor (K_H/K_V) of 10 to 100 may be expected. Vertical pore water velocities could therefore be estimated to range from 0.07 to 10 m/a using [15]. The degree of downward movement of the tailings pore water will depend on several factors such as inflow quantities, slope of the clay layer and proximity of the discharge ditch.

Hydraulic conductivity (K) measurements in the clay were performed in 1987. A hydraulic conductivity of 8.56×10^{-5} cm/s was measured at WA-15. Values obtained at Stations WA-17 and WA-18 were between 1×10^{-6} and 5×10^{-7} cm/s. The high variability in clay hydraulic conductivity could influence the flow system in the tailings. Examination of Shelby tube samples of the clay at the south end revealed horizontal to inclined varved sequences of clayey and silty materials. As previously mentioned, the methods of K measurement used in the field are biased towards the horizontal component of the conductivity. Therefore, these measured values of 80×10^{-5} to 10^{-6} cm/s should actually represent the horizontal hydraulic conductivity of the clay. The grain size distribution of the clay (presented later in Section 10.6.1) suggests that the vertical hydraulic conductivity may be lower.

Seasonal water table variations were up to 1 m and reflected the amount of water that can be stored in the tailings. For example, assuming a tailings porosity of 0.27, a water table rise of 30 cm in the tailings represents a volume of water of 32,000 cubic metres stored inside the 40 ha tailings impoundment. This represents an appreciable amount

of water which could influence the seasonal water balance at the site. It should not, however, affect the annual water balance, since it has been observed that water levels are similar at the same periods of the year.

The following sections of this report will further analyze the water balance at the tailings site and its influence on pore water movement and acid drainage production.

7. HYDROLOGY

7.1 Water Balance Equation

The acidic pore waters will flow through the tailings and exit as seepage. The volume of seepage produced will depend on the water balance of the site, as described by the following water balance equation adapted from Linsley et al, (1975):

$$P - ET - R - L - \Delta ST = S \quad [17]$$

where: P = precipitation
ET = evapotranspiration
R = run-off
L = leakage into deeper soil layers
 ΔST = change in storage
S = seepage

Figure 7.1 illustrates the components of the hydrological cycle for the tailings deposit. Input of water is by precipitation, as rainfall or snow. The quantity of water entering the tailings as infiltration will be equal to the amount of water left after evapo-transpiration and surface run-off. The amount of storage in the tailings will depend on precipitation and the physical properties of the tailings. The volume of water in excess of storage either becomes seepage, which is captured in collection ditches and then treated, or leakage into the underlying clay.

Two monitoring stations were installed in July 1987 to evaluate the water balance components at locations illustrated in Figure 7.2. Station 1 was located on the top of the northern tailings section to monitor precipitation, evaporation and surface run-off quantity and quality on the northern part of the tailings. Station 2, located along the western seepage face, monitored seepage quantity and quality at the toe of the western half of the main tailings dam.

7.2 Evaporation and Precipitation

Monthly rainfall was measured between May and September, 1988. Values obtained were between 47 and 237 mm, with monthly rainfall rates varying between 1.5 and 7.6 mm/day. The evaporation rates were between 1.8 and 3.8 mm per day. Recorded data are strictly for evaporation and do not include transpiration. From May to September, the calculated difference between evaporation and precipitation was 147.8 mm. Measured precipitation values were similar to those reported in Rouyn at the Rivière Kenojévis weather station (Gouvernement du Québec, 1989).

TABLE 7.1
MONTHLY PRECIPITATION AND EVAPORATION DATA FOR WAITE AMULET TAILINGS SITE

	MAY 11-31	JUNE 1-30	JULY 1-31	AUGUST 1-31	SEPT. 4-30	TOTAL AMOUNT (mm)
PRECIPITATION (mm)	48.8	146.2	47.4	237	93.8	573.2
RATE (mm/day)	2.3	4.87	1.5	7.6	3.47	
.....						
EVAPORATION (mm)	70	113	114	81.4	47.4	425.4
RATE (mm/day)	3.5	3.8	3.7	2.9	1.8	
DIFFERENCE	(21.2)	33.2	(66.6)	155.6	46.4	147.8

7.3 Infiltration and run-off

Infiltration rate

Infiltration and run-off rates are interrelated, and depend on several physical parameters such as soil porosity and moisture content, surface slope and degree of deformation, rain drop size and impact velocity, rainfall intensity and duration, inwash of fine materials, vegetation, and temperature (McBean, 1984). The high spatial variability of infiltration at tailings sites makes any attempt to measure a representative value very laborious. Furthermore, most field infiltrometer methods do not measure infiltration directly, but rather measure a related value, the saturated soil hydraulic conductivity. Reynolds (1984) gives a good review of infiltrometer methods.

The rate at which pore water infiltrates the tailings can be related to the measured value of saturated hydraulic conductivity (K_s) reported in section 6.2. As stated by Mein and Larsen (1973), the infiltration capacity for unsaturated soils is greater than for saturated soils. The measured K_s value of 0.03 m/day would thus represent a minimal infiltration rate for water recharging into the unsaturated zone. This rate would exist, for example, during a long, intense recharge event.

Theoretically, the infiltration rate could be higher than 0.03 m/day at the beginning of a recharge event. In this case, the top of the tailings will be unsaturated, and all precipitation will infiltrate the tailings, leaving no run-off. At a certain time during the recharge event, the tailings might gradually become saturated, and the infiltration rate should decrease asymptotically down to the value of K_s . Any amount of rain falling at a rate greater than K_s would ultimately run off the surface. In the case of a low-intensity recharge event, the infiltration rate could be lower than K_s ; in this case, the top of the tailings would remain unsaturated and all the rainfall would infiltrate.

The transition from unsaturated to saturated conditions can occur very rapidly, as noted at a similar site by Abdul and Gillham (1984), who related the phenomenon to the fine-grained nature of the tailings which induces an important tension-saturated zone immediately above the water-table.

Run-off Volumes

The rapid transition from infiltration to run-off conditions was verified, as the mean run-off flows recorded at Station 1 from May until the heavy rainfall events of August were all below $0.5 \text{ m}^3/\text{h}$. The dry conditions encountered in late spring and early summer resulted in a water table depression which, in turn, increased the rate of infiltration and limited the surface run-off on the top of the tailings to virtually zero.

Figure 7.3 shows the flow variations and the corresponding cumulated rainfall records during the month of September. The first and second rain events of approximately 10 mm each (11 and 13 September) barely influenced the overland flow which remained constant at $2 \text{ m}^3/\text{h}$. The third event of 15 mm increased the flow to approximately $5 \text{ m}^3/\text{h}$; the flow remained practically constant at this value for over a day. It was not until the rainfall events of 12 mm and 20 mm (23 and 27 September, respectively) that runoff peaks of $20 \text{ m}^3/\text{h}$ and $40 \text{ m}^3/\text{h}$ were recorded in the ditch.

The preceding observations suggest that infiltration after peak rainfalls in September gradually raised the water table in the tailings from its low summer position of 1 m below surface. Eventually, the tailings became saturated, a pond was formed on top of the tailings, and the overland ditch immediately responded to rainfall events. Continual monitoring of the water level in nearby piezometers in parallel with meteorological monitoring could be used in determining the dynamics of the water table rise and the effect of the tension-saturated zone.

An estimation of the total area drained by the the western ditch during the rainfall events can be attempted by dividing the discharge volumes by the rainfall quantities. Five major rainfall events, inducing important variations in flows during this period, can be used to do this. The events occurred in August (26th), September (23rd and 27th) and November (5th), and corresponded respectively to 17.2, 13.4, 20.6 and 27.4 mm of precipitation; the total volumes of water flowing through the Station 1 flume as a direct hydrological response for each event were respectively 891, 437, 1045 and 4086 cubic meters (corresponding storm hydrographs are illustrated in Figure 7.4).

The drainage area calculated using the rainfall-discharge ratio would vary between 3 and 15 ha. These variations would depend on the intensity of the rainfall and the water table level preceding the event. As the water table rises during the wet season, the infiltration capacity of the tailings decreases and the drainage area around Station 1 increases.

Run-off Quality

Twenty-six water samples were taken at Station 1 in May, August and November 1988. Table 7.2 shows sampling times, concentrations and calculated loadings. The metal concentrations were rather low, compared to concentrations observed in the collection pond (usually less than 10 mg/L Fe, 1 mg/L Cu, 0.2 mg/L Pb, and 5 mg/L Zn. This suggests that the run-off collected at this location contains a very small fraction of the total metal loading to be treated at the lime neutralization plant. Samples collected in the overland ditch below the Station 1 flume at various occasions indicate an increase in metal concentrations. This is probably due to intermittent seepage coming out of the tailings downstream of Station 1.

7.4 Seepage

Seepage Volumes

West dam seepage base flows measured at Station 2 (excluding rainfall events) varied from 1.5 to 4.1 m³/h, with a mean of approximately 2.5 m³/h during the study period. Seepage flows measured at twelve different high flow conditions, which were related to rainfall events and/or snow melts, are presented in Table 7.3. The data indicate the duration of rainfall, the number of rainfall sequences, the intensities, and the peak flows reached for each major event. Graphs for each of these events (cumulative rainfall and flow vs time) are given in Appendix D.

TABLE 7.2

CONCENTRATIONS AND LOADING VALUES FROM SAMPLES COLLECTED AT STATION 1

DATE	MONTH	HOUR	FLOW (m ³ /h)	CONCENTRATIONS								LOADING							
				Cu mg/l	Pb mg/l	Zn mg/l	Ca mg/l	Fe mg/l	Fe +2 mg/l	Mg mg/l	SO ₄ mg/l	Cu g/h	Pb g/h	Zn g/h	Ca Kg/h	Fe g/h	Fe +2 g/h	Mg Kg/h	SO ₄ Kg/h
12	5	10	0.46	0.69	0.15	3.38	391	6.02		138.9	1550.0	0.32	0.07	1.56	0.18	2.79	0.06	0.72	
13	5	16	0.35	0.10	N.D.	1.26	219	0.87		56.8	865.4	0.03	N.D.	0.44	0.08	0.31	0.02	0.30	
14	5	13	0.52	0.09	N.D.	1.14	209	0.88		55.6	859.7	0.05	N.D.	0.59	0.11	0.46	0.03	0.45	
15	5	17	0.84	0.12	N.D.	1.47	230	0.97		58.3	925.8	0.10	N.D.	1.23	0.19	0.81	0.05	0.77	
16	5	15	0.28	0.13	N.D.	1.43	234	0.96		58.7	903.0	0.04	N.D.	0.40	0.07	0.27	0.02	0.26	
16	5	20	0.20	0.20	N.D.	1.79	253	1.65		68.1	1009.8	0.04	N.D.	0.36	0.05	0.33	0.01	0.20	
19	5	11	0.09	0.78	0.11	3.08	352	8.02		127.1	1439.4	0.07	0.01	0.28	0.03	0.73	0.01	0.13	
20	5	9	0.41	0.85	N.D.	3.29	373	9.24		141.3	1566.7	0.35	N.D.	1.34	0.15	3.76	0.06	0.64	
25	5	15	0.02	1.27	0.21	1.69	454	30.80		172.2	1855.0	0.03	0.01	0.04	0.01	0.75	0.00	0.05	
30	5	13	0.18	0.74	0.12	3.26	452	5.69		180.6	1841.7	0.14	0.02	0.60	0.08	1.05	0.03	0.34	
3	8	10	0.80	0.31	N.D.	2.44	171	0.29	0.30	45.4	730.9	0.24	N.D.	1.94	0.14	0.23	0.24	0.04	0.58
5	8	11	1.33	0.90	N.D.	4.14	211	0.59	0.80	57.0	875.0	1.20	N.D.	5.52	0.28	0.78	1.07	0.08	1.17
8	8	5	1.33	1.30	N.D.	4.83	265	1.04	1.20	80.5	1104.8	1.73	N.D.	6.45	0.35	1.39	1.60	0.11	1.47
15	8	11	46.28	0.13	N.D.	1.77	91	0.64	0.80	17.7	326.9	6.05	N.D.	81.70	4.21	29.65	37.02	0.82	15.13
16	8	11	9.34	0.22	N.D.	2.42	120	1.57	1.10	28.0	502.1	2.05	N.D.	22.60	1.12	14.63	10.27	0.26	4.69
16	8	15	7.56	0.26	N.D.	2.13	128	1.08	0.50	29.9	519.4	1.96	N.D.	16.10	0.97	8.15	3.78	0.23	3.93
3	11	17	9.34					3.88	2.91							36.22	27.16		
3	11	22	7.56					16.36	3.90							123.72	29.46		
4	11	14	7.82					4.30	2.74							33.64	21.41		
4	11	22	12.04					3.99	1.80							47.98	21.67		
5	11	6	64.74					2.71	1.14							175.36	73.48		
7	11	20	27.08					1.67	1.41							45.26	38.30		
15	11	7	8.46	0.21	N.D.	2.37	237	5.14	3.34	46		1.74	N.D.	20.01	2.00	43.50	28.28	0.39	
16	11	0	8.45	0.22	0.00	2.50	250	0.00	1.90	49.0	746.4	1.83	N.D.	21.10	2.11	0.00	16.05	0.41	6.31
16	11	7	8.49	0.18	0.08	2.49	221	2.14	1.42	45.9	726.2	1.53	0.66	21.15	1.87	18.19	12.05	0.39	6.17
16	11	15	39.14	0.20	0.09	1.80	185	2.43	0.44	40.9	618.2	7.97	3.42	70.59	7.23	95.07	17.08	1.60	24.19

TABLE 7.3

RAINFALL DURATION AND PEAK FLOWS FOR CONDITIONS OF
HIGH SEEPAGE AT STATION 2 DURING MAY AND NOVEMBER 1988

MONTH	DATE	TOTAL DURATION (h)	RAINFALL EVENT	TOTAL RAINFALL (mm)	PEAK FLOW (m ³ /h)
MAY	13	3.0	3	15.4	44.0
	15	4.3	2	7.8	12.5
JUNE	12	0.5	1	4.2	19.0
	14	1.6	1	14.4	165.0
	19	1.0	2	5.6	31.0
	25	3.0	1	17.2	88.0
	30	3.8	1	21.2	200.0
JULY	13	2.5	1	10.6	63.0
	16	7.5	3	9.2	30.0
	25	1.2	1	9.4	140.0
NOVEMBER	5	8.0	1	14.0	66.0
	6 *	10.0	2	12.0	60.0
	16 *	5.7	1	2.8	63.0

* Rainfall combined with snowmelt.

Comparisons of the volume of water passing through Station 2 during rainfall events with the recorded rainfall accumulations suggested that the drainage area of the seepage ditch is approximately 1 ha. With the length of the ditch from the south-east end of the tailings to the Station 2 flume being 700 m, the average width of the area drained (including the ditch) would be about 14.3 meters. This area would correspond approximately to the area of the seepage face along the tailings dam. According to this estimate, most of the rain falling east of the ditch drainage area would infiltrate the tailings to later report to the ditch as seepage.

Seepage Quality

Concentrations of Fe, SO₄ and Mg at Station 2 were much higher than at Station 1, with maximum levels of 2500 mg/L for Fe (1300 mg/L Fe⁺²), 800 mg/L for Mg, and 7500 mg/L for SO₄. Total Fe values at low flow (<10 m³/h) ranged between 1100 and 1600

mg/L. About 60% of the total Fe is present as Fe^{2+} in the water samples collected in the seepage ditch. Appendix D lists the water quality values, the flow rates at the time the samples were taken, and the corresponding loadings.

High flow periods produced dilution effects such as during the rainfall/snow melting conditions of 16 November 1989, shown on Figure 7.5. During this event, the Fe_T concentrations decreased from 1440 mg/L to 890 mg/L (a drop of 40%) when the flow increased from 15 m^3/L to 62 m^3/h (a 400% increase). Assuming no contamination from rain or melted snow, the calculated Fe_T concentrations at a measured flow rate of 62 m^3/h after dilution should have been below 400 mg/L (instead of the measured 890 mg/L). The higher than expected Fe_T level could have been produced by flushing of oxidized material within the tailings, as a consequence of the sudden rise in the water table. The rise in the water table could be observed on the field during rainfall events from the position of the seepage face on the slope of the tailings dam. It should be noted that the levels of total iron did not reach the "pre-rainfall" levels, even after a 36 hour period due to a continued flushing of pore water after the rainfall event.

Watershed studies by Sklash (1975) showed that a significant portion of the water from peak run off could be pore water. Blowes and Gillham (1987) made similar observations at the Elliot Lake Uranium Tailings and concluded that groundwater represents an important pathway for the movement of oxidation products in tailings.

Linear regression analysis indicated a high correlation ($r^2 = 0.92$) between the overall Fe_T loading values (mass of iron per unit time) and the corresponding flow. Variations in metal concentrations were rather small (C.V. 20%). The total loading along the western dam was obtained from the regression analysis as follows:

$$\text{Iron Loading} = [1.35 \times \text{Concentration}] \text{ discharge} + 0.15 \quad [18]$$

The metal concentrations were measured at seven different periods between May and August in the western seepage ditch upstream and downstream from the Station 2 flume. The results were similar to the range of values (Fe_T values varied between 900 and 1400 mg/L) found from water samples collected automatically at Station 2.

7.5 WATER BALANCE EVALUATION

An estimate of the water balance components can be obtained using empirically derived curves from the U.S. Soil Conservation Service (Mockus, 1972). The SCS curve number (CN) method is widely used for predicting direct run-off and infiltration from rainfall. The method is based on values of soil water content and porosity. Three other soil moisture properties were estimated using tables from Schroeder et al. (1984): the tailings wilting point or lower limit of soil water storage in volume/volume; the tailings field capacity or water content at which any additional water will percolate through the soil; the minimal infiltration rate. The SCS method has been incorporated in several computer programs including the Hydrologic Evaluation of Landfill Performance (HELP) model (Schroeder et al, 1984), which is described in Appendix C. The HELP model was used to perform a set of simulations using data from Table 7.4.

The HELP model incorporates four types of soil layers: the vertical percolation layer, the lateral percolation layer, a waste layer, and a barrier layer. To perform the HELP simulation, the tailings section was described using the different type layers. Thus, the unsaturated top layer was assumed to act as a vertical percolation layer, the saturated zone as a lateral drainage layer, and the underlying clay as a barrier layer.

Results indicated that, in most parts of the tailings surface, approximately one fifth of the total precipitation would infiltrate the tailings, which would amount to approximately 200 mm of water for the year 1988. Infiltration would be less than this value on the tailings dam faces due to the 3:1 slope and the high water table levels. More infiltration would occur in the spring and fall than in the summer months. Computed infiltration values were 166 mm from October to April and 34 mm from May to September. Other values are shown in Table 7.5. Annual water storage inside the tailings was assumed to be zero, which is realistic considering the small difference in water levels in the tailings on a yearly basis. The values in Table 7.5 are compatible with values measured during the study period (Table 7.1) and those reported by the Quebec Ministry of Environment at the Kinojevis River weather station, near Rouyn. Table 7.5 also shows volume estimates for the entire 40 ha surface of the tailings. Estimated values of infiltration and run-off, which add up to a total annual volume of

TABLE 7.4
INPUT PARAMETERS FOR HELP MODEL
(AVERAGE BETWEEN SECTIONS A-A' AND B-B')

	LAYER 1 UNSATURATED TAILINGS	LAYER 2 SATURATED TAILINGS	LAYER 3 CLAY
THICKNESS (CM)	152.4	304.8	457.2
POROSITY (VOL/VOL)	0.2700	0.2700	0.4300
FIELD CAPACITY (VOL/VOL)	0.2000	0.2000	0.3600
WILTING POINT (VOL/VOL)	0.1200	0.1200	0.2800
INITIAL SOIL WATER CONTENT (VOL/VOL)	0.1500	0.2700	0.4300
SATURATED HYDRAULIC CONDUCTIVITY (CM/S)	0.00009999	0.0000100	0.00000010
SLOPE (DEGREES)		0.00	
DRAINAGE LENGTH (M)		200.00	

GENERAL SIMULATION DATA

SCS RUNOFF CURVE NUMBER	90.00
TOTAL AREA OF COVER	40. HA
EVAPORATIVE ZONE DEPTH	38.10 CM
UPPER LIMIT VEG. STORAGE	10.28 CM
INITIAL VEG. STORAGE	5.71 CM
INITIAL SNOW WATER CONTENT	7.62 CM
INITIAL TOTAL WATER STORAGE IN SOIL AND WASTE LAYERS	301.75 CM

TABLE 7.5
ANNUAL WATER BALANCE AT THE WAITE AMULET SITE

COMPONENT	AMOUNT (cm)	VOLUME (1000 m ³ /a)
Precipitation (P)	99.0	396.0
Run-off (R)	19.1	76.4
Evapotranspiration (ET)	55.6	222.4
Infiltration (I)	24.3	97.2
Change in storage (ΔS)	0.0	0.0
Seepage & leakage ($\Delta S + L$)	24.3	97.2

1.73 x 10⁵ m³ compare well with volumes of water treated at the treatment plant in 1986 and 1987, which were respectively 6.38 x 10⁵ m³ and 1.15 x 10⁶ m³, considering that the total drainage area for the collection pond is approximately 230 ha, or 5.7 times the area of the tailings.

The estimated infiltration value of 0.2 m/a (Table 7.5) can be verified by calculating a corresponding base flow, assuming an average length of section of 180 m contributing to flow into the 700 m long ditch. Resulting calculated base flows would be in the order of 2.8 m³/h, which is well within the observed range of 1.5 to 4.1 m³/h mentioned at the beginning of Section 7.4.

Future studies could concentrate on refining water balance estimation techniques, especially in the case of infiltration. Uncertainties in the infiltration estimate are evaluated to 30 percent, and would be due to the variable thickness of the tailings and clay layers, the hydraulic conductivity measurements, and the anisotropic nature of the tailings deposit.

A better estimate of infiltration values using the SCS method could be obtained after measuring tailings wilting point, field capacity and minimum infiltration rate on tailings samples. The advantages of using the HELP model is that it incorporates the SCS method, and that it can be used to simulate different layer configurations such as in the case of a composite soil cover. Other methods for measuring infiltration and water balance should be evaluated for the possibility of obtaining more accurate estimates, as these will be directly related to volumes of AMD produced by tailings impoundments. Differentiation between the leakage and seepage components of the water balance will be discussed in the next section.

8. FLOW MODELLING

8.1 Method

Pore water flow along sections A-A and B-B (Figure 8.1) of the tailings was simulated by two-dimensional numerical flow modelling. The model used was a steady state finite element model based on Frind and Matanga (1985).

Typical boundary conditions along the sections are illustrated in Figure 8.2. A list of the parameters involved in the simulations and their respective units is given in Table 8.1. The origins of the sections ($x=0$) were taken at the approximate location of the groundwater divide, at the center of the tailings, where a zero-flux boundary ($dq/dx = 0$) was specified. The limit of the section ($x = L$) was set at the location of the seepage collection ditch, at which point the potential (ϕ) was assumed to be constant and equal to the mean elevation of the water table along the seepage face at the toe of the tailings dam.

In order to simulate observed field conditions, anisotropy factors between vertical and horizontal hydraulic conductivities were incorporated in the models. This anisotropy is likely to be produced by the fine-grained horizontal ("slime") layers observed in the tailings. The infiltration flux value along the sections was kept near the value of 0.20 m/a estimated in Section 7.3. To simulate the difference in grain size between the north and south section of the tailings, hydraulic conductivity and infiltration fluxes used for Section A-A' was slightly lower than the one used for Section B-B'.

For the calibration of the model, hydraulic conductivities and infiltration values were adjusted within the estimated limits until the simulated hydraulic head distribution agreed with the hydraulic heads measured in the field.

TABLE 8.1
DESCRIPTION OF FLOW SIMULATION PARAMETERS

Parameter	Description	Units
q_I	Infiltration flux	L/T
q_c	Leakage flux	L/T
K	Hydraulic conductivity	L/T
K_n	Horizontal conductivity	L/T
K_y	Vertical conductivity	L/T
K_x/K_y	Anisotropy factor	-
h	Hydraulic head at ditch boundary	L
H	Hydraulic head at divide boundary	L
L	Length of section	L
q_o	Outflux at ditch boundary	L/T
Q_o	Outflow at ditch boundary	L ³ /T

8.2 Results

The simulated flow nets for Sections A-A and B-B are shown in Figures 8.3 and 8.4. A comparison between predicted and measured hydraulic head values in each piezometer in the two sections are presented in Tables 8.2 and 8.3. Mean differences for simulations were 4% for Section A-A (Figure 8.3) and 8% for Section B-B (Figure 8.4). Figures 8.3 and 8.4 also list parameter values used for each flow net.

The total length of Section A-A (L) was 150 m. The bottom of the model was set at an elevation corresponding to the level of the tailings-clay interface, which is sloped at approximately 5%. Hydraulic head at the ditch (h) was set at 2.5 m, approximately equal to the vertical distance between the bottom of the ditch and the mean position of the seepage face. Horizontal hydraulic conductivity (K_x) was set to 100 m/a (3.2×10^{-4} cm/s), while vertical hydraulic conductivity (K_y) was 1 m/a (3.2×10^{-6} cm/s), giving an anisotropy ratio (K_x/K_y) of 100. An infiltration flux of 0.15 m/a was set over the section. A leakage across the bottom boundary into the clay (q_b) of a value of 0.01 m/a was incorporated. Resulting total outflow into the ditch (Q_d) was 22.4 m³/a.

Because of a simpler geometry, Section B-B' was easier to model than Section A-A'. The total length (L) of Section B-B was 200 m. The bottom of the section was assumed to be horizontal. Hydraulic head at the ditch boundary (h) was set to 3.5 m. K_x and K_y were respectively set to 160 m/a and 1.6 m/a (5×10^{-4} and 5×10^{-6} cm/s). With an infiltration flux equal to 0.2 m/a over the total 200 m length of the section, the outflow at the ditch boundary, by continuity, was equal to 40 m³/a.

8.3 Discussion

The use of the stream function model enables a good representation of streamlines and potential lines within the flow domain. Assuming the selected boundary conditions are correct, the flow nets of Figures 8.3 and 8.4 can be used to trace the pore water flow paths in the tailings. It can be seen that, because of the tailings geometry and the effect of anisotropy in the hydraulic properties, flow in the tailings would be dominantly

TABLE 8.2

CALIBRATED AND MEASURED POTENTIALS OF PIEZOMETERS ALONG SECTION A-A'

Piezometer	Calibrated Potential (m)	Measured Potential (m)	% Difference
15-1	6.68	7.05	+5.2
15-2	7.00	7.53	+7.0
15-3	-	-	-
15-4	6.61	6.89	+4.0
28-1	6.10	6.2	+1.6
28-2	6.24	6.54	+4.6
28-3	-	-	-
28b-1	5.89	6.06	+2.8
29-1	5.31	5.34	+0.5
29-2	-	-	-
30-1	4.88	4.83	-1.0
30-2	5.16	5	-3.2
21-1	4.35	4.44	+2.0
21-2	4.79	4.67	-2.5
31-1	-	-	-
31-2	3.73	3.27	-14.0
31-3	-	3.46	-
32-1	-	-	-
32-2	-	2.30	-

TABLE 8.3

CALIBRATED AND MEASURED POTENTIALS OF PIEZOMETERS ALONG SECTION B-B'

Piezometer	Calibrated Potential (m)	Measured Potential (m)	% Difference
11-1	7.16	7.74	+7.5
11-2	7.35	8.27	+11.1
11-3	7.51	8.79	+14.5
33-1	6.40	6.13	-4.4
33-2	6.70	6.51	-2.9
33-3	-	-	-
34-1	5.52	5.26	-4.9
20-1	4.47	4.1	-9.0
20-2	4.87	4.5	-8.2
35-1	3.94	3.58	-10.0

horizontal and shallow. For example, in Section B-B', pore water from the shallowest well at Station WA-11 would be travelling along the same streamtube as pore water from WA-34 although the two stations are located almost 100 m apart. The very tight succession of streamtubes at the end of the flow sections can explain the rapid changes in pore water chemistry with depth at Stations WA-20 and WA-21, as discussed in Section 5.2. Indeed, the chemistry of the pore water along each streamtube should reflect the reactions which occurred along the path of the streamtube; minimal mixing of water between streamtubes would have occurred.

Stream function contour intervals were selected so that each flow tube carried $5 \text{ m}^3/\text{a}$ of flow through the section. The amount of flow crossing each boundary of the section can therefore be visually estimated by simply counting the number of stream tubes crossing the boundary. Simulated outflows to the seepage collection ditch for Sections A-A' and B-B' of respectively $22.4 \text{ m}^3/\text{a}$ and $40 \text{ m}^3/\text{a}$ compare well with the average field-measured baseflow of $31.2 \text{ m}^3/\text{a}$.

The amount of leakage flux of $0.01 \text{ m}/\text{a}$ was incorporated in Section A-A' based on evidence from field observation of the clay unit sampled in the north portion of the site. Because leakage flux and anisotropy in hydraulic conductivity have a very similar effect on the flownet, it is impossible to determine the magnitude of these two parameters independently. Unless a measurement of one of these parameters on the north portion of the site is made, no definite evaluation of leakage or anisotropy can be made using the numerical modelling.

Average horizontal velocities calculated from the simulations were $7.5 \text{ m}/\text{a}$ for Section A-A and $9.3 \text{ m}/\text{a}$ for Section B-B. Average vertical velocities in the tailings were $0.45 \text{ m}/\text{a}$ (Section A-A) and $0.49 \text{ m}/\text{a}$ (Section B-B). The pore water horizontal velocities within the tailings were previously estimated to range from 0.4 to $9.0 \text{ m}/\text{a}$, with higher velocities of $35 \text{ m}/\text{a}$ in the tailings dam (Siwik, 1986). The average velocities calculated with the flow model would therefore correlate well with the previous estimates.

9. PORE WATER EVOLUTION

As described in section 5.2, acidic pore waters are generated from oxidation of sulphides in the unsaturated zone of the tailings. The low-pH plume then moves downwards with slight buffering in the unsaturated and shallow saturated zones. In the saturated zone, pore water will flow in predominantly east-west directions, and will be controlled in part by the clay layer underlying the tailings, as shown in the simulated flownets of Figures 8.3 and 8.4. The simulated flowlines suggest that flow occurring in the vicinity of the seepage ditch is horizontal. Acid water produced at the limits of the impoundment will therefore move horizontally towards the seepage ditches. Acid waters generated in the central portion of the impoundment will flow downwards and reach the tailings-clay interface, along which it will flow. A small amount of seepage will slowly infiltrate into the clay.

As seen in section 5.2, the metals travelling along with the acidic pore water are mainly iron and zinc. Zinc levels remain constant and relatively low, and zinc is released into the surface ditches without undergoing any chemical reaction. On the other hand, iron levels, which are relatively high near the active oxidation zone, can precipitate from solution either as siderite (FeCO_3) or ferric hydroxide ($\text{Fe}(\text{OH})_3$) to form minerals, such as jarosite, goethite, lepidocrocite and siderite.

The review of acid generation processes occurring in the unsaturated zone of the tailings (Section 3.1) showed how most of the ferric iron generated in the tailings will be either precipitating as ferric hydroxide or consumed by secondary pyrite oxidation reactions. Most of the iron remaining in solution in the saturated zone will be in reduced form.

Any ferric iron, still in solution when seepage is released to the surface drainage system, is the main contributor to acidification; Fe^{2+} oxidizes to Fe^{3+} rapidly once oxygen becomes readily available, iron hydroxide forms and coats the bottom of the ditch with red sludge and releases acidity.

As indicated above, iron precipitation does not take place within pore water originating from the edges of the impoundment. Hence, this area is currently the major contributor to acid loading. It is expected that, as time goes on, the pH at the bottom of the tailings

will become more acidic and iron precipitation will cease. More acid loading to the collection ditches will then be produced at the centre of the impoundment. Ultimately, reduction of acid loading will occur once all the pyrite in the tailings unsaturated zone becomes oxidized and all acid pore water has drained out of the impoundment. Acid generation should first terminate in the northern section of the tailings, where the water table is high. In the southern section and along the tailings dam, acid generation should still continue for several hundred years due to the larger volume of unsaturated sulphide material.

10. GEOTECHNIQUE AND HYDROGEOCHEMISTRY OF CLAYEY SUBSOIL

10.1 Introduction

The results of the flow modelling (Chapter 8) suggested that some leakage of tailings pore water into the underlying clay layer could be occurring. A laboratory investigation of the hydrogeochemistry of the clay was therefore undertaken, to verify the presence of tailings pore water in the clay. The field and laboratory methodologies are described in detail below, and the results are interpreted regarding the movement of tailings water into the underlying clay.

10.2 Sampling

10.2.1 Field Sampling of Clay

In order to obtain high quality samples of clay soil for the aforementioned investigation, two auger holes were drilled beside WA-11 and WA-20. To provide background uncontaminated clay, a third hole was drilled south of the dam next to the roadway, along a section line through WA-11 and WA-20 (Figure 4.1). Sampling of the clay in these holes was carried out with 7.6 cm (3 -in) diameter and 61 cm (2 ft) long Shelby tubes in the hollow stem augers below the tailings. Care was taken to ensure that the tailings/clay interface was accurately and sufficiently sampled. The Shelby tubes containing the recovered clay samples were waxed at their ends and then transported to the laboratory. Upon arrival in the laboratory, the tubes were stored in a temperature-controlled (approximately 8° C) room. Samples used in the current investigation were extruded within 10 days after drilling.

10.2.2 Laboratory Sampling

Extruded clay samples were sectioned into 15 cm subsamples, sealed with microcrystalline wax and then stored at 8° C to preserve the in situ water content and pore water composition. During the extension, subsamples of clay were also taken for bulk density and water content measurements.

Clay pore water was sampled by squeezing of subsamples in a pneumatic squeeze apparatus at 12 MPa in a stainless steel loading cell. Each squeezing operation was performed to approximately 100% primary consolidation which was completed within 5 to 8 h, depending on the in situ water content of the clay. Squeezed pore waters were collected in clean, plastic vials tightly sealed and stored in a laboratory refrigerator at 7° C prior to analysis. Pore water samples used for metal analyses were acidified with concentrated nitric acid prior to storage.

As described later (Section 10.5), pressure dependency on pore water chemistry was assessed to ensure that, at the squeeze pressure of 12 MPa, only free pore water was released from the clay.

10.3 Analyses

10.3.1 Pore Water Analysis

Metal, major cation, and anion analyses and pH measurements were performed on pore waters obtained, as described in Section 10.2.2. Total dissolved Al, Si, Fe, Cu, Cd, Zn and Pb were determined by ICP (inductively-coupled plasma) to an analytical precision of ±3 percent. Pore water Na, K, Ca and Mg were determined by AAS (atomic absorption spectrophotometry), also to a precision of ±3 percent. The detection limit for these elements was 0.02 mg/L, with the exception of Cd which had a minimum detection limit of 0.005 mg/L. Dissolved anions (SO_4^{2-} , Cl^- and NO_3^-) were determined by ion chromatography to an analytical precision of ±10 percent. The detection limit was 5 mg/L. All the pore water analysis, with the exception of pH, was contracted to Enviroclean, an analytical laboratory in London, Ontario. The pH measurements were performed at the Noranda Technology Centre using a combination electrode calibrated in suitable buffers.

10.3.2 Soil Analysis

Clay soil samples were analyzed for total metal and sulphate concentrations. These analyses were performed by X-ray Assay Laboratories Limited of Toronto, Ontario. Total metals were determined by acid digestion of bulk soil samples using HF, HCl, HNO₃ and HClO₄ and subsequent analysis of the resulting extract by ICP. Soil sulphate was determined by wet chemistry.

The pH of the soil was measured on 1:5 soil : distilled water ratio using a combination electrode calibrated as previously described (Section 10.3.1).

10.3.3 Mineralogy

The mineralogy of the clay was determined on two samples located within the top 30 cm of the clay underlying the tailings dam at station WA-20. For comparison, the mineralogy of a background clay sample was also determined. The mineralogical analysis involved X-ray random powder diffraction of pulverized bulk soils and oriented diffraction of -2 μm fines of both natural and potassium-saturated specimens.

10.4 Geotechnical Testing

10.4.1 Index Properties

Index properties (bulk density, grain size distribution, specific gravity, Atterberg limits and natural water contents) were measured on clay soils located below the tailings at Station WA-11 and WA-20. For comparison, a few samples from the background hole were also analyzed for index properties. All the measurements were performed in accordance with standard geotechnical procedures (Bowles, 1986).

10.4.2 Shear Strength

The undrained shear strength of the clay was determined on clay samples from WA-11 and WA-20 by a laboratory vane method with a Geonor H-60 Inspection Vane Tester to an accuracy of +/- 10 percent. The measurements were made on Shelby tube samples held vertically in a floor-mounted ELE23-495 Universal extruder. The samples were extended to the desired depth and the vane measurements performed directly in the Shelby tube.

10.4.3 Hydraulic Conductivity

Equipment

The hydraulic conductivity, K , of the clay was determined in the laboratory using a Geostore Brainard-Kilman triaxial permeability equipment. This equipment is presented in Figure 10.1. The system consists of triaxial cell, control panel, bladder accumulator for supply of permeant to the cell, and a data acquisition system. The plexiglas cell is capable of testing samples up to 102 mm in diameter. The use of the stainless steel bladder accumulator allows potentially corrosive permeants (for example, acid mine drainage) to be used outside of the burrettes on the panel.

Pressures required for hydraulic conductivity testing were provided by a central air pressure source. The pressure is directed to three fluid reservoirs through a system of regulators on the control panel. The regulators control the inflow, outflow and confining fluid pressures applied to the sample. A four-way valve on the panel allows the selected cell, inflow and outflow pressures, to be read on a digital read-out. Double tube volume change indicators located between the reservoirs and the sample measure flow in and out of the sample to the nearest 0.05 mL.

Permeant is supplied to the bottom of the sample and exits through the top of the cell. The hydraulic gradient is selected by the difference between the inflow and outflow pressures. Side wall leakage is minimized by confining pressure which also simulates

the overburden pressure on the sample. A special burette system was designed to collect effluent exiting the top of the sample. This system prevents the effluent from going into the outflow burette mounted on the panel.

Sample Preparation and Saturation

The samples used in the K tests consisted of clay soils located below the tailings at Station WA-20. The samples were extruded from 7.3 cm diameter Shelby tubes and sliced to the desired length for the K tests without the need for trimming. The test specimen was sandwiched between filter papers and porous stones, and set on the base pedestal of the triaxial permeameter. The top cap was placed on the sample, and a rubber member was used to enclose the top cap, sample, and the pedestal. The membranes were then sealed to the top and bottom caps with O-rings.

The samples were saturated by application of 10.55 kPa back pressure prior to permeation. A relatively low cell pressure of approximately 14 kPa was applied to keep the membrane in contact with the sample. Following this, the cell, inflow and outflow pressures were increased to 145.0, 124.1 and 96.5 kPa respectively. The pressures were maintained for 24 h prior to testing to ensure complete saturation. A pore pressure reaction test was performed on the sample and gave a B-value of 0.98 which suggested that the sample was sufficiently saturated and that testing could proceed.

Oedometer consolidation tests were also performed to provide indirect estimates of the hydraulic conductivity.

Sample Permeation

Two hydraulic conductivity tests were performed. The first test was on a 11.8 cm length specimen with deionized distilled water as the permeant and a gradient of 19. The second test was performed on a shorter specimen (6.96 cm long) at a gradient of 30 with simulated pore water as the permeant. The chemical composition of this permeant is presented in Table 10.1.

TABLE 10.1
 CHEMICAL COMPOSITION OF SIMULATED PORE WATER
 USED IN THE HYDRAULIC CONDUCTIVITY TESTS

<u>Species</u>	<u>Concentration (mg/L)</u>
Sodium	25
Potassium	9.2
Calcium	80
Magnesium	11
Sulphate	380
pH	6.90 (pH units)

The selected cell, inflow and outflow pressures used in the distilled water tests were equivalent to inflow and outflow effective stresses of 35 and 60 kPa, respectively. The corresponding effective stresses in the test with the simulated pore water were 30 kPa for inflow and 65 kPa for outflow, respectively.

10.5 Quality Assurance and Quality Control

Pore water samples for metal analysis were acidified and stored at 4°C prior to shipping. The samples were tightly sealed in plastic culture tubes to prevent losses by spillage during shipping. In order to ensure analytical accuracy, both spiked and blank water samples were submitted along with the squeezed clay pore water for ICP and IC analyses. The results obtained on the spikes and blanks were very good. Total metal analyses were done on the spikes and samples, and the results were within 5 percent.

It is conceivable that squeezing of clay soils at very high pressures could affect the lattice structure of the clay minerals and the composition of the diffuse double layer. Release of double layer or adsorbed water along with free pore water could result in erroneous pore water chemistry. The pressure dependency of the pore water chemistry

was investigated for the range of stresses used in all the squeezing operation. Subsamples of clay soil were squeezed at incremental stresses from 0 to 12 MPa, and the calcium, magnesium, sodium, and potassium concentrations in the resulting pore waters were determined at each stress increment. The results of the analyses, shown in Figure 10.2, indicate that the concentrations are constant for all the species analyzed, with the exception of Ca^{++} , within the range of applied squeeze pressures. The slightly lower Ca^{++} concentrations at 12 MPa are most probably experimental errors. Since none of the species increased in concentration with increase in applied squeeze pressure, it can be concluded that adsorbed cations and hence adsorbed water were not released.

10.6 Results

10.6.1 Geotechnique

Index properties obtained on the saturated tailings and the clayey subsoil at Stations WA-11 and WA-20 are presented in Figures 10.3 and 10.4, respectively, and also in Table 10.2. The water content of the tailings at WA-11 is about 24 percent with a slight increase to 35 percent below the interface with the clay. In the clay the water contents are higher and average about 50 percent in the profile. The lower contents (30 to 35 percent) observed near the interface suggest mixing of tailings with clay or the existence of a desiccated crust in the upper part of the clay. The mixing and/or the crust is also responsible for the slightly higher undrained shear strength, C_u , (85 kPa) of the interface 'clay'. The average C_u of the deeper clay is about 20 kPa. As shown in Figure 10.2, the mixing zone also gave a slightly higher bulk density of 1.90 Mg/m^3 , compared to 1.70 Mg/m^3 for the deeper clay. The higher density correlates with the lower water content and the higher shear strength observed in the upper part of the clay layer.

At WA-20, the water content and undrained shear strength profiles show essentially the same trends as those at Station WA-11. Water contents in the clay average 50 percent with a slight decrease to about 35 to 40 percent in the clay/tailings interface. The undrained shear strength decreases from about 50 kPa in the mixing zone to an average of 25 kPa in the deeper clay. The bulk density of the clay at Station WA-20 shows a slight increase (from 1.70 to about 1.84 Mg/m^3) with depth. The reason for this increase is not known and does not correlate with the water content and strength data.

TABLE 10.2
SUMMARY OF INDEX PROPERTIES OF CLAY
UNDERNEATH THE TAILINGS IMPOUNDMENT

Borehole	Depth m	% Clay ($<2 \mu\text{m}$)	% Silt ($>2 \mu\text{m}$)	Liquid Limit %	Plastic Limit %	Specific Gravity Gs
WA-20	5.72	-	-	-	-	2.70
	5.96	82	18	-	-	2.70
	6.11	85	15	-	-	-
	6.33	78	22	62	24	-
	6.78	-	-	-	-	2.71
	7.92	-	-	-	-	2.72
	8.62	52	48	-	-	-
WA-11	12.50	-	-	-	-	2.70
XF3	5.94	-	-	-	-	2.70
	6.10	65	28	-	-	-

Figure 10.5 shows a typical grain size distribution curve for the clayey subsoil at Station WA-20. The grain size data are summarized in Table 10.1 along with specific gravities, and Atterberg limits. The data indicate that the clay is generally a silty clay and contains 52 to 85% clay size particles ($<2 \mu\text{m}$). From the Atterberg limits presented in Table 10.2, a plasticity index of 38 percent is obtained for the clay. The specific gravity of the clay ranges from 2.70 to 2.73; with 2.70 being representative.

The results of the hydraulic conductivity, K, tests obtained on the clay soil directly below the tailings dam at WA-20 are presented in Figures 10.6, and 10.7. Figure 10.7 shows the K data on a 11.8 cm long and 6.92 cm diameter sample permeated at a hydraulic gradient of 19 with deionized distilled water. The final inflow and outflow hydraulic conductivities were 6.5 and 7.5×10^{-8} cm/s, respectively, at 22,400 minutes or approximately 0.22 pore volumes. The slight difference in the final inflow and outflow conductivities is explained by the fact that steady state was not attained. The values, however, provide a rough estimate of K with respect to water. A shorter sample (6.96 cm long), but of the same diameter, was used for the K test involving simulated pore water at a gradient of 30. The results, shown in Figure 10.7, indicate that the equilibrium or steady state hydraulic conductivity of the clayey subsoil with respect to the pore water is approximately 9.0×10^{-8} cm/s at 45,000 minutes or 1.35 pore volumes. The use of simulated pore fluid ensures that potential changes in K resulting from chemical influences are minimized. The slightly lower K value for the distilled water test may be attributed to the greater sample length (Carpenter et al., 1968).

The hydraulic conductivity of the clay beneath the tailings dam at WA-20, calculated from oedometer tests, was of the order of 1 to 2×10^{-8} cm/s.

10.6.2 Hydrogeochemistry

Chemical Profiles at WA-11

The total soil and pore water chemical profiles for the clayey subsoil at Station WA-11 are presented in Figures 10.8 to 10.13 inclusive for iron, zinc, lead, copper, aluminum, and sulphate. The corresponding pH profiles are shown in Figure 10.14.

Total iron occurs in the overlying tailings at about 25 percent, mostly as a result of the presence of unoxidized pyrite and pyrrhotite, and oxidized products such as jarosite. In the clayey subsoil, the total iron occurs at about 4.5 percent and is uniform at this value in the 5-meter profile. The iron concentration in the tailings pore water is about 0.65 mg/L. The values in the clay are much lower and range from 0.01 to 0.14 mg/L. The iron profile in the clay does not show any particular trend and suggests that the observed levels are probably background uncontaminated values.

The total zinc concentrations in the tailings range from 17,100 to 33,600 mg/kg and reflect the presence of sulphides (probably sphalerite). The levels in the clay are much lower, with a value of about 140 mg/kg near the interface with the tailings. The levels drop slightly to about 105 mg/kg at 1 m and remain at this value till the end of the profile at 16.5 m. The value of 105 mg/kg represents background level. The zinc level in the tailings pore water averages about 0.36 mg/L directly above the clay layer. The levels in the clay are lower (0.025 to 0.20 mg/L) and do not provide any evidence of contamination from acidic pore water in the tailings.

Lead concentrations in the tailings range from 618 to 882 mg/kg. The clay levels range from about 3.5 mg/kg near the tailings/clay interface and then drop to only 2 mg/kg in the rest of the profile. These values are relatively low. In the clay pore water the lead concentrations are below 0.2 mg/L at all depths.

The total copper levels in the tailings range from 3200 to 8000 mg/kg. In the clayey subsoil, total copper is 48 mg/kg near the interface and decreases slightly to about 40 mg/kg in the rest of the profile. The clay pore water copper ranges from 0.02 to 0.23 mg/L and, again, does not reflect contamination from the overlying tailings.

The total aluminum concentrations in the tailings range from 3.0 to 4.0 percent. As expected, the level in the clay is much higher (8.5 to 9 percent) and reflects the presence of alumino-silicates. Dissolution of some alumino-silicates in the tailings is probably responsible for the pore water aluminum level of 1.0 mg/L in the tailings. The corresponding values in the clay are low and range from 0.2 to 0.60 mg/L. It is quite obvious that there has not been any dissolution of the clay. Most probably, acidic pore water from the tailings has not entered the clayey subsoil. Dissolved silicon concentrations in the clay pore water below the tailings at WA-11 range from 4 to 10 mg/L and are even much lower than the value of 12 mg/L observed in the background uncontaminated borehole (XF3) located outside the tailings impoundment. This confirms the proposition that the clay soil underneath the tailings has not been attacked by acidic pore water.

The total sulphate in the tailings solids is about 0.5 to 0.8 percent. In the clay, the levels are much lower and range from 0.1 to 0.3 percent. The pore water sulphate levels show a value of about 1000 mg/L in the tailings and decrease to about 50 to 460 mg/L in the clay, in the top

1 m zone directly below the tailings. In the deeper section of the profile the levels average about 150 mg/L. The background uncontaminated pore water outside the impoundment gave a sulphate concentration of 30 mg/L. The above background levels observed at WA-11 are most probably derived from sulphate in the original mill process water which has now entered the clay as a result of diffusion. Copper and ammonium sulphates were among the reagents used in the flotation of zinc from milling of the West MacDonald ore at Waite Amulet (CIM, 1957).

As shown in Figure 10.8, the pH at WA-11 ranges from 7.0 to 8.2 for the tailings solution and then increases to 8.50 in the clay. The clay soil solution and the squeezed pore water show essentially the same pH trend, that is, remains constant at about 8.50 in the entire profile. The slightly higher pH of the clay may be explained by buffering from soil hydroxides or alumino-silicates.

Chemical Profiles at WA-20

Chemical profiles for WA-20, similar to those discussed above for WA-11, are presented in Figures 10.15 to 10.21. A comparison of the profiles shows that the trends observed at WA-20 are similar to those noted for WA-11. The SO_4^{2-} levels in the clay pore at WA-20 are slightly lower (less than 100 mg/L) than those observed for WA-11 and decrease slowly with depth. The SO_4^{2-} concentration above 30 mg/L may be explained, again, by diffusion.

The pH profiles at WA-20 (Figure 10.21) begin in the clay and show a slight increase with depth from 6.8 to about 7.7 for the soil solution. The pH of the clay pore water is about 8.20 and remains essentially constant with depth. The slight decrease in the pH of the soil solution at WA-20 may be attributed to the presence of sulphides in the 'mixing zone' at the clay-tailings interface.

10.7 DISCUSSIONS

The clay soil underneath the Waite Amulet tailings constitutes part of varved sequences deposited some 8,000 to 10,000 years ago during the last phase of glacial Lake Ojibway (Quigley, 1980). Mineralogical analyses indicate that the clay consists of quartz, feldspars, interlayered illite, chlorite and smectite, and small amounts of carbonates.

The pore waters of the tailings directly above the clay at WA-11 and WA-20 are neutral and contain metals (iron, zinc and copper) at near background concentrations of 2 mg/L or less. However, sulphate levels are higher than background (350 and 1000 mg/L at WA-20 and WA-11, respectively). The lower metal concentrations may be explained by retardation reactions such as precipitation, co-precipitation, and adsorption in the tailings (Section 5.2). Jarosite and gypsum precipitation will reduce the sulphate levels in the pore waters moving through the tailings. All the original mill waters would have been displaced, based on pore water velocity calculations (see Section 8) and a travel time of 50 years. Therefore, the high sulphate levels in the tailings pore water directly above the clay are most probably derived from sulphide oxidation in the unsaturated zone. At WA-20, flushing of oxidized products out of the tailings into the nearby collection ditch may have reduced the sulphate level to 350 mg/L.

Sulphate profiles in the clay at WA-11 and WA-20 show concentrations that are higher than the estimated background value of 30 mg/L to depths of 3 to 5 m. The ground water velocity of the clayey subsoil is much lower than that of the tailings. Using an observed vertical hydraulic gradient of 0.25, a porosity of 0.46 and a hydraulic conductivity of 1×10^{-7} cm/s for the clay, the vertical velocity is calculated to be 1.7 cm/a. For a period of 50 years, the distance travelled by advection will be 0.85 m. The grain size distribution of the clay and the results already presented (Section 10.6.1) indicate that the hydraulic conductivity of 1×10^{-7} cm/s used in this calculation is reasonable. Therefore, flow of oxidized water from the tailings unsaturated zone cannot explain the sulphate concentrations in the clay. It is most probable that SO_4^{2-} , contained in the original mill water in the tailings, has migrated through the clay by diffusion. High sulphate levels in the original tailings pore water at the time of tailings deposition (approximately 50 years ago), compared to low levels in the clay deposit, will result in a chemical concentration gradient. This gradient will result in a diffusive flux which depends on the diffusion coefficient of SO_4^{2-} in the clay. SO_4^{2-} concentration in the clay pore water will also be controlled by chemical reactions such as gypsum precipitation.

The slightly higher values of total iron, lead, zinc and copper in the clay observed at the clay/tailings interface confirm the presence of a mixing zone. Mineralogical analysis revealed the presence of pyrite in this zone. This was inferred from measured values of geotechnical parameters (shear strength, water content and density) presented in Section 10.6.1.

Diffusive transport may also explain the sodium, calcium, and magnesium profiles shown in Figures 10.22 and 10.23. At WA-11, the potassium profile shows an increase in concentration with depth reflecting, most probably, K^+ desorption due to Ca^{++} or Mg^{++} adsorption. The adsorbed cation composition of the clay at WA-20 is presented in Table 10.3 and indicates that the cation exchange capacity is about 22.8 meq/100 g. Adsorbed metals (iron, zinc, copper and aluminum) were found to be very low in concentration (less than 0.025 meq/100 g for each species).

In conclusion, it should be mentioned that the concept of transport by diffusion in clay soils mentioned above is not new. Several authors, (including Desaulniers et al (1980), Crooks and Quigley (1984), Quigley and Rowe (1986), and Rowe (1988) have shown that chemical species move farther in fine-grained clayey soils by diffusion than by bulk pore water flow.

TABLE 10.3
 ADSORBED CATION COMPOSITION OF CLAY
 BENEATH TAILINGS DAM WA-20

Na^+	2.56	meq/100 g
K^+	2.47	"
Ca^{++}	11.86	"
Mg^{++}	5.89	"
Cation Exchange Capacity	22.78	"
Sodium Adsorption Ratio	6	(meq/L) ^{1/2}
Exchangeable Sodium Percentage	10	

Note: Adsorbed iron, zinc, copper, and aluminum were each less than 0.025 meq/100 g.

11. CONCLUSIONS

The study of acid pore water generation and movement in the Waite Amulet tailings has demonstrated that:

- 1) The most important control on the pyrite oxidation process is the availability of oxygen. In addition to contributing directly to oxidation, oxygen influences the production of ferric iron and the density of bacterial populations.
- 2) Oxygen concentration distribution with depth in the tailings define the depth of active oxidation. Oxygen movement within the tailings is controlled by diffusion.
- 3) Oxidation of sulphides in the deep unsaturated zone occurs at a rate dependent on pH, and will be very low. As sulphide in the shallow zone is depleted, the oxidation front will move downwards.
- 4) Acidic pore water is partly neutralized by buffering reactions occurring in the deeper unsaturated zone. The remaining acidity and dissolved metals will flow downwards with the pore water in the unsaturated zone until it reaches the water table.
- 5) Acid conditions in the shallow saturated zone become more neutral with depth due to buffering reactions, such as mineral dissolution and precipitation of minerals.
- 6) Pore water in the saturated zone will flow in a direction which varies across the area of the tailings. Flow in the central part of the tailings will be vertical and downwards; flow along the perimeter of the tailings will be horizontal.
- 7) Anisotropy in the hydraulic properties of the tailings is a major control on the flow of pore water in the tailings. The anisotropy is produced by the presence of fine-grained, horizontal ("slime") layers. It has the effect of promoting horizontal flow over vertical downward flow.

- 8) Along the west side of the tailings, the surface ditch collects most of the water infiltrating the tailings; in the northwest section of the impoundment, a small portion of the pore water flows through the bottom of the tailings into the underlying geological units.
- 9) Acid water collected in surface ditches around the tailings impoundment is produced by seepage rather than run-off.
- 10) Analysis of pore water quality and calculation of groundwater velocity in the clay suggest that tailings pore water does not penetrate deep into the clay layer on the south side of the tailings. Sulphate levels above background values, observed in the deeper layer of the clay, may be attributed to migration by diffusion.
- 11) Acid generation will last longer along the tailings dam and in the south section of the impoundment. In these areas, coarser tailings grain sizes induce lower water table levels, and larger volumes of unsaturated tailings available for oxidation.

12. RECOMMENDATIONS

Following are general recommendations which should apply to present and future tailings impoundments.

- 1) Measurement of hydrogeochemical parameters, such as mineralogy, dissolved metal and major ion concentrations should be performed at reactive tailings impoundments where information on AMD generation and loading is needed.
- 2) Measurement of infiltration and hydraulic conductivity of tailings should be performed at reactive tailings impoundments to evaluate the tailings pore water flow systems.
- 3) Characterization of soil layers underneath reactive tailings impoundments should be performed routinely to evaluate the potential for downward migration of oxidation products.

- 4) High water tables should be promoted by selective placement of fine-grained tailings across the site. Coarse-grained material, such as rock fill, should be avoided in tailings dam core construction, unless design features are incorporated to prevent water tables from dropping excessively.
- 5) Horizontal flow should be promoted by selective placement of horizontal fine-grained layers across the area of the tailings deposits. This could reduce downward vertical flow considerably, and facilitate the collection of AMD around the perimeter of the impoundments.
- 6) A standardized method for computation of water balances in inactive tailings impoundments should be developed. This could be based on methods used in the present study, such as the Guelph permeameter, the SCS method, and/or the HELP model.

Specific recommendations are made for the Waite-Amulet site, which might have later implications for other tailings sites.

- 1) Small-scale monitoring of rainfall and pore water pressures in the Waite-Amulet tailings should be done during rainfall events to confirm the effect of the rapid rise of the water table in the tension-saturated zone and its effect on seepage water quality.
- 2) The long-term compatibility of Waite-Amulet clay with acid water solutions should be determined through laboratory-scale testing.
- 3) Data collected at the Waite-Amulet site should be used to model the long-term acid generation rates of the tailings.
- 4) Data from the Waite-Amulet site should be used as background to study the effect of remediation options such as natural soil barriers.

REFERENCES

- Abdul, A.S. and R.W. Gillham (1984). Laboratory studies of the effects of the capillary fringe on streamflow generation, *Water Resources Research* 20 (6), p 691-698.
- Bowles, J.E. (1978). *Engineering properties of soils and their measurement*. McGraw-Hill Book Company, New York. 3rd edition.
- Blowes, D.W. and J.A. Cherry (1986). Hydrogeochemical investigations of the unsaturated zone of the Waite Amulet tailings site, WRI Award No. 1142401. A final report prepared for Noranda Research Centre.
- Blowes, D.W., J.A. Cherry, and E.J. Reardon (1987). The hydrogeochemistry of four inactive tailings impoundments: perspectives on tailings pore water evolution. Proceedings of the National Symposium on Mining, Hydrology, Sedimentology, and Reclamation, University of Kentucky, Lexington, Kentucky, 7-11 December, p. 253-261.
- Blowes, D.W., and R.W. Gillham (1988). The generation and quality of streamflow on inactive uranium tailings near Elliot Lake, Ontario. *Journal of Hydrology*, 97, p. 1-22.
- Blowes, D.W., and J.L. Jambor (1989). The pore water geochemistry and the mineralogy of the vadose zone of sulphide tailings, Waite Amulet, Quebec. Report to CANMET, DSS Contract 23440-7-9161/01-SQ.
- Brooks, B.W. (1981). Revegetation of the Waite Amulet tailings discharge areas. Noranda Mines Limited for Canadian Mineral Processors Conference, Ottawa, 20-22 January 1981.
- Caruccio, F.T., J.C. Ferm, J. Horne, G. Geidel, and B. Bagaz (1977). Paleoenvironment of coal and its relation to drainage quality. U.S. EPA Report EPA-600/7-77-067, 118 p.
- Caruccio, F.T., and G. Geidel (1987). The in-situ mitigation of acidic drainages - management of hydro-geochemical factors. Proceedings of the Acid Mine Drainage Seminar/Workshop, Halifax, Nova Scotia, 23-26 March, p. 479-497.

- Cornelius, R.J., and J.T. Woodcock (1958). Pressure leaching of manganese ore, Part I: Kinetic aspects. *Proc. Australian Inst. Mining Metall.*, 65.
- Crooks, V.E., and R.M. Quigley (1984). Saline leachate migration through clay: a comparative laboratory and field investigation. *Canadian Geotechnical Journal*, 21, p. 349 - 362.
- Daniel, J.A., J.R. Harries, and A.I.M. Ritchie (1980). Temperature distributions in an overburden dump undergoing pyritic oxidation. *Proceedings of the 4th International Symposium on Environmental Biogeochemistry and Conference on Biogeochemistry in Relation to the Mining Industry and Environmental Pollution*, p. 630-636.
- Dave, N.K., T.P. Lim, R.S. Siwik, and R. Blackport (1986). Geophysical and biogeochemical investigations of an inactive sulphide tailings basin, Noranda, Quebec. 1986 National Symposium on Mining, Hydrology, Sedimentology and Reclamation, University of Kentucky, Lexington, Kentucky.
- Davis, G.B., and A.I.M. Ritchie (1986). A model of oxidation in pyritic mine wastes, part 1 - equations and approximate solution. *Appl. Math. Modelling*, 10, p. 314-322.
- Davis, G.B., and A.I.M. Ritchie (1987). A model of oxidation pyritic mine wastes, part 3 - import of particle size distribution. *Appl. Math. Modelling*, 11, p. 417-422.
- Desaulniers, D.E., J.A. Cherry, and P. Fritz (1981). Origin, age and movement of pore water in argillaceous Quaternary deposits at four sites in southwestern Ontario. *Journal of Hydrology*, 50, pp. 231 - 257.
- Dubrovsky, N.M., J.A. Cherry, E.J. Reardon, and A.J. Vivurka (1985). Geochemical evolution of inactive pyritic tailings in the Elliot Lake uranium district. *Canadian Geotechnical Journal*, 22, p. 110-128.

- Feenstra, S., R.D. Blair, J.A. Cherry, J.L. Chakravitti, and C. Larocque (1981). Hydrogeochemical investigations of the two inactive tailings areas in the Elliot Lake uranium district, Ontario. Proceedings of the 4th Symposium on Uranium Mill Tailings Management. Geotechnical Engineering Program, Civil Engineering Department, Colorado State University, Fort Collins, Co.
- Frind, E.O., and G.B. Matanga (1985). The dust formulation of flow for contaminant transport modelling, 1 - review of theory and accuracy aspects. Water Resources Research, Vol. 21, No. 2, p. 159-169.
- Geidel, G, and F.T. Caruccio (1977). Time as a factor in acid mine drainage pollution. Proceedings of the 7th Symposium on Coal Mine Drainage Research, Louisville, Kentucky, 18-20 October, p. 41-50.
- Gouvernement du Québec, Ministère de l'environnement. Sommaire Quotidien, Station Rivière Kinévis, Ste-Foy, Québec.
- Harris, J.R., and A.I.M. Ritchie (1981). The use of temperature profiles to estimate the pyritic iron oxidation rate in a waste rock dump from an open cut mine. Water, Air and Soil Pollution, 16, p. 405-423.
- Harris, J.R., and A.I.M. Ritchie (1983). The microenvironment within waste rock dumps undergoing pyritic oxidation. Int. Symp. on Biohydrometallurgy, Cagliari, 1-4 May 1983.
- Hurlbut Jr., C.S., and C. Klein (1977). Manual of mineralogy, 19th edition, John Wiley and Sons, New York, 532 p.
- IUPAC (1985). Standard potentials in aqueous solution. Edited by A.J. Bard, R. Parsons, and J. Jordan. International Union of Pure and Applied Chemistry, Marcel Dekker Inc., New York, 834 p.
- Jambor, J.L. (1987). Character and depth of oxidation on the reactive acid tailings at the Waite Amulet tailings mine site, Noranda, Quebec. CANMET, MSL, Ottawa, July 1987.

- Kimball, B.A., and E.R. Lemon (1971). Air turbulence effects upon soil gas exchange. *Soil Sci. Soc. Am. Proc.*, 35, p. 16-21.
- Knapp, R.A. (1987). The biogeochemistry of acid generation in sulphide tailings and waste rock. *Proceedings of the Acid Mine Drainage Seminar/Workshop*, Halifax, Nova Scotia, 23-26 March, p. 47-65.
- Lacey, D.T., and F. Lawson (1970). Kinetics of the liquid-phase oxidation of acid ferrous sulphate by the bacterium *Thiobacillus ferrooxidans*. *Biotechnology and Bioengineering*, 12, p. 29-50.
- Landesman, J., D.W. Duncan, and C.C. Walden (1966). Iron oxidation by washed cell suspensions of the chemoautotroph, *Thiobacillus ferrooxidans*. *Can. J. Microbiol.*, 12, p. 25-33.
- Lowson, R.T. (1982). Aqueous oxidation of pyrite by molecular oxygen. *Chemical Reviews*, 82 (5), p. 461-497.
- Linsley, R.K., M.A. Kohler, and J.L.H. Paulhus (1975). *Hydrology for Engineers*, McGraw-Hill, New York.
- MacKintosh, M.E. (1978). Nitrogen fixation by *Thiobacillus ferrooxidans*. *J. Gen. Microbiol.*, 105, p. 215-218.
- McBean, E.A. (1984). Surface techniques to control leachate generation, Notes to students in Landfill Engineering course, University of Waterloo, Dept. of Civil Engineering.
- Mein, R.G. and C.L. Larson (1973). Modeling infiltration during a steady rain, *Water Resources Research* 9 (2), p. 384-394.
- Mockus, V. (1972). Estimation of direct runoff from storm rainfall. *U.S. Soil Conservation Service National Engineering Handbook*, Section 4, Hydrology, Chapter 10, p. 10.1-10.23.

- Myerson, A.S. (1981). Oxygen mass transfer requirements during the growth of *Thiobacillus ferrooxidans* on iron pyrite. *Biotech & Bioeng.*, 23, p. 1413-1416.
- Nicholson, R.V. (1984). Pyrite oxidation in carbonate-buffered systems: experimental kinetics and control by oxygen diffusion in a porous medium. Unpublished Ph.D. Thesis, University of Waterloo, Ontario, 176 p.
- Nicholson, R.V., R.W. Gillham, E.J. Reardon (1988). Pyrite oxidation in carbonate-buffered solution. No. 1 Experimental Kinetics. *Geochemica et Cosmochemica Acta*, Vol. 52, p. 1077 - 1085.
- Nicholson, R.V., R.W. Gillham, J.A. Cherry, and E.J. Reardon (1989). Reduction of acid generation in mine tailings through the use of moisture-retaining cover layers as oxygen barriers. *Canadian Geotechnical Journal*, 26 (1), p. 1-8.
- Nordstrom, D.K. (1982). Aqueous pyrite oxidation and the consequent formation of iron minerals. In *Acid Sulphate Weathering*, Soil Sci. Soc. Amer. Spec., Publ. No. 10, 37-56.
- Petruk, W.R., and R. Pinard (1986). Mineralogical and image analysis study of samples for core WA-20 of the Waite Amulet tailings. CANMET, MSL, Ottawa, June 1986.
- Pugh, C.E. (1979). Influence of surface area and morphology on the oxidation of pyrite from Texas lignite. *Dissertation Abstract International*, B1979, 39, 4788.
- Quigley, R.M., and R.K. Rowe (1986). Leachate migration through clay below a domestic waste landfill, Sarnia, Ontario, Canada: Chemical interpretation and modelling philosophies. *American Society for Testing and Materials, Specialty Publication on Industrial and Hazardous Waste*, STP 933, p. 93 - 102.
- Razzell, W.E., and P.C. Trussell (1963). Microbiological leaching of metallic sulfides. *Appl. Microbiol.*, 11, p. 105-110.
- Reynolds, D. (1984). Some methods for measuring hydraulic conductivity in the absence of a water table. Unpublished document, Dept. of Land Resource Science, University of Guelph, Ontario. 27 p.

- Ritchie, J.T. (1972). A model for predicting evaporation from a row crop with incomplete cover. *Water Resources Research*, Vol. 8, No. 5, p. 1204-1213.
- Robertson, R. (1985). A review of process control for wastewater lime facilities. Noranda Technology Centre internal report, May 1985. Project N-8305.
- Rowe, R.K. (1988). Eleventh Canadian Geotechnical Colloquium; Contaminant migration through groundwater - the role of modelling in the design of barriers. *Canadian Geotechnical Journal*, 25, p. 778 - 798.
- Schroeder, P.R., A.C. Gibson, and M.D. Sinden (1984). The hydrologic evaluation of landfill performance (HELP) model, Vol. II. Documentation for Version I. EPA/530-SW-84-010, U.S. Environmental Protection Agency, Office of Solid Waste and Emergency Response, Washington, DC, 256 p.
- Silverman, M.P., and D.G. Lundgren (1959). Studies on the chemi-autotrophic iron bacterium *Ferrobacillus ferrooxidans*. *J. Bacteriol.*, 77, p. 642-647.
- Singer, P.C., and W. Stumm (1970). Acidic mine drainage: the rate- determining step. *Science*, 167, p. 1121-1123.
- Siwik, R. (1986). Hydrogeochemical investigation of reactive tailings at the Waite Amulet tailings site, Noranda, Quebec - 1985 program. DSS File No. 23SQ.23440-5-9120.
- Siwik, R.S., R. Prairie, and S. Payant (1987). Hydrogeochemical investigation of reactive tailings at the Waite Amulet tailings site, Noranda, Quebec, Phase 2. Report to CANMET, DSS Contract No. 23440-6-9099/01-SQ, July 1987.
- Siwik, R.S., R.V. Nicholson, and J.E. Smith (1987). Development of laboratory methodology for evaluating effectiveness of engineered covers for reactive tailings. National Uranium Tailings Program Report No. DSS 15SQ.23317-6-1737.

- Siwik, R.S., L. St-Arnaud, R. Prairie, and L. Labrosse (1988). Hydrogeochemical investigation of reactive tailings at the Waite Amulet tailings site, Noranda, Quebec - Phase 3. Report to CANMET, DSS Contract No. 03SQ.23440-7-0161, April 1988.
- Sklash, M.G., and R.N. Farvolden (1975). The role of groundwater in storm runoff. *Journal of Hydrology*, 43, p. 45 - 65.
- Smith, E.E., and K.S. Shumate (1970). *Water Poll. Cont. Res.*, Report No. 14010 FPS DAST-40, U.S. Dept. Inc., FWPCA.
- Smyth, D.J.A. (1981). Hydrogeological and geochemical studies above the water table in an inactive uranium tailings impoundment near Elliot Lake, Ontario. M.Sc project, University of Waterloo, Ontario.
- St-Arnaud, L.C., E.K. Yanful, R. Prairie, and N.K. Dave (1989). Evolution of acidic pore water at the Waite Amulet tailings site, Noranda, Quebec. *Proceedings of the International Symposium on Tailings and Effluent Management, Halifax, CIM, Vol. 14, p. 93-102.*
- Stenhouse, J.F., and W.M. Armstrong (1952). The aqueous oxidation of pyrite. *Trans. Can. Inst. Mining and Metall. Min. Soc., N.S.*, 55, p. 38-42.
- Stumm, W., and G.F. Lee (1961). Oxygenation of ferrous iron. *Ind. Eng. Chem.*, 53, p. 143-146.
- Stumm, W., and J.J. Morgan (1981). *Aquatic chemistry: an introduction emphasizing chemical equilibria in natural waters.* Wiley-Interscience, New York, p. 583.
- Torma, A.E., C.C. Walden, and R.M. Branion (1970). *Biotechnol. Bioeng.*, 12, p. 501-517.
- Tuovinen, O.H., and D.P. Kelly (1972). Biology of *Thiobacillus ferrooxidans* in relation to the microbiological leaching of sulphide ores. *Z. Allg. Mikrobiol.* 12, p. 311-346.
- Veldhuizen, H., D.W. Blowes, and R.S. Siwik (1987). The effectiveness of vegetation in controlling acid drainage from base metal tailings. *Proceedings of the Acid Mine Drainage Workshop/Seminar, Halifax, Nova Scotia, 23-26 March 1987.*

Vick, G. (1983). Planning, design and analysis of tailings dams. Wiley Interscience, New York, NY, 369 p.

Walsh, F., and R. Mitchell (1972). An acid-tolerant iron-oxidizing metallogenium. J. Gen. Microbiol., 72, p. 369-376.

Warren, I.H. (1956). The generation of sulphuric acid from pyrite by pressure leaching. Aust. J. Appl. Sci., 7, 346.

FIGURES

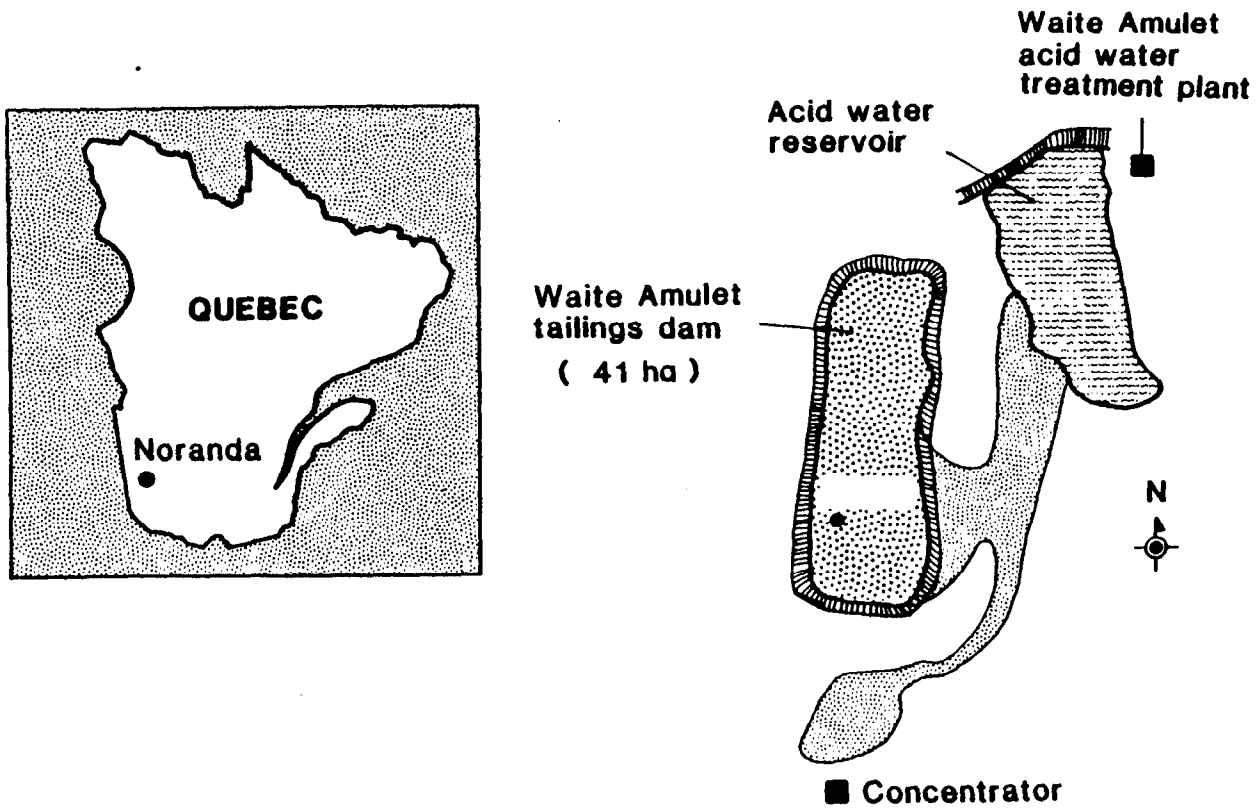


Figure 1.1 Location of Waite Amulet Tailings Area

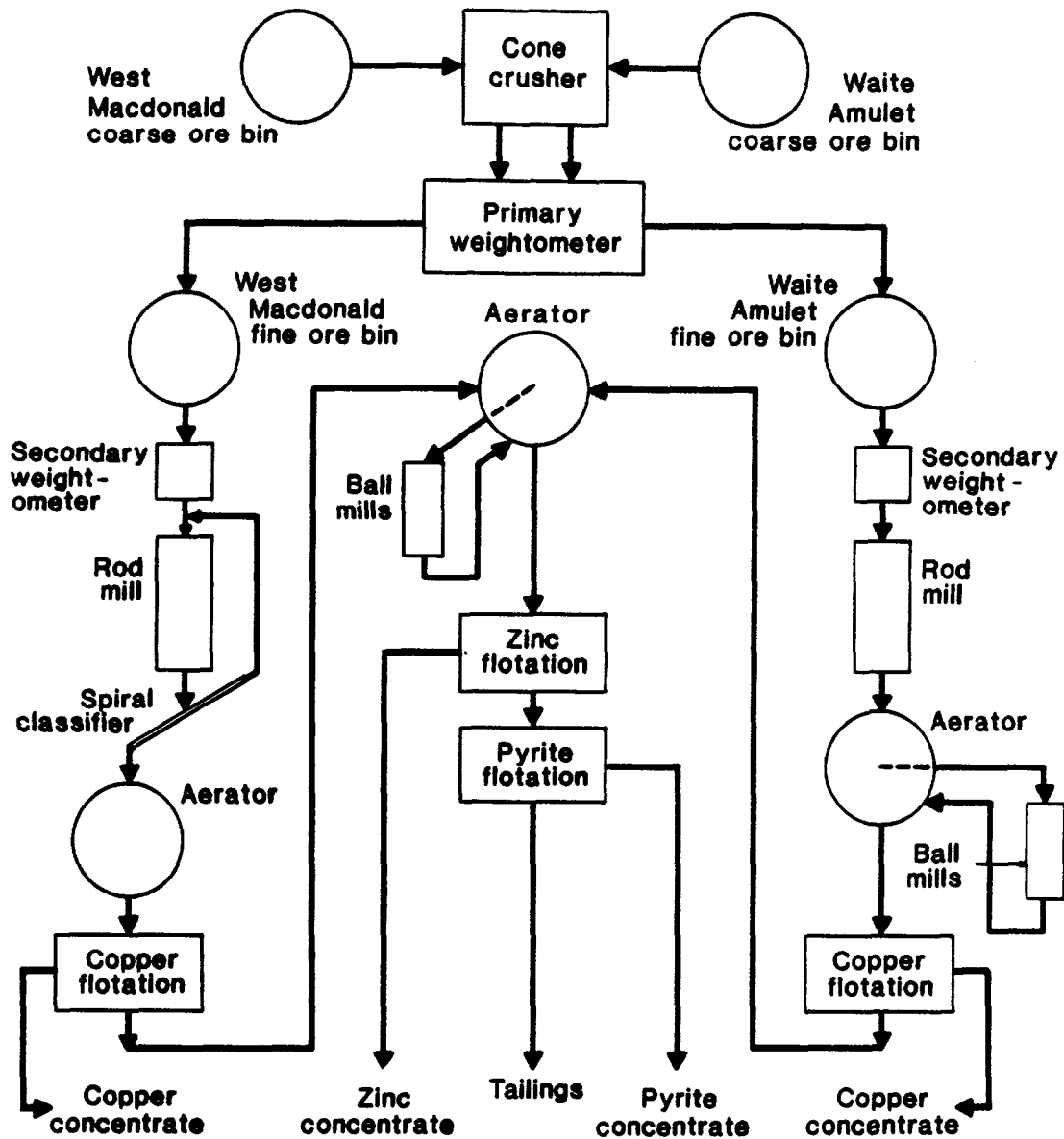


Figure 1.2 Waite Amulet Concentrator Flowsheet

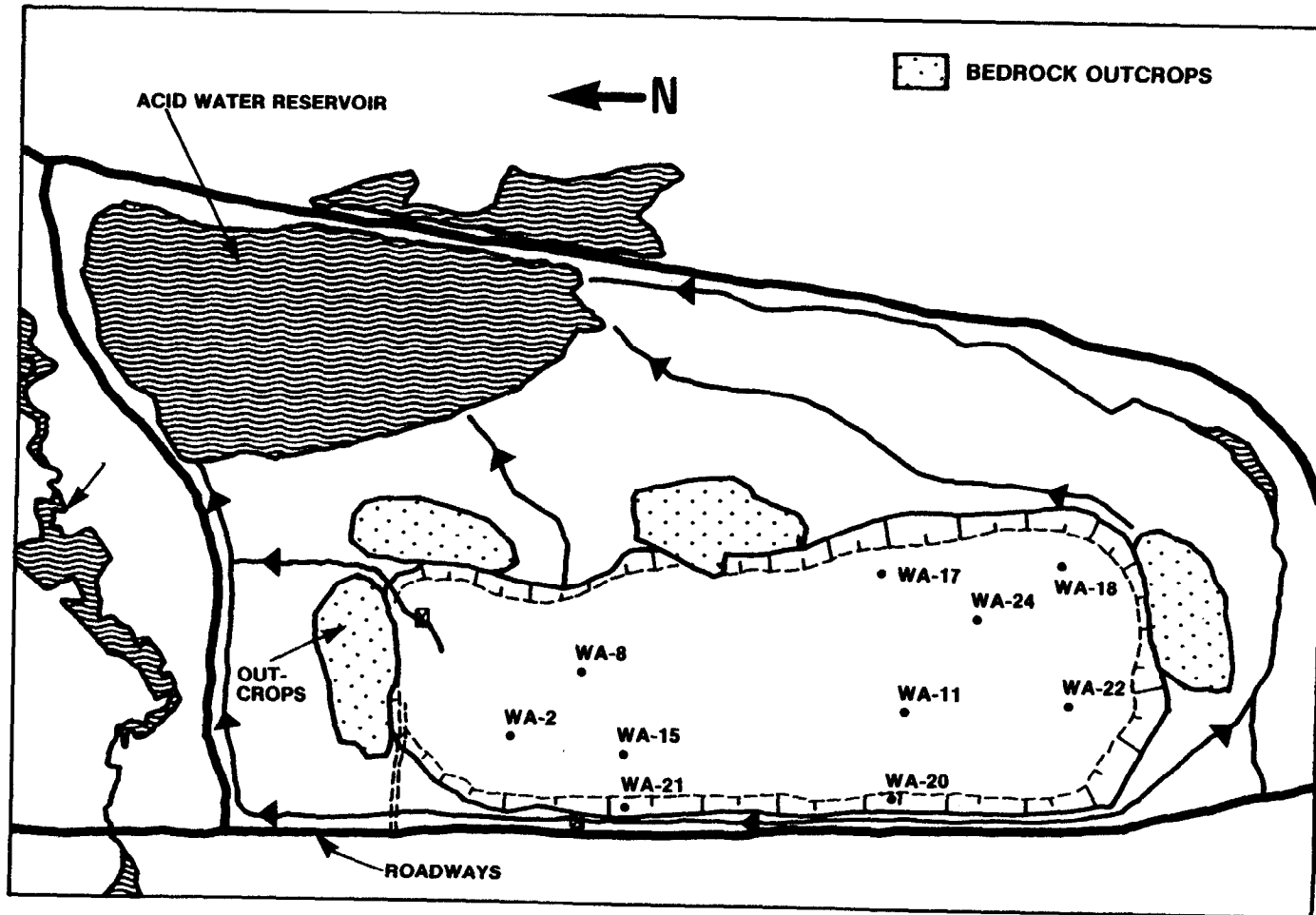


Figure 4.1 Location of Waite Amulet Monitoring Stations

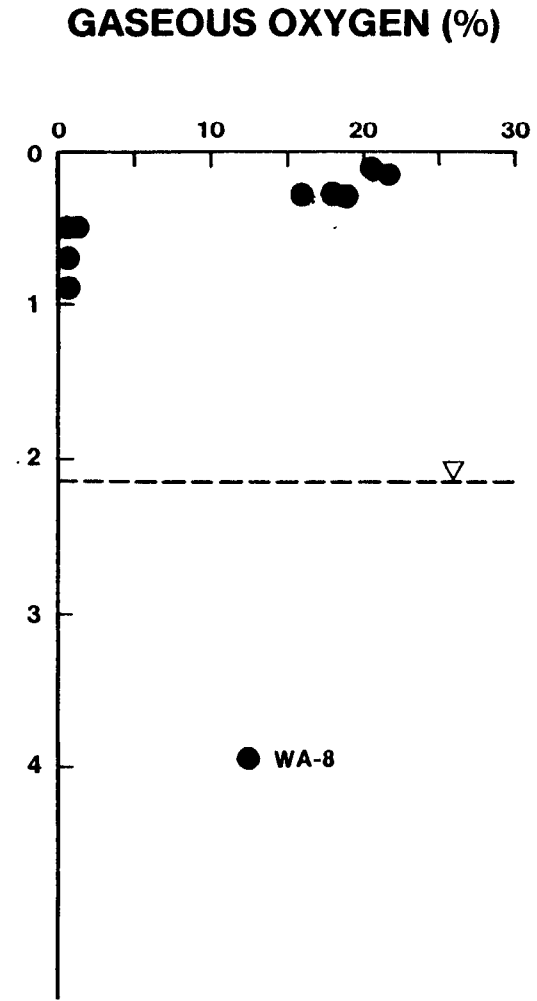
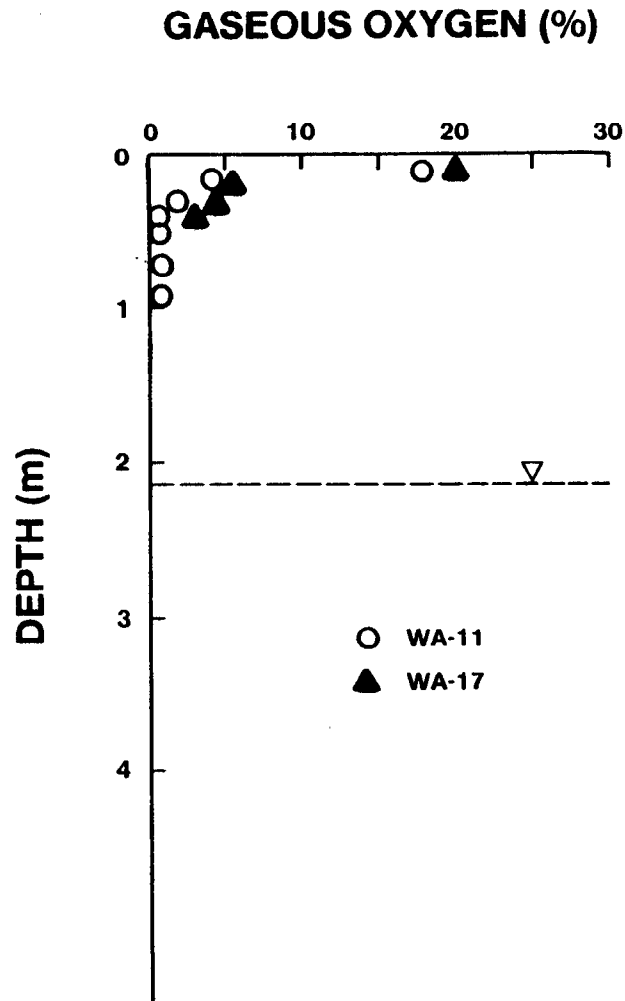


Figure 4.2 Gaseous Oxygen Concentration versus Depth at (a) Locations WA-11, WA-17 in 1986 and (b) Location WA-8 in 1987

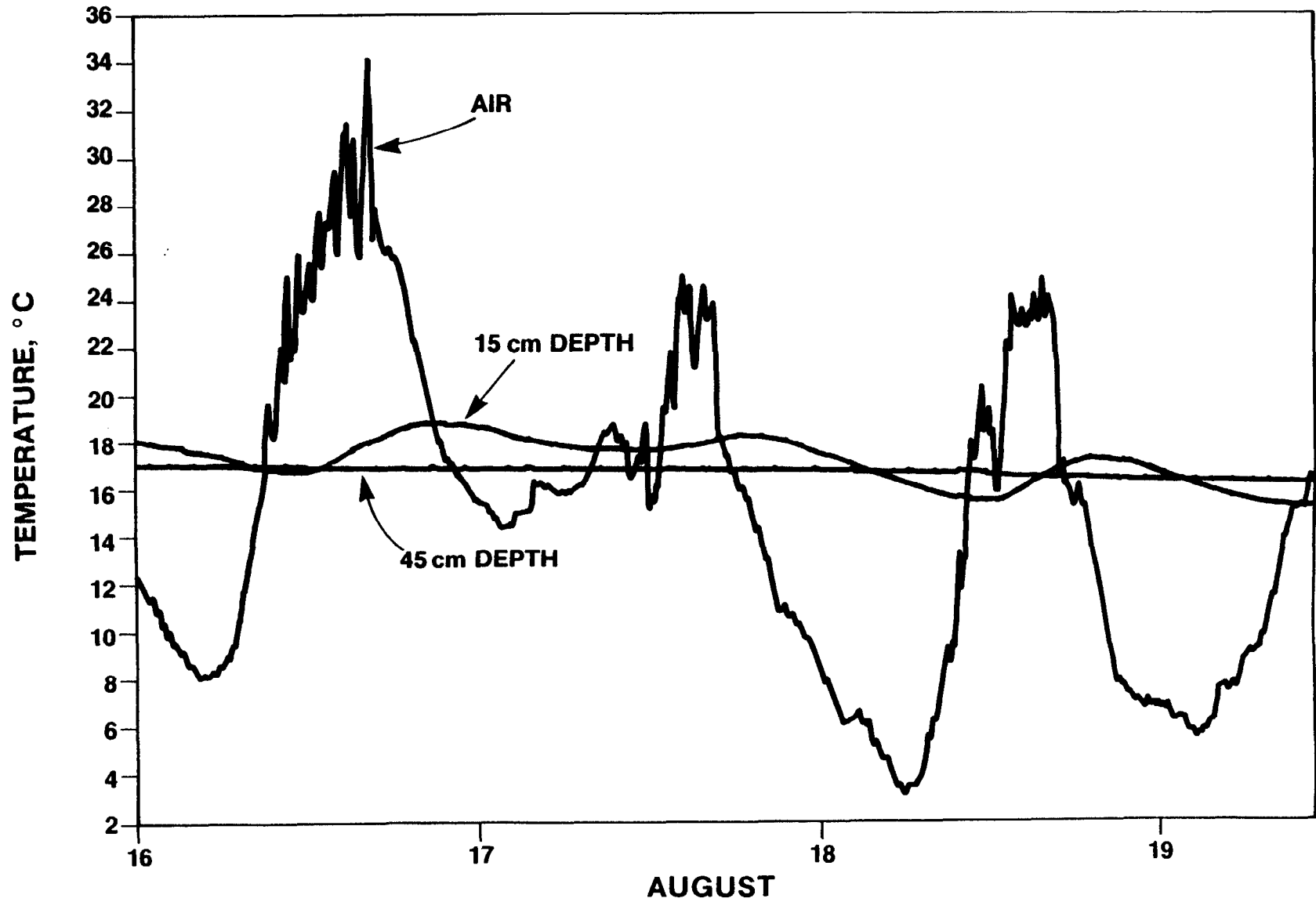


Figure 4.3 Diurnal Temperature Variations of Air and Tailings at 15 and 45 cm Depth in August 1988

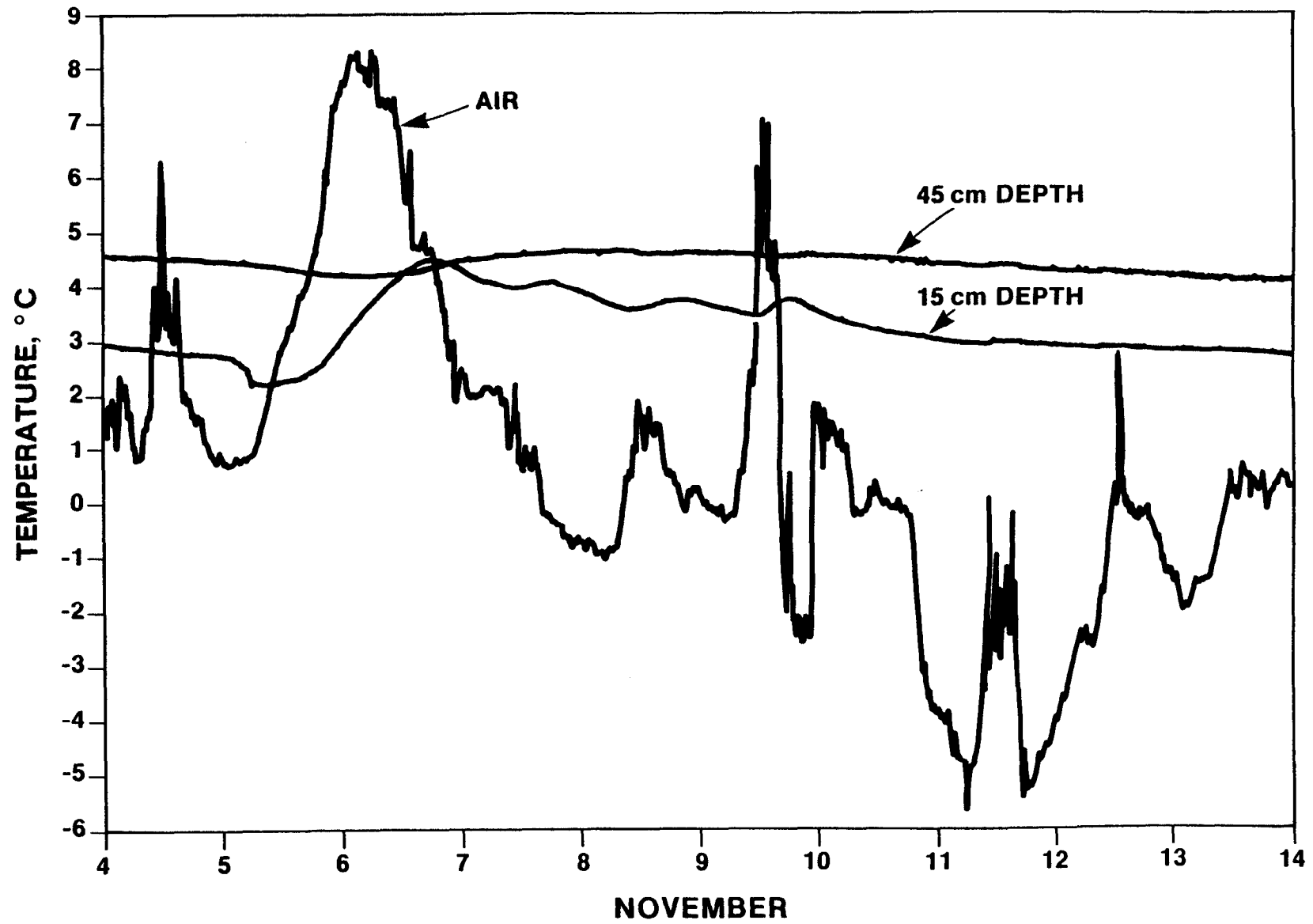


Figure 4.4 Diurnal Temperature Variation of Air and Tailings at 15 and 45 cm Depth in November 1988

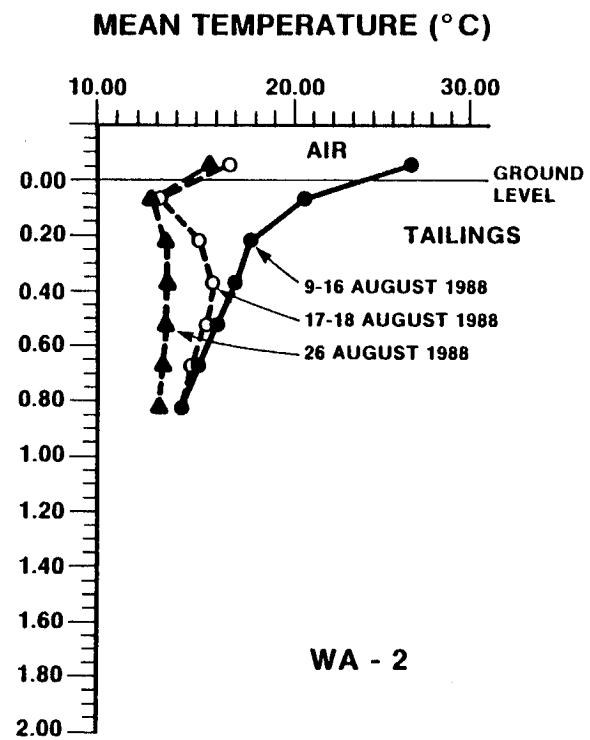
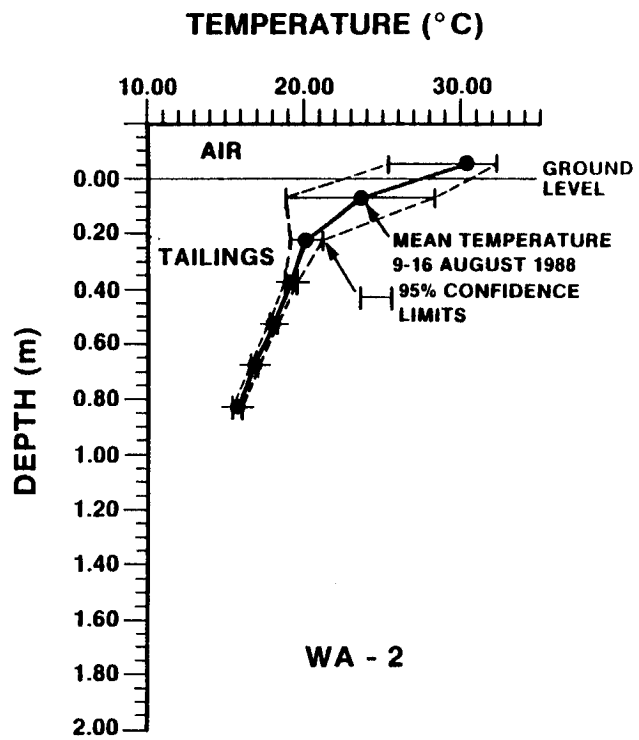


Figure 4.5 Temperature versus Depth at Location WA-2

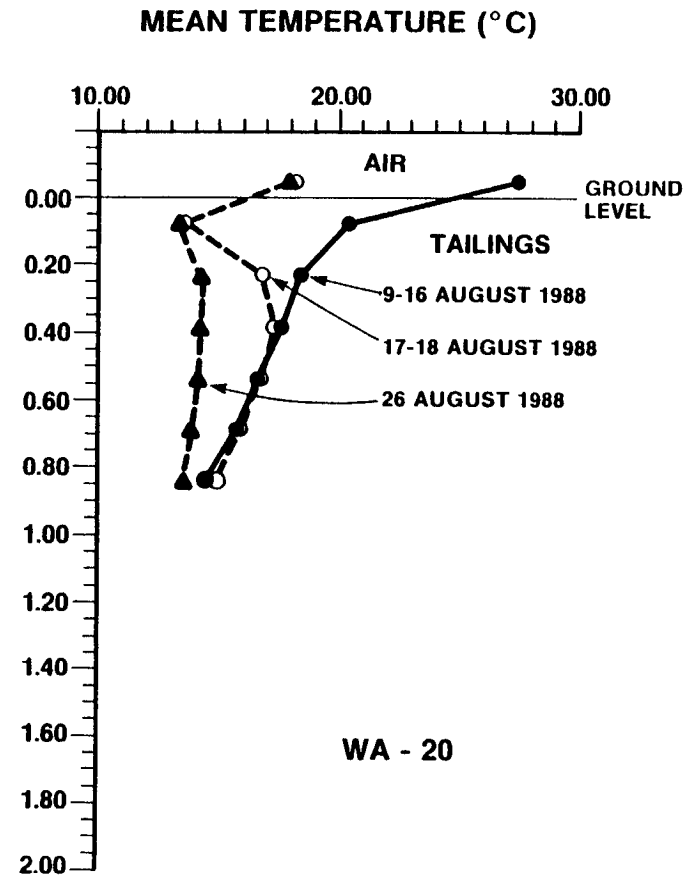
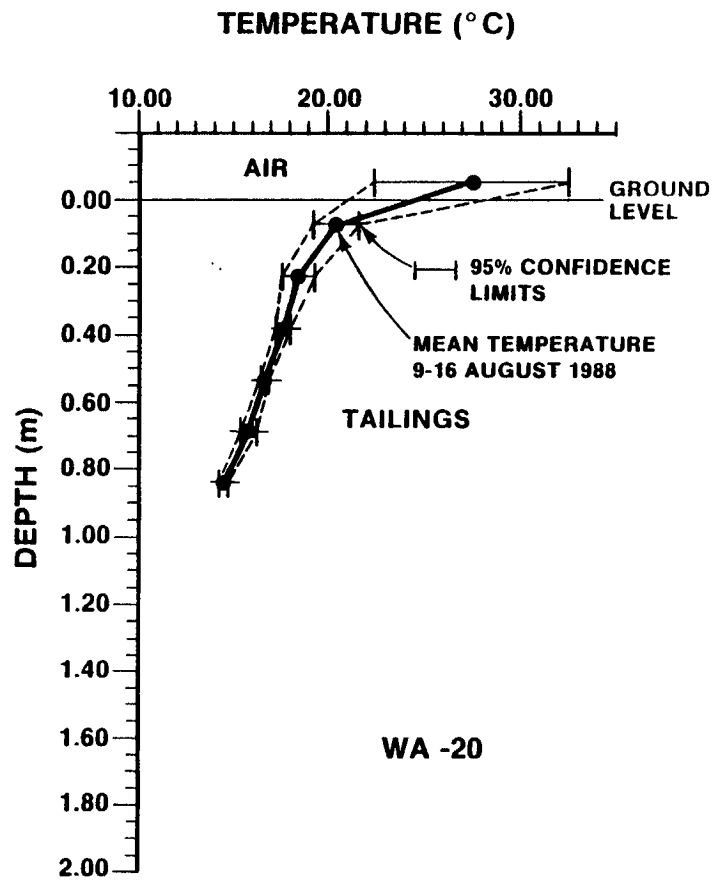


Figure 4.6 Temperature versus Depth at Location WA-20

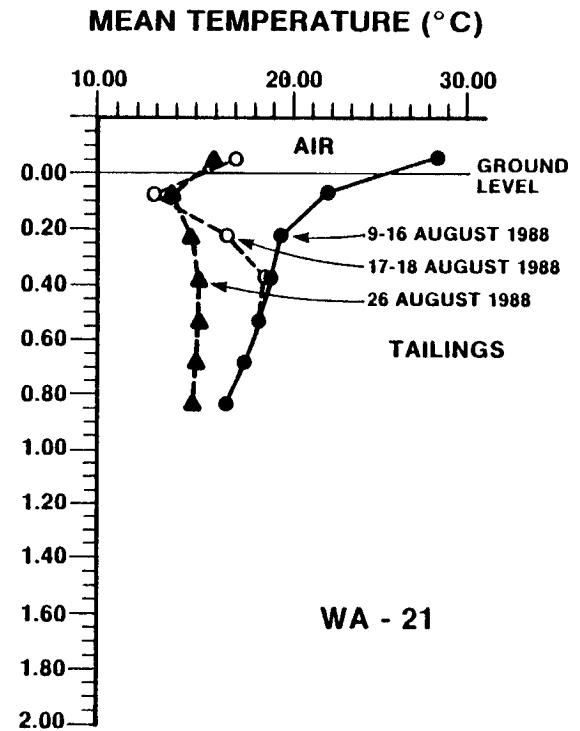
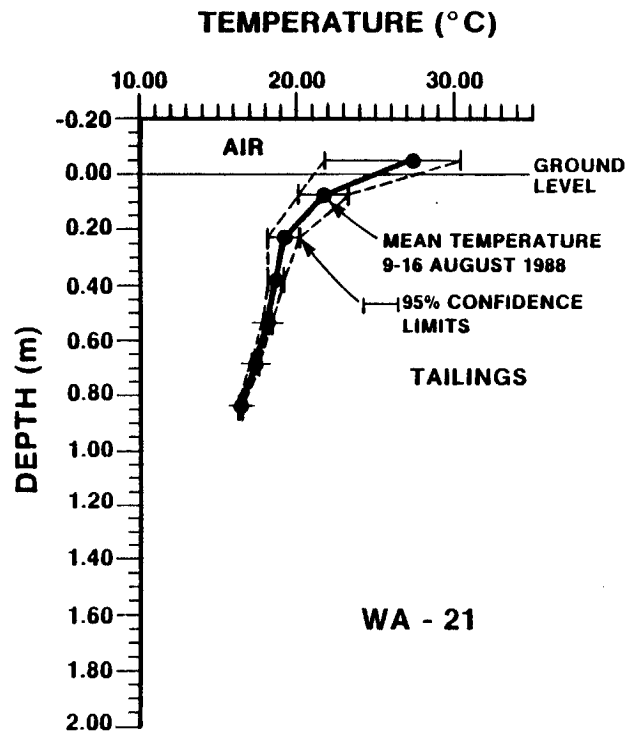


Figure 4.7 Temperature versus Depth at Location WA-21

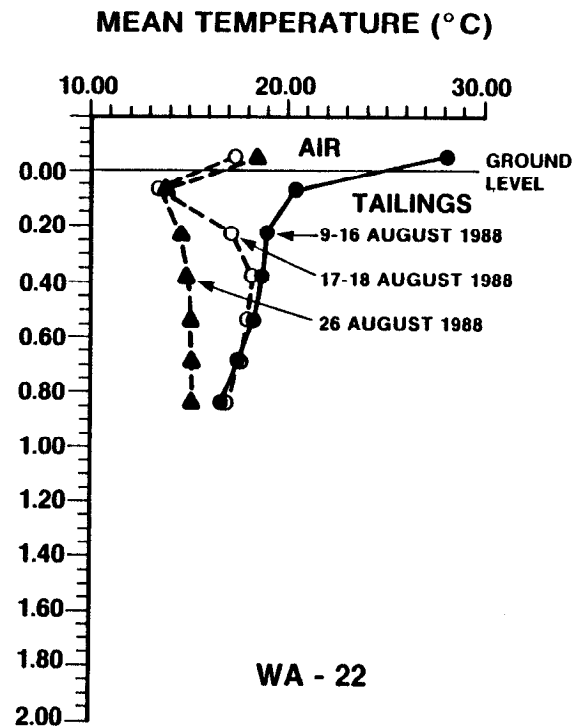
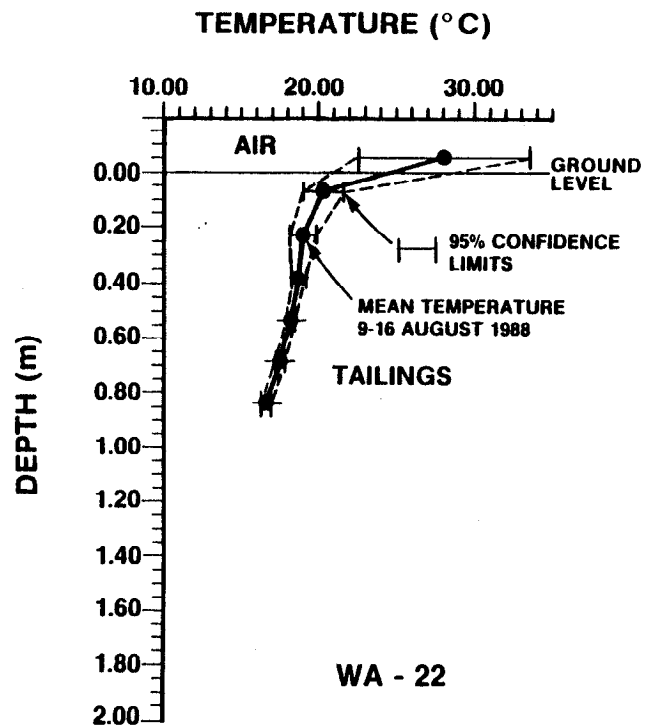


Figure 4.8 Temperature versus Depth at Location WA-22

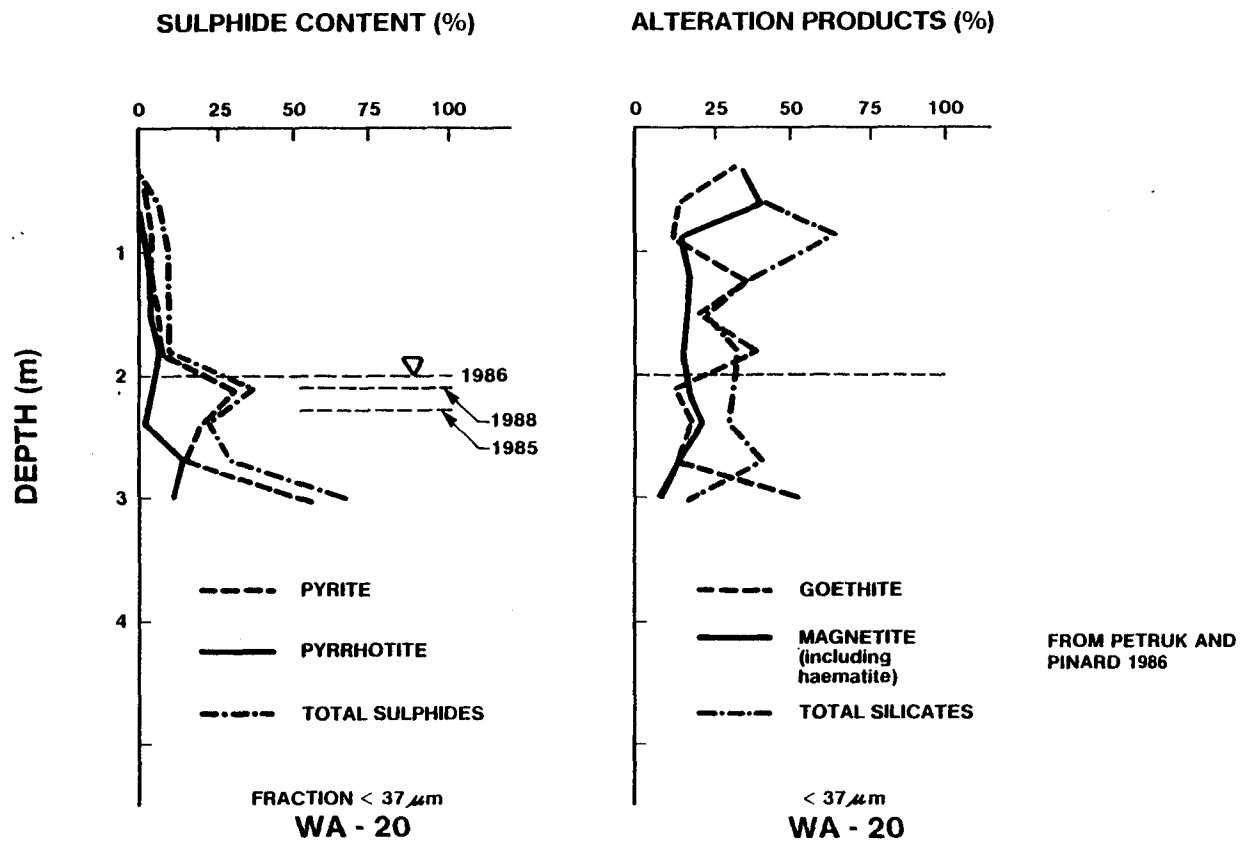


Figure 4.9 Variation in Sulphides and Alteration Products versus Depth for <37 micron Particles at WA-20

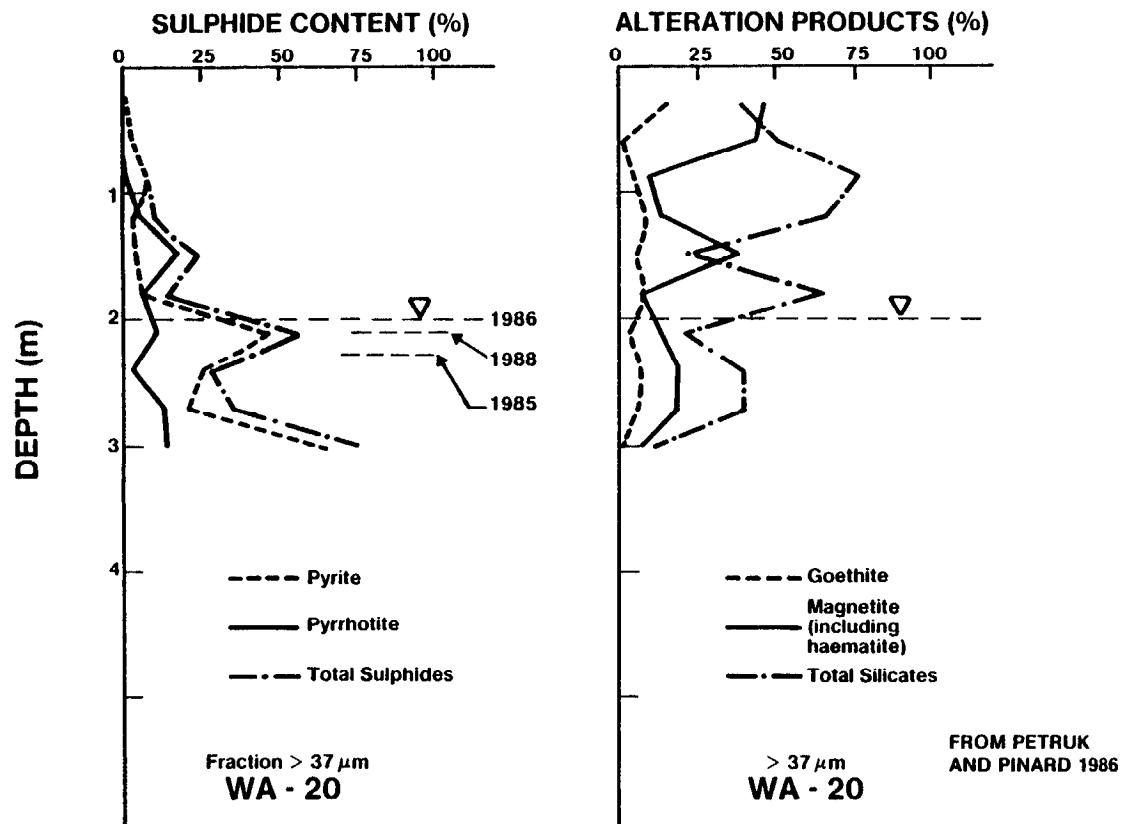


Figure 4.10 Variation in Sulphide and Alteration Products versus Depth for >37 micron Particles at WA-20

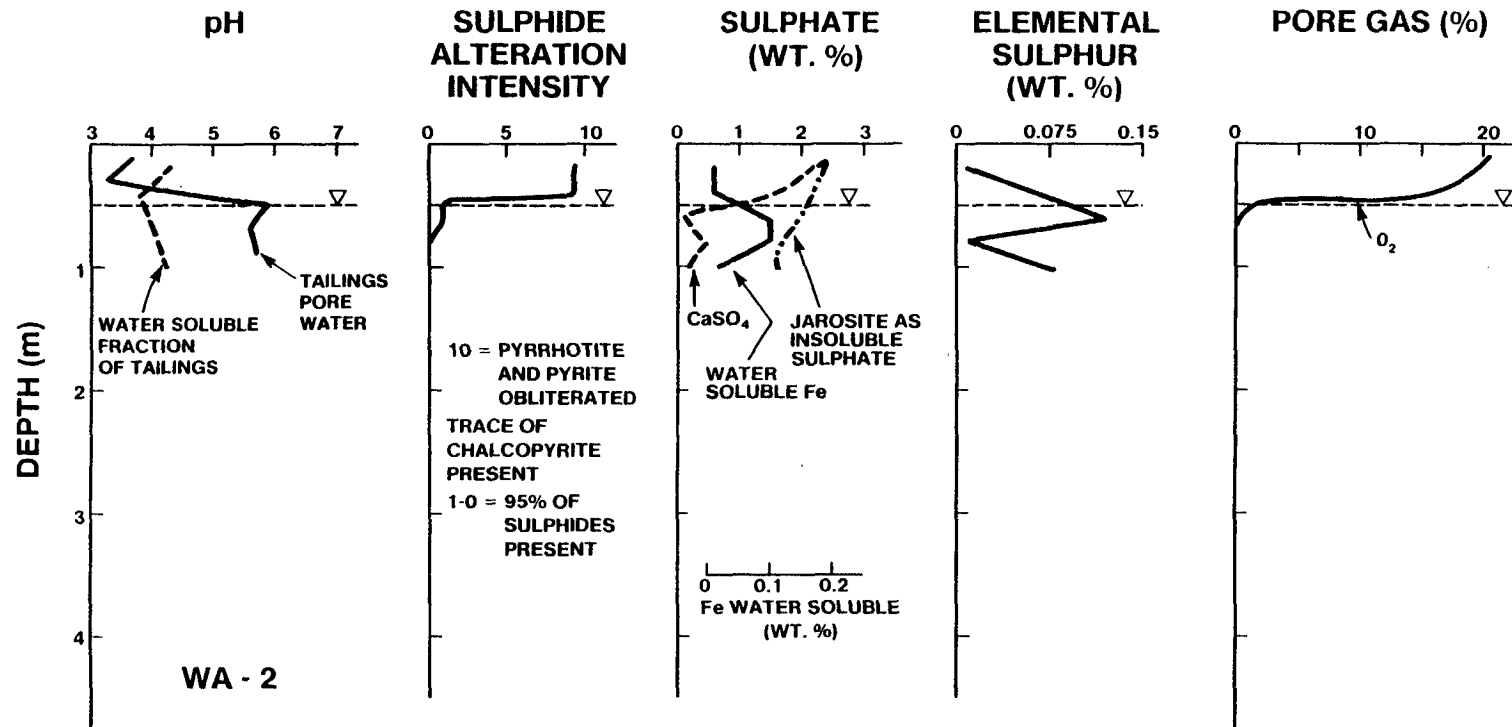


Figure 4.11 Variation in pH, Sulphide Alteration Intensity, Sulphate, Elemental Sulphur and Pore Gas with Depth at WA-2

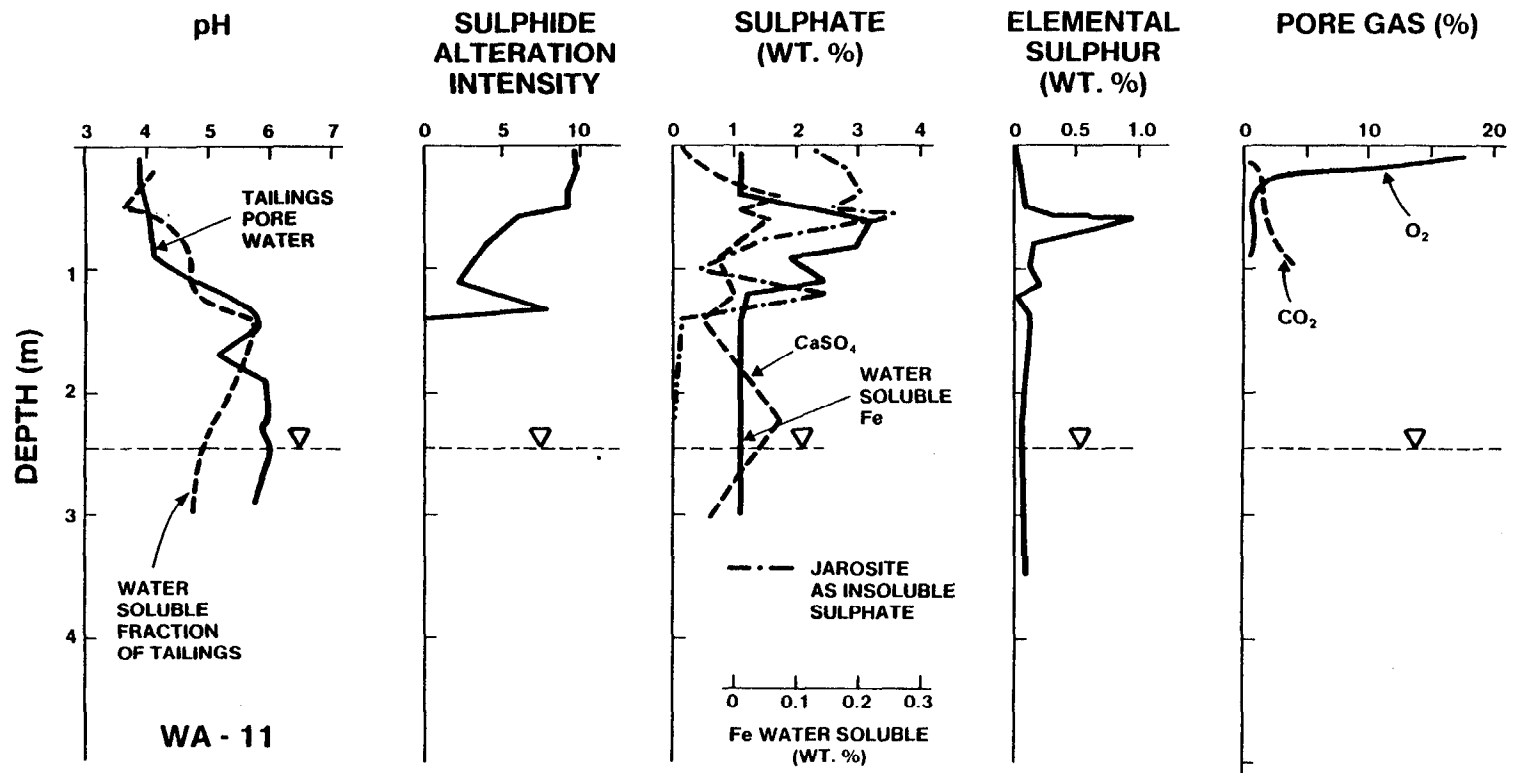


Figure 4.12 Variation in pH, Sulphide Alteration Intensity, Sulphate, Elemental Sulphur and Pore Gas with Depth at WA-11

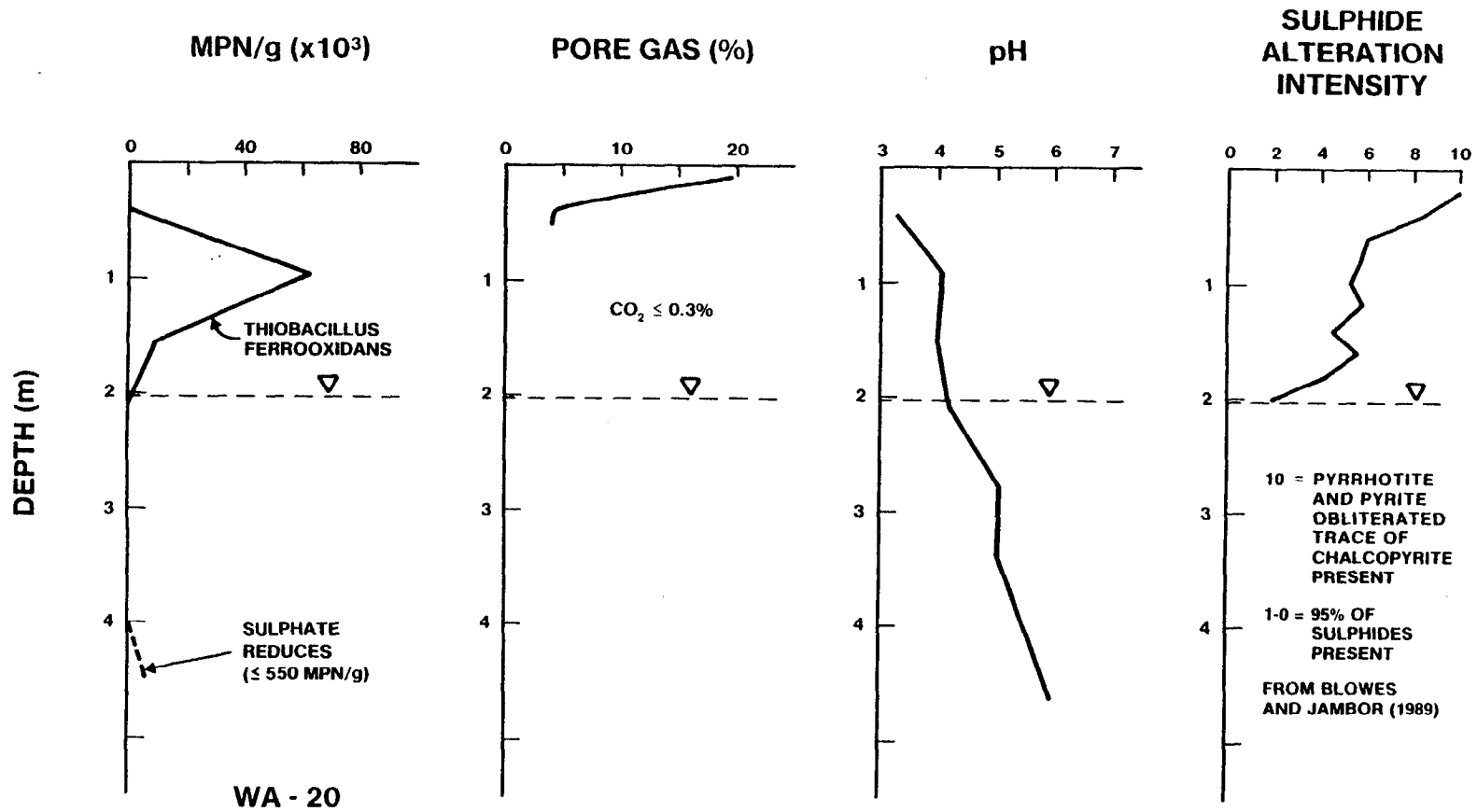


Figure 4.13 T. Ferrooxidans, Sulphate Reducers, Pore Gas, pH and Sulphide Alteration Intensity versus Depth for WA-20

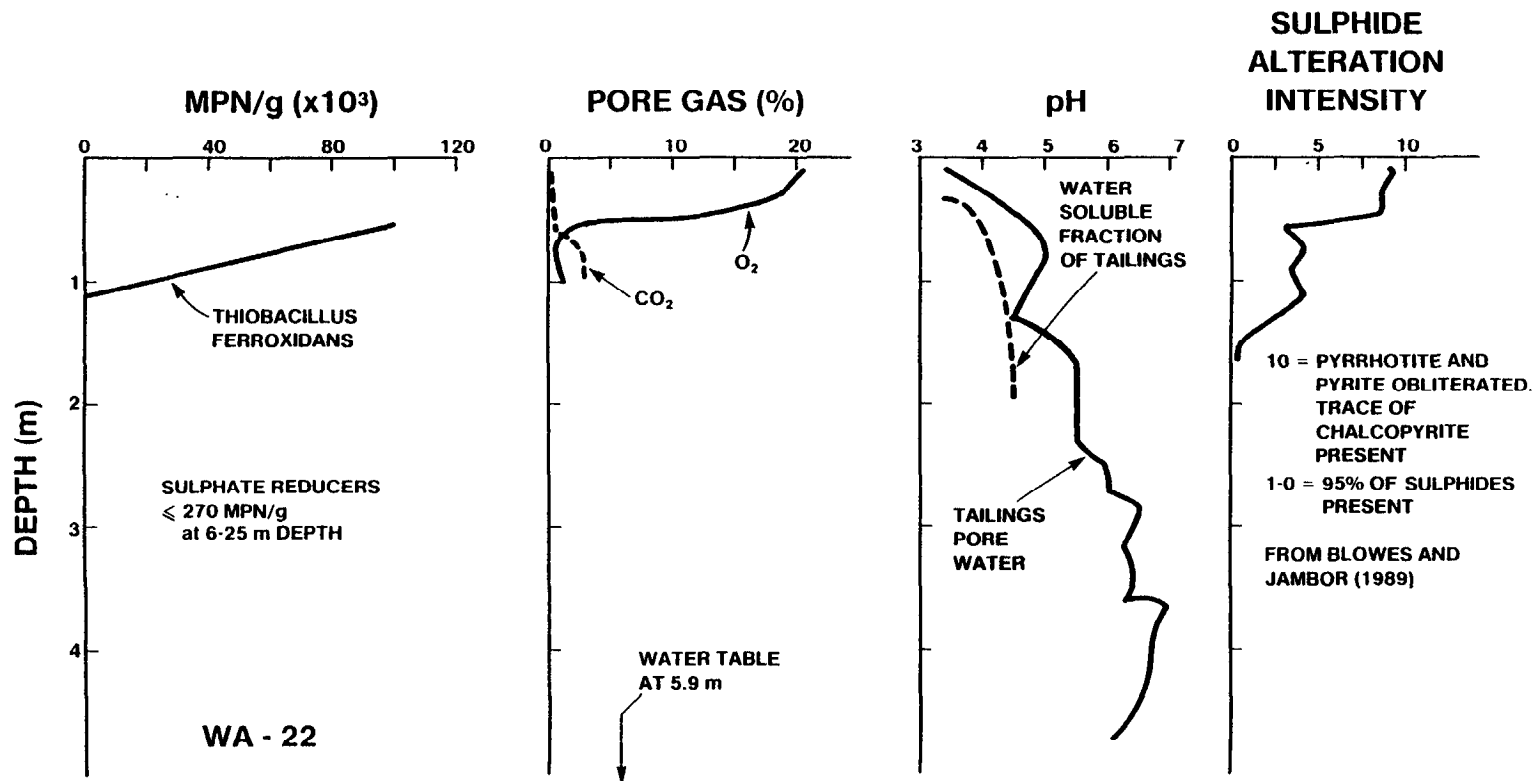


Figure 4.14 T. Ferrooxidans, Sulphate Reducers, Pore Gas, pH and Sulphide Alteration Intensity versus Depth for WA-22

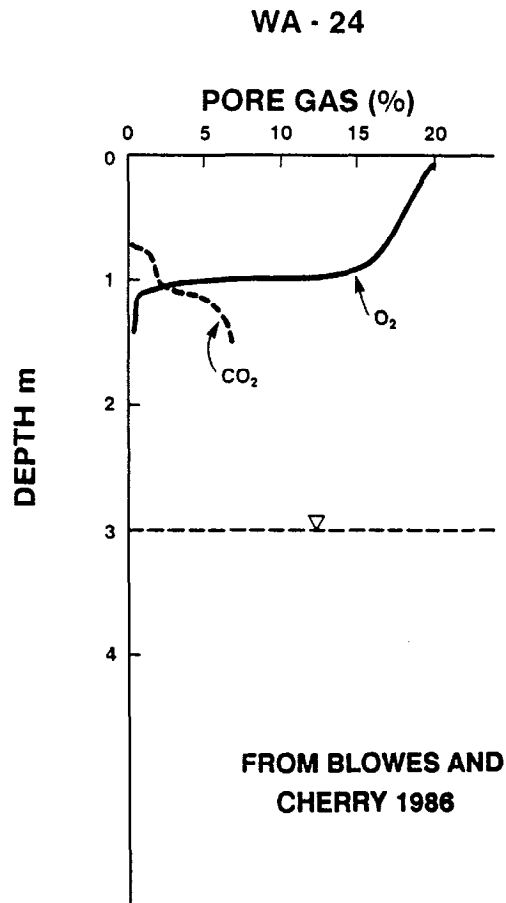


Figure 4.15 Variation in Oxygen and Carbon Dioxide versus Depth at WA-24

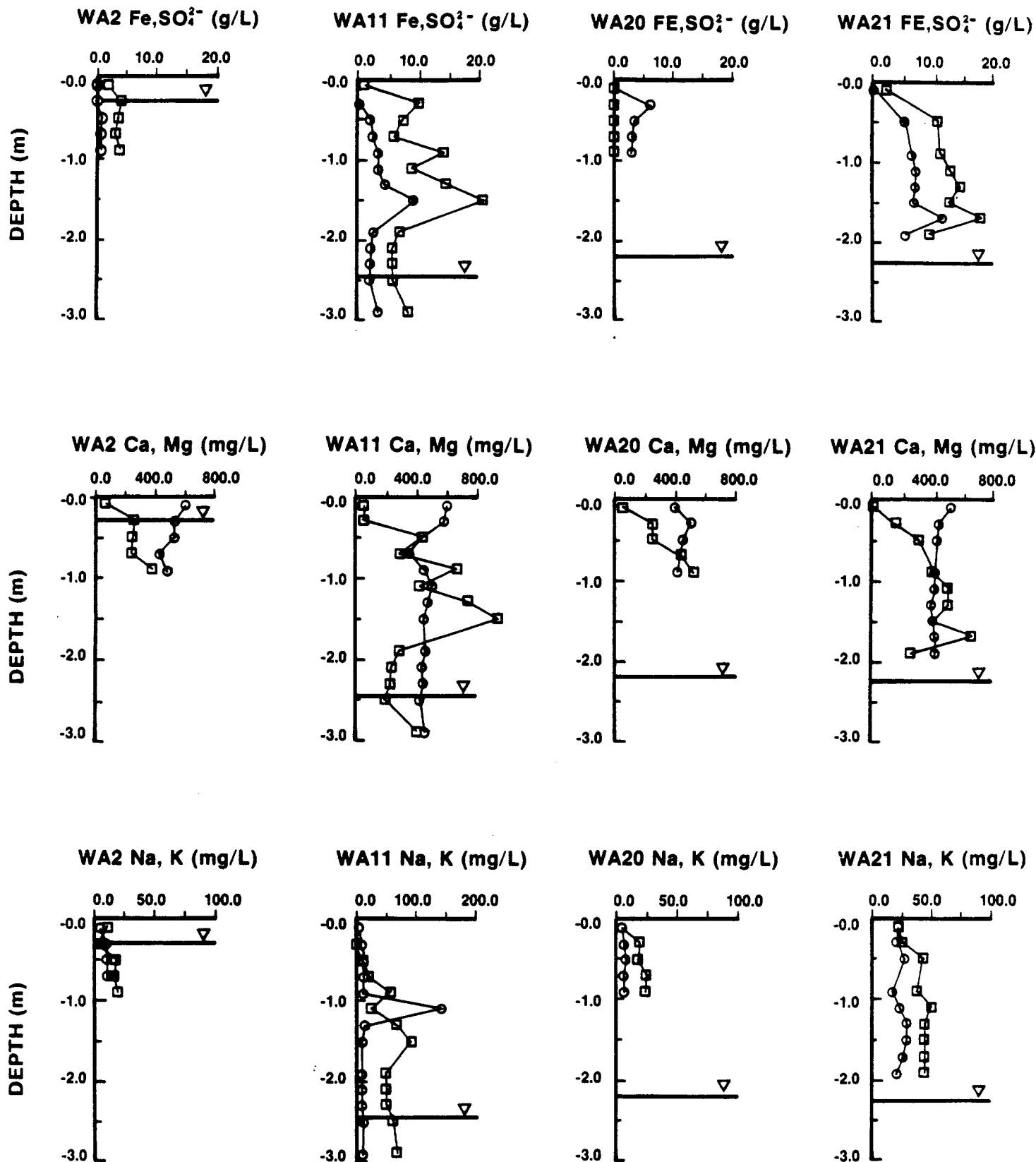


Figure 5.1 Ion Concentration Profiles at WA-2, WA-11, WA-20, and WA-21, October 1986. Fe, Ca and Na are represented by circles; SO₄, Mg and K are represented by squares.

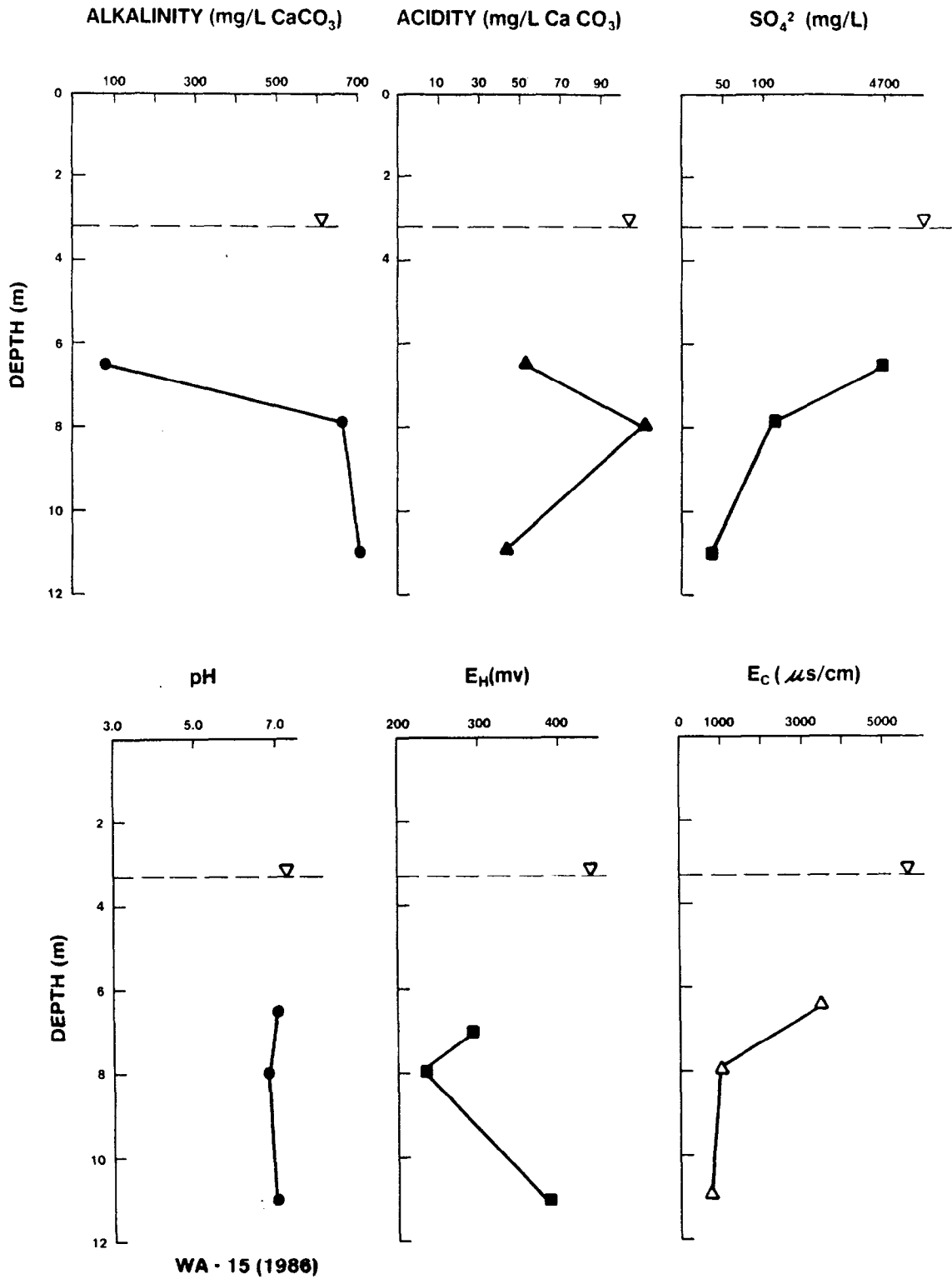
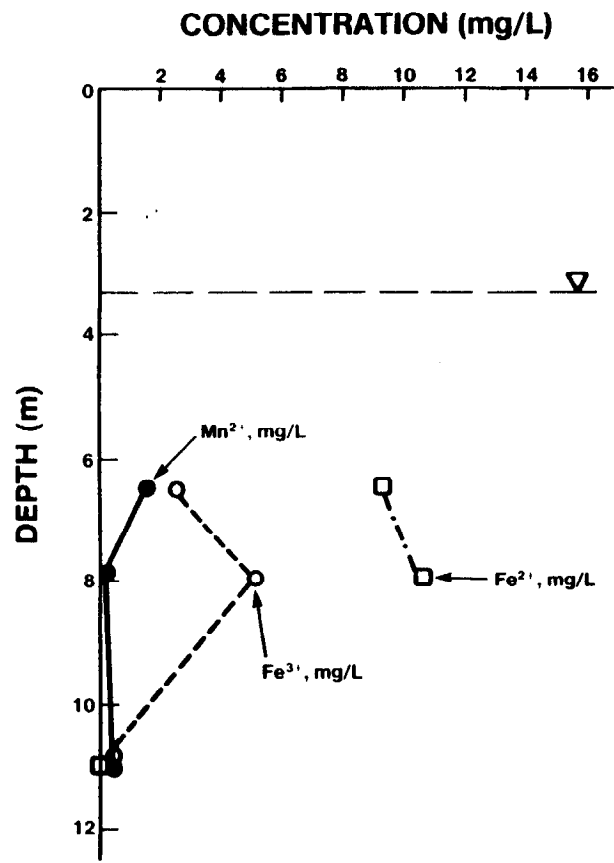


Figure 5.2 Pore Water Chemistry Profiles at WA-15, October 1986



WA - 15 (1986)

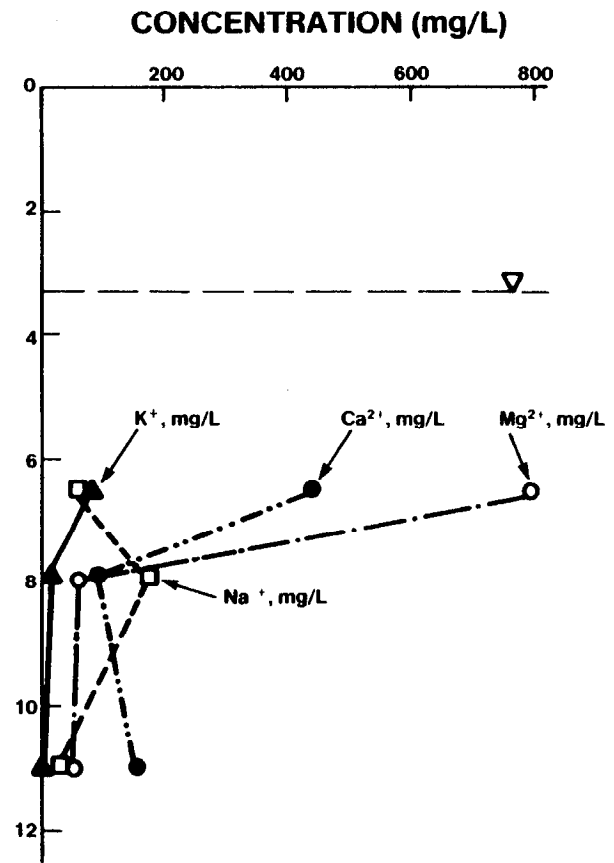


Figure 5.3 Pore Water Chemistry Profiles at WA-15, October 1986

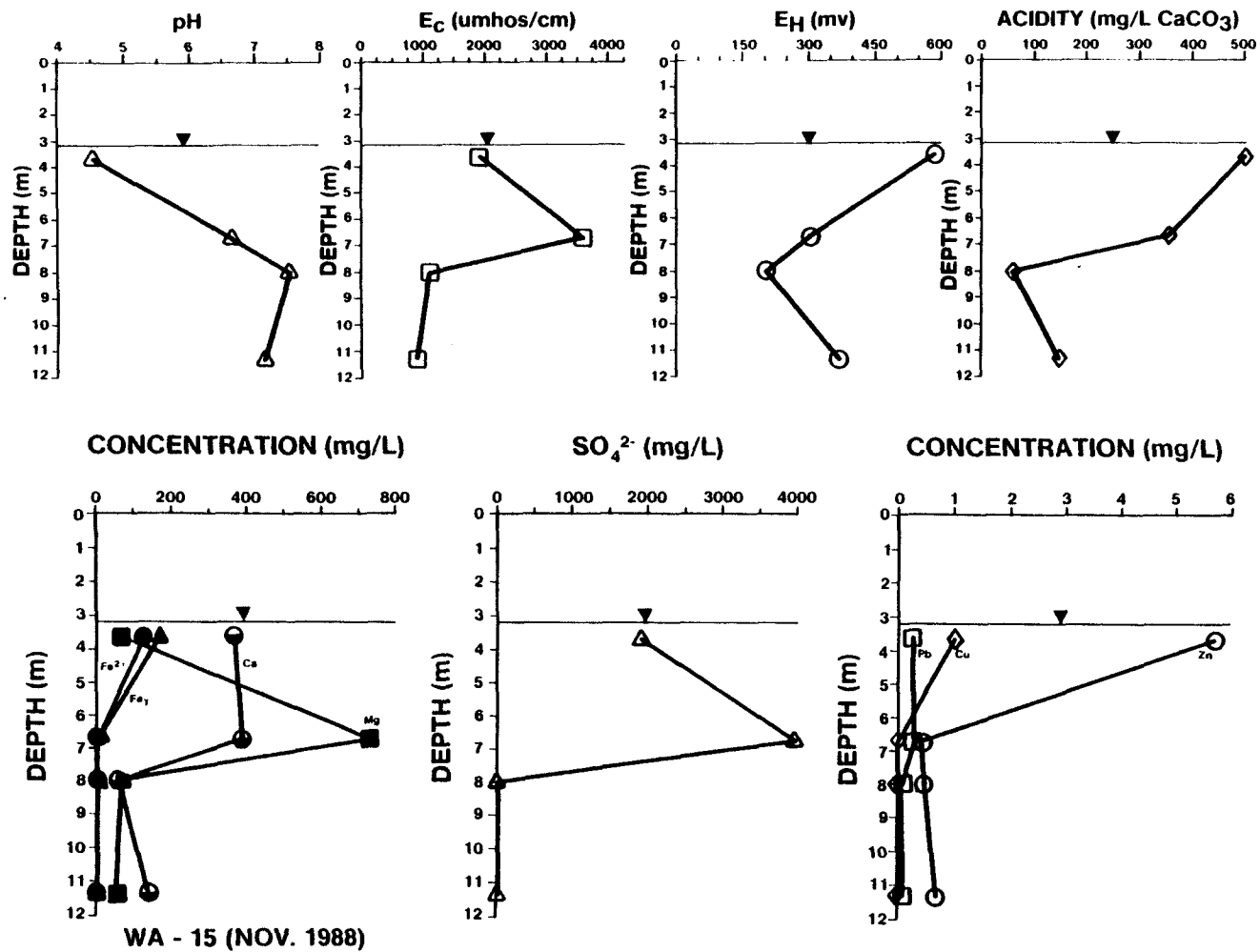


Figure 5.4 Pore Water Chemistry Profiles at WA-15, November 1988

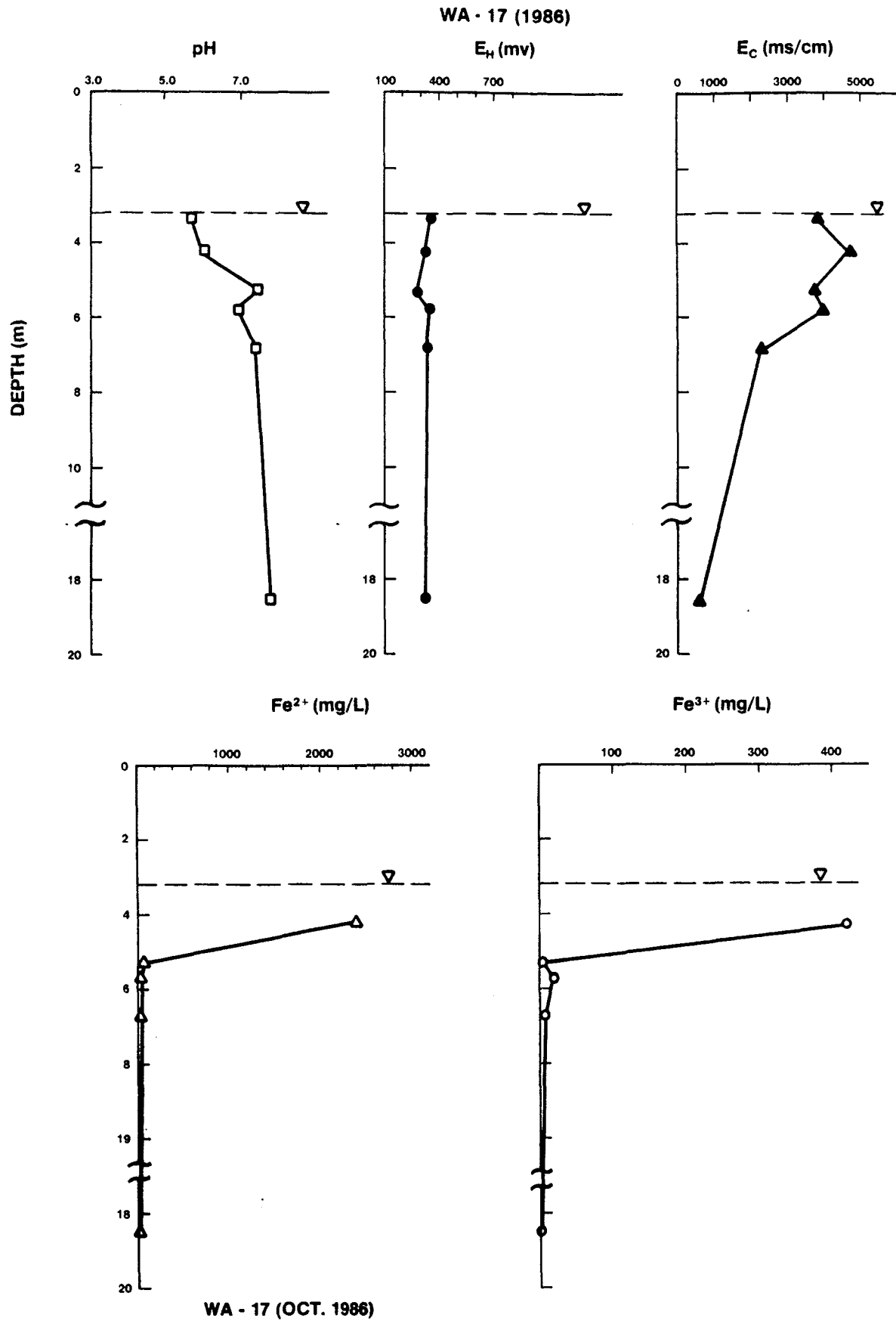


Figure 5.5 Pore Water Chemistry Profiles at WA-17

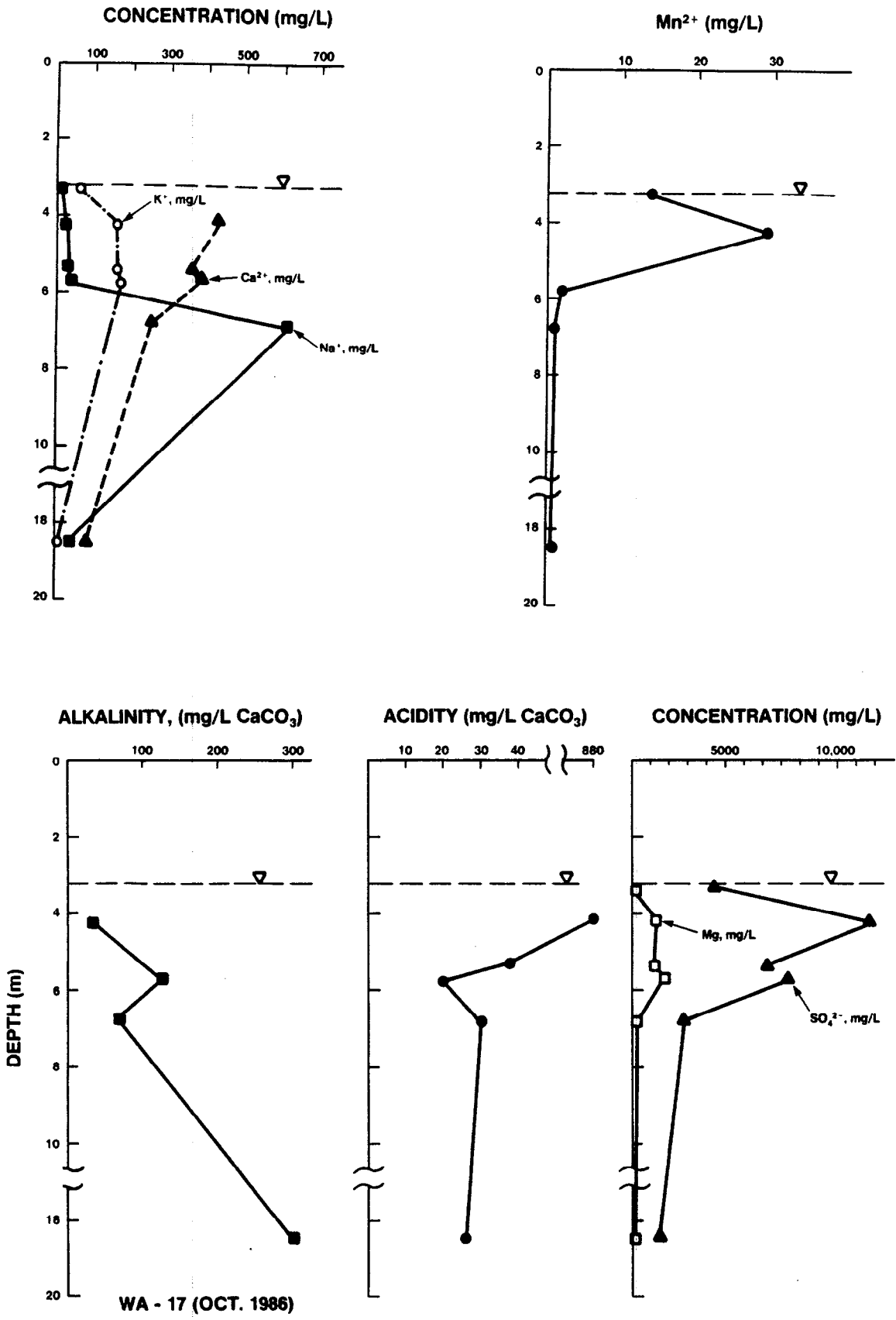
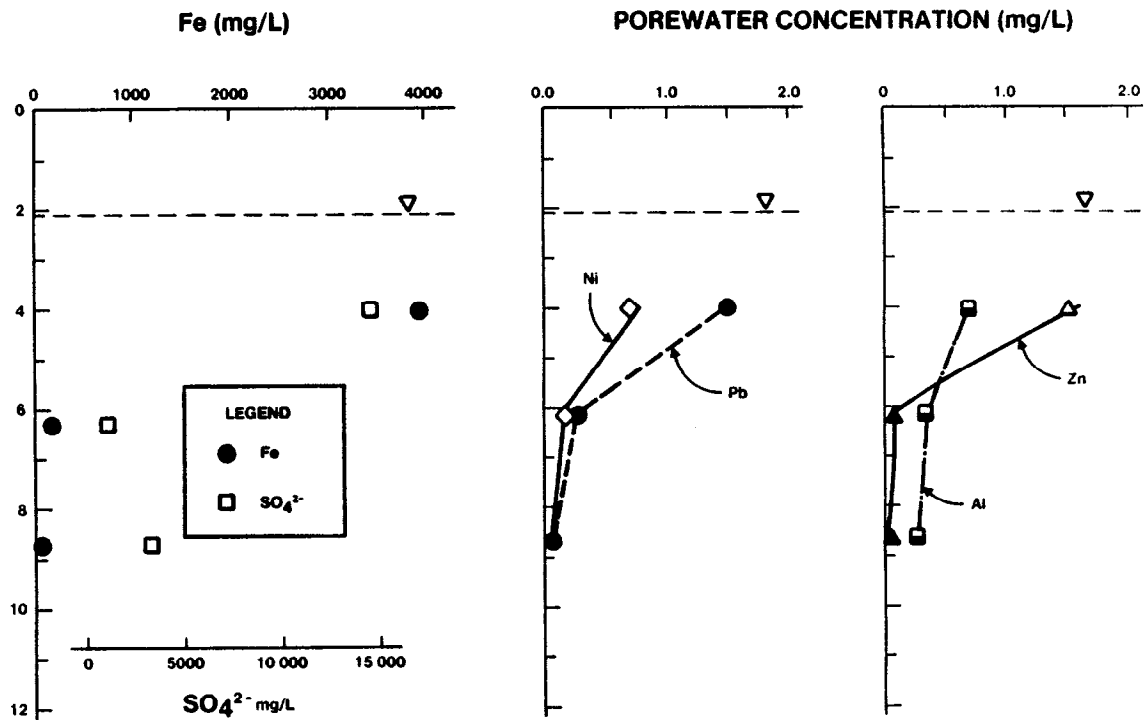
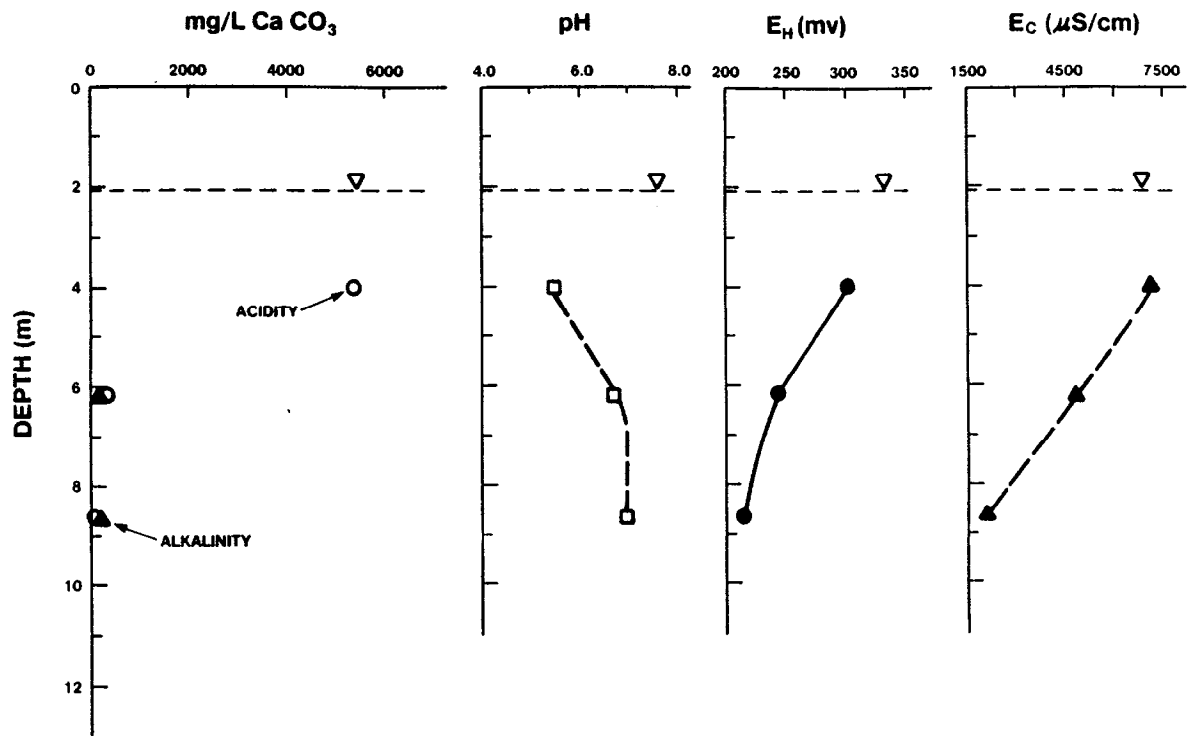


Figure 5.6 Pore Water Chemistry Profiles at WA-17



WA - 11 (DEC. 1985)

Figure 5.7 Pore Water Chemistry Profiles at WA-11

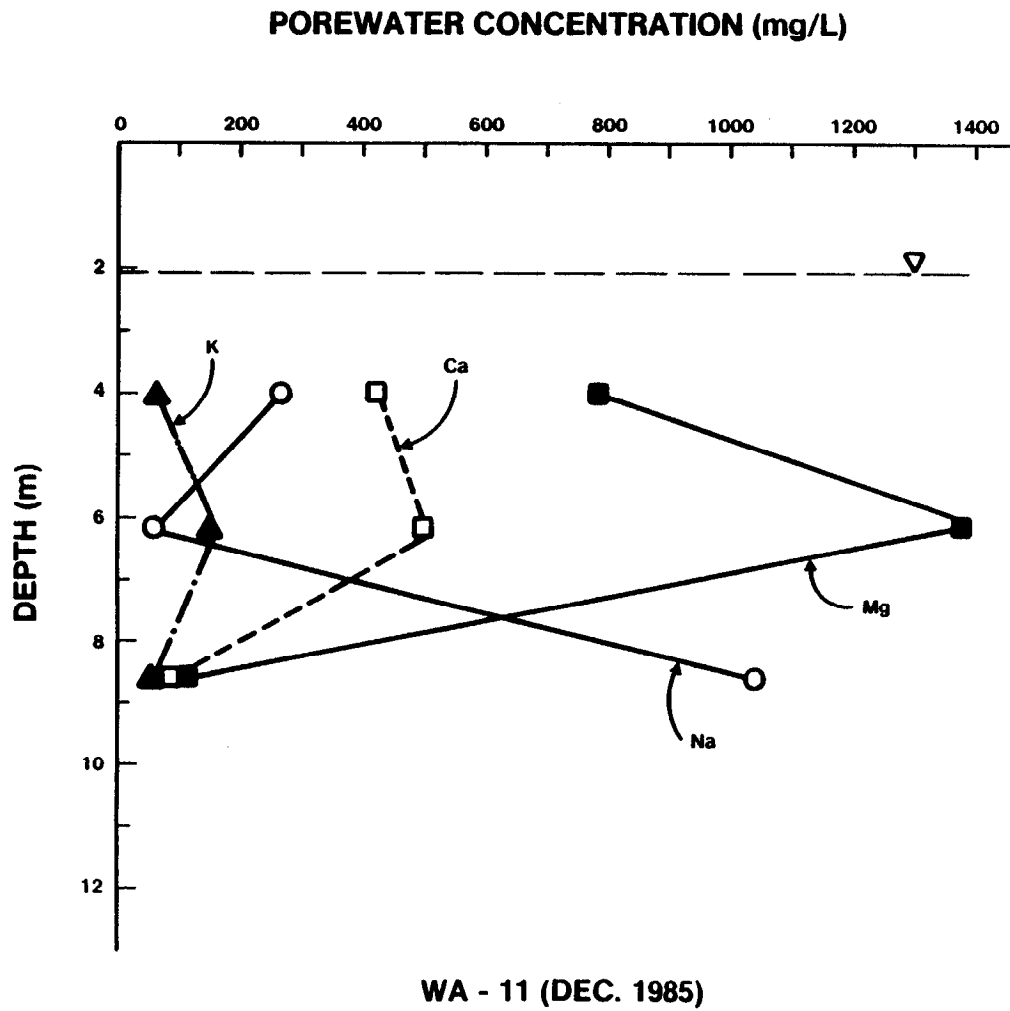
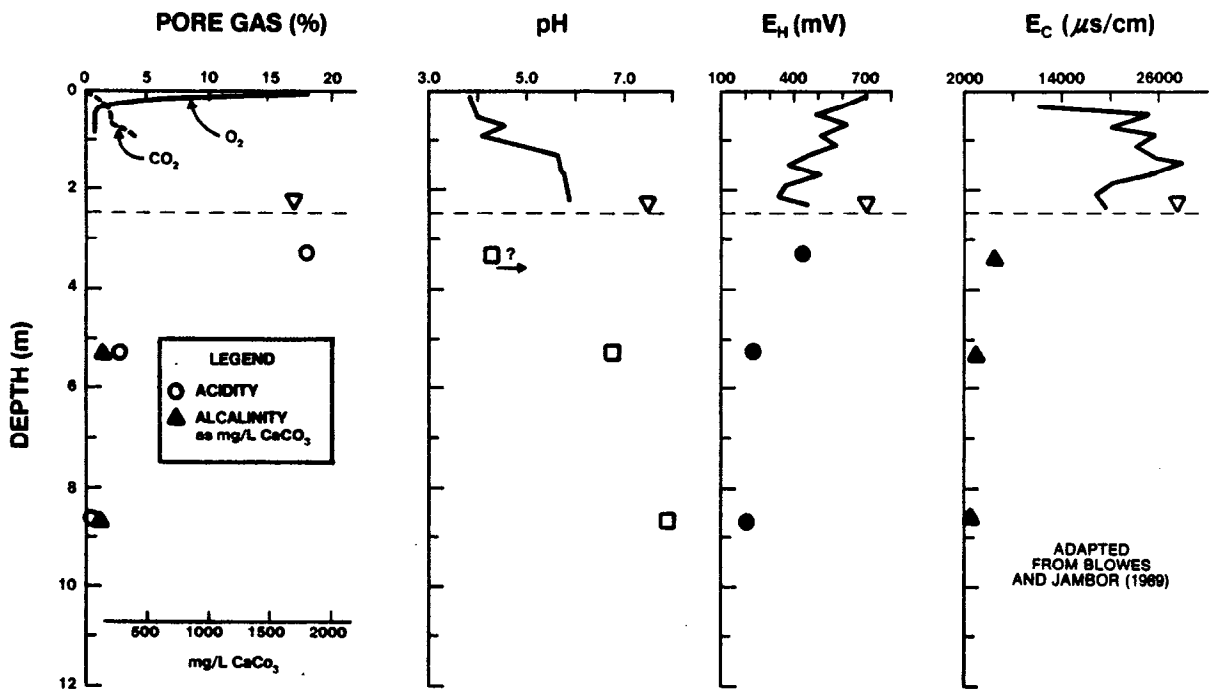
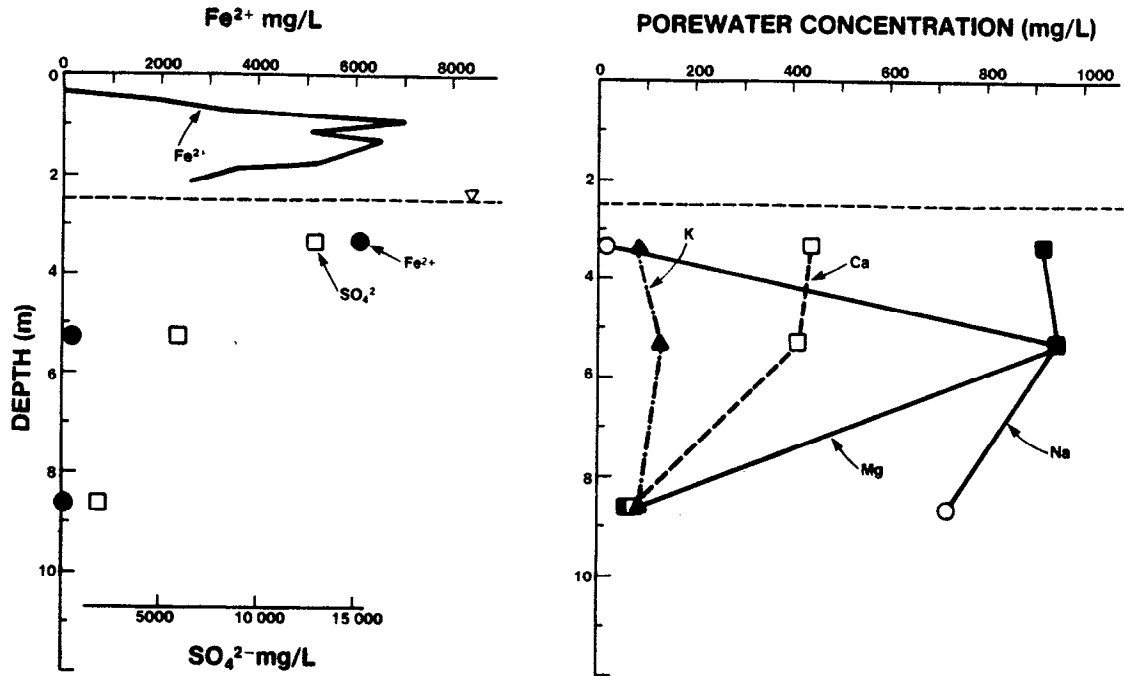


Figure 5.8 Pore Water Chemistry Profiles at WA-11



WA - 11 OCTOBER 1986

Figure 5.9 Pore Water Chemistry Profiles at WA-11

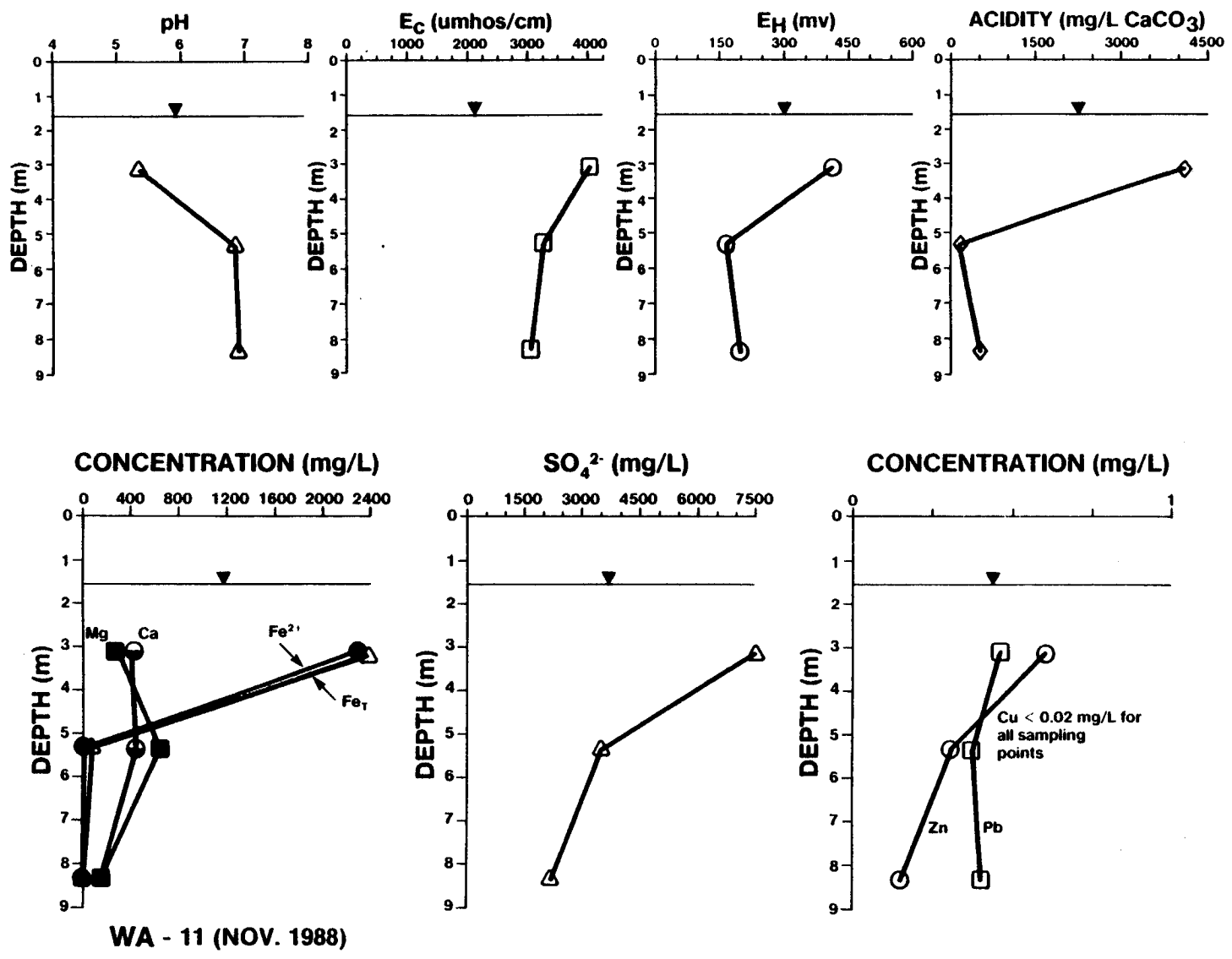


Figure 5.10 Pore Water Chemistry Profiles at WA-11

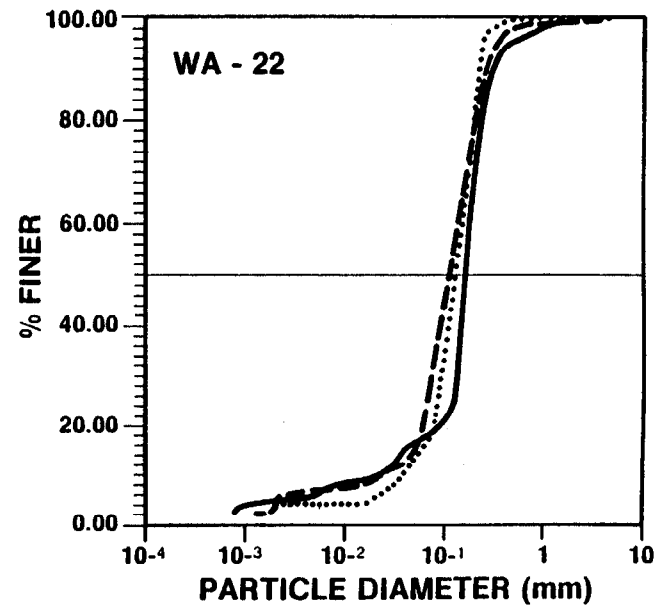
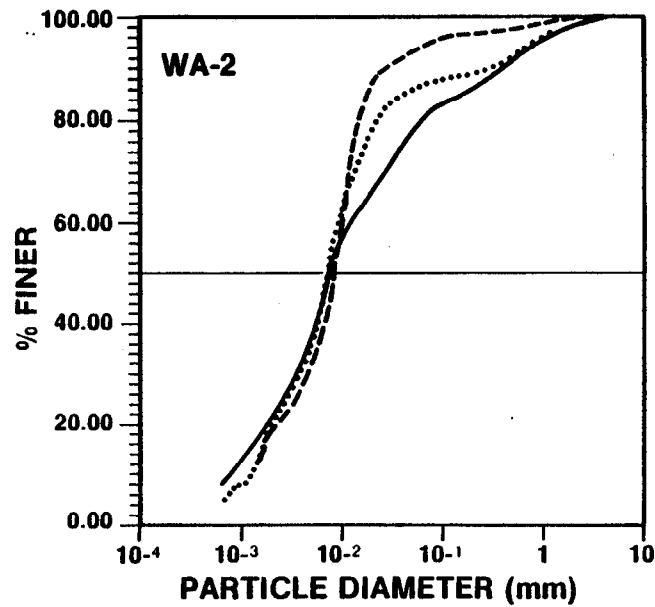


Figure 6.1 Grain Size Distribution Curves for Waite Amulet Tailings at WA-2 and WA-20. Solid, dotted and dashed lines represent, respectively, shallow, intermediate and deep sample depths.

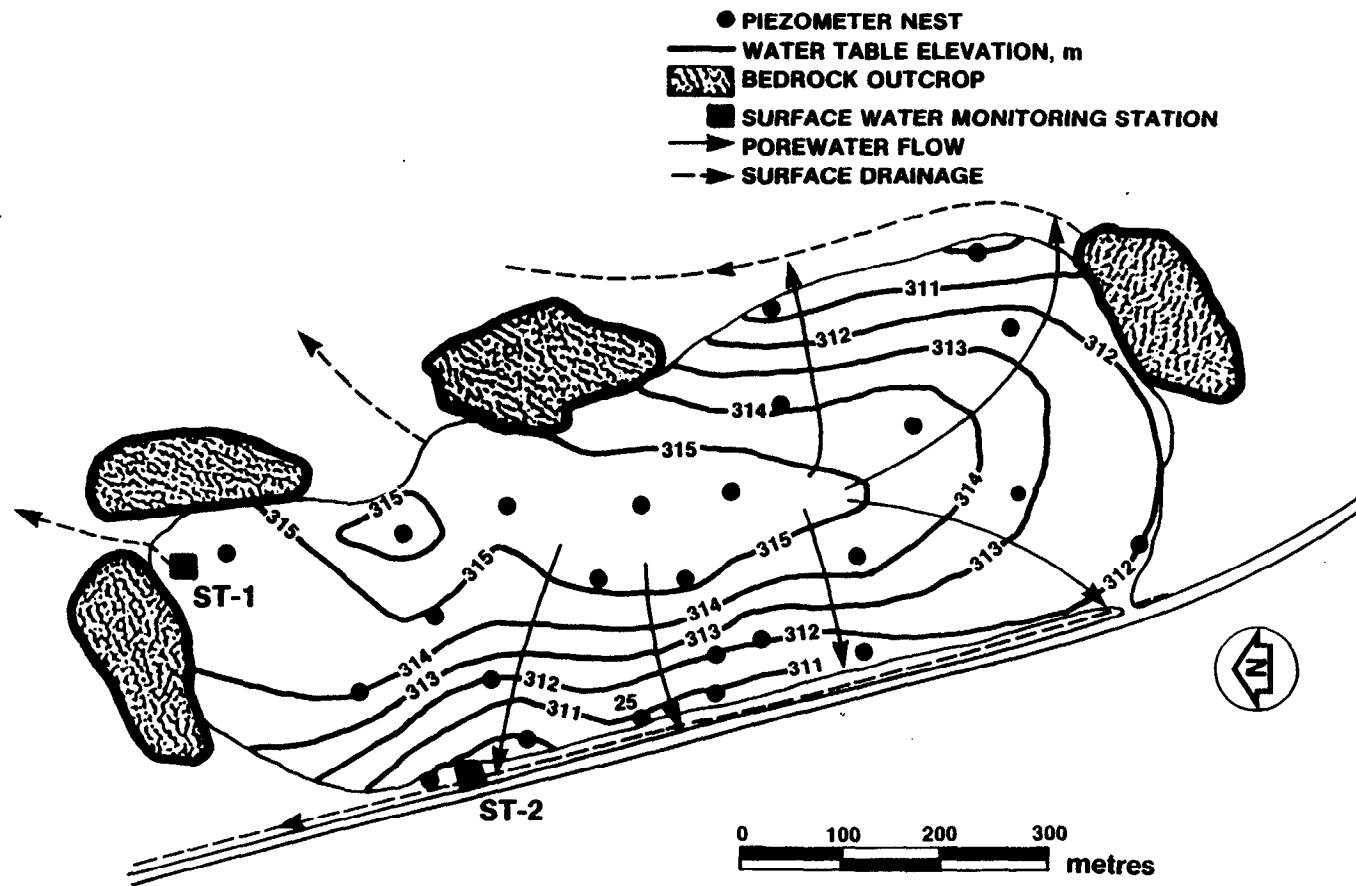


Figure 6.2 Water Table at Waite Amulet, October 1986

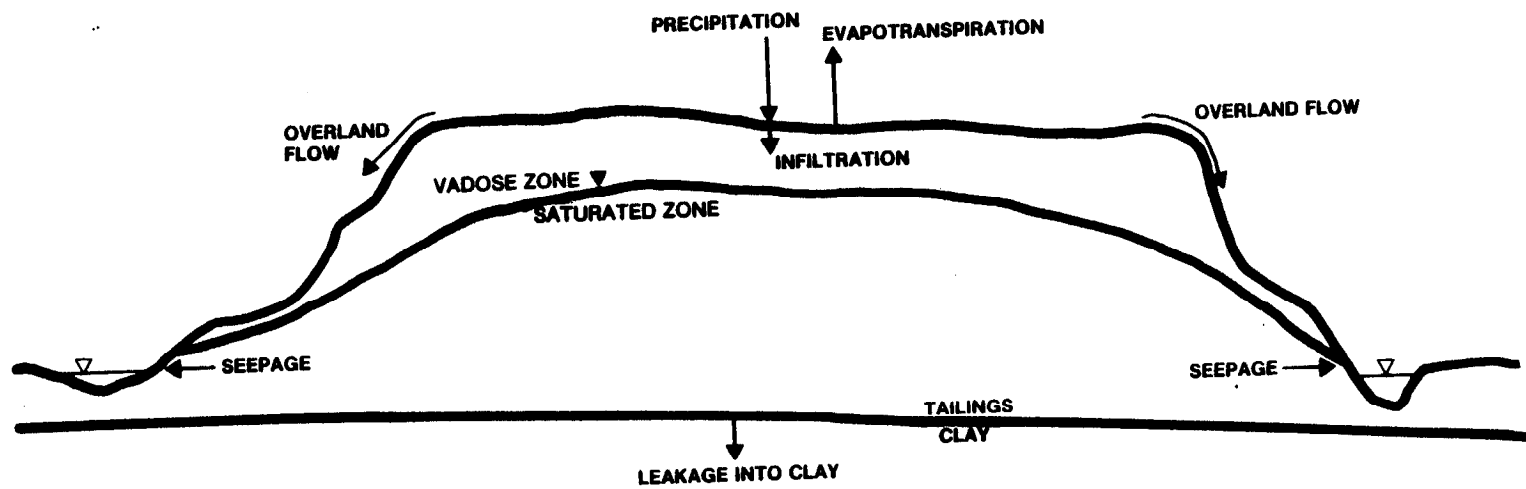


Figure 7.1 Hydrogeologic Cycle for Waite Amulet Tailings Site

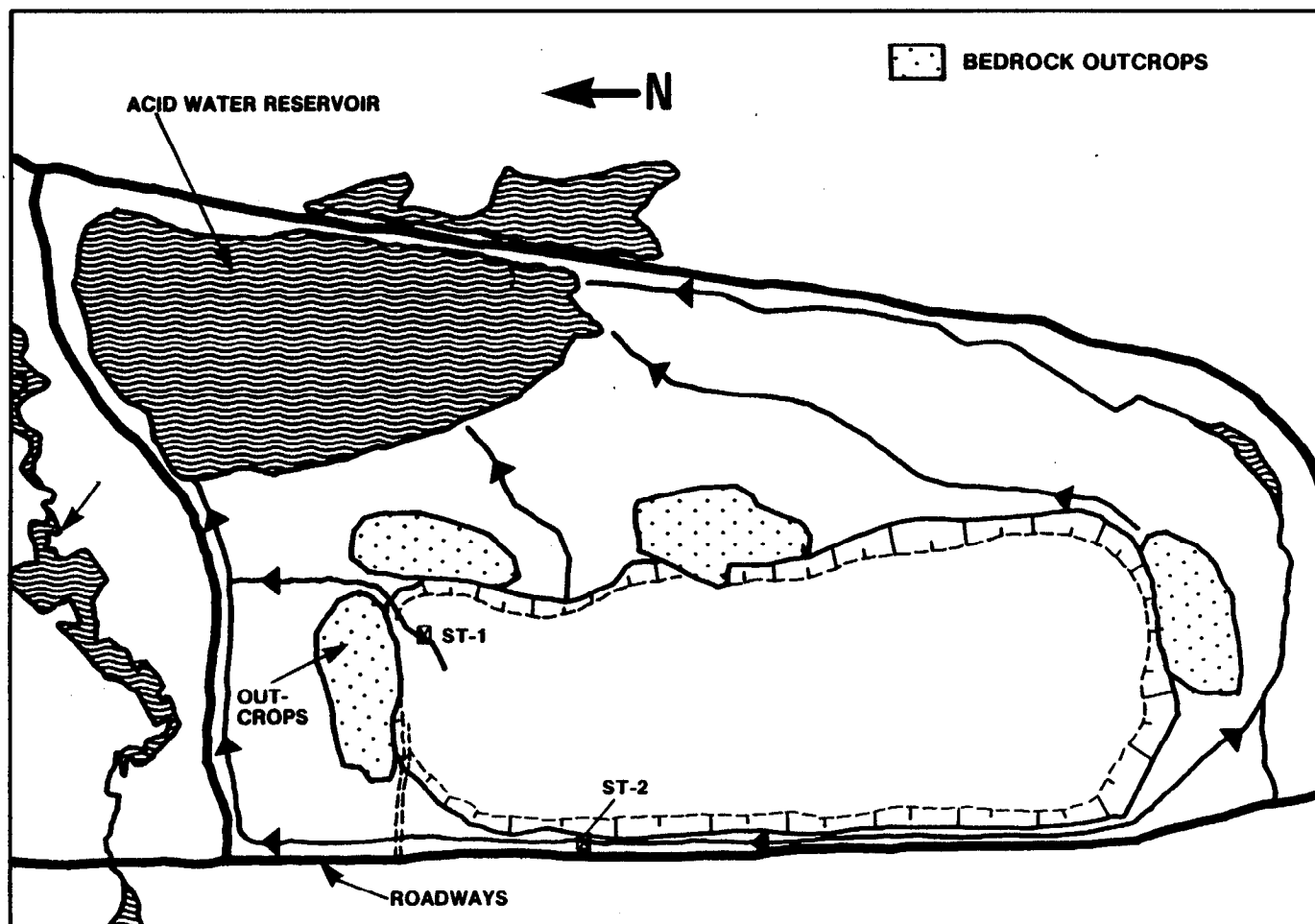


Figure 7.2 Location of Meteorological and Surface Water Monitoring Stations

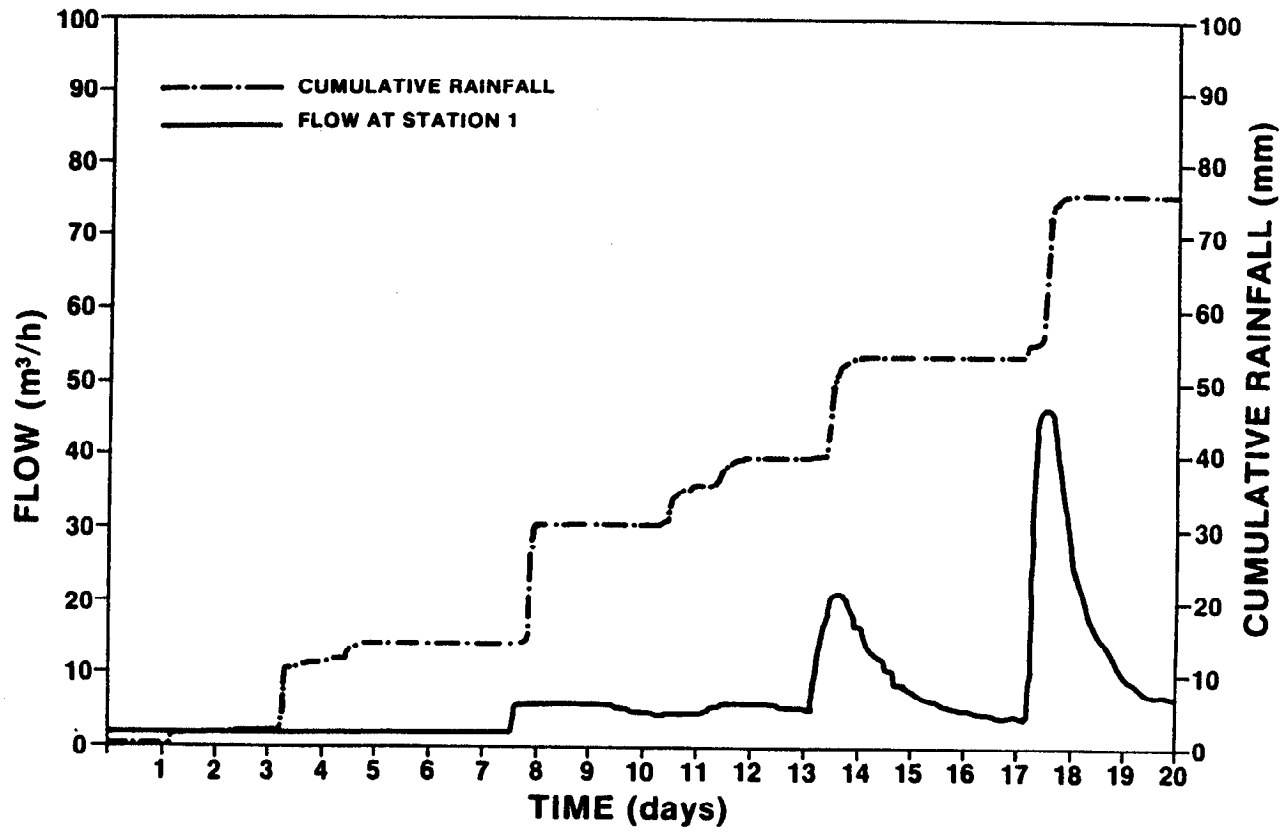


Figure 7.3 Cumulative Rainfall and Storm Hydrograph at Station 1 for September 1988

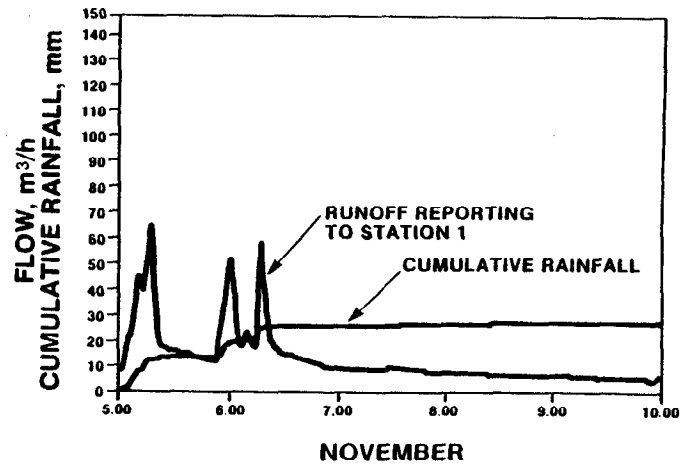
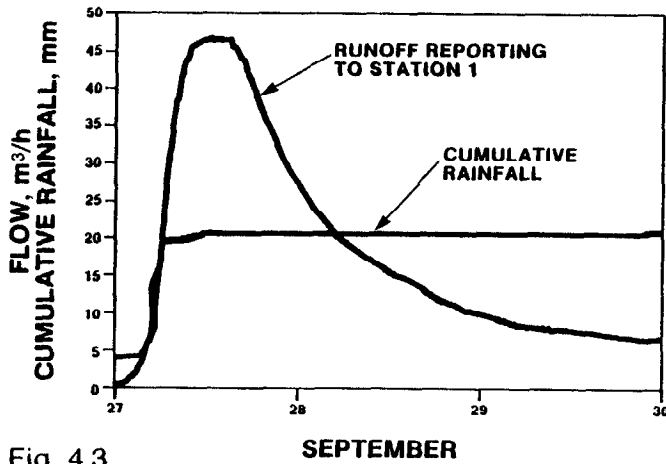
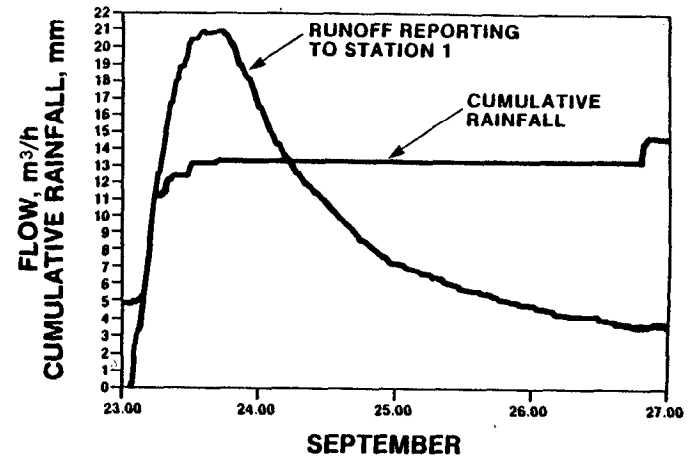
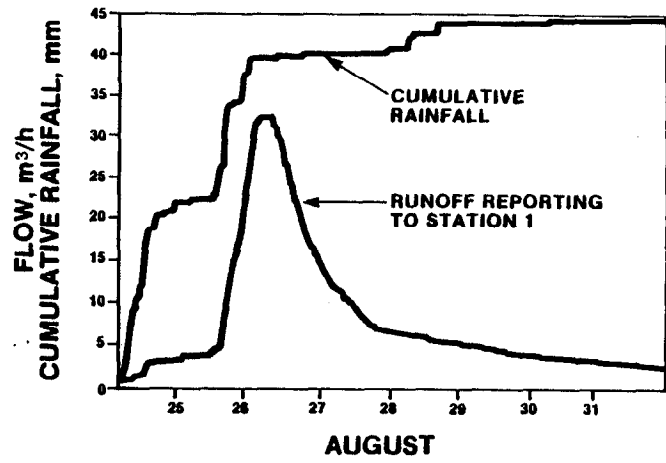


Fig. 4.3

Figure 7.4 Cumulative Rainfall and Storm Hydrographs at Station 1 for 26 August, 24 and 27 September, and 5 November 1988

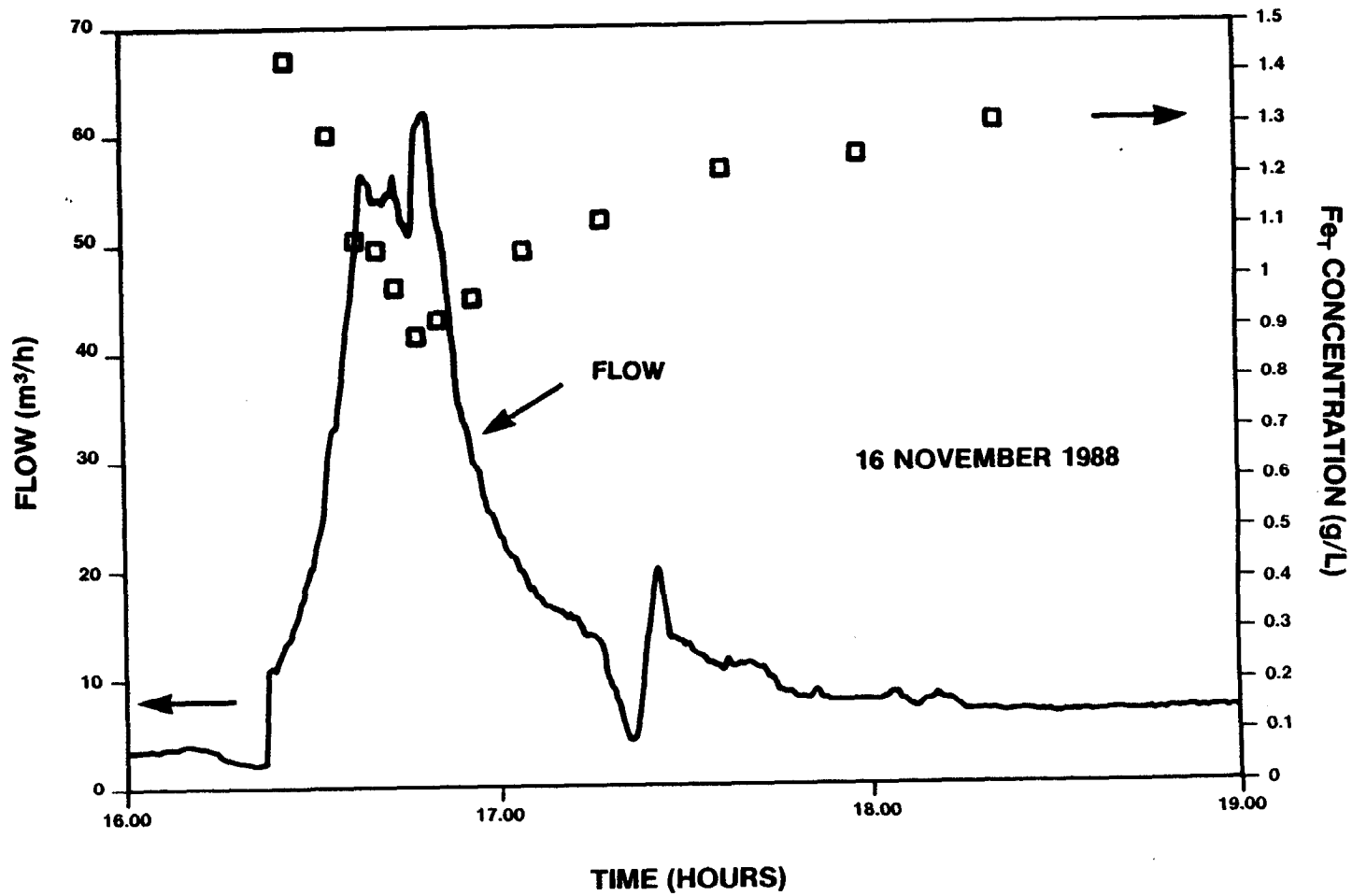


Figure 7.5 Flow and Fe_T Concentrations Versus Time at Station 2, November 1988

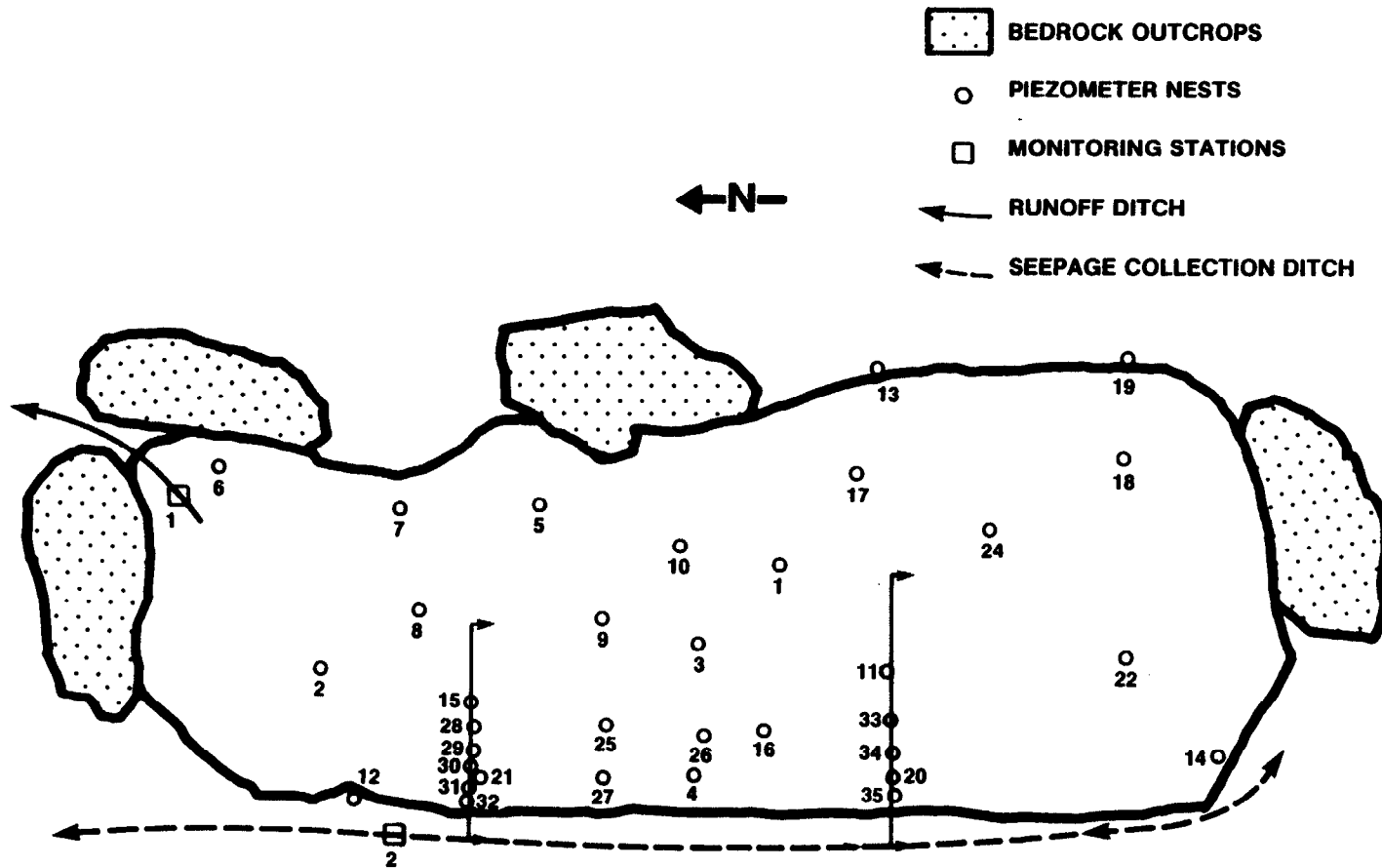


Figure 8.1 Plan of Tailings Showing Locations of Piezometer Nests and Sections A-A' and B-B'

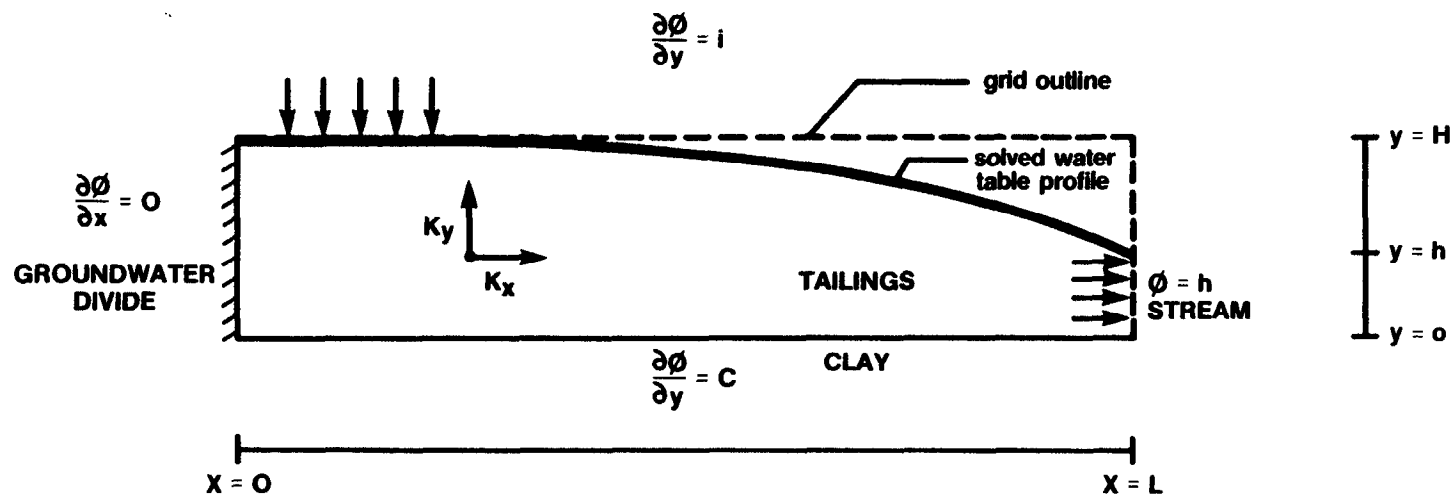


Figure 8.2 Boundary Conditions for Two-Dimensional Flow Modelling of Waite Amulet Tailings

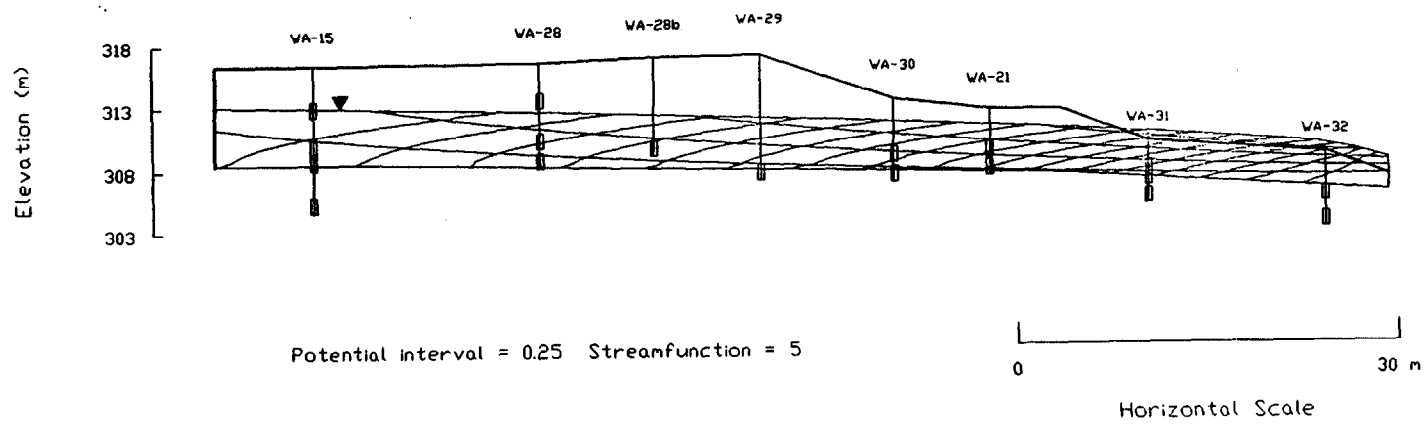


Figure 8.3 Calibrated Flow Net Section A-A, Waite Amulet Tailings

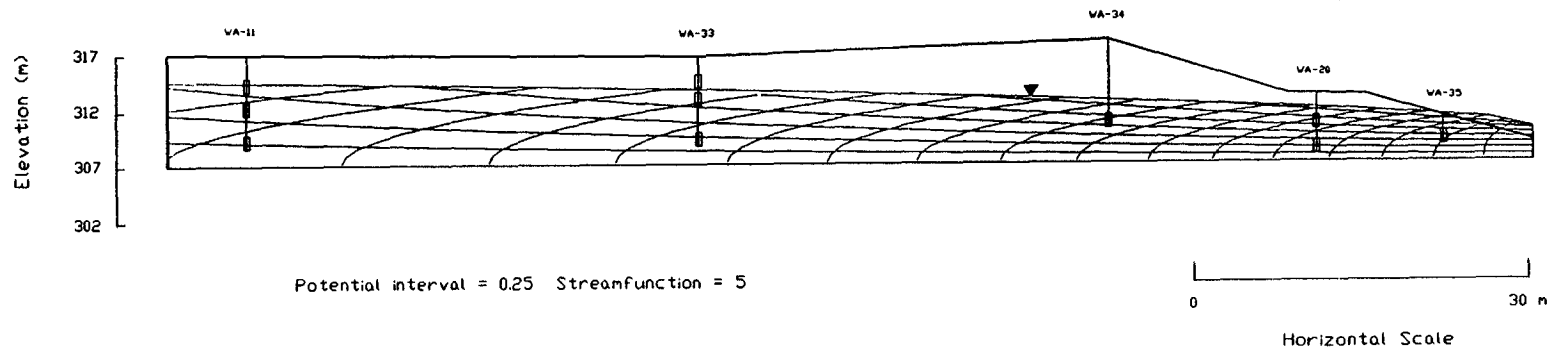


Figure 8.4 Calibrated Flow Net Section B-B, Waite Amulet Tailings

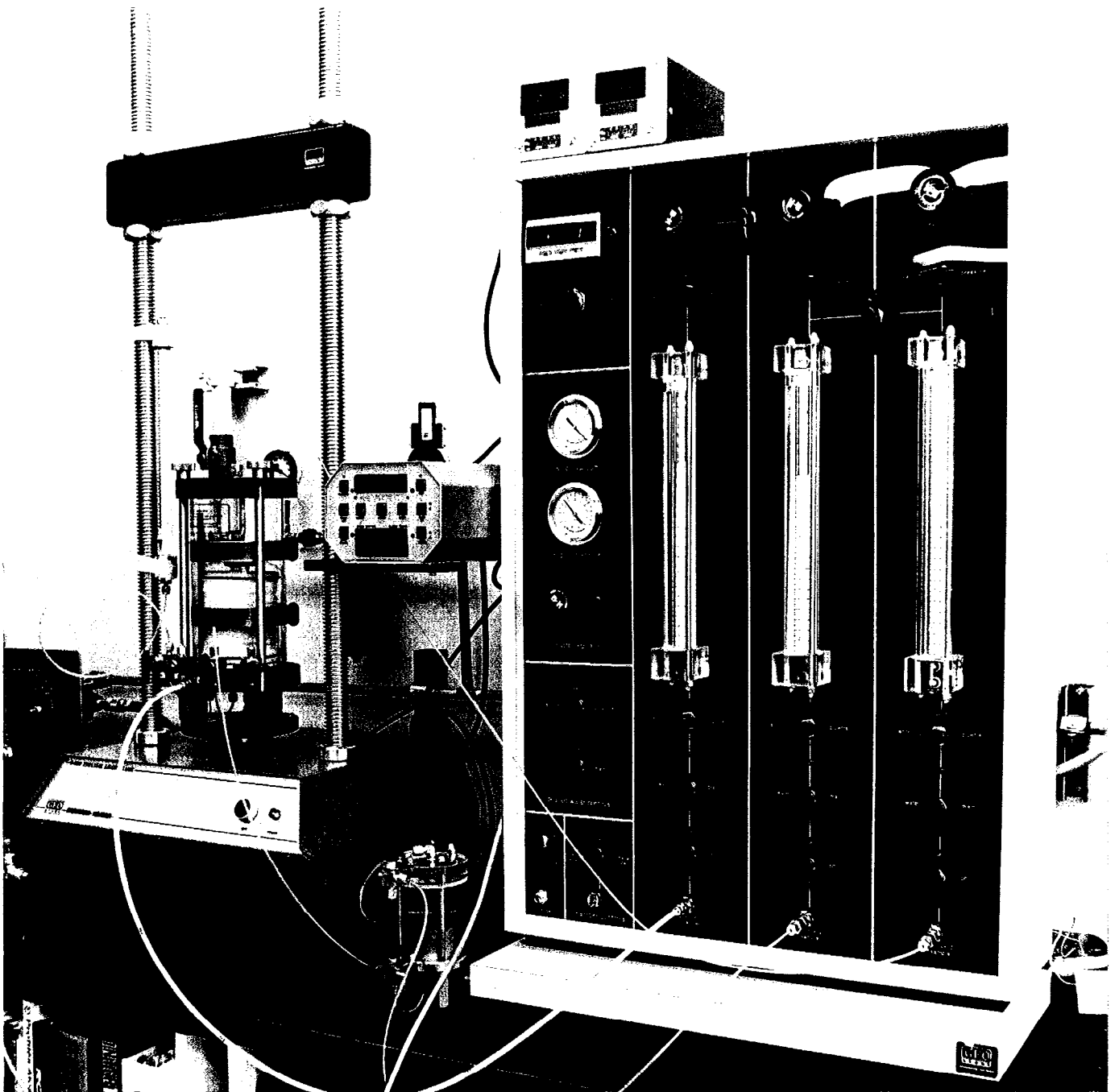


FIGURE 10.1 Triaxial panel and cell used in the hydraulic conductivity tests.

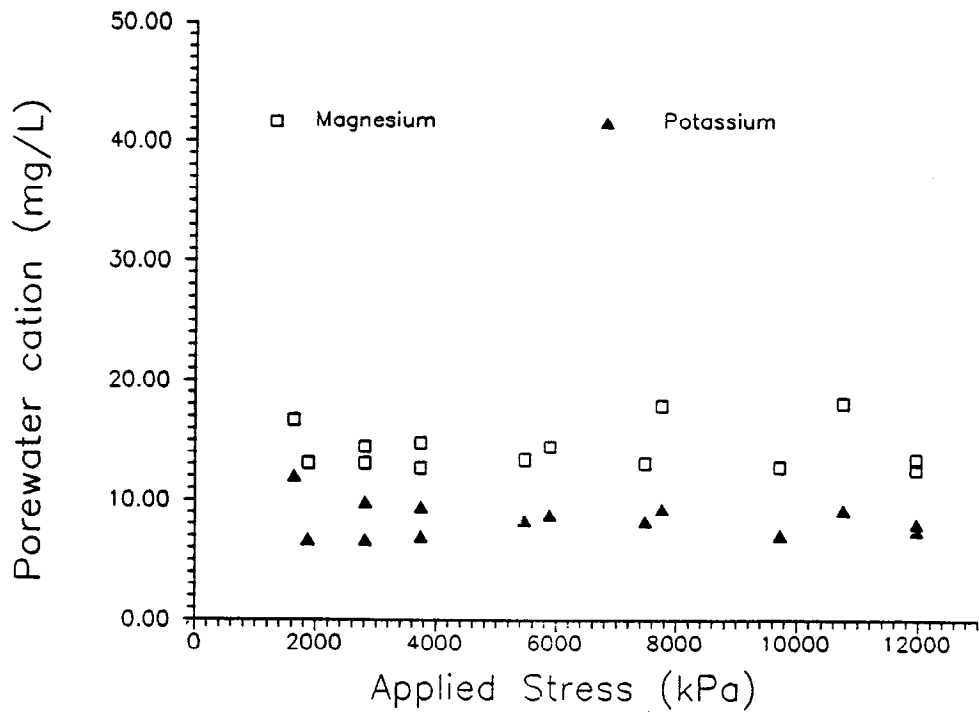
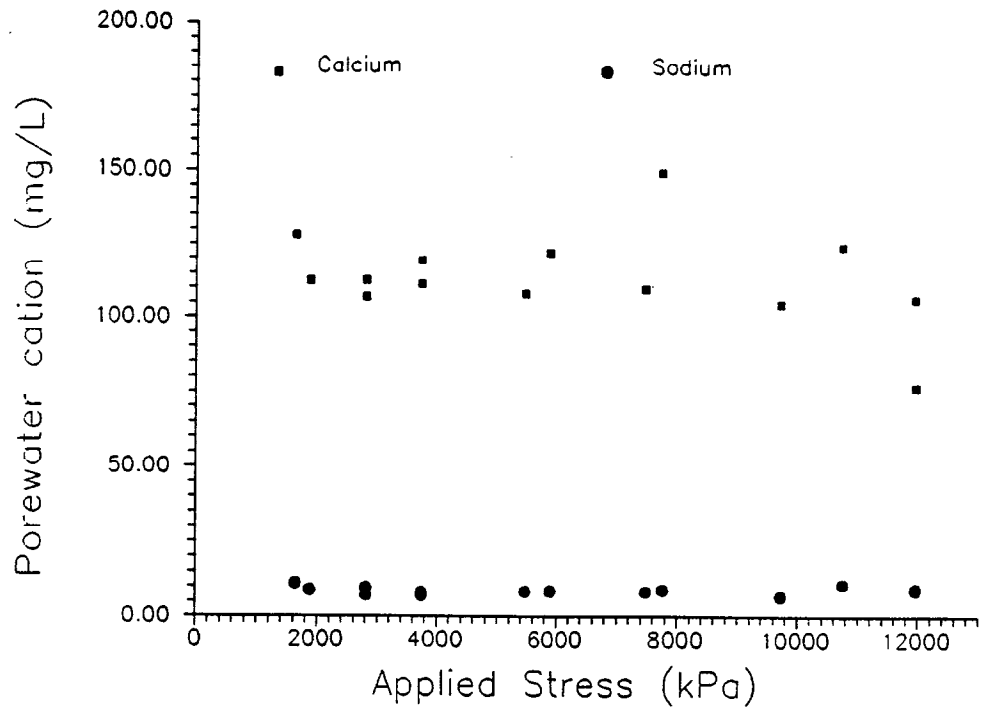


Figure 10.2 Applied Squeeze Pressures vs Pore Water Cation Concentrations in Background Waite Amulet Clay.

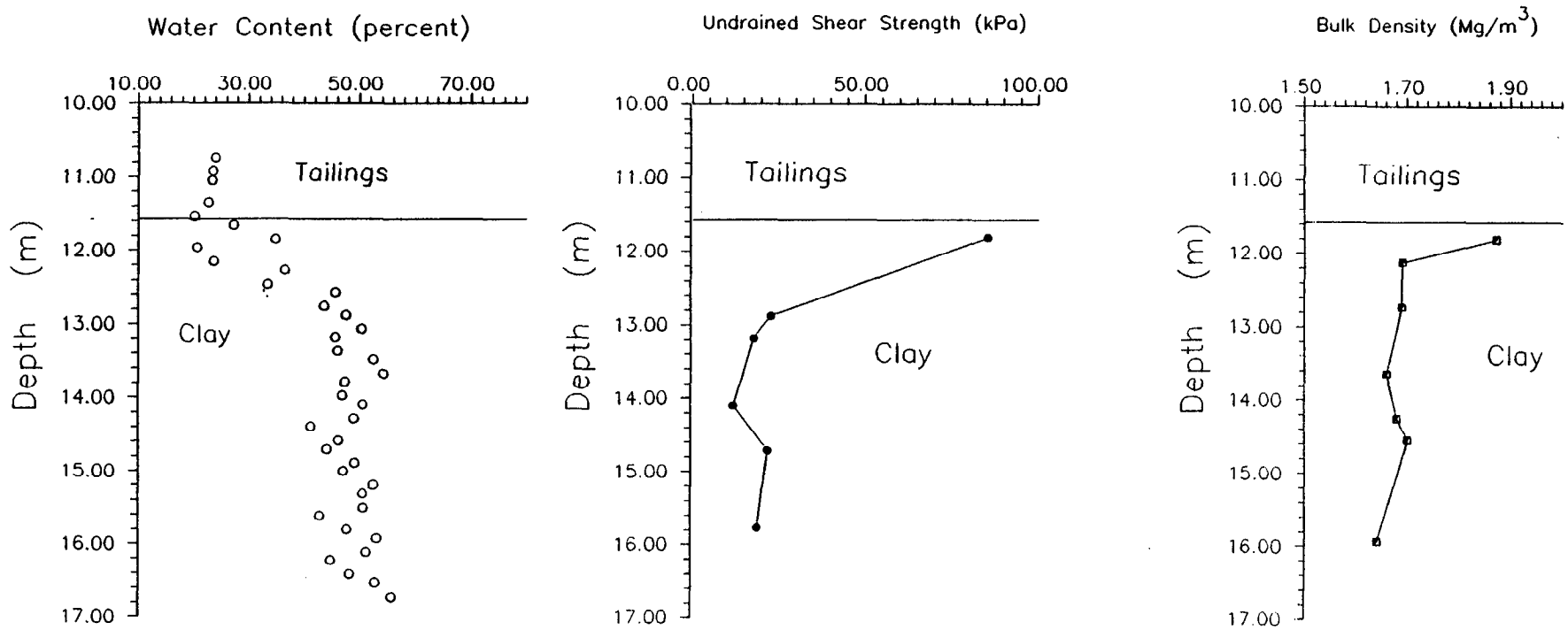


Figure 10.3 Geotechnical Profiles at WA-11.

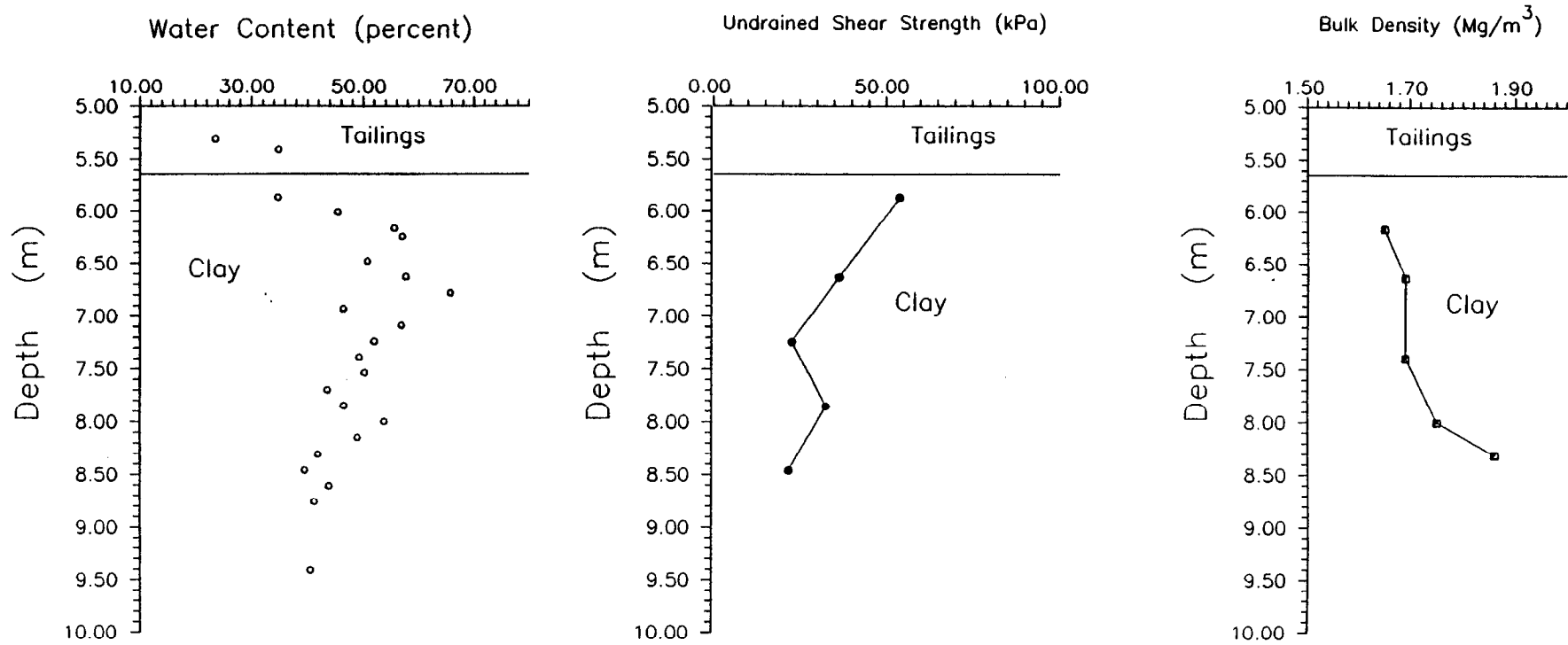


Figure 10.4 Geotechnical Profiles at WA-20.

<p style="text-align: center;">HYDROMETER</p> <p style="text-align: center;">CENTRE DE TECHNOLOGIE NORANDA</p> <p>ENVIRONMENT & MINING LABORATORY</p>	HYDROMETER NO.	SHEET	OF
	TEST NO.		
	LOCATION <i>WAITE AMULET</i>		
	B.H. NO. <i>WA-20</i>	SAMPLE NO. <i>XF2-5</i>	
	DEPTH FROM <i>6.27m</i> TO <i>6.40m</i>		
	DATE <i>18 Jan 1990</i>	TESTED BY <i>KSS</i>	

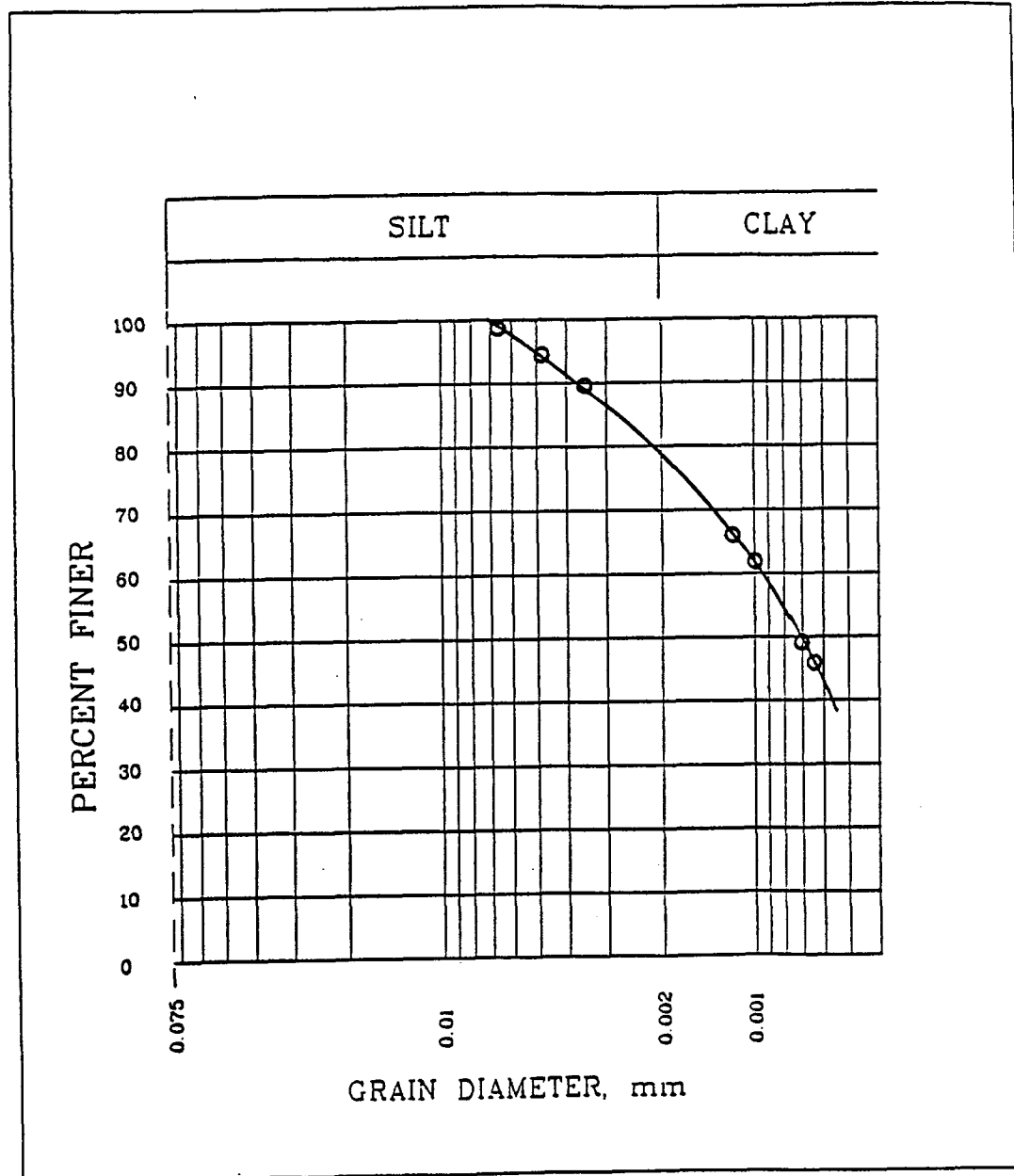


Figure 10.5 A Typical Grain Size Distribution of Waite Amulet Clay.

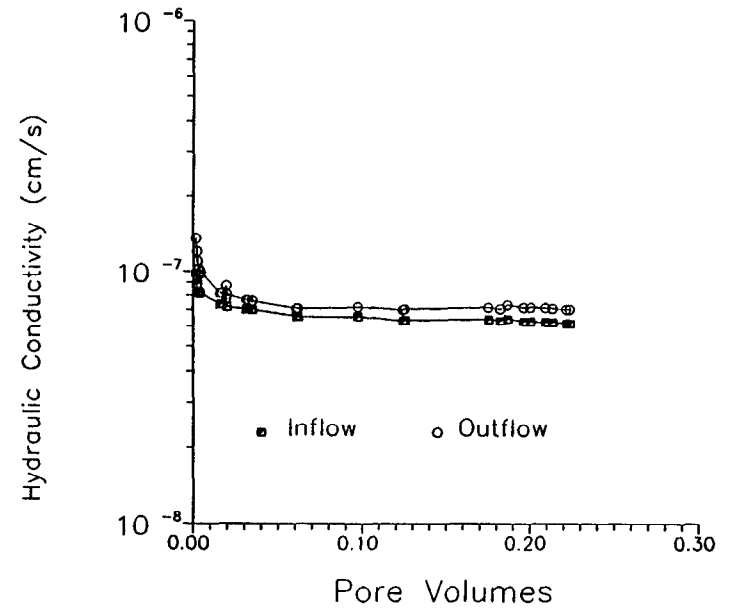
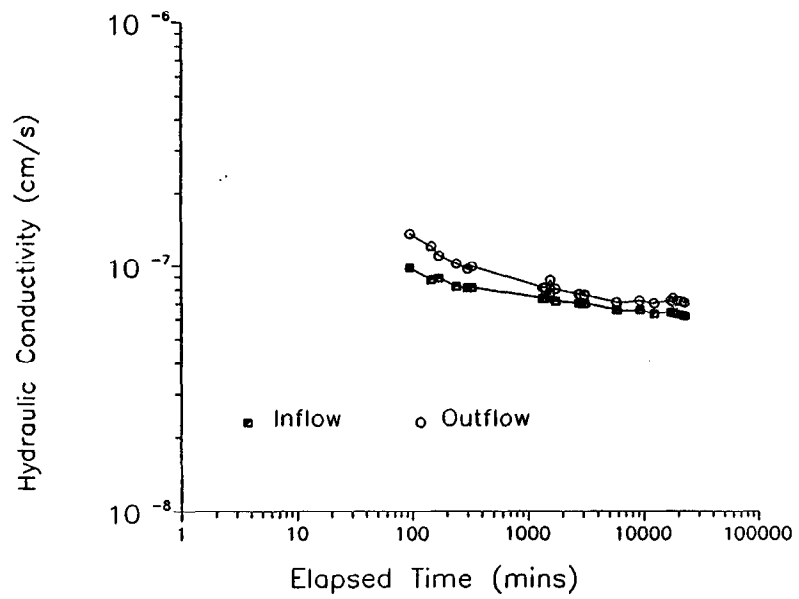


Figure 10.6 Hydraulic Conductivity of Clay Soil Near the Tailings/Clay Interface at WA-20 Permeated with Distilled Water.

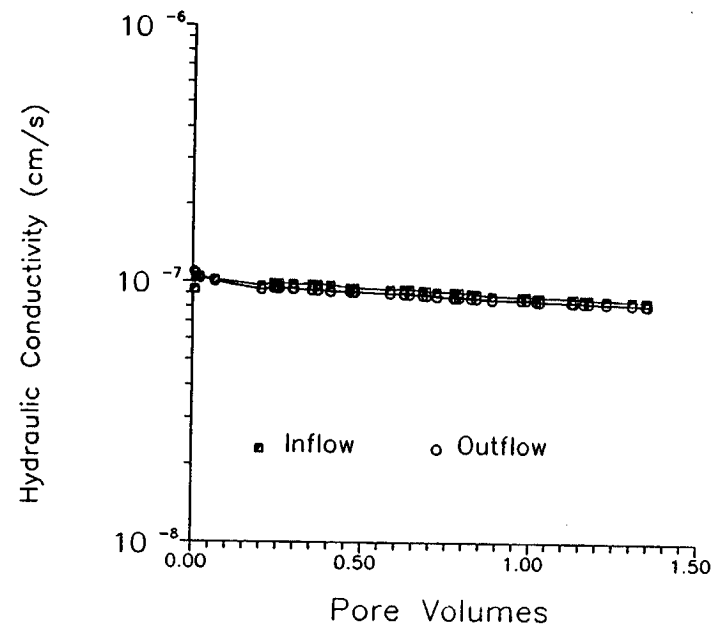
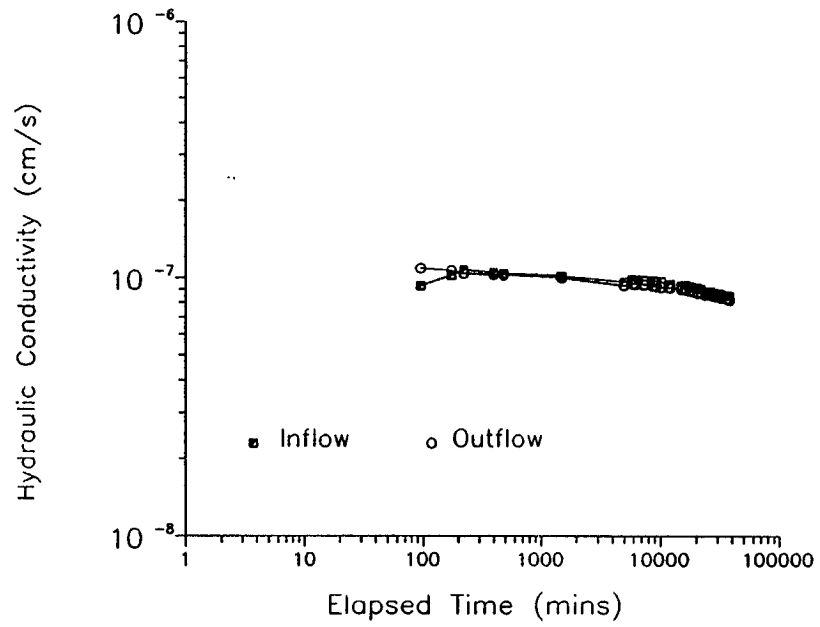


Figure 10.7 Hydraulic Conductivity of Clay Soil Near the Tailings/Clay Interface at WA-20 Permeated with Simulated Pore Water.

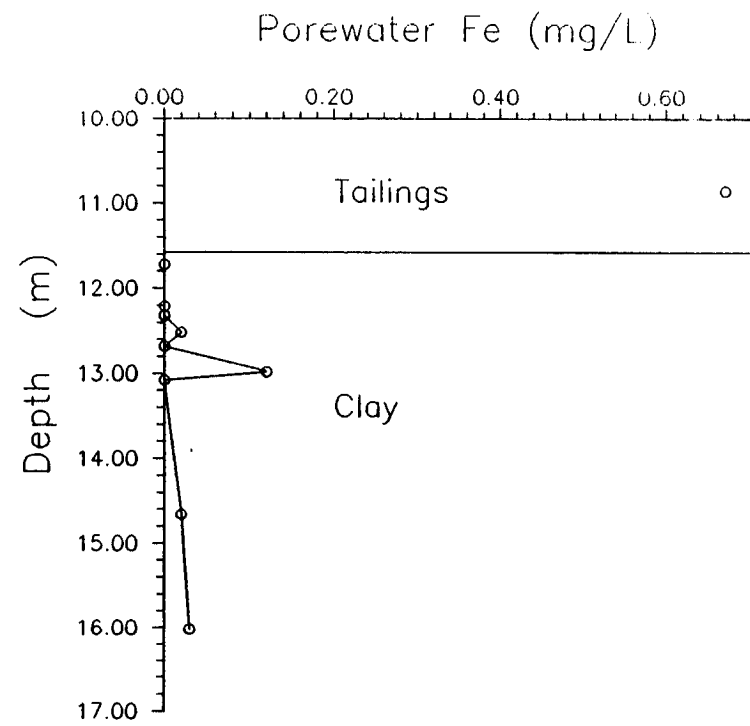
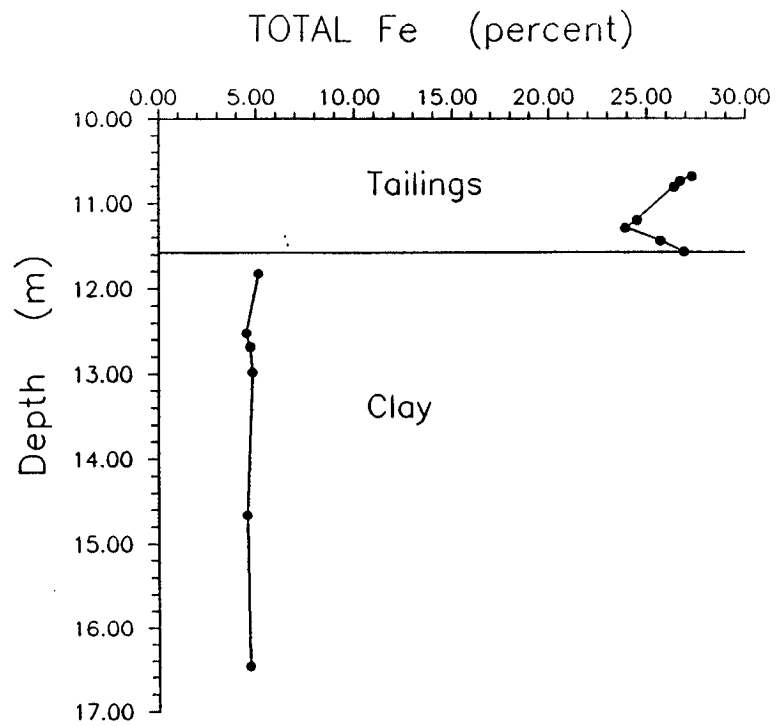


Figure 10.8 Iron Concentrations in Bulk Clay Soil and Pore Water at WA-11.

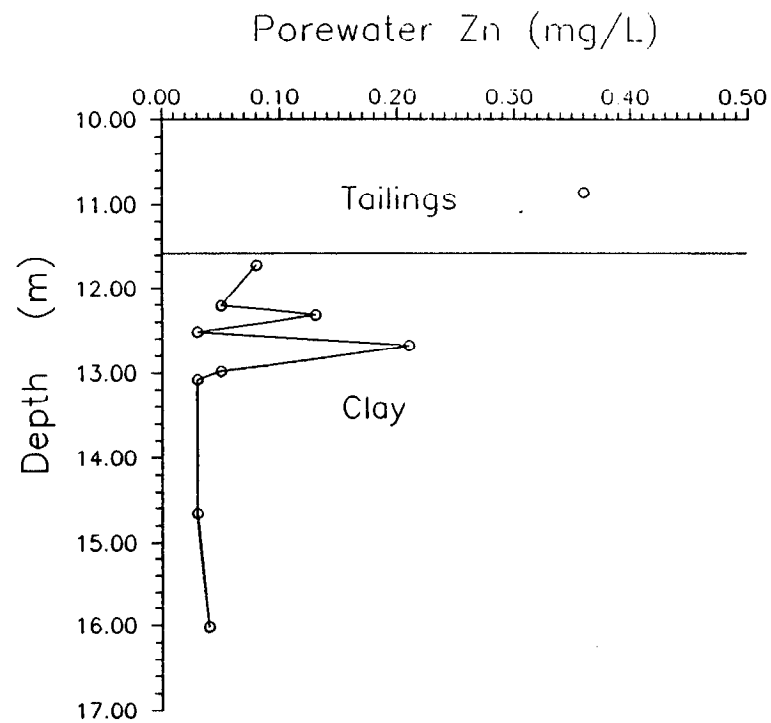
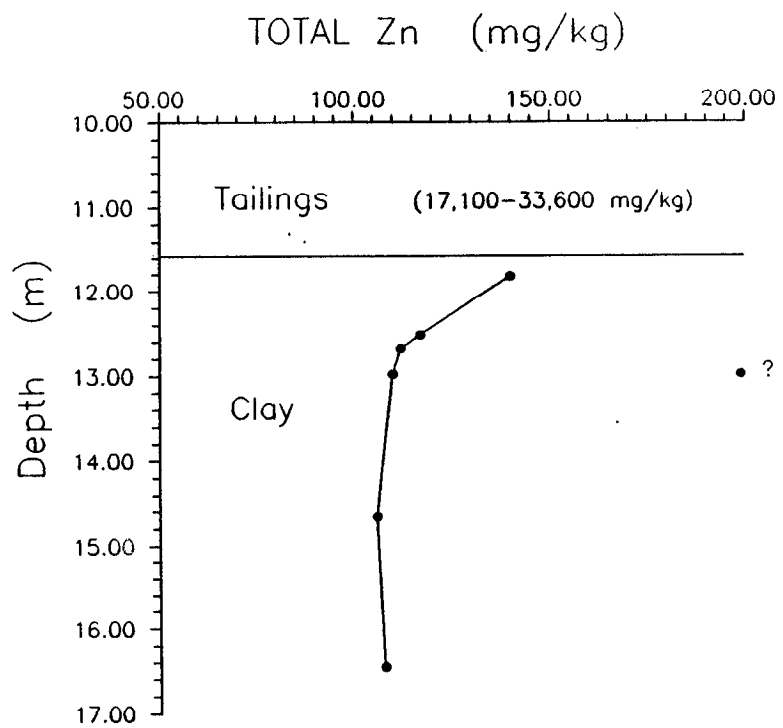


Figure 10.9 Zinc Concentrations in Bulk Clay Soil and Pore Water at WA-11.

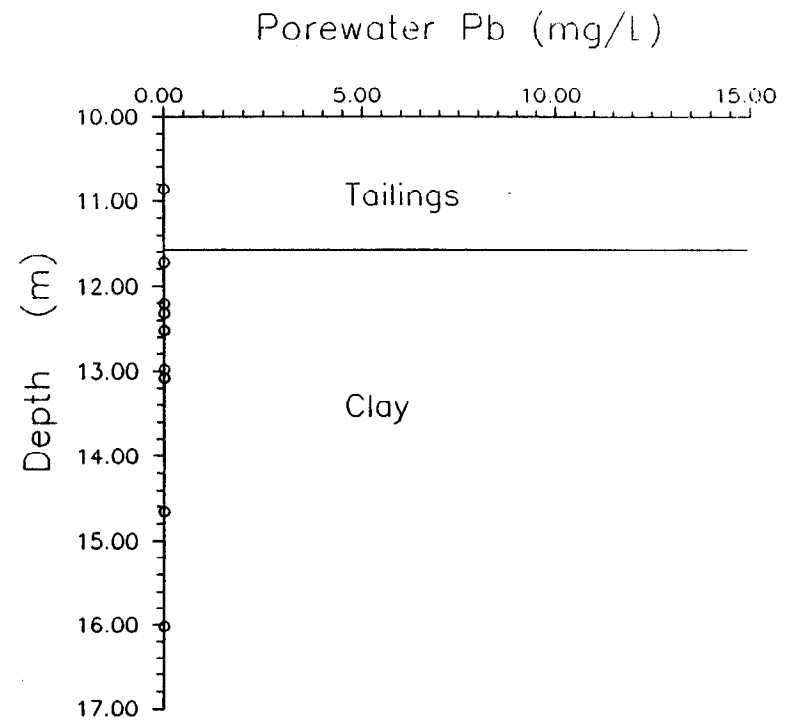
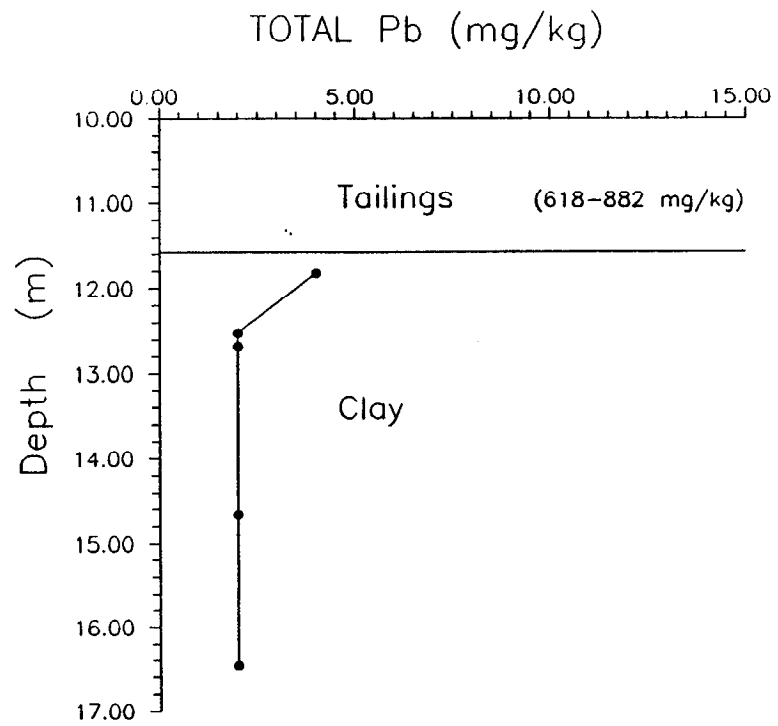


Figure 10.10 Lead Concentrations in Bulk Clay Soil and Pore Water at WA-11.

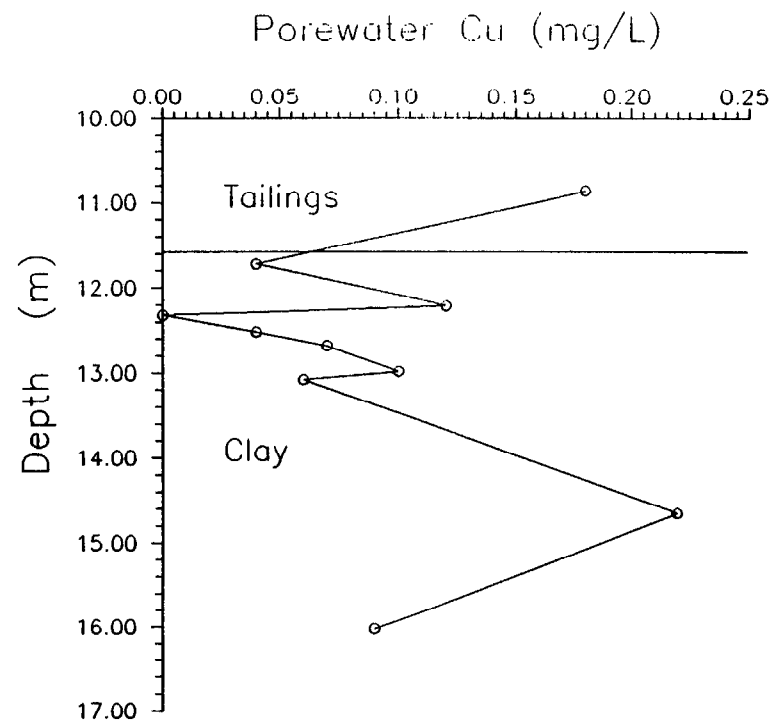
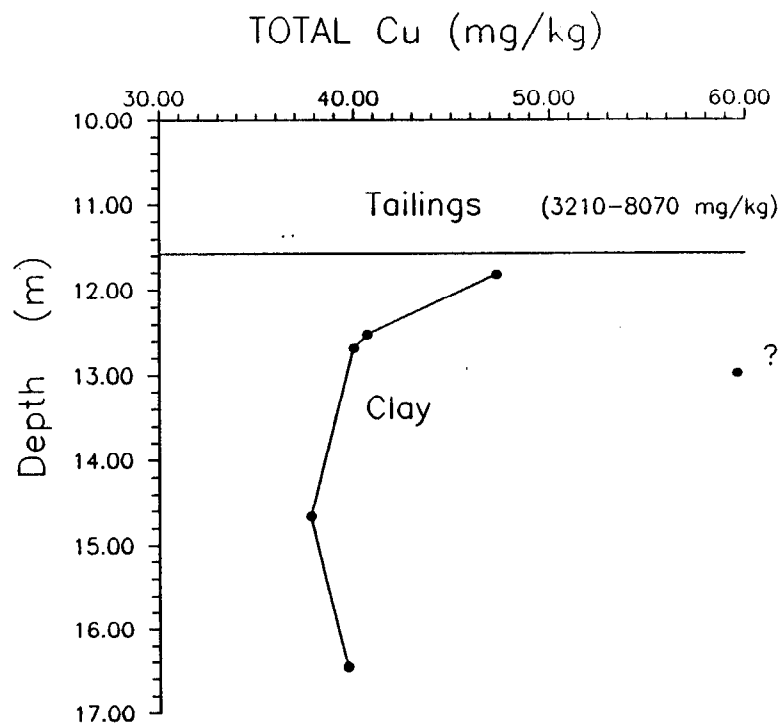


Figure 10.11 Copper Concentrations in Bulk Clay Soil and Pore Water at WA-11.

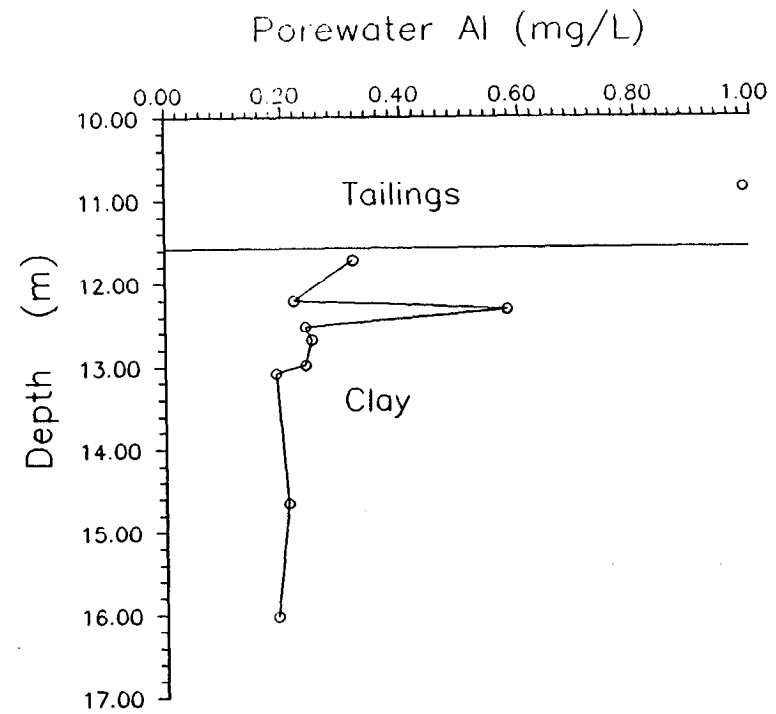
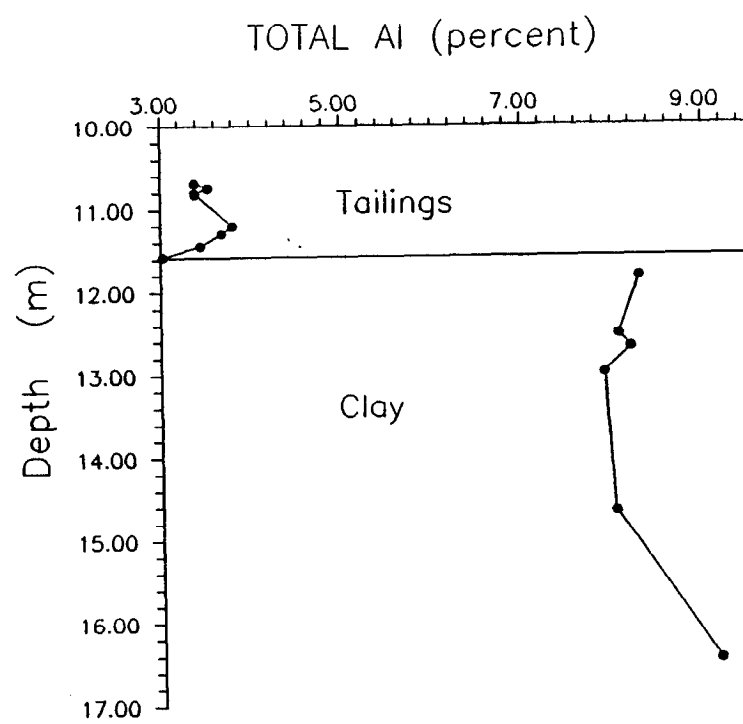


Figure 10.12 Aluminum Concentrations in Bulk Clay Soil and Pore Water at WA-11.

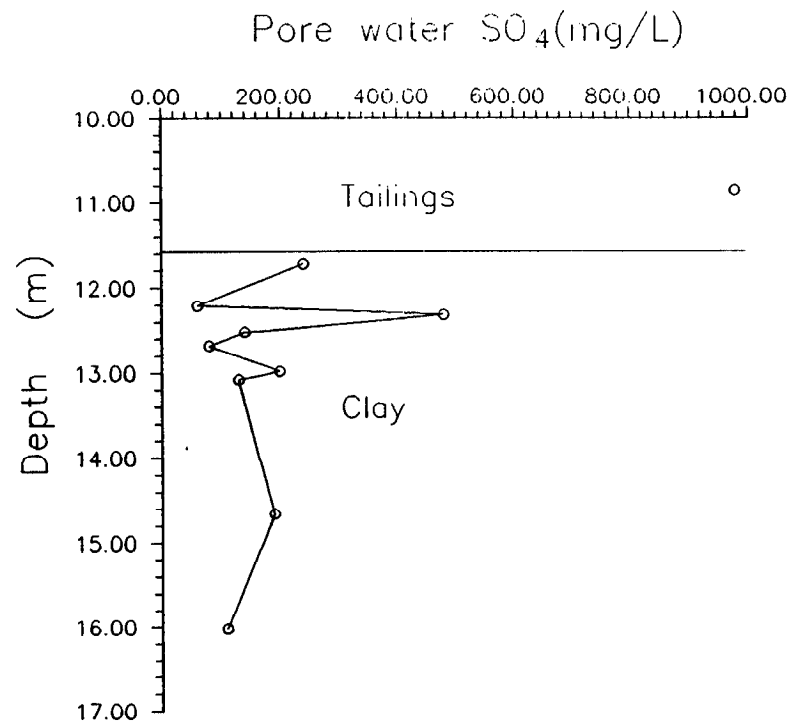
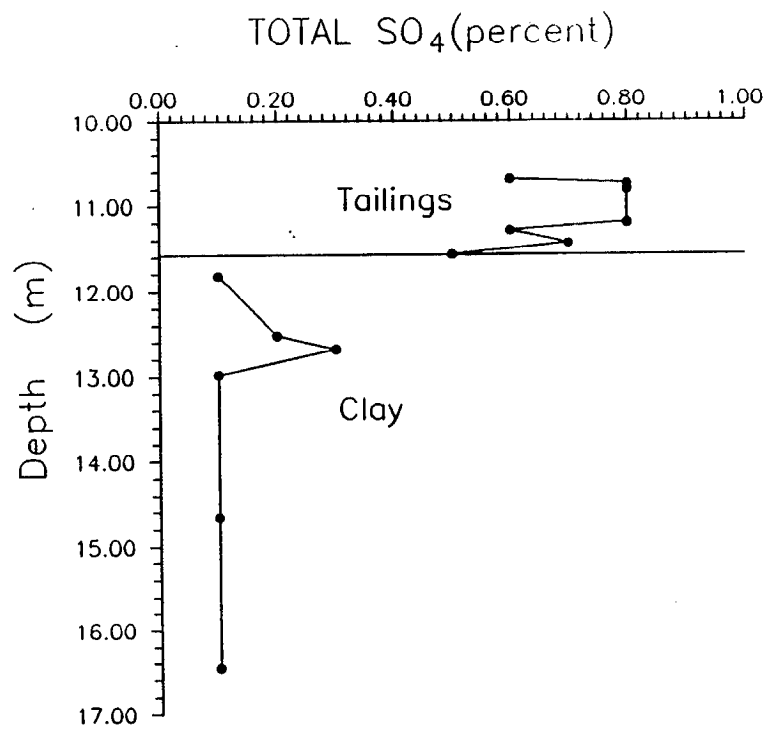


Figure 10.13 Sulphate Concentrations in Bulk Clay Soil and Pore Water at WA-11.

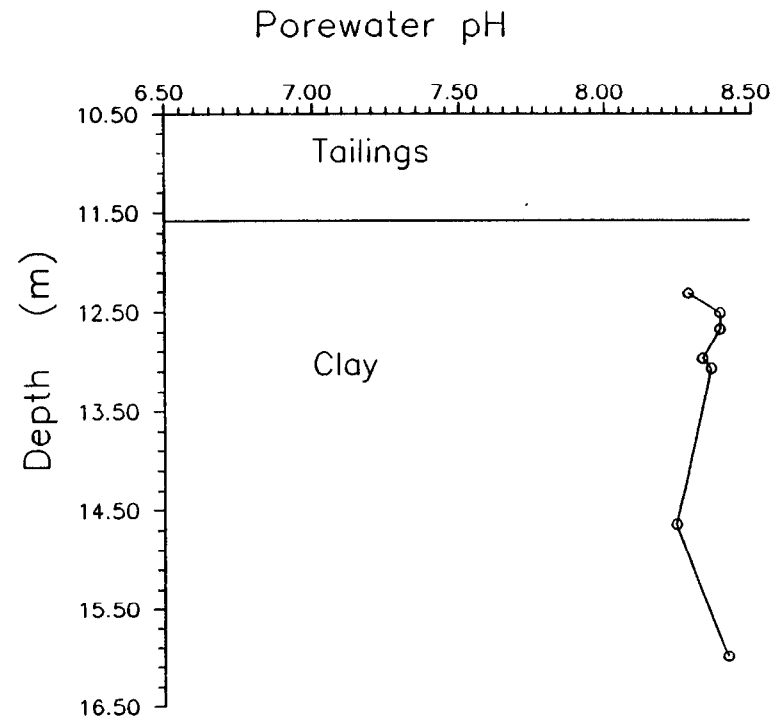
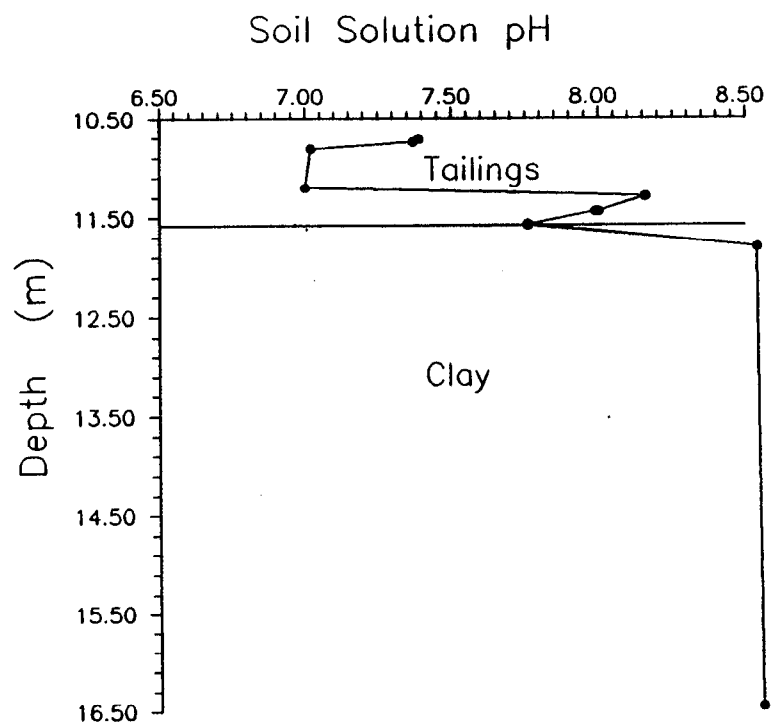


Figure 10.14 Soil Solution and Clay Pore Water pH Profiles at WA-11.

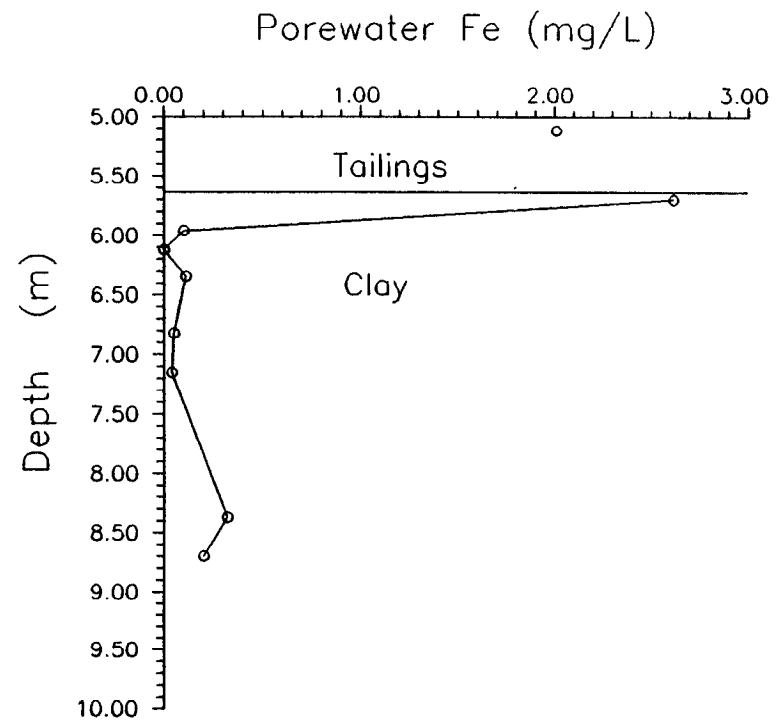
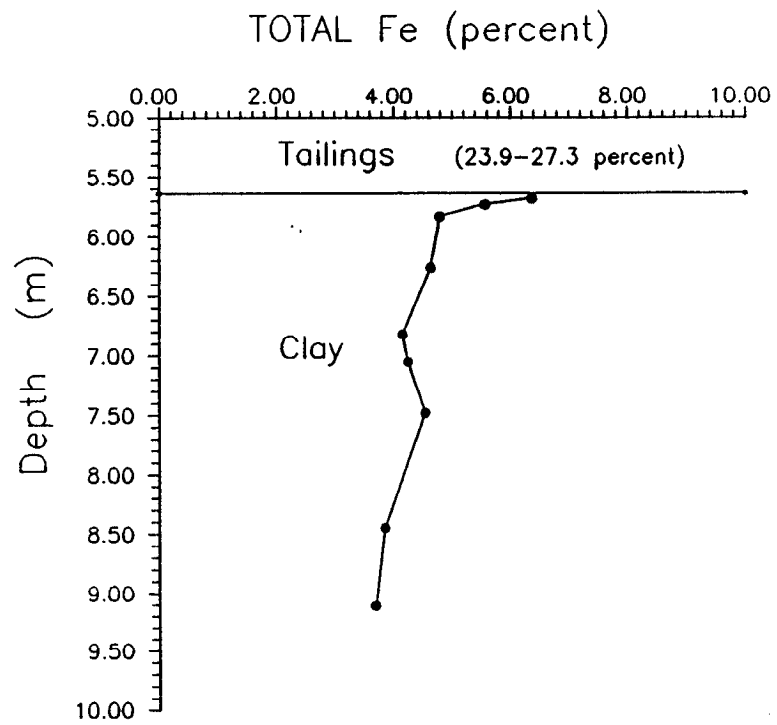


Figure 10.15 Iron Concentrations in Bulk Clay Soil and Pore Water at WA-20.

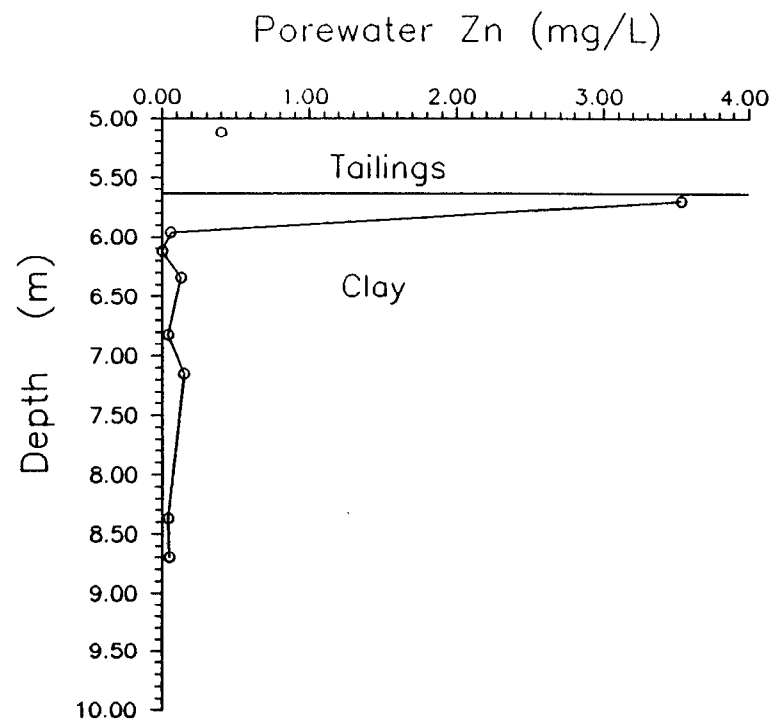
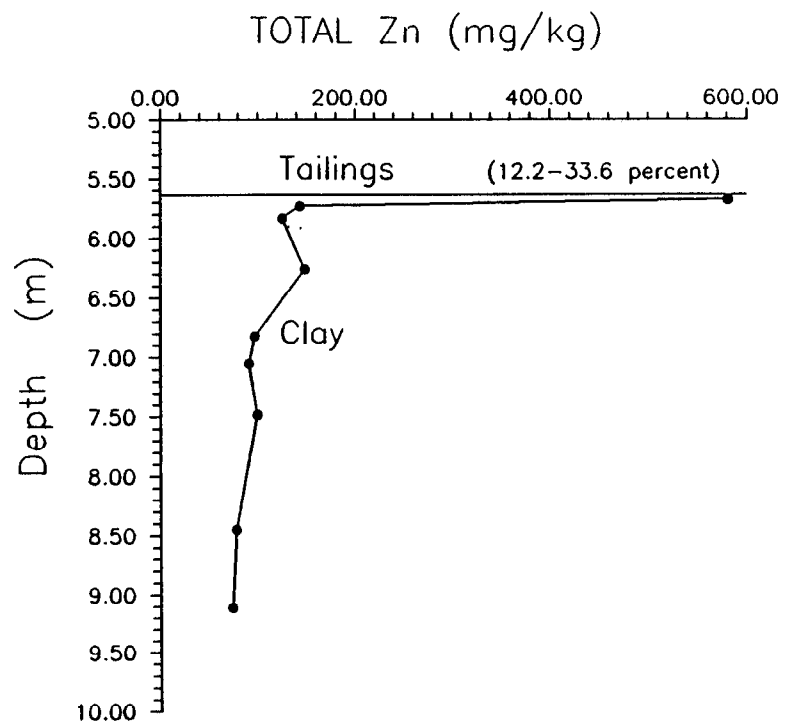


Figure 10.16 Zinc Concentrations in Bulk Clay Soil and Pore Water at WA-20.

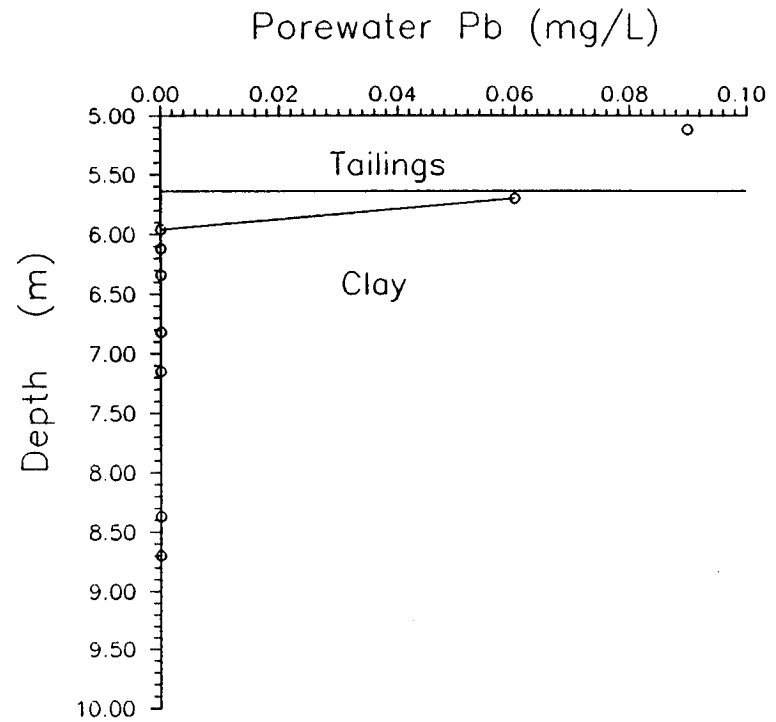
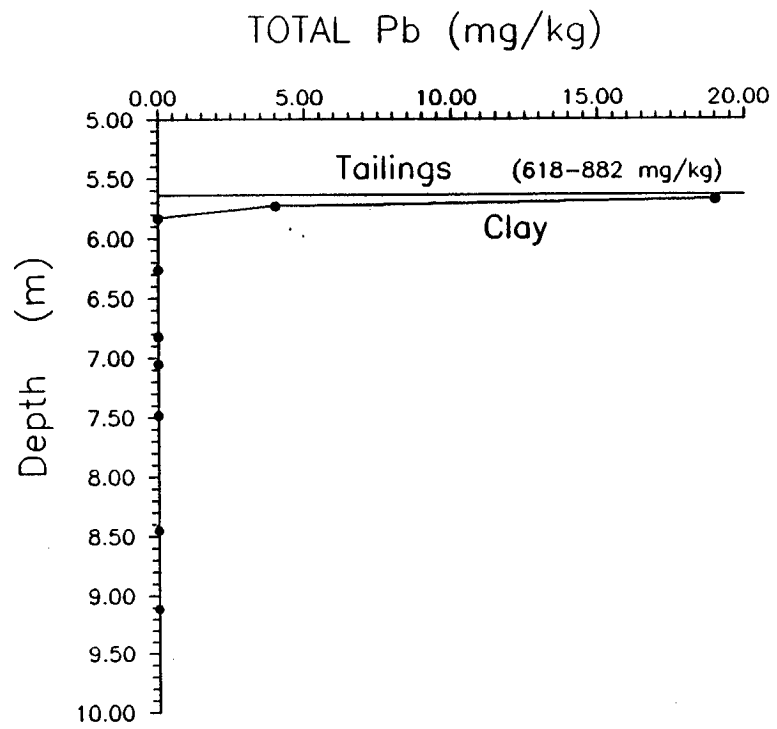


Figure 10.17 Lead Concentrations in Bulk Clay Soil and Pore Water at WA-20.

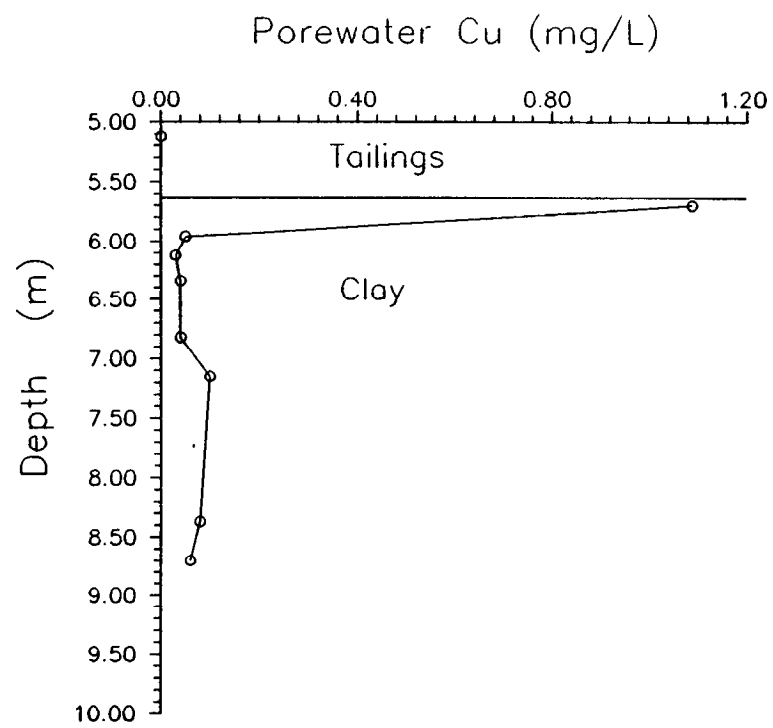
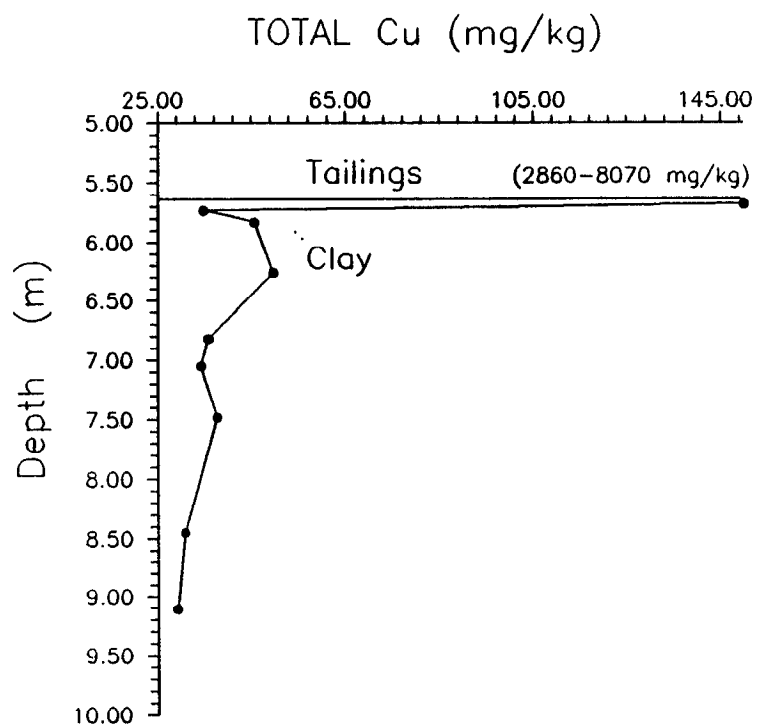


Figure 10.18 Copper Concentrations in Bulk Clay Soil and Pore Water at WA-20.

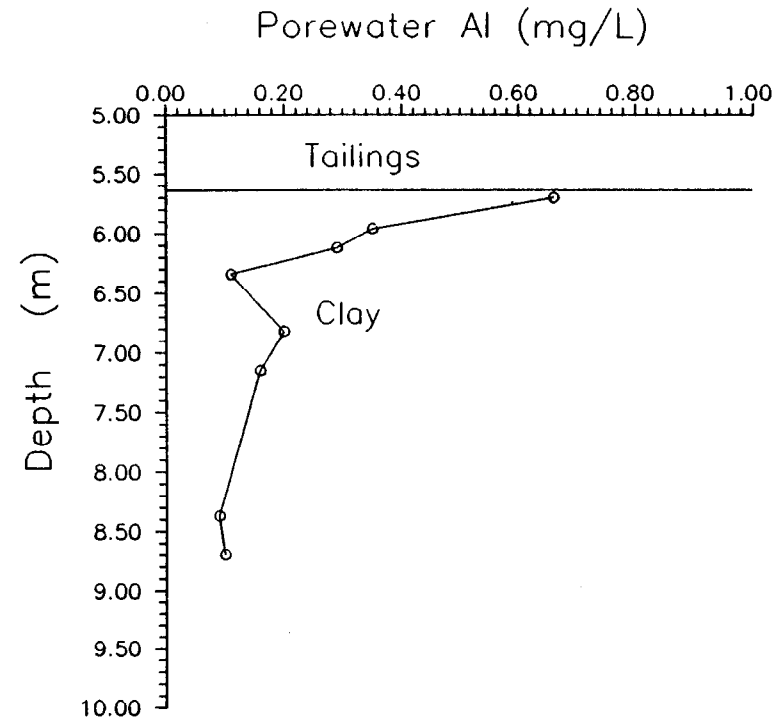
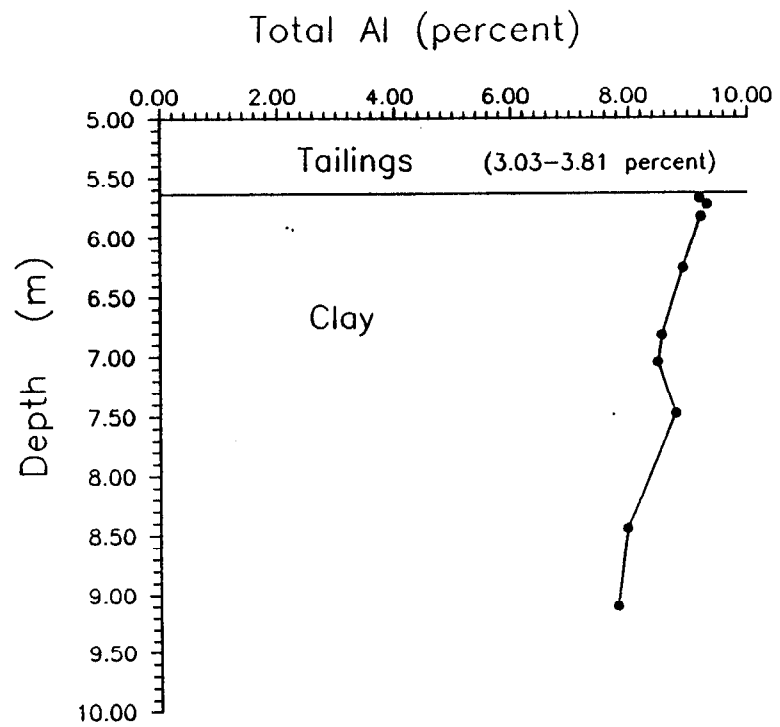


Figure 10.19 Aluminum Concentrations in Bulk Clay Soil and Pore Water at WA-20.

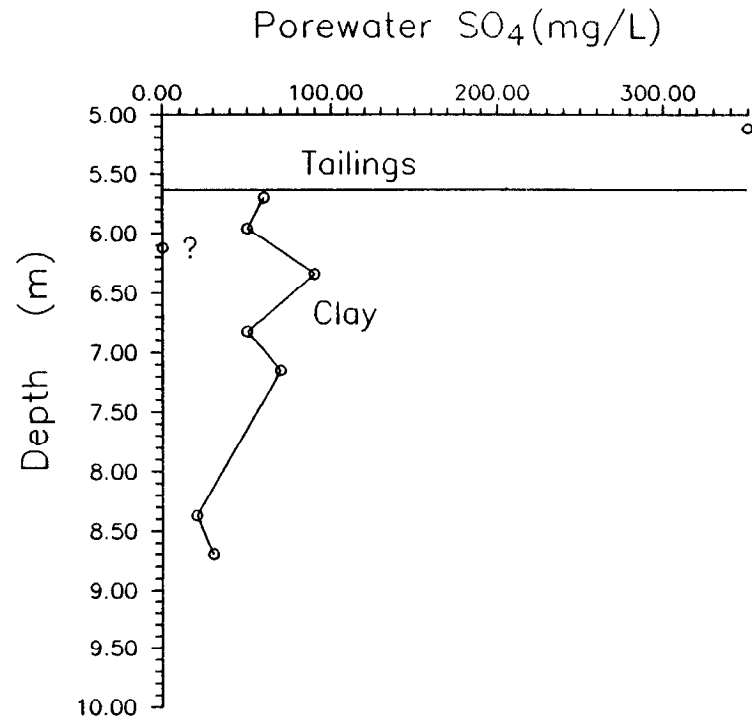
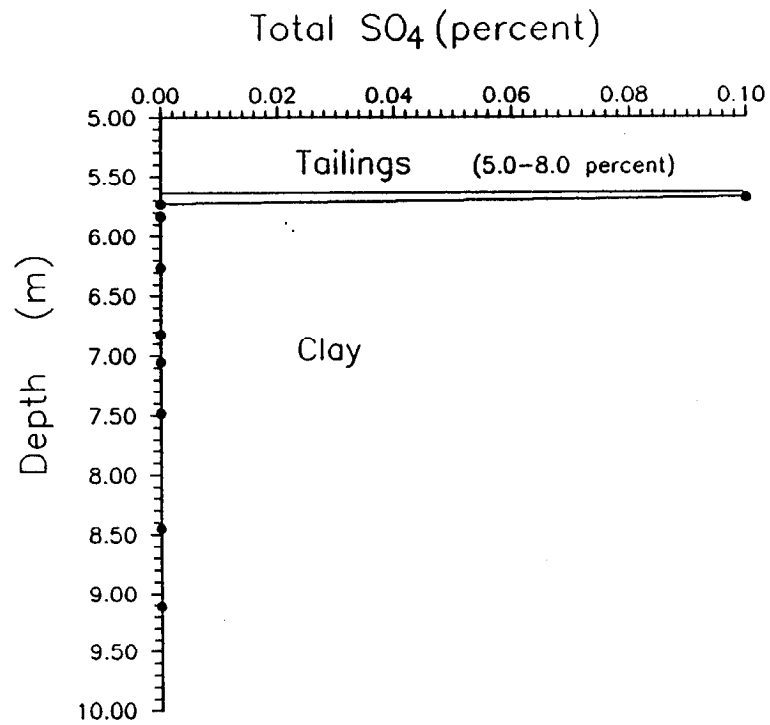


Figure 10.20 Sulphate Concentrations in Bulk Clay Soil and Pore Water at WA-20.

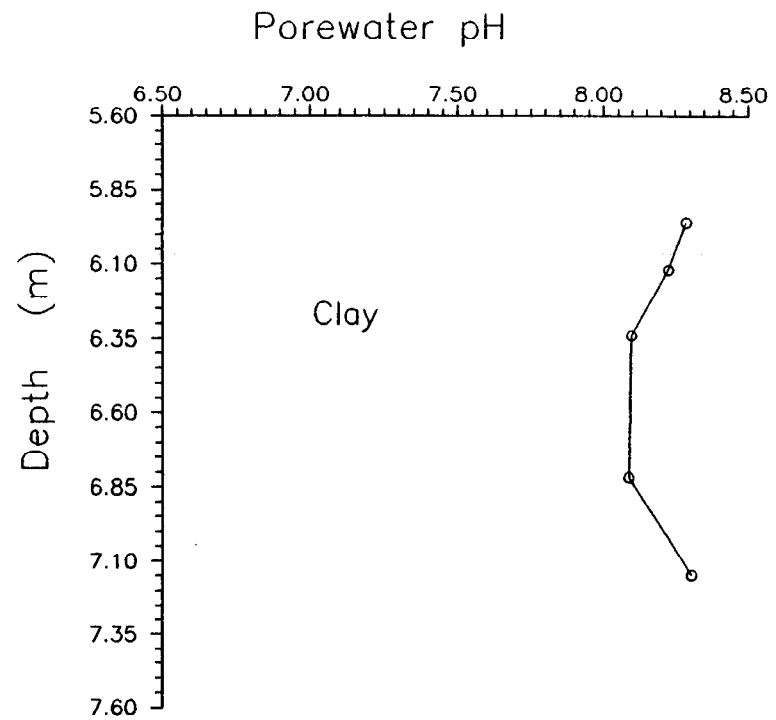
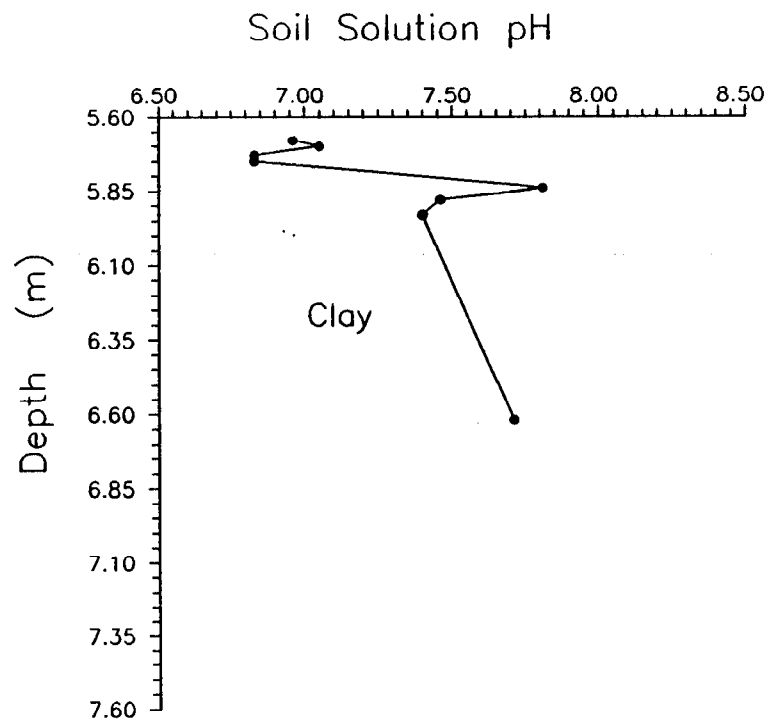


Figure 10.21 Soil Solution and Clay Pore Water pH Profiles at WA-11.

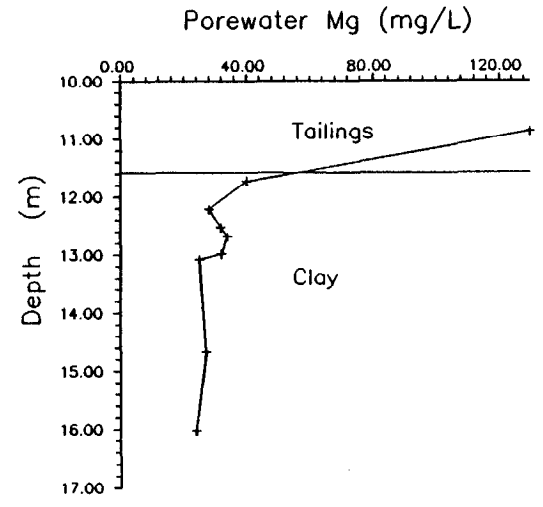
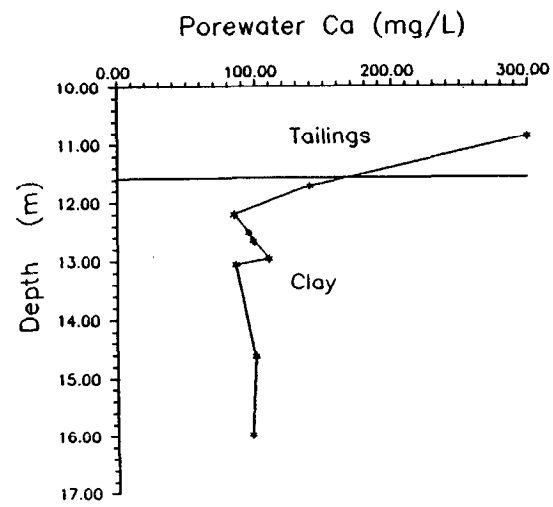
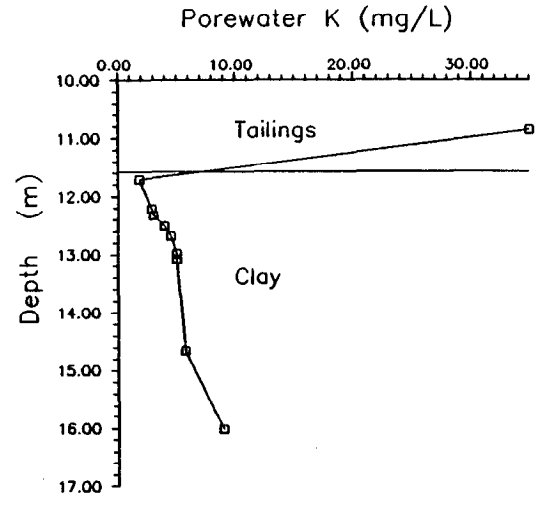
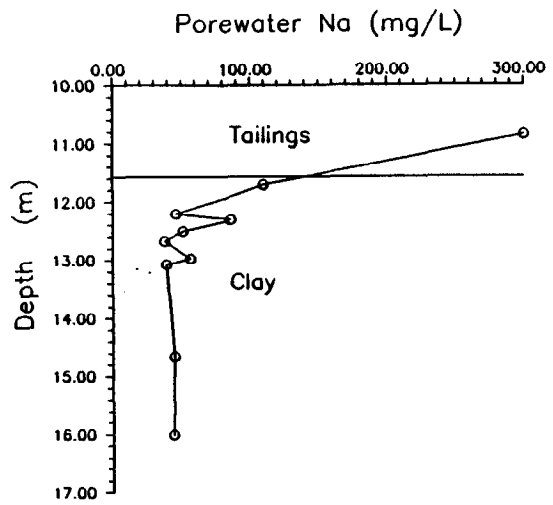


Figure 10.22 Major Cation Profiles at WA-11.

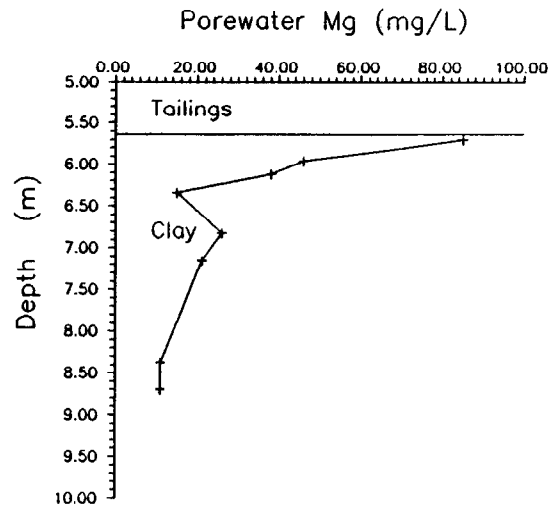
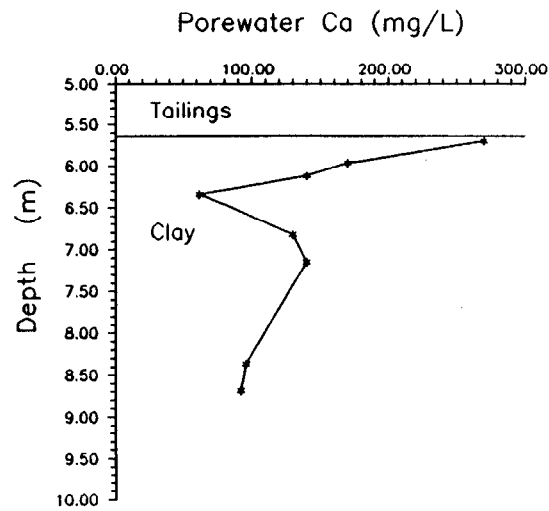
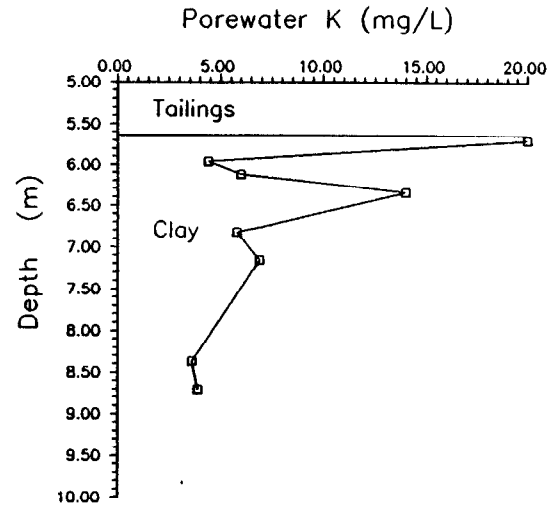
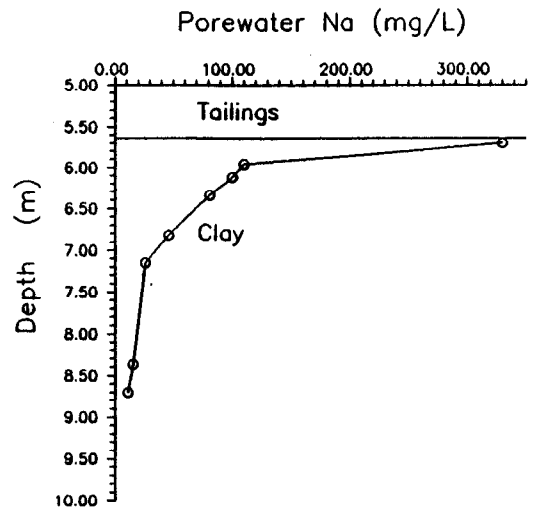


Figure 10.23 Major Cation Profiles at WA-20.

APPENDIX A

WATER TREATMENT

APPENDIX A WATER TREATMENT

Figure A-1 shows the process diagram for the Waite Amulet water treatment plant. Hydrated lime (Robertson, 1985) is received in 30-tonne truckloads and stored in a 60-tonne bin. The rotary valve discharges lime through a rubber skirt into the slurring tank equipped with a 1/3 HP Greey-Lightnin mixer. The overflow discharges by gravity to the first, or optionally the second, neutralization tank. Agitators provide mixing.

Acid waters are collected in the acid water reservoir and pumped to the first, or optionally the second, of two neutralization tanks. The two 69 m³ neutralization tanks are in series. The lime/sludge mixture is allowed to overflow at constant flowrate into the first, or optionally, the second vessel via launders. Aeration for the first and second tank is injected at multiple points under the agitator impeller. Both tanks are designed with a baffled overflow into which pH probes are inserted. Normally, the pH probe in the overflow of first neutralization tank is used to control lime addition; the probe in the second tank could easily be hooked up to serve the same purpose. Flocculant is added into the base of the overflow well of the second reactor. The flow discharges into the clarifier.

Solid/liquid separation at the Waite Amulet operations centers around an 8 m diameter Axel-Johnson clarifier equipped with dual Lamella platepacks. A variable speed motor slowly rotates a picket fence-type rake to direct sludge to a bottom well. Overflow from neutralization tank No. 2 enters a baffled inlet along one side of the clarifier; the flow continues downward, then up through the inclined platepacks where solids are separated. The clarified effluent from the platepacks overflows to a launder located on the side opposite to the feed. Two pumps are located at the bottom of the thickener. One is to recycle sludge back to the lime/slurry mixing tank, and the other to direct sludge as required to sludge disposal.

Sludge is pumped to one of three sludge draining beds (12,300 m³ total) on a timed basis (~15 min.), the drainage of which reports back to the acid water reservoir. Overflow from the clarifier flows by gravity into a polishing pond. A decant tower is in place which directs the final effluent to Duprat Creek.

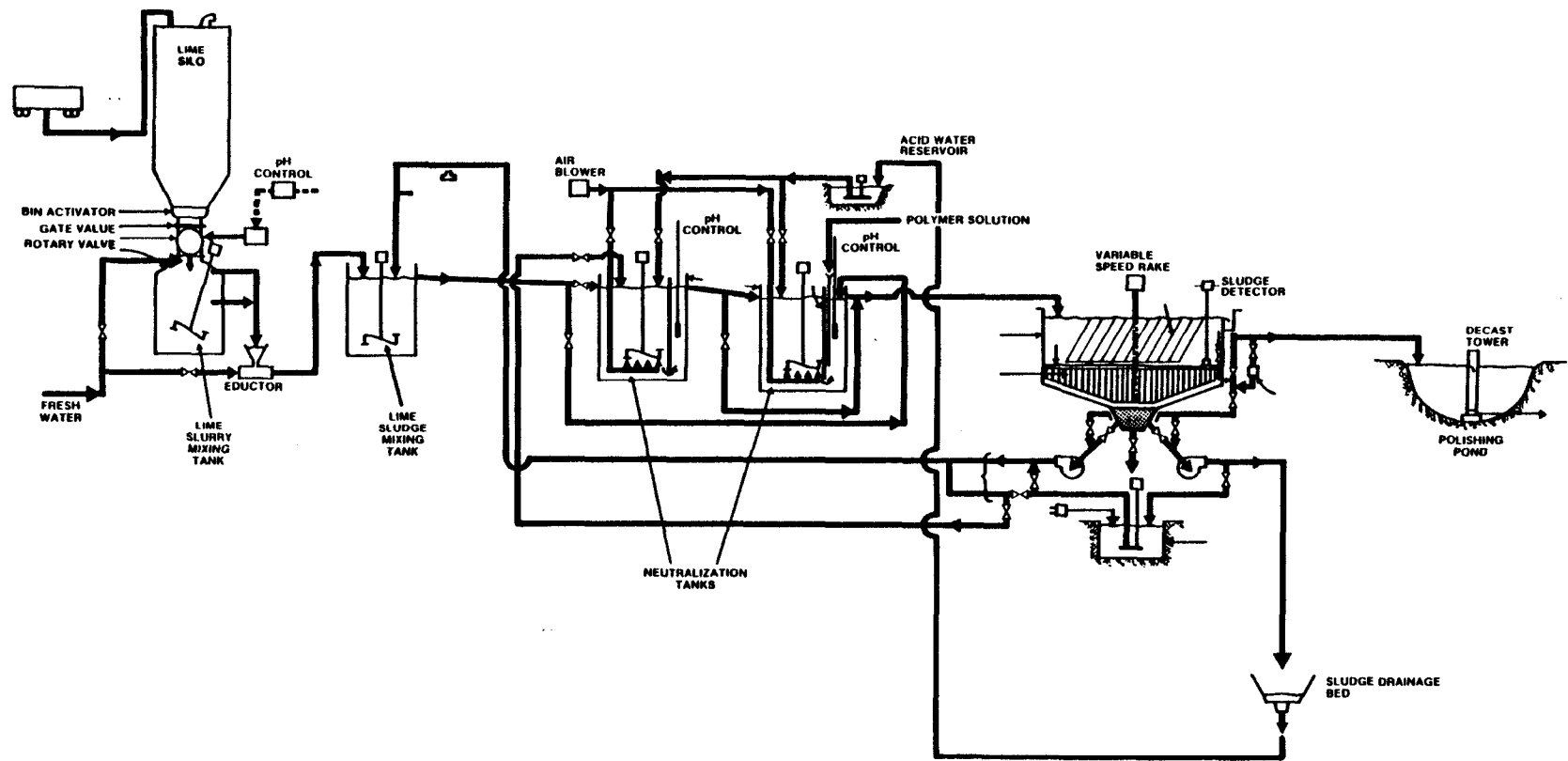


Figure A-1 Waite Amulet Treatment Plant Process Diagram

APPENDIX B

METHODS OF INVESTIGATION AND QA/QC

APPENDIX B METHODS OF INVESTIGATION

B.1 Surface Hydrology and Meteorology

Two surface water monitoring stations were installed on the Waite Amulet tailings site. Station 1 was located on the top of the northern tailings section where monitoring of precipitation, evaporation and surface run-off (quantity and quality) took place. Station 2, located along the western seepage face, monitored seepage quantity and quality of the western half of the main tailings dam.

Precipitation and evaporation were monitored to assess water available for infiltration and run-off. Because overland flow from the 40 hectare site could only exit from the northern edge of the tailings, Monitoring Station 1 was installed there to assess run-off flowrate and quality. Monitoring Station 2 was installed to assess seepage flow rates and water quality of the western half of the dam seepage discharge.

The field data acquisition system for the overland and seepage flow Monitoring Stations 1 and 2 is illustrated in Figure B-1. The data were gathered at each station in two separate 32 k byte memory data loggers (Lakewood Model LE8305C) at 10-minute intervals. The flow rates were monitored at the two stations using Lakewood float pot water level recorders in Hinde Engineering Accura-flow H flumes (0.4572 m flume for Station 1 and 0.3048 m flume for Station 2). The height of the water in the flumes was transmitted as an analog signal to the data loggers.

A 24-bottle American Sigma Model 6201 automatic sampler, installed at each location, collected water samples at frequencies controlled by the volume of water passing through the flume. This particular volume proportional sampling schedule was implemented in order to get more samples during high flow periods than during baseflow periods. The automatic sampler contained twenty-four 475 mL sample bottles, pre-filled with 90 mL of distilled water and 10 mL of reagent grade hydrochloric acid. The added distilled water was used to minimize acid evaporation, and resultant corrosion of the automatic sampler. After twenty-four samples were collected, a new sampling tray was installed in the sampler and samples were submitted for analysis (Fe_T and some Fe^{+2} , Cu, Pb, Zn, Ca, Mg and SO_4). A Signet pH monitoring sensor

was installed at the exit of each flume in order to monitor pH changes, sending an analog signal between 0.5 and 2.5 volts, which corresponded linearly to pH values ranging from 2 to 14. This piece of equipment did not perform satisfactorily; the pH readings were very unstable.

The meteorological station installed at Station 1 consisted of an OTA 34-T tipping bucket rain gauge and a Qualimetrics Model 6844-A evaporation gauge combined with an evaporation pan (approximately 1.2 m dia.). Rainfall events were recorded in the data logger as pulse signals accumulated for the number of tips (one tip = 0.2 mm of rain) encountered during each 10-minute interval. The evaporation flux was recorded at the same time interval by measuring the water level in the evaporation pan with a float system, which sent an analog signal to the data logger.

At approximately 100 m north of the piezometer WA-21, Lakewood temperature thermistors (Model LE8396) were installed in the tailings at 15 cm and 45 cm depth to measure temperature variations. Another thermistor was installed at Station 2 to record air temperature variations. The voltage data from each thermistor were recorded at 10-minute intervals by the data logger at Station 2; these data were transformed into temperature values ($^{\circ}\text{C}$).

All the data accumulated in the data loggers were retrieved at 5- to 15-day intervals by serial transfer to a Toshiba 1100 portable micro-computer, using Lakewood software. Data could be immediately viewed graphically, which facilitated maintenance and troubleshooting of the stations by revealing any problems which could have occurred during the monitoring period.

Data conversion from analog and pulse recordings were performed at NTC using a computer spreadsheet program.

The two monitoring stations (illustrated in Figure 3) were installed and functioning from May to July. During August and September, communication problems occurred between the Station 2 data logger and the computer, resulting in limited sets of data for that period. The equipment was decommissioned during the hunting season in October and re-installed for a 21-day period in November.

B.2 Hydrogeological Monitoring

Water levels were measured in the piezometers using a coaxial cable electrical water level meter. The levels were measured weekly during the summer of 1987, bi-weekly in the summer of 1988, and at three occasions in 1989. Hydraulic conductivity tests were performed and interpreted according to the method of Hvorslev (1959). Water levels and hydraulic conductivities for piezometers along sections A-A' and B-B' are reported in Table B-1.

Measurements of hydraulic conductivity in the vadose zone were performed using the Guelph permeameter of Reynolds and Elrick (1986). The Guelph permeameter consists of a graduated constant-head reservoir which operates on the Mariotte siphon principle. The hydraulic conductivity is calculated using the water inflow rate into a hand-augered borehole. For each test, two steady-state inflow values are taken at different head values. The general equation is :

$$K_{fs} = (a_1)(X)(R_2) - (a_2)(X)(R_1)$$

where K_{fs} is the field-saturated hydraulic conductivity, a_1 and a_2 are empirical constants, X is the reservoir constant, and R_1 and R_2 are the two inflow values.

Measurements at Waite-Amulet were made at two to four different depths at six locations. Results are listed in Table B-2. Values ranged from 2.34×10^{-5} to 1.0×10^{-3} cm/s and generally decreased with depth. The K_{fs} values were found to be influenced by very local soil conditions; reproducibility of measurements was within one order of magnitude. According to the method, zero or negative values are obtained when soil discontinuities, e.g. stratification, roots or rodent holes, are encountered. These values were therefore ignored. Care in test site location and borehole preparation are necessary for good results.

B.3 Pore Water Quality Sampling

Pore waters sampled from the piezometers were tested in the field for pH and conductivity, and in the laboratory for dissolved metals, E_H , acidity, and sulphate. Conductivity was determined by means of a conductivity meter which was calibrated with a potassium chloride solution before each measurement. A combination electrode was used for measurement of pH. The electrode was calibrated with suitable buffers prior to testing and between samples.

Acidity was determined within one hour after arrival in the laboratory by titration with 1N sodium hydroxide solution to a pH of 8.3. Ferrous iron, Fe^{+2} , was determined by the potassium dichromate titration technique of Waser (1966). Total dissolved iron, zinc, lead, copper, calcium, magnesium, sodium, and potassium were all determined by atomic absorption spectrophotometry. Sulphate concentrations were obtained by colorometric analysis.

With the exception of the acidity determinations, all laboratory analyses were performed by Noranda Environmental Services, Noranda, Quebec. Results of the analysis are given in Table B-3.

B.4 QA/QC Program for Water Samples

Several measures were taken to minimize saturated zone piezometer sample contamination:

- Sampling equipment, which included the sample tubes and hand-operated bailer, were rinsed with distilled water prior to sampling each piezometer.
- Each filter was disposed of after one use.
- Sample tubes were not allowed to touch the tailings and were hung up when not in use.

A special procedure was used for the water samples collected by the automatic samplers (at Station 1 and 2): each sample bottle was rinsed three times with tap and distilled water. After, 10 mL of HCl (as preservative for heavy metal and especially for Fe^{+2}) and 90 mL of distilled water were poured into each bottle.

Quality control of the analysis (from porewater, surface water and seepage samples) carried out by the Noranda Environmental Services Laboratory, Horne Division, Rouyn-Noranda, QC, was assessed using five replicates and 10 spikes (two different levels). Replicate determinations, illustrated in Table B-4 are from Piezometer WA 11-2 sampled in November.

In general, the reproducibility of analysis was good for Cu, Pb, Ca, Mg and SO₄ (C.V. <15%), but marginal for Fe_T at the low level of 5 mg/L (C.V. of 18%). The reproducibility of Zn analysis was quite poor (C.V. >70%) at low levels (.05 mg/L); however, at levels near 0.3 mg/L (replicate samples), reproducibility of Zn improved drastically (C.V.: 11.5%). The high C.V. value for Zn, due especially to two numbers, reflects common contamination problems occurring at low Zn levels. The relative error values shown for the two levels spiked samples suggest relatively good accuracy for Cu, Pb, Ca and Mg, but the Zn (at low level) and Fe Relative Error values suggest some positive bias.

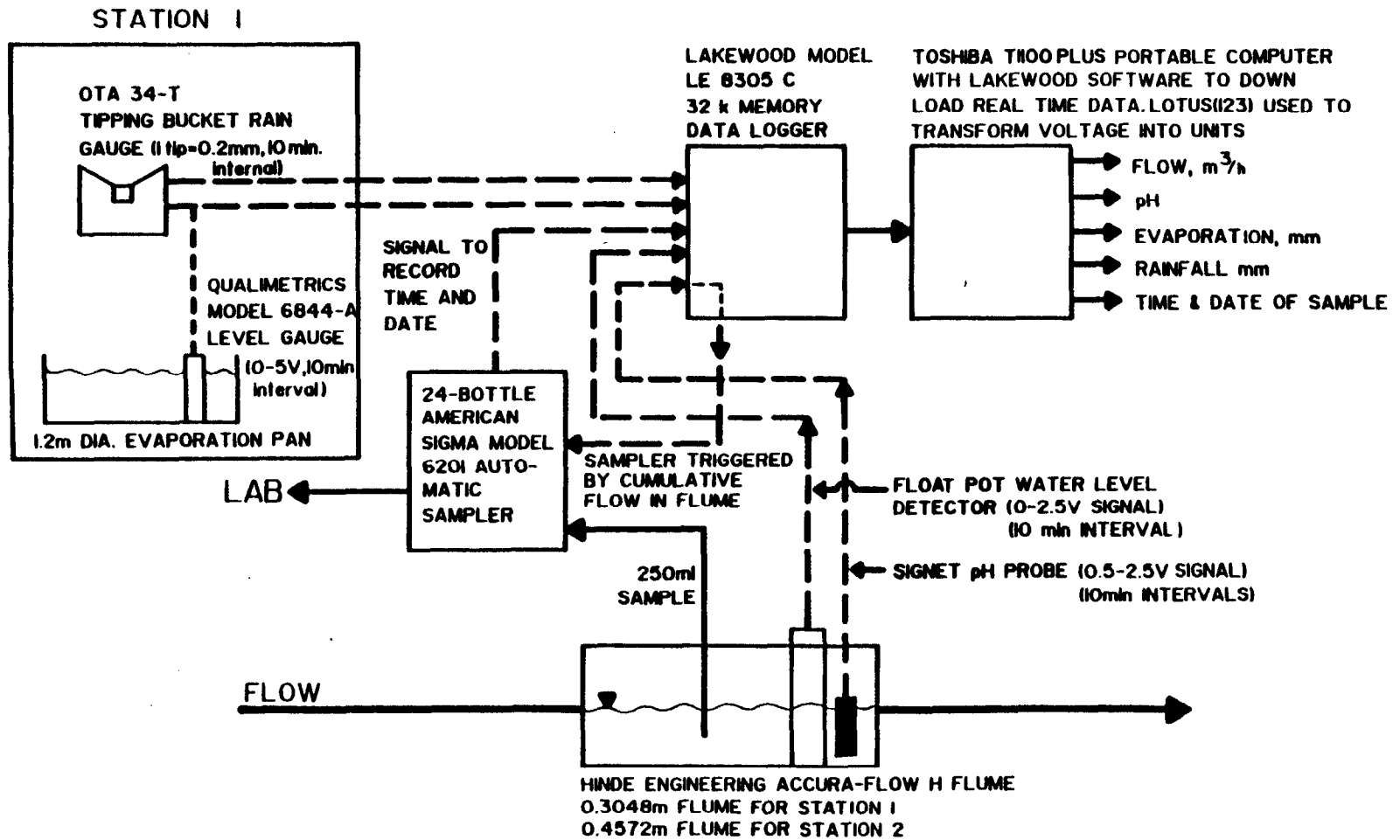


Figure B-1 Flowsheet for Monitoring Stations 1 and 2

TABLE B-1

TIP AND WATER ELEVATIONS IN PIEZOMETERS
ALONG SECTIONS A-A' AND B-B'

piezo no.	tip elev (m)	water elevation (m)			hydraulic conductivity
		11-15-88	04-18-89	05-30-89	
15-3	304.76	312.08	311.61	312.01	8.56E-05
15-4	308.12	312.76	311.38	311.79	2.23E-06
15-1	309.39	311.99	311.45	317.16	4.7E-05
15-2	312.43	312.73	--	312.76	--
28-1	308.21	309.76	310.88	311.24	2.83E-06
28-2	309.76	311.11	310.82	311.15	4.61E-05
28-3	312.97	--	--	316.77	--
28b-1	309.18	310.70	310.62	310.81	7.12E-05
29-1	307.10	307.67	310.24	310.55	1.40E-06
29-2	310.0 *	310.4 *	--	310.6 *	--
30-1	306.97	307.36	310.00	310.23	--
30-2	308.45	310.18	310.12	310.33	1.84E-05
21-1	307.41	309.84	309.87	309.86	--
21-2	308.80	309.84	309.87	309.96	--
31-1	305.00	305.15	309.26	309.25	--
31-2	306.46	309.21	309.24	309.22	1.37E-04
31-3	307.20	307.50	307.75	308.43	--
32-1	303.10	303.27	307.77	307.94	1.99E-06
32-2	305.10	305.21	307.52	307.67	--
32-3	305.7 *	305.84 *	307.43 *	307.43 *	--
11-1	309.15	314.74	314.07	314.87	7.89E-06
11-2	312.21	315.27	314.49	315.63	5.89E-06
11-3	314.37	315.79	314.90	316.24	8.89E-06
33-1	309.16	312.19	313.07	313.50	9.94E-06
33-2	312.84	313.51	313.28	313.66	1.34E-04
33-3	314.36	--	--	318.40	--
34-1	310.74	312.26	312.20	312.32	3.64E-05
34-2	311.0 *	--	--	--	--
20-1	308.30	309.97	311.56	311.59	1.97E-04
20-2	310.49	311.26	311.63	311.66	1.22E-03
35-1	309.14	310.58	310.63	310.64	7.45E-07

* estimated elevations

TABLE B-2

HYDRAULIC CONDUCTIVITY AT DIFFERENT
DEPTHS IN THE VADOSE ZONE

station	depth (in)	Kfs
WA-9	12	1.71E-04
	14	2.34E-05
WA-11	7	-5.3E-05
	9	-5.2E-05
	11	6.50E-04
	21.5	1.10E-04
WA-20	7	1.08E-03
	10	-2.9E-05
WA-24	7	1.70E-04
WA-25	6.5	0.00E+00
	13	-6.2E-03
	22	-5.0E-04
WA-27	6	6.88E-04
	12	7.43E-04

TABLE B-3

RESULTS OF POREWATER QUALITY ANALYSIS, NOVEMBER 1988

NO.	Cu mg/L	Pb mg/L	Zn mg/L	Ca mg/L	Fe mg/L	Fe +2 mg/L	Mg mg/L	SO ₄ mg/L	pH (field)	pH (lab)	S.Cond. (umhos)	redox (mV)	acidity (mg/L CaCO ₃)
28-2	<.02	0.19	0.82	452	7.11	7.1	188	2100	6.75	6.31	2030	265	50
28-1	<.02	0.09	0.43	73.3	3.03	2	84.6	115	7.25	6.71	1240	278	150
28B-1	<.02	0.26	0.65	376	12.8	9.6	388	3200	7.25	6.5	2850	218	150
21-2	<.02	0.67	0.51	369	2610	2600	449	9500	6.85	4.83	4510	325	5100
21-1	<.02	0.21	0.39	144	8.26	3.4	219	2300	7.5	7.02	3230	167	50
20-2	<.02	0.39	0.46	396	714	700	789	4700	6.65	5.66	3320	220	1550
20-1	<.02	0.09	0.4	30.4	2.01	2	11.2	350	7.3	7.01	1636	270	50
15-4	<.02	0.07	0.46	57.2	10.6	5	67.1	20	6.65	6.47	1107	304	350
15-3	<.02	0.09	0.68	141	0.67	0.2	53.7	33	7.15	6.81	900	369	150
15-2	1.01	0.24	5.68	369	170	130	72.7	1900	4.55	3.39	1919	585	500
15-1	<0.02	0.29	0.42	389	8.57	2.4	732	4000	7.55	6.8	3590	205	50
11-3	<0.02	0.6	0.46	398	2380	2300	291	7500	5.35	4.18	4040	411	4100
11-2	<0.02	0.31	0.37	431	58	22	641	3500	6.85	6.43	3260	166	150
11-1	<0.02	0.15	0.4	134	1.24	0.72	121	2200	6.9	7.21	3040	199	500
29-1	<0.02	0.15	0.72	138	13.3	--	55	600	7.4	--	1214	321	--
30-1	<0.02	0.34	0.97	104	14.9	--	44	285	7.5	--	908	453	--
30-2	<0.02	0.17	0.43	167	7.6	--	216	2200	7.45	6.51	2640	178	50
31-2	<0.02	0.62	0.56	369	2510	--	449	8000	6.3	4.43	3520	376	4800
31-3	<0.02	0.86	3.33	284	2320	--	192	6750	5.55	--	3580	444	--
33-1	<0.02	<0.05	0.43	6.3	0.09	--	3.8	525	8.5	8.85	1611	293	<50
34-1	<0.02	0.31	0.54	434	165	--	427	3400	6.65	5.75	2730	216	450
35-1	<0.02	0.27	0.5	354	313	--	616	4500	6.55	5.72	4040	195	700

Table B-4 QA/QC results assessment, Waite-Amulet 1988

	Cu	Pb	Zn	Ca	Fe	Fe +2	Mg	SO4
SPIKE LOW(mg/L)								
	0.35	0.44	0.07	46.3	7.65		47.5	215
	0.41	0.47	0.06	47.7	5.58		49.7	250
	0.42	0.44	0.04	48.1	5.36		49.8	225
	0.42	0.54	0.21	51.0	5.17		49.7	190
	0.44	0.51	0.21	48.3	5.26		50.3	210
AVG(mg/L)	0.41	0.48	0.12	48.3	5.80		49.4	218
SD(mg/L)	0.03	0.04	0.08	1.7	1.04		1.1	22
CV(%)	8	9	72	4	18		2	10
RE(%)	18	4	76	3	16		1	336
SPIKE HIGH(mg/L)								
	7.99	10.2	29.7	187	221		204	820
	8.02	10.3	29.4	211	202		221	1000
	8.15	10.8	28.8	207	200		223	1000
	8.86	12.1	32.1	189	239		197	780
	9.99	13.4	35.6	197	265		188	815
AVG(mg/L)	8.60	11.4	31.1	198	225		207	883
SD(mg/L)	0.85	1.4	2.8	11	27		15	108
CV(%)	10	12	9	5	12		7	12
RE(%)	8	14	4	1	25		3	342
REPLICATES (mg/L)								
	<0.02	0.29	0.36	452	52.9		620	4000
	<0.02	0.34	0.33	451	56.0		626	4100
	<0.02	0.34	0.29	444	58.0		635	3400
	<0.02	0.27	0.29	450	56.5		658	3500
	<0.02	0.31	0.37	431	58.0		641	3500
AVG(mg/L)	---	0.31	0.33	446	56.3		636	3700
SD(mg/L)	---	0.03	0.04	9	2.1		15	324
CV(%)	---	10	11	2	4		2	9

APPENDIX C

MODELLING

APPENDIX C MODELLING

C.1 Flow Modelling

The numerical model used for the simulations, called FLONET, was developed at the University of Waterloo and is based on the theory of streamfunctions (Frind and Matanga, 1985).

The theory is based on the existence of a potential function $\phi = \phi(x, y)$ and streamfunction $\psi = \psi(x, y)$ for the case a a two-dimensional x, y coordinate system. The specific discharge (Darcy discharge) vector q can be expressed in general form as

$$\begin{Bmatrix} q_x \\ q_y \end{Bmatrix} = - \begin{bmatrix} K_{xx} & K_{xy} \\ K_{yx} & K_{yy} \end{bmatrix} \begin{Bmatrix} \frac{\partial \phi}{\partial x} \\ \frac{\partial \phi}{\partial y} \end{Bmatrix} = \begin{Bmatrix} \frac{\partial \psi}{\partial y} \\ -\frac{\partial \psi}{\partial x} \end{Bmatrix}$$

where K_{ij} is the hydraulic conductivity tensor. (A.1) thus relates the discharge q to both ϕ and ψ . For the case where the coordinate axes coincide with the principal directions of permeability, (A.1) simplifies to:

$$\begin{Bmatrix} q_x \\ q_y \end{Bmatrix} = - \begin{Bmatrix} K_{xx} \frac{\partial \phi}{\partial x} \\ K_{yy} \frac{\partial \phi}{\partial y} \end{Bmatrix} = \begin{Bmatrix} \frac{\partial \psi}{\partial y} \\ -\frac{\partial \psi}{\partial x} \end{Bmatrix}$$

where K_{xx} and K_{yy} are the principal components of K_{ij} .

The dual continuity equations in principal direction form are:

$$\frac{\partial}{\partial x} \left[K_{xx} \frac{\partial \phi}{\partial x} \right] + \frac{\partial}{\partial y} \left[K_{yy} \frac{\partial \phi}{\partial y} \right] = 0$$

$$\frac{\partial}{\partial x} \left[\frac{1}{K_{yy}} \frac{\partial \psi}{\partial x} \right] + \frac{\partial}{\partial y} \left[\frac{1}{K_{xx}} \frac{\partial \psi}{\partial y} \right] = 0$$

The boundary conditions are also expressed in dual form. For a boundary where the head is known, the boundary conditions take the forms:

$$\phi = \phi_0$$

and

$$\vec{g}^\psi \cdot \vec{n} = -\nabla \phi \cdot \vec{r}$$

where \mathbf{n} is the unit normal vector to the boundary, \vec{r} is the corresponding tangential vector, and the gradient vector \vec{g} is defined by:

$$\begin{Bmatrix} g_x^\psi \\ g_y^\psi \end{Bmatrix} = \frac{1}{|K|} \begin{bmatrix} K_{xx} & K_{xy} \\ K_{yz} & K_{yy} \end{bmatrix} \begin{Bmatrix} \frac{\partial \psi}{\partial x} \\ \frac{\partial \psi}{\partial y} \end{Bmatrix} = \begin{Bmatrix} \frac{\partial \phi}{\partial y} \\ -\frac{\partial \phi}{\partial x} \end{Bmatrix}$$

Thus, a known head ϕ_0 enters the potential equation directly in the form of a first-type boundary condition, and indirectly in the streamfunction equation in the form of a second-type boundary condition expressed in terms of the (negative) rate of change of the head along the boundary.

For a boundary where the flux is known, the boundary conditions take the forms:

$$\vec{g}^\phi \cdot \vec{n} = (\vec{K} \nabla \phi) \cdot \vec{n}$$

and

$$\psi(\Gamma) = \psi_0(\Gamma_0) + \int_{\Gamma_0}^{\Gamma} \vec{q}_0 \cdot \vec{n} d\Gamma$$

where Γ represents the boundary. The specified flux q_0 enters the potential equation in the form of a second-type boundary condition and the streamfunction equation in the form of a first-type boundary condition by integration of the flux along the boundary. In the special case of an impermeable boundary (or a symmetry boundary), the normal flux is zero and the boundary is a streamline.

The flow region is discretized into triangular elements, and a solution for ϕ or ψ at a finite number of nodal points is obtained by the Galerkin finite element technique. A comprehensive description of the solution method is given by Frind and Matanga (1985). The solution takes place in three steps, namely:

1. the solution of (A.3) for heads ;
2. the determination of boundary fluxes on the basis of the calculated heads;
3. the solution of (A.4) for streamfunctions ψ . After the solution has been completed, the functions ϕ and ψ are contoured to produce a flownet.

During Step 1, an iterative scheme is used to determine the position of the water table required to obtain a balanced steady-state flow system. In this scheme, the finite element grid is allowed to expand or contract so that the elevation of the upper boundary nodes matches the calculated hydraulic head at these nodes. Each iteration consists of a complete solution for head, followed by a comparison of the boundary heads to the elevation of the boundary nodes and a commensurate adjustment of the nodal elevations. The iterative procedure is completed when the difference between calculated head and elevation along the upper boundary falls within a predetermined tolerance.

C.2 Geochemical Modelling

In order to assess which mineral phases have the potential to form in the saturated zone, the geochemical model MINTEQ (Felmy et al, 1984) was used.

MINTEQ is a speciation model which implements principles of chemical thermodynamics. It merely predicts the potential for metals such as iron and copper to precipitate as solid minerals. The model is unable to predict the rate at which these reactions will occur.

The way in which MINTEQ predicts the potential for mineral formation is by the calculation of saturation indices, where saturation indices are defined as the difference between the activity (or concentration) of a mineral in a formation reaction and the activity of that mineral if it were in solubility equilibrium (Stumm and Morgan 1981). Negative saturation indices indicate undersaturation of the groundwater with respect to the mineral in question; saturation indices of approximately zero indicate that precipitation will not occur; indices which are positive indicate that precipitation will occur. The more positive these indices are, the more likely it is that the precipitation of the mineral will be spontaneous.

Supersaturation of certain minerals in the groundwater indicate the occurrence of certain chemical processes. In particular, supersaturation of groundwater with jarosite indicates the oxidation of sulphides such as pyrite. If there were carbonates present which acted to buffer the acid produced, then MINTEQ would predict supersaturation with respect to gypsum.

Supersaturation of the groundwater with ferrihydrate indicates that microbial activity on the iron compounds released from the acid conditions has occurred. Further crystallization of ferrihydrate results in the formation of hematite. Therefore, groundwater supersaturated with ferrihydrate and undersaturated with hematite would indicate that iron released from the acid conditions is relatively recent.

The use of MINTEQ in modelling the chemical conditions of groundwater in the vicinity of acid producing tailings is relatively new. Information concerning the chemical history of the groundwater can be obtained by using MINTEQ to model the data obtained from chemical analysis of the groundwater. As mentioned above, the occurrence and extent of sulphide

oxidation can be determined by the MINTEQ model. In addition, the occurrence of buffer activity by carbonates can also be determined with this model. MINTEQ may also be used to assess the effect of pH changes on the solubility of the metals present.

C.3. Modelling of Infiltration and Run-off

The Hydrological Evaluation of Landfill Performance (HELP) model is a deterministic water balance model (Schroeder et al 1984). The program uses data involving precipitation, mean monthly temperatures, and solar radiation to determine the water budget of the landfill. This model is intended for use in assessing the effectiveness of soil covers on landfills containing hazardous or municipal solid waste. The objective in using a soil cover for hazardous waste is to eliminate the infiltration of water which will cause the formation of leachate. From Figure C-2 it can be seen that the characteristics of cover design for hazardous waste are similar to that of the Waite-Amulet tailings site.

The parameters describing the topsoil and vegetation are similar to those which describe the vegetated soil cover on the tailings. Also, the parameters describing the lateral drainage zone are similar to those which describe the tailings below the water table. Finally, the parameters which describe the barrier soil are comparable to the clay which underlies the tailings.

The two groups of parameters which are important in the HELP model are the parameters associated with the cover design itself, and the parameters associated with percolation and drainage. In the former, topsoil type, cover thickness, surface vegetation, and others are considered by this model. In the case of percolation and drainage, the hydraulic conductivity of the soil barrier, and the underlying soil layers are important.

Design specifications consist of the number of layers of soil, type of soil cover, thickness of the layer, and the slope of the layer. The model has stored seven default options for vegetation and twenty one soil types for use when actual datum are not available.

There are four types of layers which are defined by the HELP model: the vertical percolation layer, the lateral percolation layer, a waste layer, and a layer which acts as a barrier.

In terms of the Waite-Amulet tailings impoundment, the unsaturated top layer may be modelled by the vertical percolation layer, the saturated zone may be modelled by the lateral drainage zone, the tailings by the waste zone and the underlying clay may be modelled by the barrier zone.

In the vertical percolation layer, vertical flow downward is assumed to be unrestricted. However, water is allowed to seep upward and evaporate off. It is recommended that layers designed to support vegetation should be modelled as vertical percolation layers.

The lateral drainage layers are assumed to have hydraulic conductivity high enough so that there is little resistance to flow.

Barrier layers function to restrict the vertical flow. This program only allows for vertical movement of water in the barrier layer.

Schroeder and Peyton (1987) performed a study to evaluate the sensitivity of the input parameters in order to determine which were the most influential in terms of evaluating the water budget. The parameters which were studied in terms of their effect on the water budget were the topsoil thickness and characteristics, the vegetation, the runoff curve number, the evaporative depth, the drainage porosity, the plant available water capacity, the hydraulic conductivity, the drainage length and the liner slope. The parameters which were determined to have the greatest affect on the water budget were the hydraulic conductivity of the topsoil and lateral drainage layers, and the clay liners.

In addition to the sensitivity analysis of the input parameters, Shroeder and Peyton (1987) attempted a verification of the model with field data. The field data were obtained from seven sites for the purpose of comparison with model simulations. In some cases, it was difficult to find agreement between observed surface runoff and that determined by HELP. The probable reason for this is that runoff calculations are based on empirically determined equations, whereas in some cases, run-off is controlled by soil characteristics and evapotranspiration. In addition, in some cases, it was difficult to find agreement between evapotranspiration determined by HELP and that measured in the field. It was thought that the problem here could be related to errors in measuring evapotranspiration in the field. However, it was concluded that lack of adequate field data made it difficult to correlate the two sets of data.

Based on the sensitivity analysis and the verification of field data with the model, it was concluded that the lowest hydraulic conductivity possible should be used as a guide in soil cover design. In terms of the Waite-Amulet tailings site, this finding would indicate that a soil cover with low hydraulic conductivity would be important in terms of reducing the amount of acid mine water produced by these tailings by virtue of reducing the water seepage.

References

Schroeder, P.R., J.M. Morgan, T.M. Walski, and A.C. Gibson. The Hydrologic Evaluation of Landfill Performance (HELP) Model. U.S. Environmental Protection Agency, Office of Solid Waste and Emergency Response, Washington, DC, 1984.

Schroeder, P.R. and R.L. Peyton. Verification of the Hydrologic Evaluation of Landfill Performance (HELP) Model Using Field Data. U.S. Environmental Protection Agency, Hazardous Waste Engineering Research Laboratory Office of Research and Development, Cincinnati, OH, 1987.

APPENDIX D

METEOROLOGICAL DATA

Table D-1 Concentrations and loading values from samples collected at STATION 1

DATE	MONTH	HOUR	FLOW (m ³ /h)	CONCENTRATIONS							LOADING								
				Cu mg/l	Pb mg/l	Zn mg/l	Ca mg/l	Fe mg/l	Fe +2 mg/l	Mg mg/l	SO ₄ mg/l	Cu g/h	Pb g/h	Zn g/h	Ca Kg/h	Fe g/h	Fe +2 g/h	Mg Kg/h	SO ₄ Kg/h
12	5	10	0.46	0.69	0.15	3.38	391	6.02		138.9	1550.0	0.32	0.07	1.56	0.18	2.79		0.06	0.72
13	5	16	0.35	0.10	N.D.	1.26	219	0.87		56.8	865.4	0.03	N.D.	0.44	0.08	0.31		0.02	0.30
14	5	13	0.52	0.09	N.D.	1.14	209	0.88		55.6	859.7	0.05	N.D.	0.59	0.11	0.46		0.03	0.45
15	5	17	0.84	0.12	N.D.	1.47	230	0.97		58.3	925.8	0.10	N.D.	1.23	0.19	0.81		0.05	0.77
16	5	15	0.28	0.13	N.D.	1.43	234	0.96		58.7	903.0	0.04	N.D.	0.40	0.07	0.27		0.02	0.26
16	5	20	0.20	0.20	N.D.	1.79	253	1.65		68.1	1009.8	0.04	N.D.	0.36	0.05	0.33		0.01	0.20
19	5	11	0.09	0.78	0.11	3.08	352	8.02		127.1	1439.4	0.07	0.01	0.28	0.03	0.73		0.01	0.13
20	5	9	0.41	0.85	N.D.	3.29	373	9.24		141.3	1566.7	0.35	N.D.	1.34	0.15	3.76		0.06	0.64
25	5	15	0.02	1.27	0.21	1.69	454	30.80		172.2	1855.0	0.03	0.01	0.04	0.01	0.75		0.00	0.05
30	5	13	0.18	0.74	0.12	3.26	452	5.69		180.6	1841.7	0.14	0.02	0.60	0.08	1.05		0.03	0.34
3	8	10	0.80	0.31	N.D.	2.44	171	0.29	0.30	45.4	730.9	0.24	N.D.	1.94	0.14	0.23	0.24	0.04	0.58
5	8	11	1.33	0.90	N.D.	4.14	211	0.59	0.80	57.0	875.0	1.20	N.D.	5.52	0.28	0.78	1.07	0.08	1.17
8	8	5	1.33	1.30	N.D.	4.83	265	1.04	1.20	80.5	1104.8	1.73	N.D.	6.45	0.35	1.39	1.60	0.11	1.47
15	8	11	46.28	0.13	N.D.	1.77	91	0.64	0.80	17.7	326.9	6.05	N.D.	81.70	4.21	29.65	37.02	0.82	15.13
16	8	11	9.34	0.22	N.D.	2.42	120	1.57	1.10	28.0	502.1	2.05	N.D.	22.60	1.12	14.63	10.27	0.26	4.69
16	8	15	7.56	0.26	N.D.	2.13	128	1.08	0.50	29.9	519.4	1.96	N.D.	16.10	0.97	8.15	3.78	0.23	3.93
3	11	17	9.34					3.88	2.91							36.22	27.16		
3	11	22	7.56					16.36	3.90							123.72	29.46		
4	11	14	7.82					4.30	2.74							33.64	21.41		
4	11	22	12.04					3.99	1.80							47.98	21.67		
5	11	6	64.74					2.71	1.14							175.36	73.48		
7	11	20	27.08					1.67	1.41							45.26	38.30		
15	11	7	8.46	0.21	N.D.	2.37	237	5.14	3.34	46		1.74	N.D.	20.01	2.00	43.50	28.28	0.39	
16	11	0	8.45	0.22	0.00	2.50	250	0.00	1.90	49.0	746.4	1.83	N.D.	21.10	2.11	0.00	16.05	0.41	6.31
16	11	7	8.49	0.18	0.08	2.49	221	2.14	1.42	45.9	726.2	1.53	0.66	21.15	1.87	18.19	12.05	0.39	6.17
16	11	15	39.14	0.20	0.09	1.80	185	2.43	0.44	40.9	618.2	7.97	3.42	70.59	7.23	95.07	17.08	1.60	24.19

Table D-2 Concentrations and Loading Values from Samples Collected at Station 2

DATE	MONTH	HOUR	FLOW (c.m.)	CONCENTRATIONS							LOADING								
				Cu	Pb	Zn	Ca	Fe	Fe +2	Mg	SO4	Cu	Pb	Zn	Ca	Fe	Fe +2	Mg	SO4
				mg/l	mg/l	mg/l	g/l	g/l	g/l	mg/l	g/l	g/h	g/h	g/h	Kg/h	Kg/h	Kg/h	g/h	Kg/h
11	5	14	1.79					1.07							1.91				
12	5	10	1.76	2.19	0.46	5.98	0.36	1.18	556.6	5.81	3.84	0.81	10.51	0.64	2.07	0.98	10.20		
13	5	5	14.64	2.26	0.46	7.04	0.34	1.36	437.1	5.43	33.02	6.73	103.14	4.91	19.98	6.40	79.49		
13	5	16	5.05	2.62	0.41	7.11	0.33	1.23	450.4	5.30	13.24	2.07	35.92	1.67	6.19	2.27	26.75		
14	5	9	3.36	2.29	0.41	6.25	0.34	1.23	478.6	5.40	7.67	1.38	20.97	1.12	4.13	1.61	18.11		
15	5	2	2.57	2.07	0.43	5.84	0.35	1.20	533.4	5.60	5.32	1.11	14.99	0.89	3.07	1.37	14.38		
15	5	10	11.37	2.49	0.41	7.03	0.33	1.40	455.0	5.60	28.33	4.62	79.91	3.74	15.92	5.17	63.67		
15	5	23	5.96	2.21	0.46	6.50	0.34	1.25	484.4	5.32	13.18	2.75	38.70	2.05	7.43	2.89	31.69		
16	5	13	3.54	2.45	0.39	6.75	0.36	1.27	534.3	6.16	8.68	1.38	23.91	1.29	4.51	1.89	21.82		
16	5	22	3.58					1.17							4.18				
17	5	10	3.63	1.91	0.44	5.71	0.35	1.30	536.9	6.02	6.95	1.60	20.74	1.27	4.73	1.95	21.87		
17	5	20	3.49					1.18							4.13				
18	5	7	3.71	1.81	0.40	5.49	0.36	1.35	577.8	6.07	6.70	1.50	20.37	1.34	5.00	2.14	22.51		
18	5	17	3.54					1.11							3.95				
19	5	3	3.58	1.71	0.40	5.31	0.37	1.30	597.8	6.02	6.13	1.42	18.99	1.32	4.66	2.14	21.53		
19	5	14	3.51					1.23							4.33				
19	5	23	3.46					1.24							4.28				
20	5	9	3.43	1.69	0.47	5.30	0.37	1.28	616.3	6.23	5.79	1.60	18.18	1.27	4.40	2.11	21.39		
20	5	18	5.97	1.57	0.40	4.79	0.35	1.24	547.4	5.63	9.37	2.38	28.61	2.09	7.43	3.27	33.64		
21	5	2	3.75	1.71	0.43	5.58	0.38	1.38	599.7	6.17	6.41	1.62	20.96	1.43	5.17	2.25	23.17		
21	5	11	4.82					1.35							6.49				
21	5	20	4.96	1.71	0.47	5.86	0.41	1.29	652.7	6.19	8.47	2.33	29.07	2.03	6.42	3.24	30.70		
22	5	5	4.77					1.34							6.40				
22	5	15	3.12	1.95	0.39	6.19	0.41	1.20	649.6	6.16	6.07	1.22	19.31	1.27	3.76	2.03	19.22		
23	5		3.37					1.33							4.48				
23	5	10	3.12	1.76	0.43	5.83	0.40	1.35	644.2	6.53	5.51	1.34	18.18	1.25	4.21	2.01	20.38		
23	5	20	3.24					1.40							4.53				
24	5	7	3.46	1.74	0.49	5.66	0.41	1.38	693.9	6.66	6.02	1.69	19.59	1.44	4.78	2.40	23.08		
25	5	14	3.19	1.65	0.46	5.78	0.40	1.31	648.1	6.22	5.28	1.48	18.45	1.28	4.18	2.07	19.84		
27	5	13	2.38	1.70	0.46	6.14	0.42	1.37	683.8	6.32	4.04	1.10	14.61	0.99	3.26	1.63	15.05		
27	5	20	19.62	2.15	0.44	6.72	0.36	1.38	463.3	5.63	42.27	8.57	131.80	7.05	27.08	9.09	110.52		
28	5	9	4.82	2.00	0.42	6.56	0.38	1.32	557.6	5.77	9.64	2.04	31.63	1.85	6.38	2.69	27.83		
29	5	14	3.72	2.02	0.39	6.43	0.40	1.18	593.1	5.85	7.51	1.45	23.94	1.47	4.38	2.21	21.76		
30	5		6.30	1.77	0.37	5.96	0.35	1.30	494.4	5.60	11.16	2.32	37.58	2.19	8.21	3.12	35.26		
30	5	14	3.30	2.06	0.32	6.76	0.38	1.18	564.7	5.55	6.80	1.05	22.28	1.26	3.88	1.86	18.31		
31	5	13	2.24					1.21							2.71				
1	6	6	2.25	1.41	0.47	5.39	0.36	1.35	569.6	6.31	3.17	1.07	12.15	0.82	3.05	1.28	14.22		
1	6	16	1.68					1.37							2.30				
2	6	11	1.70	1.30	0.52	5.63	0.37	1.49	586.4	6.36	2.20	0.88	9.55	0.62	2.52	0.99	10.77		
4	6	14	1.67					1.27							2.12				
5	6	19	1.67	1.48	0.52	6.69	0.44	1.42	724.6	6.74	2.47	0.86	11.18	0.74	2.38	1.21	11.27		
8	6	14	1.56					1.42							2.22				
10	6	13	1.58	1.23	0.46	6.60	0.43	1.59	710.3	7.20	1.95	0.72	10.45	0.68	2.52	1.12	11.40		
11	6	5	2.59					1.54							3.98				
12	6	4	2.65	0.98	0.53	5.64	0.40	1.48	666.6	6.74	2.60	1.40	14.93	1.05	3.92	1.76	17.84		
12	6	23	18.40	2.18	0.45	7.43	0.37	1.60	600.0	5.73	40.15	8.28	136.76	6.80	29.36	11.04	105.40		
13	6	4	6.68	1.24	0.42	6.22	0.40	1.54	662.7	6.82	8.29	2.82	41.53	2.66	10.29	4.43	45.54		
13	6	10	6.33	1.32	0.39	6.46	0.40	1.52	681.3	6.72	8.33	2.49	40.88	2.54	9.62	4.31	42.51		
14	6	7	4.63	1.18	0.45	6.24	0.40	1.57	677.7	6.89	5.49	2.11	28.90	1.85	7.27	3.14	31.90		
14	6	18	165.55	4.39	0.42	8.26	0.28	1.20	309.7	4.93	725.98	70.33	1368.01	46.73	199.42	51.27	816.73		

Table D-2 (cont)

Concentrations and Loading Values from Samples Collected at Station 2

DATE	MONTH	HOUR	FLOW (c.m.)	CONCENTRATIONS										LOADING							
				Cu	Pb	Zn	Ca	Fe	Fe +2	Mg	SO ₄	Cu	Pb	Zn	Ca	Fe	Fe +2	Mg	SO ₄		
				mg/l	mg/l	mg/l	g/l	g/l	g/l	mg/l	g/l	g/h	g/h	g/h	Kg/h	Kg/h	Kg/h	g/h	Kg/h		
15	6	3	8.13	2.07	0.45	7.50	0.39	1.52			559.1	6.71	16.82	3.68	60.95	3.14	12.37			4.55	54.60
15	6	9	7.21	1.87	0.42	7.57	0.41	1.54			601.4	6.95	13.47	3.05	54.58	2.93	11.11			4.34	50.16
16	6		4.12	1.59	0.43	7.32	0.41	1.47			654.6	6.70	6.55	1.78	30.14	1.67	6.04			2.70	27.57
17	6	2	3.45	1.27	0.49	6.29	0.39	1.51			649.5	6.64	4.38	1.68	21.70	1.36	5.20			2.24	22.93
18	6	4	4.20	1.11	0.43	6.13	0.39	1.43			642.5	6.85	4.65	1.80	25.77	1.64	5.99			2.70	28.79
19	6	9	5.98	1.20	0.46	6.83	0.43	1.48			721.4	7.06	7.21	2.73	40.83	2.60	8.86			4.31	42.24
19	6	13	9.67	1.40	0.46	7.34	0.39	1.70			598.2	7.06	13.52	4.42	70.96	3.82	16.47			5.78	68.28
20	6	3	5.65	1.36	0.43	7.14	0.41	1.63			641.1	7.06	7.67	2.43	40.37	2.33	9.23			3.62	39.90
20	6	11	200.51	1.54	0.57	7.39	0.41	1.47			648.0		308.17	113.83	1482.56	81.62	294.29			129.93	
23	6	9	4.44	1.40	0.47	8.14	0.44	1.69			707.5	7.48	6.21	2.09	36.18	1.97	7.51			3.14	33.22
24	6	9	3.80	0.93	0.43	5.86	0.38	1.47			605.1	6.30	3.52	1.63	22.23	1.43	5.57			2.30	23.91
24	6	21	8.18	1.09	0.39	5.76	0.33	1.43			519.2	5.95	8.95	3.17	47.13	2.70	11.67			4.25	48.71
25	6	7	77.28	0.87	0.39	3.88	0.20	0.87			228.5	3.60	67.42	29.96	299.63	15.52	66.88			17.66	278.23
25	6	17	9.44	1.91	0.39	7.39	0.29	1.23			386.3	5.05	18.04	3.66	69.81	2.76	11.57			3.65	47.71
26	6		8.29	1.70	0.32	7.02	0.29	1.19			394.6	4.92	14.12	2.64	58.22	2.43	9.89			3.27	40.77
26	6	12	6.34	1.58	0.46	6.67	0.28	1.18			398.8	4.98	10.00	2.89	42.28	1.78	7.45			2.53	31.58
29	6	19	16.99	2.08	0.46	8.83	0.36	1.52			459.7	6.30	35.28	7.76	150.07	6.05	25.87			7.81	107.03
1	7	8	18.16	1.36	0.32	4.65	0.26	0.71			203.5	3.32	24.64	5.78	84.49	4.70	12.82			3.70	60.35
2	7	8	13.32	2.17	0.42	6.52	0.29	0.90			252.0	4.08	28.95	5.53	86.86	3.89	11.99			3.36	54.40
4	7	16	7.50	1.77	0.46	8.36	0.42	1.33			627.2	6.44	13.30	3.43	62.74	3.16	9.97			4.71	48.30
5	7	10	8.56	1.52	0.46	7.17	0.42	1.37			659.1	6.44	13.04	3.91	61.42	3.60	11.74			5.64	55.14
6	7	8	9.16	1.69	0.43	8.31	0.51	1.51			789.2	7.62	15.47	3.93	76.06	4.67	13.82			7.23	69.72
7	7	10		1.48	0.36	7.45	0.44	1.41			688.2	6.78									
8	7	9	1.09	1.37	0.48	7.01	0.46	1.47			710.3	6.92	1.49	0.53	7.62	0.50	1.60			0.77	7.53
13	7	16	6.70	0.87	0.42	5.70	0.36	1.11			571.8	5.75	5.85	2.78	38.25	2.43	7.43			3.83	38.52
14	7	20	8.59	1.27	0.43	7.24	0.44	1.34			681.2	6.51	10.94	3.69	62.21	3.77	11.54			5.85	55.90
20	7	18	1.66					1.25									2.07				
21	7	7	1.98					1.34									2.65				
21	7	18	1.34					1.32									1.76				
22	7	15	1.31	1.40	0.53	7.10	0.46	1.41			738.0	7.20	1.83	0.69	9.32	0.60	1.85			0.97	9.45
25	7		35.16					1.41									49.65				
25	7	18	35.16	1.18	0.54	4.62	0.37	1.23			765.7	6.78	41.38	18.98	162.58	13.00	43.08			26.92	238.52
27	7	9		1.09	0.54	5.68	0.40	1.44			600.9	6.51									
28	7		1.41					1.48									2.09				
28	7	22	1.41	1.18	0.57	6.99	0.457	1.40			696.5	6.92	1.66	0.80	9.87	0.65	1.97			0.98	9.77
29	7		1.52					1.20									1.83				
29	7	22	1.55	0.94	0.57	5.54	0.40	1.36			623.1	6.51	1.46	0.88	8.61	0.63	2.11			0.97	10.11
30	7		1.09					1.25									1.36				
30	7	20	1.09	0.90	0.53	5.75	0.41	1.41			639.7	6.51	0.98	0.57	6.25	0.44	1.54			0.70	7.08
31	7	11	1.74	0.87	0.57	5.66	0.41	1.32			661.8	6.51	1.52	0.99	9.85	0.71	2.29			1.15	11.32
2	8	10	4.72	1.15	0.60	6.54	0.41	1.62	0.90		627.2	6.85	5.43	2.81	30.85	1.92	7.65	4.25		2.96	32.36
2	8	14	14.26	1.02	0.60	5.54	0.40	1.54	0.79		632.8	6.44	14.62	8.49	79.00	5.73	21.92	11.30		9.03	91.84
2	8	16	12.35	1.90	0.73	6.49	0.36	1.34	0.66		447.8	5.42	23.47	9.04	80.14	4.42	16.52	8.16		5.53	66.93
3	8	1	36.08	2.17	1.78	6.02	0.29	1.39	0.53		298.9	4.53	78.20	64.40	217.22	10.32	50.09	19.19		10.78	163.55
15	8	23	7.52	2.76	0.57	8.23	0.34	1.18	0.74		377.3	5.29	20.72	4.29	61.86	2.53	8.90	5.56		2.84	39.77
16	8	9	7.42	2.44	0.57	7.97	0.35	1.24	0.78		410.0	5.29	18.07	4.27	59.16	2.62	9.21	5.79		3.04	39.29

Table D-2 (con't)

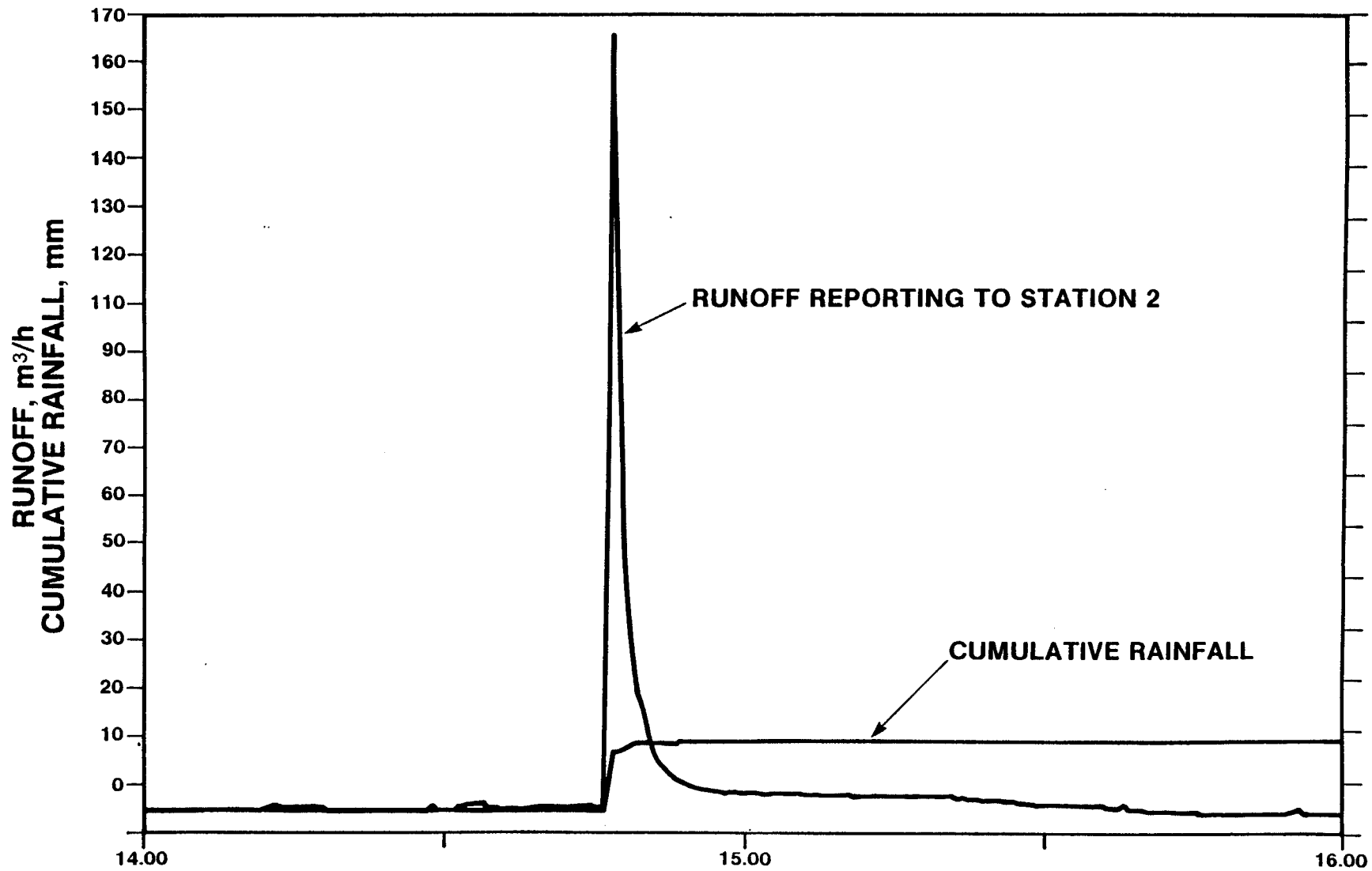
Concentrations and Loading Values from Samples Collected at Station 2

DATE	MONTH	HOUR	FLOW (c.m.)	CONCENTRATIONS										LOADING					
				Cu	Pb	Zn	Ca	Fe	Fe +2	Mg	SO4	Cu	Pb	Zn	Ca	Fe	Fe +2	Mg	SO4
				mg/l	mg/l	mg/l	g/l	g/l	g/l	mg/l	g/l	g/h	g/h	g/h	Kg/h	Kg/h	Kg/h	g/h	Kg/h
17	8	19	2.63	2.34	0.59	7.80	0.36	1.33	0.93	427.5	5.47	6.15	1.54	20.50	0.94	3.51	2.45	1.12	14.39
18	8	9	3.45	2.05	0.55	7.33	0.39	1.29	0.75	485.3	5.70	7.07	1.91	25.31	1.33	4.47	2.58	1.67	19.67
19	8	10	4.05	1.75	0.59	7.02	0.41	1.50	1.01	550.5	6.15	7.09	2.38	28.43	1.65	6.09	4.10	2.23	24.88
31	8	2	4.17	1.78	0.60	7.14	0.41	1.61		553.0	6.30	7.42	2.51	29.80	1.72	6.72		2.31	26.29
3	11		4.11					1.62	1.16							6.64	4.74		
3	11	21	6.35					1.57	1.17							9.95	7.42		
4	11	6	6.96					1.58	0.84							11.01	5.85		
4	11	15	12.14					2.54	1.29							30.83	15.68		
4	11	23	8.33					2.37	1.31							19.71	10.92		
5	11	3	44.02					2.41	1.16							106.02	51.14		
5	11	5	44.02					2.34	1.21							102.95	53.05		
5	11	6	65.90					2.25	0.88							148.10	57.80		
7	11	15	8.89					1.35	0.89							11.99	7.92		
16	11	10	15.21	1.39	0.35	6.84	0.32	1.44	1.05	389.7	5.35	21.17	5.35	104.05	4.79	21.83	16.04	5.93	81.32
16	11	13	36.64	1.41	0.33	6.99	0.27	1.29	0.94	315.9	4.87	51.82	12.09	256.24	9.85	47.27	34.55	11.57	178.50
16	11	15	56.18	1.26	0.26	5.78	0.23	1.08	0.77	244.9	4.08	70.97	14.71	324.57	12.81	60.85	43.28	13.76	229.37
16	11	16	54.35	1.43	0.31	5.96	0.23	1.06	0.71	237.7	4.10	77.69	16.59	323.85	12.31	57.79	38.41	12.92	222.59
16	11	17	51.79	1.48	0.30	5.97	0.21	0.99	0.67	225.6	3.89	76.54	15.31	309.38	11.12	51.24	34.64	11.68	201.42
16	11	19	62.18	1.46	0.25	5.59	0.22	0.89	0.60	204.9	3.54	91.00	15.33	347.73	13.60	55.56	37.36	12.74	220.32
16	11	20	43.64	1.63	0.22	5.85	0.21	0.93	0.59	206.9	3.58	71.28	9.50	255.25	9.03	40.39	25.80	9.03	156.14
16	11	22	28.91	1.84	0.24	6.24	0.23	0.97	0.63	225.0	3.90	53.33	6.94	180.37	6.55	28.01	18.21	6.50	112.73
17	11	2	17.64	2.17	0.21	6.98	0.24	1.06	0.68	249.5	3.99	38.28	3.65	123.17	4.17	18.70	11.98	4.40	70.31
17	11	6	9.16	2.23	0.26	7.54	0.27	1.12	0.73	291.5	4.81	20.41	2.38	69.05	2.49	10.25	6.71	2.67	44.03
17	11	8	4.42	2.07	0.26	7.98	0.33	1.31	0.92	404.7	5.68	9.17	1.16	35.28	1.45	5.78	4.07	1.79	25.10
17	11	14	10.89	2.14	0.23	7.68	0.29	1.22	0.84	339.9	4.98	23.29	2.55	83.60	3.21	13.26	9.09	3.70	54.24
17	11	23	7.85	2.10	0.24	7.45	0.30	1.24	0.84	359.3	5.13	16.48	2.07	58.46	2.39	9.76	6.59	2.82	40.28

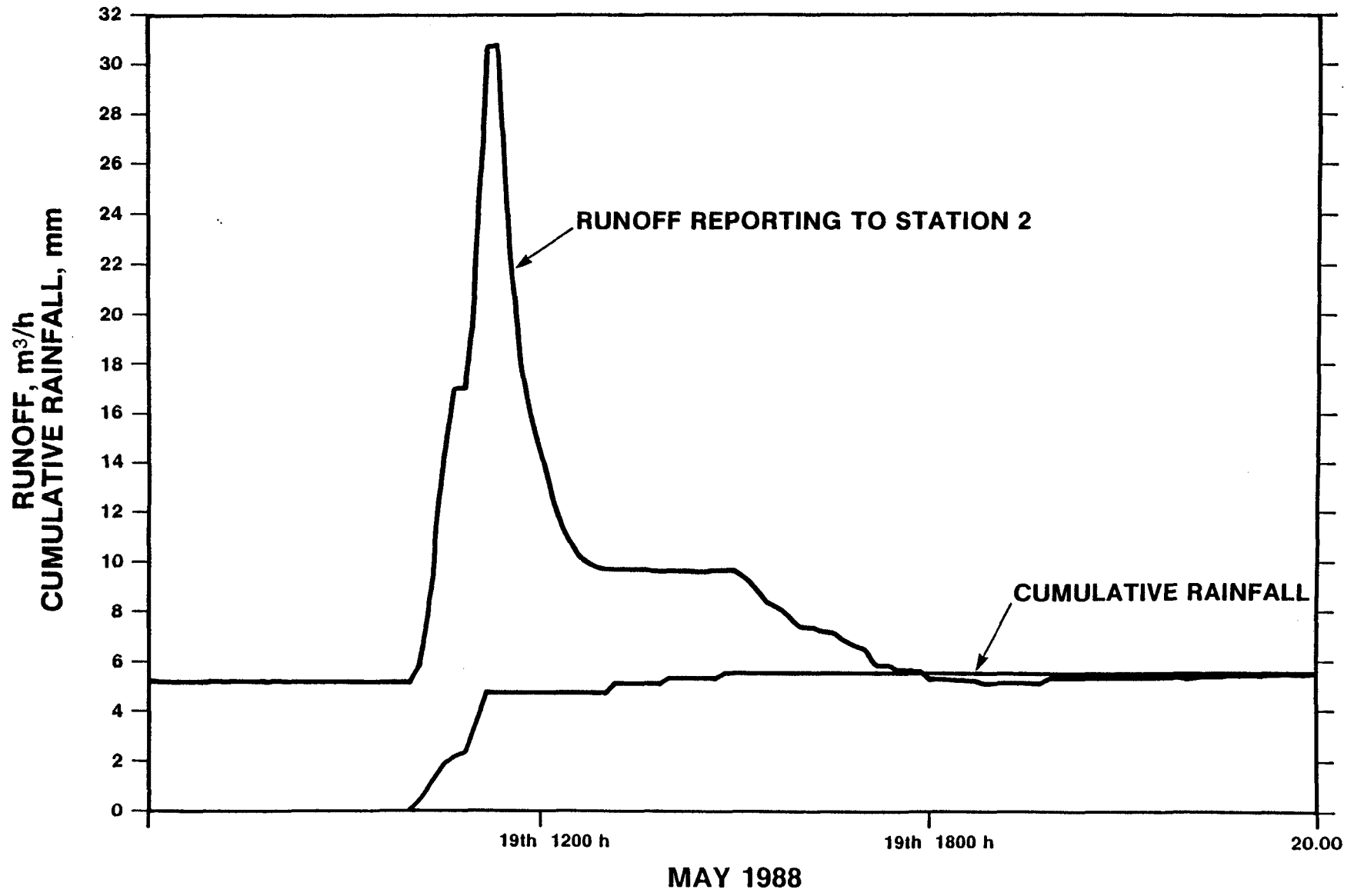
Table D-3 Metal Concentrations in Run-off and Seepage Ditches, 1988

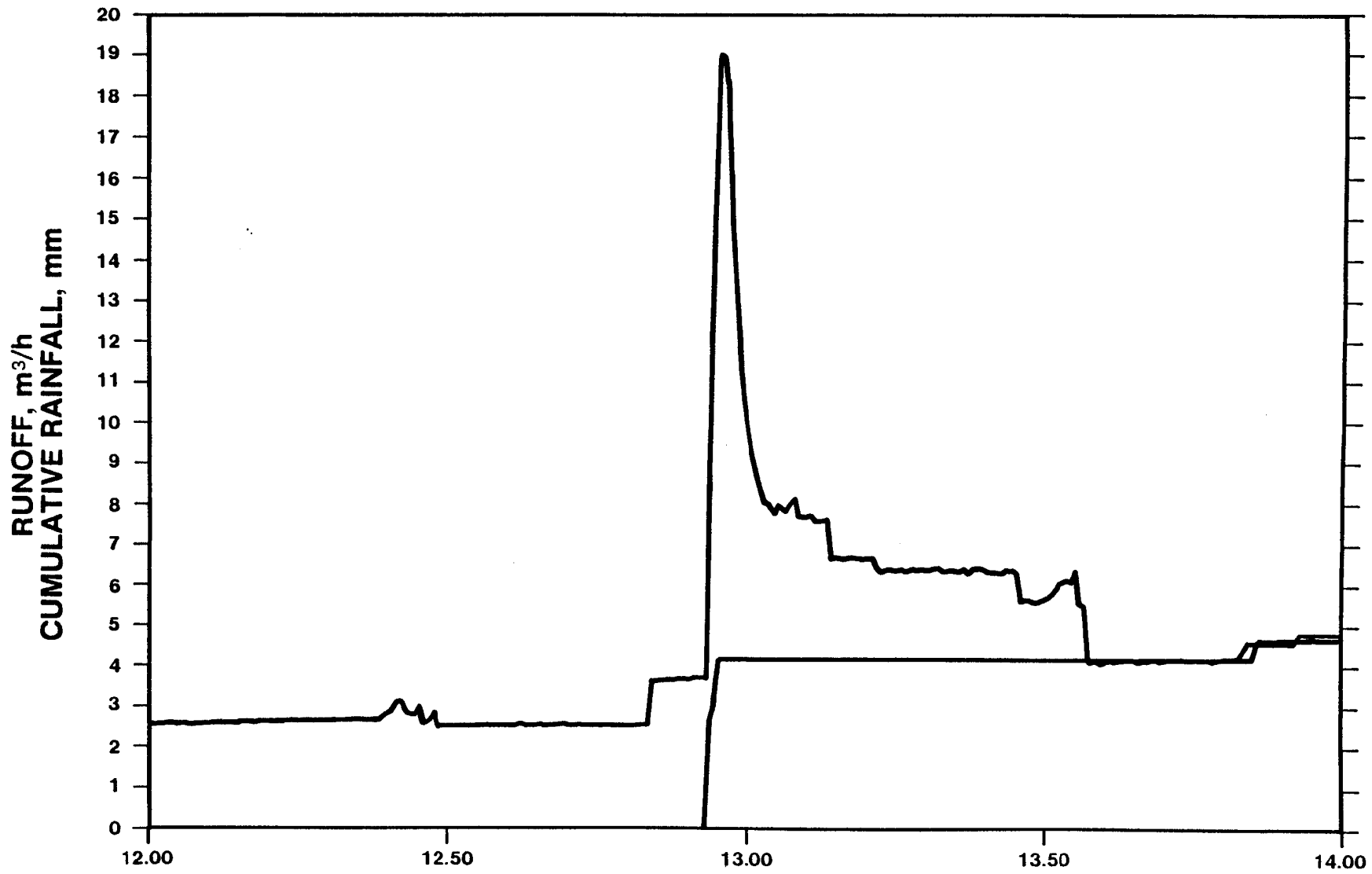
STATION	DATE	MONTH	Cu mg/l	Pb mg/l	Zn mg/l	Ca mg/l	Fe(t) mg/l	Fe +2 mg/l	Mg mg/l	SO4 g/l
ST 1.1	1	6	1.61	0.22	5.72	476	7.0		287.1	2.34
ST 1.2	1	6	0.38	0.26	12.04	457	349.5		217.8	3.48
ST 1.2	17	6					1334.3			0.00
ST 1.1	4	8					1.9	1.3		0.00
ST 1.2	4	8					14.1	12.0		0.00
ST 1.1	5	8	1.27	0.00	4.42	207	2.2	1.2	59.5	1.05
ST 1.2	5	8	0.86	0.00	4.75	221	26.0	20.0	66.7	1.11
ST 1.1	8	8					2.9	1.7		0.00
ST 1.2	8	8					35.4	29.0		0.00
ST 1.1	15	8					0.9	1.0		0.00
ST 1.2	15	8					2.3	2.0		0.00
ST 2.1	1	6	1.73	0.38	6.66	373	1338.8		596.4	6.38
ST 2.2	1	6	1.80	0.37	6.66	380	1397.8		629.0	6.44
ST 2.3	1	6	1.87	0.39	7.28	390	1379.2		645.4	6.63
ST 2.4	1	6	1.90	0.34	7.40	365	1334.6		642.0	6.32
ST 2.5	1	6	2.23	0.32	8.15	376	1354.4		711.7	6.77
ST 2.6	1	6	1.03	0.25	6.71	351	1272.3		641.2	6.05
ST 2.7	1	6	0.89	0.32	6.02	345	1085.1		619.7	5.66
ST 2.1	16	6					1501.9			0.00
ST 2.2	16	6					1450.0			0.00
ST 2.3	16	6					1458.0			0.00
ST 2.4	16	6					1364.4			0.00
ST 2.5	16	6					1308.6			0.00
ST 2.6	16	6					1259.6			0.00
ST 2.7	16	6					1075.0			0.00
ST 2.1	19	6					1567.8			0.00
ST 2.5	19	6					1328.6			0.00
ST 2.1	4	8					1301.5	488.0		0.00
ST 2.1	4	8					866.3	490.0		0.00
ST 2.3	4	8					1242.2	556.0		0.00
ST 2.4	4	8					1234.9	472.0		0.00
ST 2.5	4	8					879.1	406.0		0.00
ST 2.6	4	8					1045.6	621.0		0.00
ST 2.7	4	8					1002.4	616.0		0.00
ST 2.1	5	8	2.09	0.31	7.59	340	966.0	369.0	425.6	5.11
ST 2.2	5	8	1.69	0.37	7.30	315	1272.7	701.0	432.5	5.51
ST 2.3	5	8	1.53	0.33	6.79	273	1038.2	512.0	366.4	4.75
ST 2.4	5	8	1.94	0.37	8.32	314	1221.7	608.0	480.7	5.65
ST 2.5	5	8					995.4	452.0		5.04
ST 2.6	5	8	1.92	0.28	8.44	351	1174.6	715.0	585.2	5.74
ST 2.7	5	8	1.86	0.28	7.08	315	1098.4	624.0	478.8	5.07
ST 2.1	8	8					1064.0	620.0		0.00
ST 2.2	8	8					1344.0	744.0		0.00
ST 2.3	8	8					1248.3	660.0		0.00
ST 2.4	8	8					1216.0	615.0		0.00
ST 2.5	8	8					1133.3	571.0		0.00
ST 2.6	8	8					1106.7	662.0		0.00
ST 2.7	8	8					1085.9	623.0		0.00
ST 2.1	15	8					602.5	384.0		0.00
ST 2.2	15	8					1162.0	758.0		0.00
ST 2.3	15	8					1095.9	700.0		0.00
ST 2.4	15	8					1114.2	653.0		0.00
ST 2.5	15	8					942.9	567.0		0.00
ST 2.6	15	8					905.6	555.0		0.00
ST 2.7	15	8					866.7	582.0		0.00

Note: ST 1.1 : 20 m upstream from Station 1
 ST 1.2 : 10 m downstream from Station 1
 ST 2.1 : 200 m downstream from Station 2
 ST 2.2 : 100 m downstream from Station 2
 ST 2.3 : 100 m upstream from Station 2
 ST 2.4 : 200 m upstream from Station 2
 ST 2.5 : 300 m upstream from Station 2
 ST 2.6 : 400 m upstream from Station 2
 ST 2.7 : 500 m upstream from Station 2

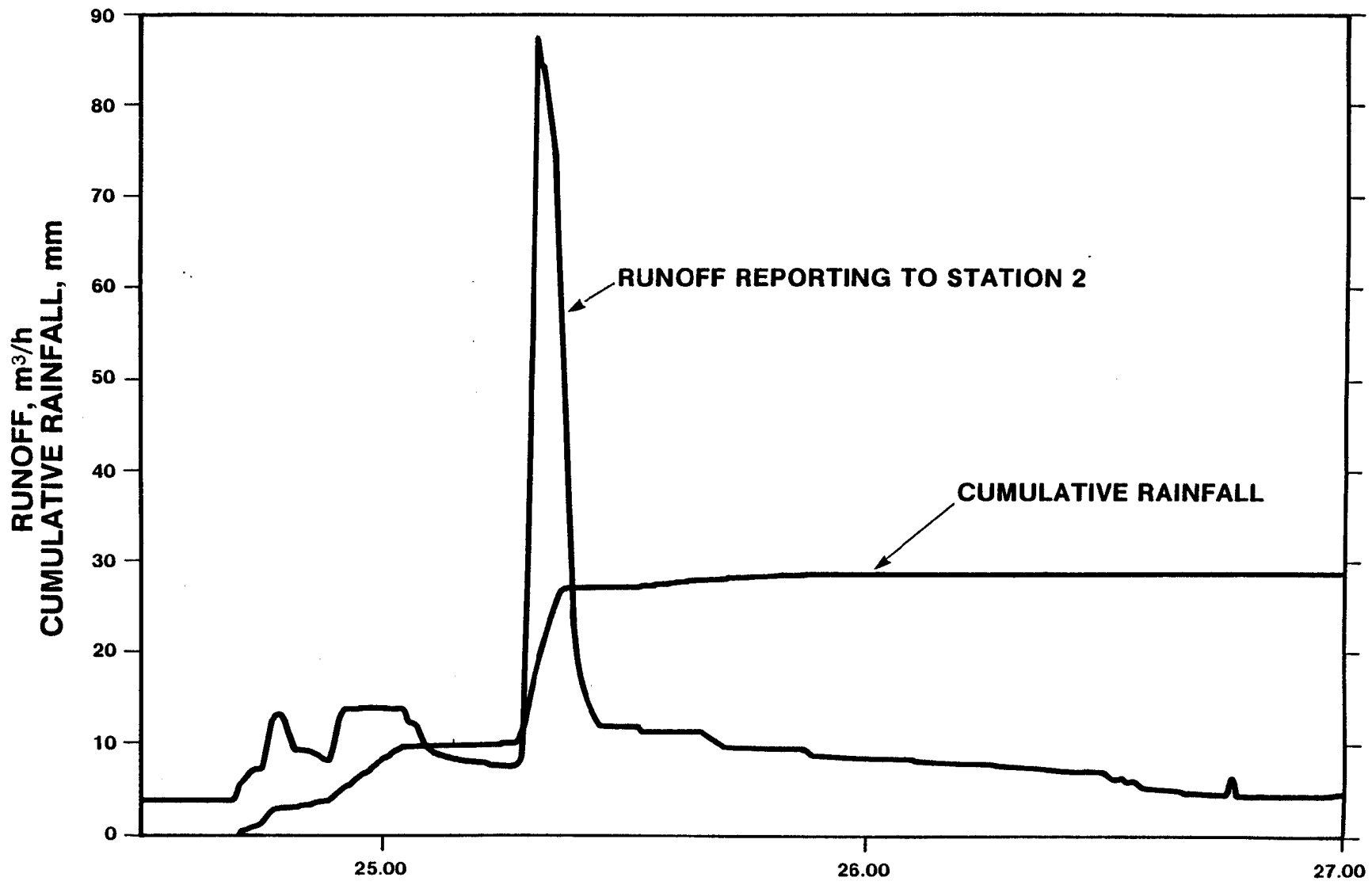


JUNE 1988

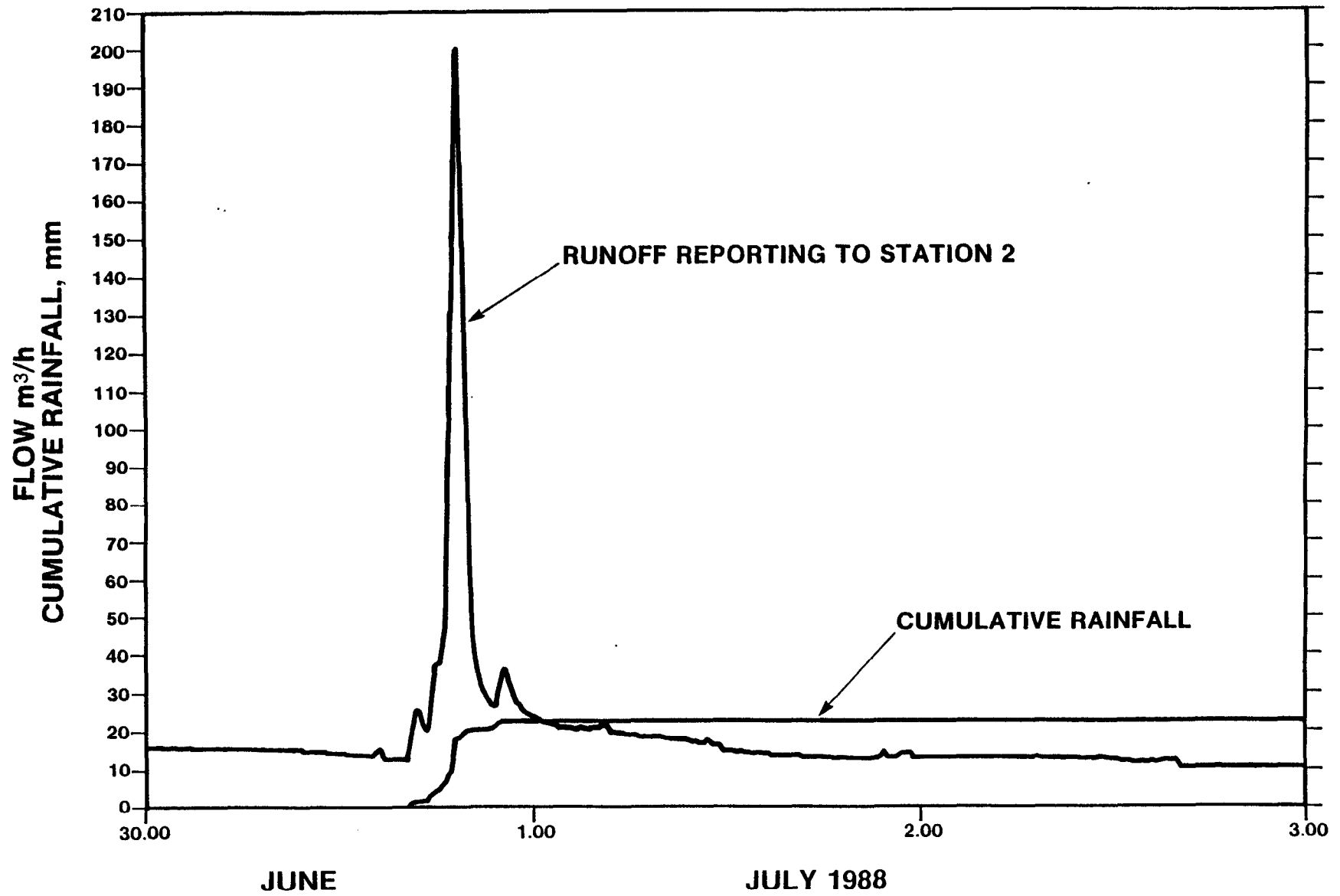


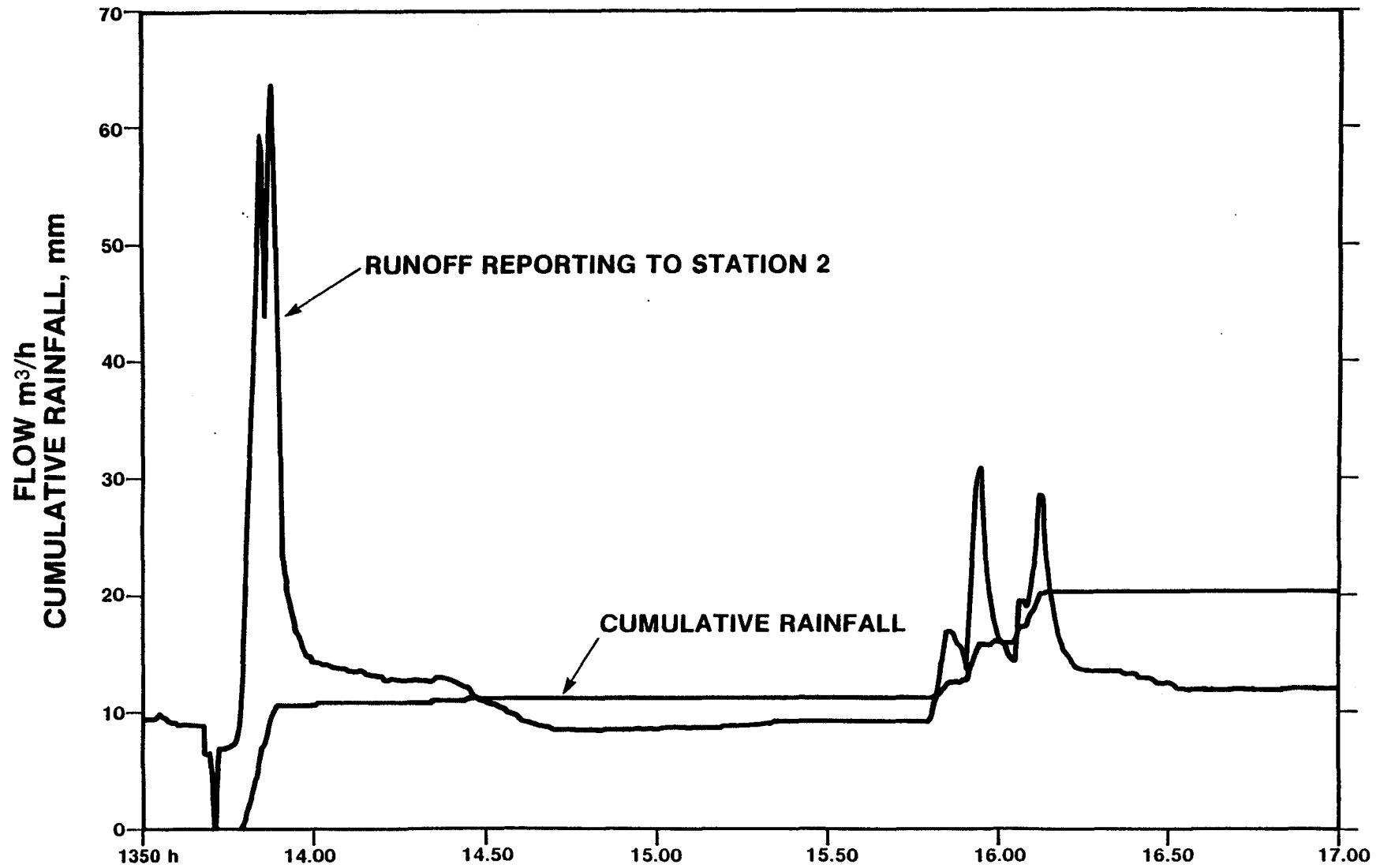


JUNE 1988

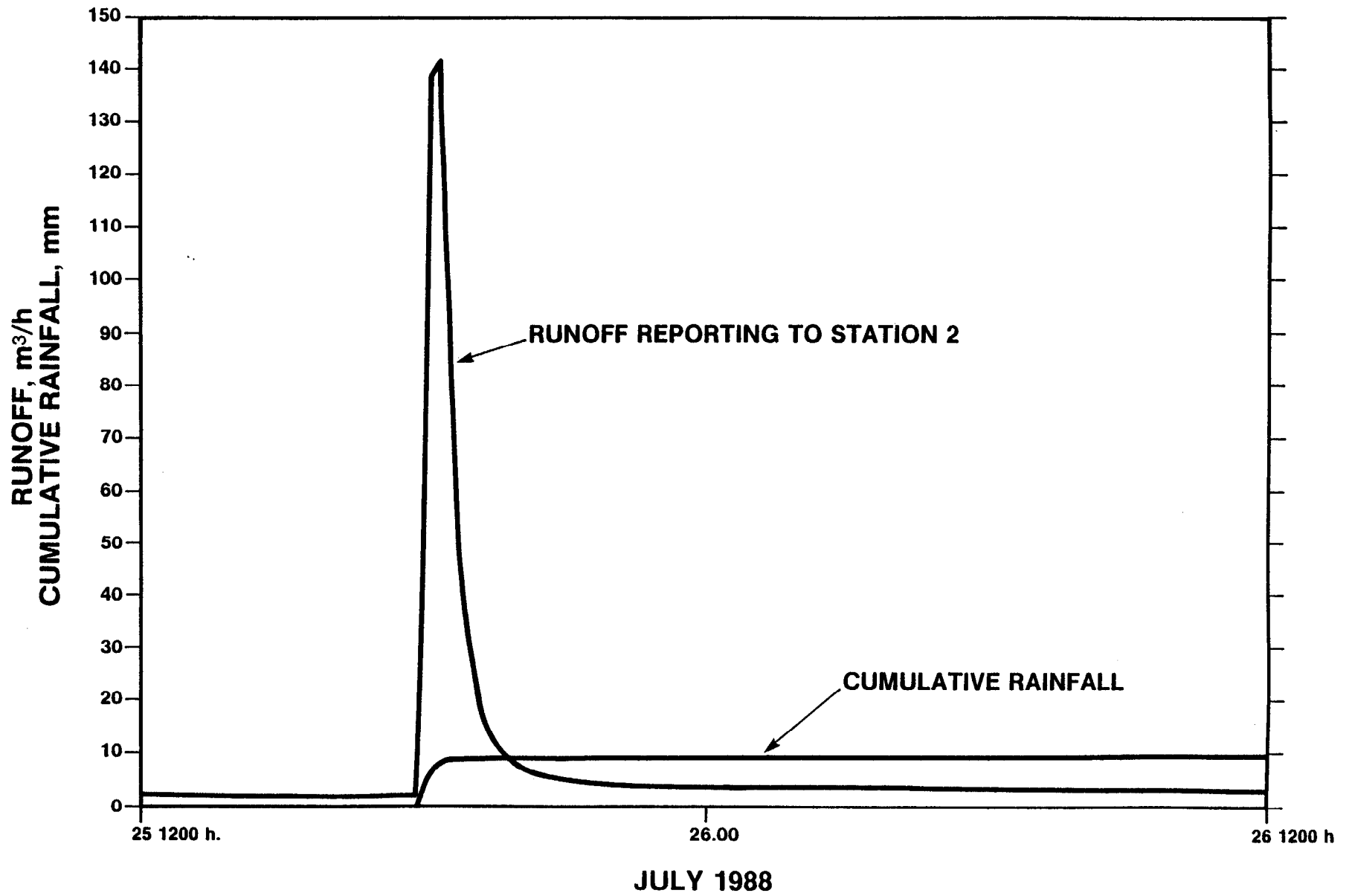


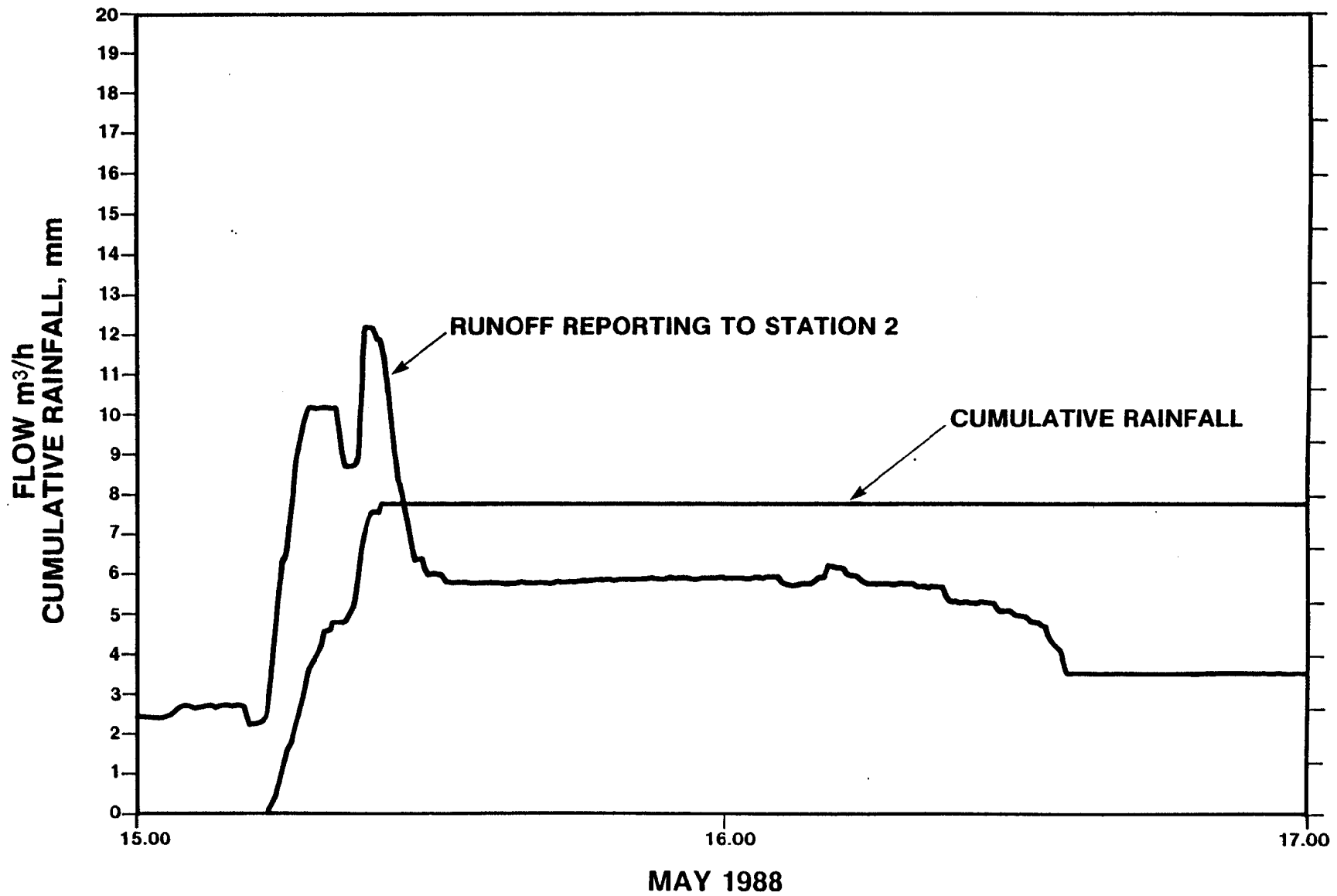
JUNE 1988

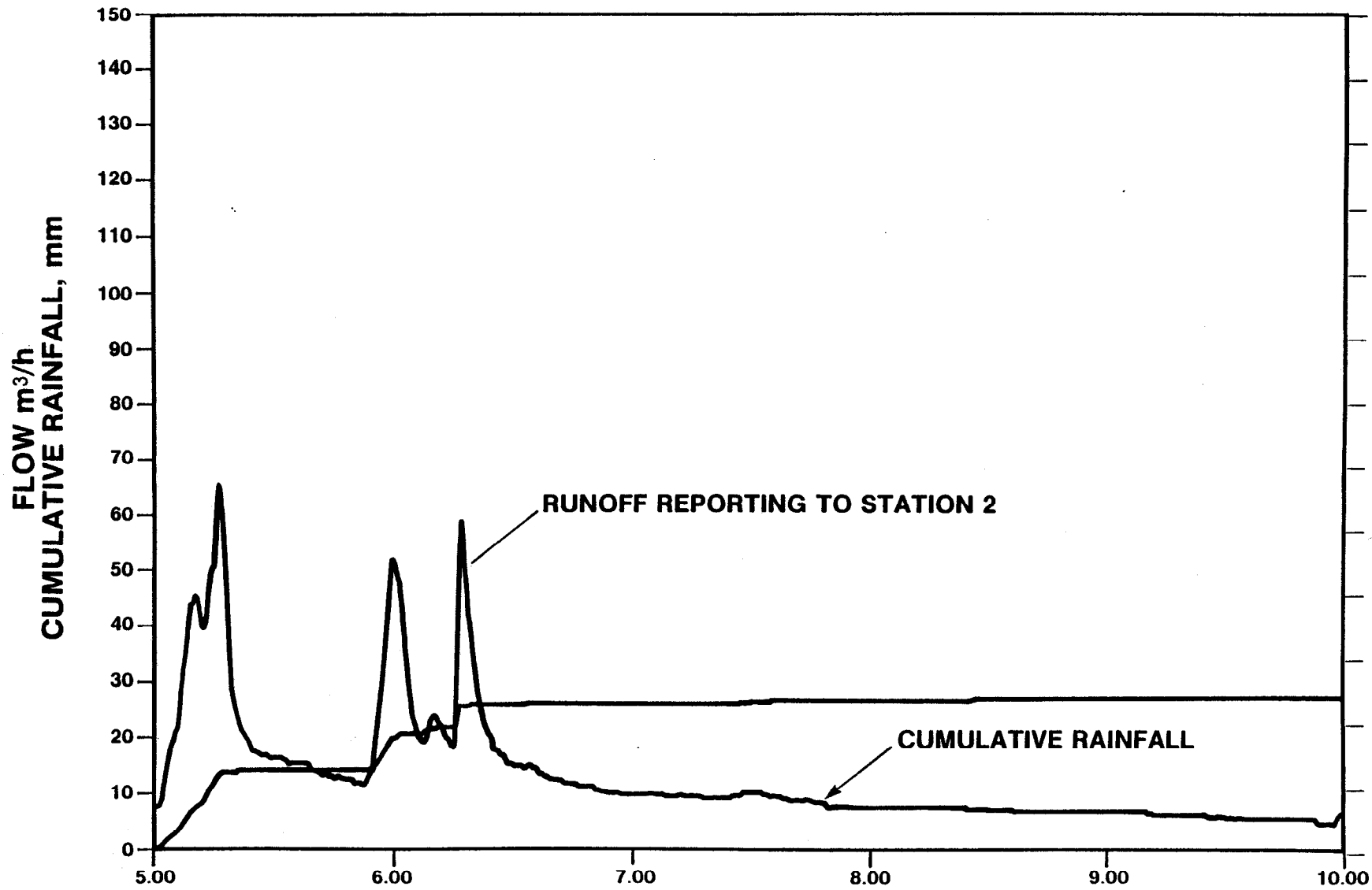




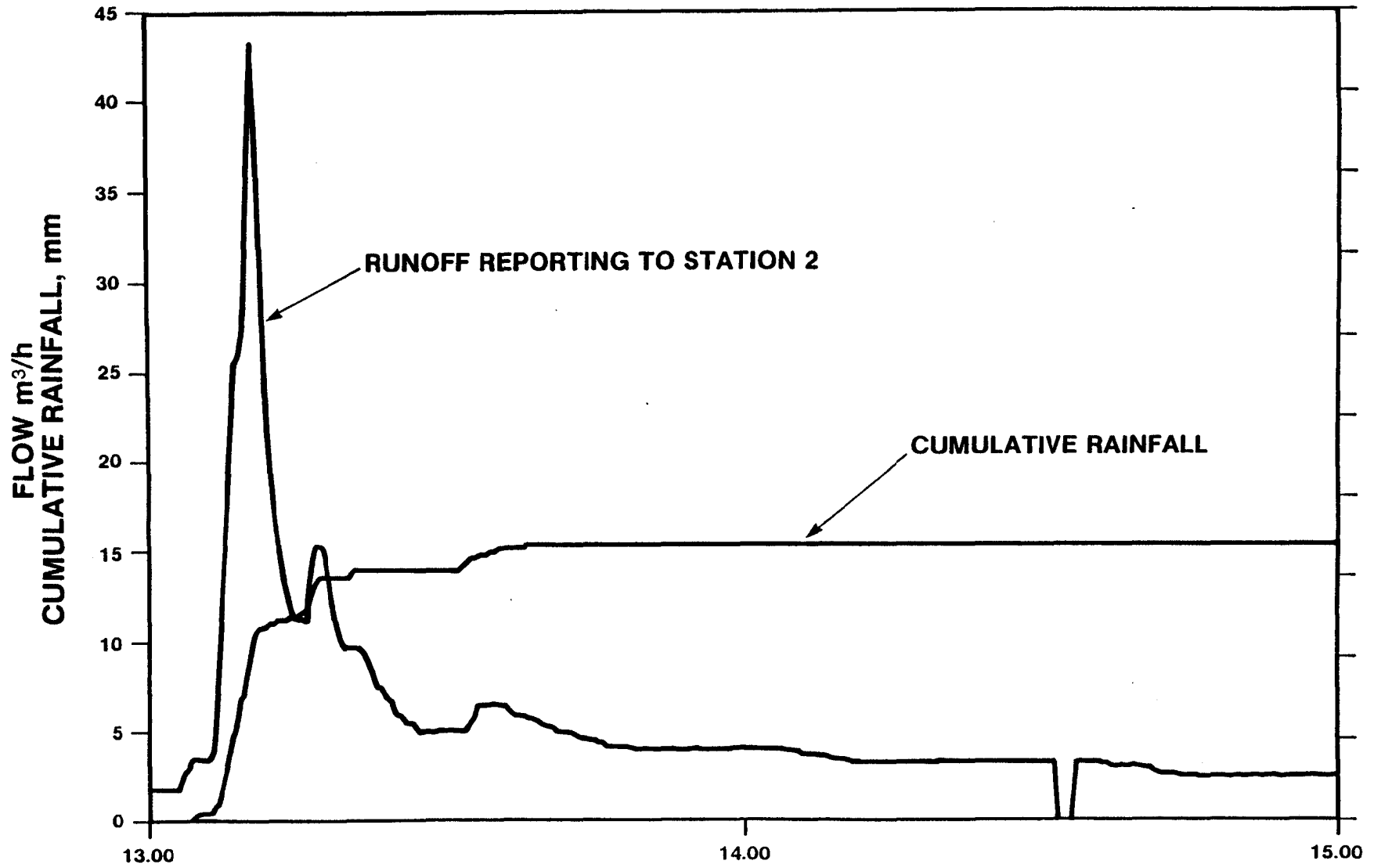
JULY 1988







NOVEMBER 1988



MAY

CENTRE DE TECHNOLOGIE NORANDA

November 15, 1989
Dr. E.K. Yanful

PROPOSAL FOR FURTHER WORK Project 1.17 WAITE AMULET HYDROGEOCHEMISTRY

A draft of the final report on the Waite Amulet hydrogeochemistry study was issued in October 1989. The report was distributed to all members of the MEND Prediction Committee for review and was discussed at a meeting of the Committee in Toronto on 10 November 1989. The report inferred, among other things, that flow of acid pore water from the tailings impoundment into the underlying clay deposit could be occurring. The Prediction Committee agreed with a recommendation in the report that the clay be studied to validate this proposition. This work, in the view of the Committee, should involve both laboratory and field studies.

This document presents a two-phased proposal for the additional work. The laboratory investigation, which has already commenced at the Noranda Technology Centre, is presented as Phase I. It is believed that the laboratory investigation will provide sufficient information to assess whether or not acid pore water from the tailings is entering the clay. If further work in the field is deemed necessary for the evaluation, it will be conducted during spring/summer 1990 as Phase II.

Phase I: Laboratory Investigation

Three boreholes were drilled in October 1989 into the clay and Shelby tube samples were taken for laboratory investigation. Laboratory testing will include hydraulic conductivity (permeability) measurements, clay chemical assessment by dissolved, adsorbed, and total metal analyses, and mineralogy. The clay pore water will be sampled by soil squeezing at pre-determined stresses to 100 percent primary consolidation. Clay soils directly beneath the tailings impoundment will be used in the evaluation. Results obtained on these soils will be compared with those to be obtained from background soils obtained outside the impoundment.

The results from the above-mentioned tests will be analyzed and geochemical and hydrogeological modelling will be conducted. The draft report will then be revised to include the results of the additional work.

The estimated cost for Phase I is \$50,511.00 which includes the cost for drilling. The breakdown is as follows:

(i)	Sampling including drill and mobilization (already incurred)	\$17,011.00
(ii)	5 hydraulic conductivity tests at field stresses using simulated pore water to at least 1.5 pore volumes and 3 consolidation tests	\$ 7,500.00
(iii)	Mineralogical analysis (external contract)	\$ 2,000.00
(iv)	Clay soil analyses for cation exchange, metals and sulphate and pore water squeezing and analyses for dissolved metals, pH, acidity, cations and anions	\$11,500.00
(v)	Data Processing, modelling, and reporting	\$12,500.00
	TOTAL	<u>\$50,511.00</u>

Phase II: Field work to supplement laboratory study, if required

This phase of the evaluation, if required, will involve drilling and installation of three piezometer nests in the clay with three piezometers in each nest. One piezometer nest will be located close to the groundwater divide and the other two down-gradient on the west dam face. Field hydraulic conductivities and hydraulic gradients will be determined in all the piezometers. The piezometers will also be sampled for pore water. The pore water will subsequently be analyzed for pH, acidity, conductivity, metals, cations and anions.

As in the case of the laboratory evaluation, data processing and modelling will be conducted. The report will then be revised to incorporate the additional information.

The estimated cost for Phase II is \$40,100 and the cost distribution for the various components are as follows:

(i)	Drilling including mobilization	\$ 11,100.00
(ii)	Piezometer installation, field testing, sampling, and chemical analyses	\$ 16,500.00
(iii)	Data processing, modelling, and reporting	\$ 12,500.00
	TOTAL	<u>\$ 40,100.00</u>